SAND2020-9203R

SANDIA NATIONAL LABORATORIES
WASTE ISOLATION PILOT PLANT

UPDATE TO TRANSPORTATION ANALYSIS FOR THE WASTE ISOLATION PILOT PLANT

REVISION 01

Authors: Elena Kalinina
Print | Signature | Date

Robert Kalan
Print | Signature | Date

Douglas Ammerman
Print | Signature | Date

Steven Maheras
Print | Signature | Date

Cathy Farnum
Print | Signature | Date

Lucas Lujan
Print | Signature | Date

Technical Review: Fotini Walton
Print | Signature | Date

Management Review: Paul Shoemaker
Print | Signature | Date

Sandia National Laboratories is a multimission laboratory managed and operated by National Technology & Engineering Solutions of Sandia, LLC, a wholly owned subsidiary of Honeywell International Inc., for the U.S. Department of Energy's National Nuclear Security Administration under contract DE-NA0003525. SAND2020-XXXX X

This page intentionally left blank.

Table of Contents

LIST OF TABLES

LIST OF FIGURES

ACRONYMS AND ABBREVIATIONS

ASME	Society of Mechanical Engineers
CCC	criticality control container
CCO	criticality control overpack (also 55-gal drum with criticality control overpack)
CGOC	center-of-gravity-over-corner
CH	contact-handled
DOE	(U.S.) Department of Energy
DSP	Disposition of Surplus Plutonium
EQPS	equivalent plastic strain
FARS	Fatality Analysis Reporting System
FR	Federal Register
HAC	hypothetical accident conditions
ICV	Inner Containment Vessel
INL	Idaho National Laboratory
IWM	Integrated Waste Management
LCF	latent cancer fatality
MCMIS	Motor Carrier Management Information System
MEI	maximum exposed individual
NEPA	National Environmental Policy Act
NNSS	Nevada National Security Site
NRC	(U.S.) Nuclear Regulatory Commission
NRD	Nuclear Radiation Development
OCA	outer confinement assembly
OCV	outer containment vessel
ORNL	Oak Ridge National Laboratory
POC	pipe overpack container also 55-gal drum with pipe overpack container
RH	remote-handled
RNS	reactive nitrate salts
SA	Supplement Analysis
SCA	shielded container assembly
SEIS	Supplemental Environmental Impact Statement
SLB2	standard large box 2
SNF	spent nuclear fuel
SNL	Sandia National Laboratories
SRS	Savannah River Site
SWB	standard waste box
START	Stakeholder Tool for Assessing Radioactive Transportation
TA	transportation analysis
TDOP	ten drum overpack
TI	transportation index
TRU	transuranic
TRUPACT-II	Transuranic Packaging Transporter-II
URF	unit risk factor
U.S.	United States
WAC	waste acceptance criteria
WIPP	Waste Isolation Pilot Plant

This page intentionally left blank.

EXECUTIVE SUMMARY

The goal of this transportation analysis (TA) is to update the 2008 TA in order to evaluate the impacts associated with the transportation of transuranic (TRU) waste from waste generator sites to the Waste Isolation Pilot Plant (WIPP) facility and from waste generator sites to the Idaho National Laboratory (INL).

This TA serves as an update to the 2008 TA. A similar approach was used in this revision to calculate radiological and non-radiological impacts. However, the input data used in this analysis has been updated to include the most recent route, accident, traffic count, and population data. The transportation index (TI) values were derived from analysis of the actual data (measured dose rates at 1 m from the package surface) for WIPP shipments. Bounding contact-handled (CH) and remote-handled (RH) inventories were developed based on the analysis of WIPP-bound CH and RH waste streams. The data used in this analysis are from the updated inventory as of December 31, 2018, which includes about 6 MT of surplus, non-pit plutonium and about 42.2 MT of surplus, pit plutonium (included in the WIPP inventory so that potential impacts can be estimated). The impacts on the Transuranic Packaging Transporter-II (TRUPACT-II) in an extra-regulatory accident was determined from structural finite element modeling (impacts onto unyielding surface at velocities greater than 30-mph) and thermal modeling (engulfing fire). These modeling capabilities were not feasible in 2008. As a result, the impacts on the TRUPACT-II from the extra-regulatory accidents in the 2008 TA were assumed to be the same as the impacts on the spent nuclear fuel (SNF) truck transportation cask. Extra-regulatory in this context means evaluating the impacts of accident scenarios beyond the hypothetical accident conditions (HAC) defined for regulatory accidents in 10 CFR Part 71. The intent of the radioactive material transportation HAC is to assure that the package will maintain containment in most, but not all, accidents. Consideration of low probability extra-regulatory accidents (probability-based analysis) are included per Department of Energy (DOE) National Environmental Policy Act (NEPA) accident analysis guidance. The modeling results were used to calculate the probability of an accident with the release of radioactive materials. The probability of this accident was estimated to be 5.00×10^{-5}.

The TA results include radiological impacts from incident-free transport, non-radiological impacts, and radiological impacts from transportation accidents with and without release of radioactive materials. The results are presented in a similar format to that of the 2008 TA.

The impacts associated with the transportation of TRU waste were evaluated using conservative input parameters and conservative models. As a result, the calculated impacts are conservative. The actual impacts will be lower than the impacts reported in this TA.

Radiological Impacts from Incident-Free Transport and Transportation Accidents without Release of Radioactive Materials

The maximum annual collective population dose calculated in this TA is 4 person-rem. This population dose includes multiple persons, the number of which differs depending on the exposure scenario. Note that the maximum annual individual occupational dose is limited to 5 rem (10 CFR Part 835). The collective doses calculated for an accident without release are significantly lower than the collective doses calculated for incident-free transport because the number of exposed persons is significantly lower.

The collective population doses (people along the transportation routes, people sharing the route, residents near stops, and people at refueling stations) calculated in this TA are slightly higher than in the 2008 TA. This is due to the difference in routes, increase in population density along the routes, additional stops not considered in the 2008 TA, and differences in the state-specific vehicle densities.

The maximum annual individual doses for receptors in the incident-free scenarios and a receptor (maximum exposed individual) in the accident without release of radioactive material scenario calculated in this TA are below the US average annual background (natural and anthropogenic) dose of 0.62 rem. The individual doses calculated in this TA are slightly lower than in the 2008 TA, except the individual doses to a person in a traffic jam and to the maximum exposed individual (MEI) in an accident without release scenario are slightly higher in this TA.

Non-Radiological Impacts

The total non-radiological impacts estimated for the duration of the WIPP transportation campaign are small – 49 accidents, 18 injuries, and 1 fatality. The estimated number of accidents per year is 0.94. The total non-radiological impacts in the 2008 TA were 366 accidents and 1 fatality for the assumed duration of the WIPP transportation campaign. The number of injuries was not estimated in the 2008 TA. The estimated number of accidents per year in the 2008 TA was 10.5. The differences are due to the higher assumed accident rates in the 2008 TA. The actual number of accidents from 1999 (beginning of WIPP transportation campaign) to October 2019 is 21 over 12,603 shipments. There have been no injuries or fatalities as of June 2020. Including the three-year interruption in the WIPP transportation campaign, the number of accidents per year is 1.17.

Radiological Impacts from Transportation Accidents with Release of Radioactive Materials

The radiological impacts from a transportation accident with release of radioactive materials were calculated for rural, suburban, and urban segments for each state crossed by the transportation route and for each route. Two scenarios were considered – an accident with a TRUPACT-II with contact-handled (CH)-TRU waste and an accident with a HalfPACT with remote-handled (RH)-TRU waste in shielded container assemblies (SCAs).

In both scenarios the dose risks (dose times the accident probability) are very low. The dose risk of an accident with a RH shipment is more than 2 orders of magnitude lower than for an accident with a CH shipment because of the lower number of RH shipments. In the 2008 TA the collective dose risks per CH shipment were higher and their ranges were larger for all (rural, suburban, and urban) links compared to this TA. This is primarily related to the higher (about one order of magnitude) assumed curie and A_2 content and higher assumed accident rates in the 2008 TA.

The radiological impacts were also calculated for two severe accident scenarios. The consequences of a severe accident are reported in terms of doses without taking in account the accident probability, which is extremely low. A severe accident was assumed to occur under conditions which maximize the radiological impacts - urban area and stable meteorological conditions. In this TA, the urban population density was defined based on the analysis of the actual route data. The collective population doses and MEI doses calculated in this TA are small, but somewhat higher than in the 2008 TA. This is mainly because of the higher release fraction calculated in this TA. The release fraction in the 2008 TA was assumed to be the same as in an accident with a SNF transportation cask which is structurally very different from TRUPACT-II and HalfPACT and has content (SNF assemblies) very different from the TRU waste.

This page intentionally left blank.

1. INTRODUCTION

This Transportation Analysis (TA) was performed in accordance with the Analysis Plan "*Analysis Plan for Update to Transportation Analysis for the Waste Isolation Pilot Plant*" (Kalinina, 2020). The analysis plan summarized the approach to the TA, the required input data, and the software. The TA is an update to the 2008 TA (Weiner and Dunagan, 2009).

The Waste Isolation Pilot Plant (WIPP) facility, located near Carlsbad, New Mexico, is a facility authorized to dispose of transuranic (TRU) waste generated by the U.S. Department of Energy (DOE) defense activities. The goal of this TA was to evaluate the impacts associated with the transportation of TRU waste from waste generator sites (sites) to the WIPP facility (direct routes) and from the waste generator sites to Idaho National Laboratory (INL) (indirect routes). Twelve routes, including 9 direct routes and 3 indirect routes, were considered in this TA.

This TA uses the updated estimate for the WIPP facility final closure date, the updated estimates of the quantities and characteristics of TRU wastes from DOE generator/storage sites and considers the impacts of transporting these wastes. The DOE requires re-evaluation of the impacts associated with the transportation of TRU waste from waste generator sites to the WIPP facility in order to support National Environmental Policy Act (NEPA) documentation associated with the proposed action of excavation and use of additional TRU waste disposal panels. These additional disposal panels will provide for the disposal of defense TRU waste up to the total TRU waste volume capacity limit of 6.2 million cubic feet (175,564 cubic meters) established in section 7(a)(3) of Public Law 102-579, *The Waste Isolation Pilot Plant Land Withdrawal Act of 1992* (as amended). Sandia National Laboratories (SNL) with support from the Pacific Northwest National Laboratory (PNNL) conducted this transportation analysis to evaluate the transportation impacts of this action.

The approach used in this TA is documented in Section 2. It is similar to the approach used in the 2008 TA (Weiner and Dunagan, 2009). Any modifications to the 2008 TA approach are defined and explained. The most recent versions of software (RADTRAN 6.02 and WebTragis) were used.

A large amount of input data was required for the new TA. Section 3 describes the inputs needed for the assessment of radiological impacts from incident-free transportation and non-radiological impacts.

Some transportation routes changed since 2008 and some were terminated. Also, a few new routes were only recently introduced. The updated (or new) routes were generated using WebTragis and the route specific data including the population density within 800 m (2,625 ft) of the highway were obtained as described in Section 3.1.

The population densities in WebTragis are based on the 2010 Census data. The data on state specific population increase since 2010 to 2018 (most recent available) were collected and used to adjust the population densities from WebTragis. In addition, the change in population multipliers were developed for 2030 and 2040 to be considered in the sensitivity analysis. The details are provided in Section 3.2.

The most recent state specific traffic count data (2017-2018) were collected and analyzed to obtain state specific average number of vehicles per hour. Section 3.3 provides the details of this analysis.

The most recent data on the state specific number of accidents, injuries and fatalities and miles traveled for large trucks was collected. These data were used to derive the state specific accident, injuries, and fatalities rate in the form of incident per vehicle-km. The data and data analysis are described in Section 3.4.

The annual number of shipments by package type was estimated for each generator site in Attachments D and E of WIPP Nuclear Waste Partnership, 2020. This information was used to define the number of shipments by shipment type for each site as described in Section 3.5.

The major parameter required for the assessment of the radiological impacts due to the external radiation during the routine transportation and transportation accidents without release of radioactive materials is the transportation index (TI). The TI represents the radiation dose rate at 3.3 ft (1 m) from the surface of the package. In this TA the TIs were derived from the actual data (measured TIs) of the WIPP shipments from the beginning of the transportation campaign through October 4, 2019 (except for surplus plutonium). The dose rate data are from Attachment C of WIPP Nuclear Waste Partnership, 2020. Section 3.6 describes the data analysis and the resulting bounding values of TI for each shipment type.

The input data developed in Section 3 were compared to the corresponding input data used in the 2008 TA. This comparison is important for understanding the differences in the results of radiological impacts from incident-free transportation and non-radiological impacts.

The radiological impacts from incident-free transportation are evaluated using the unit risk factor approach. The unit risk factors were calculated using RADTRAN 6.02 as described in Section 4.1.

Section 4.2 describes the results of the impacts from the incident-free transportation assessment. This includes radiation exposures to the general public (along the transportation route, sharing the road, and people at refueling stations), transportation workers (crew while the truck is moving and during stops), refueling station employees, site and state border inspectors, and for a hypothetical person in a traffic jam next to the WIPP truck with cargo. The results are presented in a format similar to the one in the 2008 TA (Weiner and Dunagan, 2009). The results are compared to the corresponding 2008 TA results.

Section 5 describes the results of the non-radiological impact assessment. The results are presented in a format similar to the one in the 2008 TA (Weiner and Dunagan, 2009). The results are compared to the corresponding 2008 TA results.

Section 6 describes the input data needed for the evaluation of the radiological impacts from transportation accidents.

One of the major parameters required for the assessment of the radiological impact related to accidents that are severe enough to breach the waste package and to release some of the radioactive material is the radionuclide inventory. This TA uses updated inventory information as of December 31, 2018, which includes ~6MT of surplus, non-pit plutonium (Van Soest 2019). In addition, ~42.2MT of surplus, pit plutonium is included in the WIPP inventory so that potential impacts can be estimated (Toothman 2019). The inventory was analyzed to derive bounding compositions for the different types of packages. Section 6.1 describes the details of this analysis.

The consequences of extra-regulatory accidents that may result in breach of TRUPACT-II were evaluated using a finite-element impact model. The analyses considered impacts on the top, the side, and the upper corner of the TRUPACT II package onto an unyielding target at different velocities. Section 6.2 describes the model and the modeling results. Section 6.3 extends the modeling results to impacts onto yielding targets. Section 6.3 and 6.4 provide the data for developing the accident conditional probabilities and corresponding release fractions as described in Section 6.5. Note that at the time of the 2008 TA no finite element model capable of determining hole sizes generated from an extra-regulatory impact of any of the WIPP packages existed.

The radiological impacts from transportation accidents are evaluated using the unit risk factor approach. The unit risk factors were calculated using RADTRAN 6.02 as described in Section 7.1.

Sections 7.2 and 7.3 describes the results of the impacts from transportation accidents. This includes:

- Radiological impacts related to the potential accidents that are severe enough to breach the TRU waste package and to release some of the radioactive materials.
- Radiological impacts from potential accidents that do not result in a release of radioactive material. These impacts represent the radiation exposes to the general public and to a maximum exposed individual (MEI) while the truck is stopped due to the accident.

The results are presented in a format similar to the one in the 2008 TA (Weiner and Dunagan, 2009). The results are compared to the corresponding 2008 TA results.

Section 8 summarizes the major results of this TA.

Note that the 2008 TA considered the pollution health effects that could be the result of vehicle emissions (diesel exhaust) while traveling through urban areas. The pollution health effects were not re-evaluated in this TA. The WIPP SEIS-II showed that latent cancer fatalities (LCFs) attributed to diesel exhaust exposure in an urban area are very small relative to the impact of accidents, fatalities, or injuries.

The 2008 TA also considered the impacts from hazardous chemical exposures during transportation accidents. The impacts from hazardous chemical exposures were not re-evaluated in this TA because these impacts continue to be bounded by the scenario evaluated in the 2008 TA that considered an accident with a TRUPACT-II. The updated inventory, shipment, and route data will not affect the hazardous chemical exposure scenario.

The types of shipments considered in this TA are illustrated in Figure 1-1 reproduced from DOE (2017).

a. Shipment of Two TRUPACT-II and One HalfPACT

b. Shipment of One TRUPACT-III

c. Shipment of Three HalfPACT

d. Shipment of One RH-TRU 72-B

Figure 1-1. Types of TRU Waste Shipments Considered in this TA.

2. METHODS

This TA uses the unit risk factors approach to calculate the radiological and non-radiological impacts. The unit risk factors were calculated using RADTRAN 6.02 for each shipment type for incident-free transport and transportation accidents. The unit risk factor approach is an effective way to incorporate greater details regarding route specific and other parameters. This allows for multiple exposure calculations without re-running RADTRAN 6.02.

In the 2008 TA each transportation route was divided into one rural, one suburban, and one urban segment within each state that the route crossed. The route specific data were used as an input into RADTRAN 6.02. The RADTRAN 6.02 calculations were done for a CH shipment and a RH shipment for each route. In this TA RADTRAN 6.02 was used to calculate the unit risk factors. The route specific data were used as an input into the spreadsheet calculations.

Section 2.1 describes the calculations of the impacts from the incident-free transport. Section 2.2 describes the calculations of the impacts from the transportation accident. Section 2.3 describes the calculations of the non-radiological impact.

2.1 Incident-Free Transport Calculations

The unit risk factors were calculated using RADTRAN 6.02 for different shipment types assuming:

- Dose rate at 1 m (TI) equal to 1 mrem/hr
- Shielding factor equal to 1 (no shielding)
- Link distance equal to 1 km (0.62 mi), if applicable
- Vehicle speed equal to 1 km/hr (0.62 mph), if applicable
- Population density equal to 1 person per km^2 (0.39 persons/mi^2), if applicable
- Traffic count equal to 1 vehicle/hr, if applicable
- Vehicle occupancy equal to 1 person per vehicle, if applicable
- Exposure time equal to 1 hr, if applicable
- Accident rate equal to 1 accident per km (0.62 accident per mi), if applicable

The calculations of the unit risk factors for incident-free transportation are described in Section 4.1. The unit risk factors are summarized in Table 4-3. The notations in this table correspond to the notations used in the equations below.

The external collective dose to a receptor from each shipment type and each route is calculated using unit risk factors, shipment specific and route specific data, and the receptor specific scenario parameters. The details of these calculations are provided below.

The probability that the transportation is routine and without incident with release of radioactive materials is close to 1. Due to a very small conditional probability of a release, the collective doses in this group of scenarios are reported in terms of doses and not dose risks as in the case of an accident with release of radioactive materials.

2.1.1 Non-Occupational Dose Calculation

The route-specific data for these calculations are: rural, suburban, and urban distances traveled within each state crossed by the route and corresponding rural, suburban, and urban population densities within an 800

m corridor on either side of the transportation route. These data are obtained from WebTragis and described in Section 3.1. The population bins in WebTRAGIS are:

• rural: up to 139 persons/mi^2 (53.73 persons/km^2)
• suburban: more than 139 to 3,326 persons/mi^2 (more than 53.73 to 1,286 persons/km^2)
• urban: more than 3,326 persons/mi^2 (more than 1,286 persons/km^2)

The 800 m was historically used in AEC (1972) and in RADTRAN applications. Retaining the 800-m value is extremely conservative, but it provides comparability with older analyses.

The route data are summarized in Tables 3-2 – 3-13. The suburban and urban distances within each state are divided into two segments – the segment to which the rush hour-speed is applied and the segment with the non-rush hour speed. The percent of the total urban and suburban distance that is affected by the rush hour speed is an input parameter and is described in Section 4.2. The stops are defined for each route based on the requirements for safety check stops, refueling, break, and inspections as described in Section 3.1.

The population densities along the route are adjusted using the population change multipliers to account for the population change from the 2010 census to 2018 (base case) and from 2010 to 2030 and 2040 (cases used in the sensitivity analysis). The percent population change analysis is described in Section 3.2. The percent population changes are summarized in Table 3-15.

The package specific data are the transportation indexes (TIs) that are defined for each package in Section 3.6, Table 3-22. The number and type of each shipment are defined for each site in Section 3.5, Table 3-20. The traffic count data are described in Section 3.3. The data used in the calculations are summarized in Table 3-17.

The receptor and scenario specific parameters are described for each receptor below.

2.1.1.1 Residents along the Transportation Route

The external collective dose to residents $D_{off,p}$ (person-rem) along the route segment (link) L from the shipment of type p (off link collective dose) is calculated as:

$$D_{off,p} = \frac{PD_L}{v_L} \cdot SF_L \cdot DIST_L \cdot URF_{off,p} \cdot TI_p \qquad (2\text{-}1)$$

where

PD_L = adjusted population density within 800 m corridor of the route segment L (persons/km^2)
v_L = vehicle speed (km/hr) during the rush hour or non-rush hour depending on the link type
SF_L = shielding factor with default values of 1 (rural), 0.87 (suburban), and 0.018 (urban) links
$DIST_L$ = link distance (km)
$URF_{off,p}$ = off-link unit risk factor for shipment type p (km^2)
TI_p = external dose rate at 1 m from the shipment surface (TI), mrem/hr

The collective dose to residents along the route from shipment of type p is a sum of the collective doses of all the route segments. This dose is multiplied by the number of shipments of type p along the route to obtain the transportation campaign collective dose Note that the transportation campaign begins in 2020.

2.1.1.2 Occupant of Vehicles Sharing the Transportation Route

The external collective dose to the occupants of the vehicles sharing the route with the shipment (on link collective dose) includes the following receptors:

- Occupants of vehicles traveling in the opposite direction to the shipment
- Occupants of vehicles traveling in the same direction as the shipment, and
- Occupants of passing vehicles.

The collective dose to the occupants of the vehicles $D_{on,p}$ (person-rem) sharing the route segment L with the shipment of type p is calculated as:

$$D_{\text{on,p}} = DIST_L \cdot PPV_L \cdot N'_L \cdot URF_{on,p} \cdot TI_p \quad (2\text{-}2)$$

PPV_L = vehicle occupancy (average number of persons per vehicle)
N'_L = one-way traffic count (average number of vehicles per hour in all lanes)
$URF_{on,p}$ = rush or non-rush hour on-link unit risk factor for shipment type p depending on link type (hr^2/km)

Note that the $URF_{on,p}$ accounts for all three types of receptors listed above.

The 2008 TA assumed two persons per vehicle. The same assumption was used in this TA. The state specific and population area specific traffic count data are described in Section 3.3.

The collective dose to the occupants of the vehicle sharing the route from shipment of type p is a sum of the collective doses of all the route segments. This dose is multiplied by the number of shipments of type p along the route to obtain the transportation campaign collective dose.

2.1.1.3 Collective Dose to Residents Near Stops

It is assumed that when a truck stops, the residents in the vicinity of the stop are exposed. In this case, the population in RADTRAN is modeled as a population uniformly distributed within the annulus surrounding the stop with the vehicle in the center of it. The dose is then integrated over this population from the minimum radial distance x_{min} to the maximum radial distance x_{max} from the truck. As discussed in Section 4.1, the unit risk factors were calculated assuming x_{min} equal to 30 m and x_{max} equal to 800 m. It was assumed that the truck does not stop in urban areas. This is the same assumption as in the 2008 TA.

The external collective dose to population in the vicinity of a stop $D_{st,p}$ (person-rem) on link L from the shipment of type p is calculated as:

$$D_{\text{st,p}} = PD_L \cdot T_{st} \cdot SF_L \cdot URF_{st,p} \cdot TI_p \quad (2\text{-}3)$$

T_{st} = duration of stop (hr)
$URF_{st,p}$ = population near the stop unit risk factor for shipment type p (km^2)

The stop can be a refueling stop, a safety check stop, a break stop, or an inspection stop. The stops assumed for each route are described in Section 3.1. The duration of the different types of stops is an input parameter into the calculations and is discussed in Section 3.1.

The total collective dose to the residents near the stops along the route from the shipment of type p is the sum of the doses from all the stops. This dose is multiplied by the number of shipments of type p along the route to obtain the transportation campaign collective dose.

2.1.1.4 Collective Dose to People at Refueling Stops

It is conservatively assumed that when a truck stops, people at the refueling station get exposed. The collective external dose $D_{pst,p}$ (person-rem) to the people at stop from the shipment of type p is calculated as:

$$D_{\text{pst,p}} = PD_{pst} \cdot T_{st} \cdot URF_{pst,p} \cdot TI_p \quad (2\text{-}4)$$

$$PD_{pst} = N_{pst}/A$$

$URF_{pst,p}$ = people at stop unit risk factor for shipment type p (km^2)
N_{pst} = number of people at the refueling station
A = annular area defined by x_{min} and x_{max} (km^2)

The 2008 TA assumed 7 people at the refueling station, x_{min}=1 m and x_{max}=15 m. The same assumptions were made in this TA.

The refueling stops assumed for each route are described in Section 3.1. The duration of the refueling stop is an input parameter into the calculations and is discussed in Section 3.1.

The total collective dose to the people at the refueling stops along the route from the shipment of type p is the sum of the doses from all the refueling stops. This dose is multiplied by the number of shipments of type p along the route to obtain the transportation campaign collective dose.

2.1.1.5 Dose to a Person in a Traffic Jam Next to the WIPP Truck with Cargo

The external dose to a person in a traffic jam $D_{ptrf,p}$ (person-rem) from the shipment of type p is calculated as:

$$D_{\text{ptrf,p}} = T_{trf} \cdot URF_{ptrf,p} \cdot TI_p \quad (2\text{-}5)$$

T_{trf} = time in a traffic jam (hr)
$URF_{ptrf,p}$ = person in a traffic jam unit risk factor for shipment type p (unitless)

In the 2008 TA it was assumed that the person is exposed only once, the exposure distance is equal to 2 m, and the exposure time is 30 min. The same assumptions were made in this TA.

2.1.2 Occupational Dose Calculation

The shipment specific data are the TIs that are defined for each shipment type in Section 3.6, Table 3-22. The number and type of each shipment is defined for each site in Section 3.5, Table 3-20.

The receptor and scenario specific parameters are described for each receptor below.

2.1.2.1 Inspector at the Generator Site

The dose to an inspector at the generator site $D_{gins,p}$ (person-rem) inspecting the shipment of type p leaving the site is calculated as:

$$D_{gins,\text{p}} = T_{gins} \cdot URF_{ins,p} \cdot TI_p \cdot P_{gins} \cdot K_p \cdot \frac{T_{exp}}{Tcmp} \quad (2\text{-}6)$$

T_{gins} = inspection time (hr)
$URF_{ins,p}$ = inspector unit risk factor for shipment type p (unitless)
P_{gins} = percent of all shipments inspected by an inspector at the generator site
K_p = total number of packages of type p shipped from the generator site
T_{exp} = total exposure period (yrs)
T_{cmp} = campaign duration (yrs)

The 2008 TA assumed that the inspector at the generator site would have an exposure distance of 1 meter for an hour (T_{gins}=1), the inspector would work at the same job for 10 years (T_{exp}=10), and there would be two shifts working the same job (P_{gins}=0.5). The same assumptions were made in this TA. The assumed campaign duration was 52 yrs.

2.1.2.2 Inspector at the State Border

The dose to an inspector at state border $D_{bins,p}$ (person-rem) inspecting the shipment of type p is calculated as:

$$D_{bins,\mathrm{p}} = T_{bins} \cdot URF_{ins,p} \cdot TI_p \cdot P_{bins} \cdot K_p \cdot \frac{T_{exp}}{Tcmp} \quad (2\text{-}7)$$

T_{bins} = inspection time (hr)
P_{bins} = percent of all shipments inspected by an inspector at the state border

The 2008 TA assumed that the state border inspector would be involved in 20 percent of the inspection (P_{bin}S=0.2) over a 10-year period with an average exposure distance of approximately 1 meter and inspection time of 1 hr. The same assumptions were made in this TA, except the inspection time (T_{bins}) as described in Section 4.2.7.

2.1.2.3 Refueling Stop Employee

The external dose $D_{emp,p}$ (person-rem) to a refueling station employee from the shipment of type p is calculated for each route as:

$$D_{emp,\mathrm{p}} = PD_{emp} \cdot T_{emp} \cdot P_{emp} URF_{emp,p} \cdot TI_p \cdot K_p \cdot \frac{T_{exp}}{T_{cmp}} \quad (2\text{-}8)$$

$URF_{emp,p}$ = refueling station employee unit risk factor for shipment type p (km^2)
T_{emp} = total refueling stop time on the route
P_{emp} = percent of total shipments to which the refueling station employee is exposed

PD_{emp}=1421.026 persons/km^2 is calculated assuming that one person is exposed within the annular area with the minimum exposure distance of 1 m and maximum exposure distance of 15 m.

The 2008 TA assumed that the individual will be exposed to approximately 20 percent of shipments (P_{emp}=0.2) over a 10-year period. This assumption is made on the basis that trucks stop at the same location, an individual works for 10 years at the truck stop, and 3 shifts work at the truck stop. The assumed stop duration was 50 minutes. The same assumptions were made in this TA. The stop duration is an input parameter and is described in Section 4.2.6.

2.1.2.4 Truck Crew while Driving and while at Stops

The external dose to the truck crew while driving $D_{crdr,p}$ (person-rem)with the shipment of type p is calculated as:

$$D_{\text{crdr,p}} = T_{crdr} \cdot URF_{crdr,p} \cdot TI_p \quad (2\text{-}9)$$

T_{crdr} = total time of driving from a generator site to the WIPP (hr) with the shipment p
$URF_{crdr,p}$ = crew while driving unit risk factor for shipment type p (unitless)

Note that the unit risk factors were calculated assuming the crew of two people.
The external dose to the truck crew while at stops $D_{crst,p}$ (person-rem) with the shipment of type p is calculated as:

$$D_{\text{crst,p}} = T_{crst} \cdot URF_{crst,p} \cdot TI_p \cdot N_{cr} \cdot P_{crst} \quad (2\text{-}10)$$

T_{crst} = total stop time (hrs) on the route from a generator site to the WIPP with the shipment type p
$URF_{crst,p}$ = crew while at stop unit risk factor for the shipment type p
N_{cr} = number of people in the crew
P_{crst} = percent of time spent next to the truck at the stop

The total external dose to the truck crew while driving $D_{cr,p}$ (person-rem) with the shipment of type p from a generator site to the WIPP (INL) is calculated as:

$$D_{\text{cr,p}} = D_{crdr,p} + D_{crst,p} \quad (2\text{-}11)$$

Note that this calculation does not take into account that per current regulations any monitored crew member who receives a radiation dose that approaches 2 rem (the administrative limit for occupational doses) in any given year is to be reassigned to other duties involving no further dose for the remainder of the year (DOE 2004). These are the same assumptions as in the 2008 TA.

The 2008 TA assumed that the truck crew consists of two people and that the drivers spend half time each standing next to the truck at the stops. The same assumptions were made in this TA.

2.2 Transportation Accident Calculations

The majority of the transportation accidents (99.993 percent -in the 2008 TA) are the accidents in which there is no release of radioactive materials. In this TA the probability of an accident with release is even lower. The calculation of the exposure from these accidents is described in Section 2.2.1.

Calculation of the radiological impacts related to the potential accidents that are severe enough to breach the TRU waste package and to release some of the radioactive materials are described in Section 2.2.2.

The unit risk factor approach was used in both, transportation accidents with and without release of radioactive materials.

2.2.1 Radiological Impacts from the Transportation Accident without Release of Radioactive Materials

A truck involved in an accident in which no radioactive materials were released will stay at or near the place of the accident for many hours. The nearby population will be exposed to the external radiation from

the package(s) on the truck as well as an individual who happened to be in the vicinity (this also applies to a first responder).

The 2008 TA considered one such accident scenario that took place in a densely populated area (2,750 persons/km^2). The residents were located within the annular area defined by the minimum distance of 30 m and maximum distance of 800 m from the truck. The maximum exposed individual (MEI) was assumed to be at the 30 m distance from the truck. The exposure time was assumed to be 10 hours. The radiological impacts were reported as a population dose. The same assumptions were made in this TA.

The unit risk factors were calculated using RADTRAN 6.02 for the different shipment types assuming:

- Dose rate at 1 m (TI) equal to 1 mrem/hr
- Shielding factor equal to 1 (no shielding)
- Population density equal to 1 person per km^2 (0.39 persons/mi^2), if applicable
- Exposure time equal to 1 hr

The calculations of the unit risk factors are described in Section 7.1. The unit risk factors are summarized in Table 7-2. The notation in this table correspond to the notations used in the below equations.

The collective external doses were calculated using the unit risk factors, shipment specific TIs, and the population density and exposure time defined in Section 7.2.3. Note that the calculations are similar to the ones in Section 2.1 because the radiological impacts from potential accidents without release of radioactive material are treated as long duration stops.

The external collective dose to population in vicinity of the place of an accident $D_{nracc,p}$ (person-rem) from the shipment of type p is calculated as:

$$D_{\text{nracc,p}} = PD_{nracc} \cdot T_{nracc} \cdot URF_{nracc,p} \cdot TI_p \qquad (2\text{-}12)$$

TI_p = transportation index for shipment p (mrem/hr)
PD_{nracc} = population density in vicinity of an accident (persons/km^2)
T_{nracc} = exposure time (hr)
$URF_{nracc,p}$ = population near the place of an accident unit risk factor for shipment type p (km^2)

The external dose to the MEI $D_{MEI\_nr,p}$ (person-rem) from the shipment of type p is calculated as:

$$D_{\text{MEI\_nr,p}} = T_{nracc} \cdot URF_{MEI\_nr,p} \cdot TI_p \qquad (2\text{-}13)$$

$URF_{MEI\_nr,p}$ = MEI near the place of an accident unit risk factor for shipment type p (unitless)

2.2.2 Radiological Impacts from Transportation Accidents with Release of Radioactive Materials

The radiological impacts from transportation accidents with release of radioactive materials are calculated for rural, suburban, and urban segments for each state crossed by the transportation route. Credit is not taken for the fact that an accident will occur at only one place. A few rural segments may exist in one state and combining them in one segment with aggregated population may result in overestimating the population density and thus, the radiological impacts. The same concerns exist for the suburban segments. The radiological impacts in an urban segment will not be overestimated in states that have only one urban population center. This is the same approach as in the 2008 TA.

The radiological impacts are calculated using the unit risk factor approach. The unit risk factors were calculated using RADTRAN 6.02 for the bounding package inventory assuming:

- Accident rate equal to 1 accident/km
- Link distance equal to 1 km
- Population density equal to 1 person per km^2 (0.39 persons/mi^2)

The radiological impacts in the rural and suburban areas are calculated in RADTRAN 6.02 using the same pathway-specific equation. The population dose in an urban area includes a factor that takes into account the population inside buildings and the population outside (pedestrians). As a result, the unit risk factors are the same for the rural and suburban links and different for the urban links.

The bounding inventories are described in Section 6.1 and summarized in Table 6-5. The other inputs into the unit risk factor calculations are the conditional probability of each type of accident (severity fractions) and associated release fractions. Note that the accident conditional probabilities and the corresponding release fractions used in this TA are different from the 2008 TA. The consequences of the extra-regulatory accidents that may result in a breach of TRUPACT-II were evaluated using the finite-element impact model (Section 6.2). The model provided the data for developing the accident conditional probabilities and corresponding release fractions as described in Section 6.5. At the time of the 2008 TA no finite element model capable of determining hole sizes generated from extra-regulatory impact of any of the WIPP packages existed.

The calculations of the unit risk factors for transportation accidents involving a release of radioactive materials are described in Section 7.1. The unit risk factors are summarized in Table 7-1. The notation in this table correspond to the notations used in the below equations.

The route specific inputs are:

- Rural, suburban, and urban distances traveled within each state crossed by the route
- Rural, suburban, and urban population densities within an 800 m corridor on either side of the transportation route
- State specific accident rates

The distance and population data were obtained from WebTragis and are described in Section 3.1. The route data are summarized in Tables 3-2 – 3-13.

The population densities along the route were adjusted using population change multipliers to account for the population change from the 2010 census to 2018 (base case) and from 2010 to 2030 and 2040 (cases used in the sensitivity analysis). The percent population change analysis is described in Section 3.2. The percent population changes are summarized in Table 3-15. The state specific accident data are described in Section 3.4.

The results for the accident case are reported in terms of the total population dose risk, which is the sum of the dose risks calculated for each accident category. The category specific dose risk is a product of the category conditional probability and population dose. The population dose in RADTRAN 6.02 is calculated as the sum of the inhalation, cloudshine, resuspension, and groundshine doses.

The total population dose risk for the rural/suburban route segment from the bounding inventory i ($DR_{L,i}$) (person-rem) is calculated as:

$$DR_{L,i} = P_{acc,L} \cdot PD_L \cdot DIST_L \cdot URF_{acc,i} \quad (2\text{-}14)$$

$P_{acc,L}$ = accident rate on the route segment L (accident/km)
PD_L = adjusted population density within 800 m of the route segment L (persons/km^2)
$DIST_L$ = link distance (km)
$URF_{acc,i}$ = rural/suburban accident unit risk factor for bounding inventory i (km^2)

The total population dose risk for the urban route segment from the bounding inventory i ($DRU_{L,i}$) (person-rem) is calculated as:

$$DRU_{L,i} = P_{acc,L} \cdot PD_L \cdot DIST_L \cdot URF_{u\_acc,i} \quad (2\text{-}15)$$

$URF_{u\_acc,i}$ = urban accident unit risk factor for bounding inventory i (km^2)

The total population dose risks were also calculated for all shipments relevant to the corresponding bounding inventory. This is the same approach as in the 2008 TA. As was pointed out in the 2008 TA, multiplying by the number of shipments is accurate because it increases the probability that a shipment will be involved in each type of accident.

2.3 Non-Radiological Impact Calculations

The non-radiological impacts are expressed as the number of potential traffic accidents and non-radiological fatalities and injuries likely to occur as a result of transporting the TRU waste containers round trip between the generator sites and the WIPP facility and between the generator sites and INL. The type of shipment is not relevant in this case, only the total number of shipments along the route is.

The inputs into the non-radiological impact calculations are described in Section 3. They are:

- Total distance along each route, Table 3-14.
- Number of shipments along each route, Table 3-20.
- State specific accident, injury, and fatality rates for the states crossed by the WIPP routes, Table 3-18.

The number of accidents along the route N_{acc} is calculated as:

$$N_{acc} = N_{shp} \cdot \sum_i^{Nst} P_{acc,i} \cdot 2 \cdot DIST_i \quad (2\text{-}16)$$

N_{shp} = total number of shipments along the route
N_{st} = total number of states crossed by the route
$P_{acc,i}$ = accident rate in state i (accidents/km)
$DIST_i$ = distance traveled in state i (km)

The number of injuries along the route N_{inj} is calculated as:

$$N_{inj} = N_{shp} \cdot \sum_i^{Nst} P_{inj,i} \cdot 2 \cdot DIST_i \quad (2\text{-}17)$$

$P_{inj,i}$ = injury rate in state i (injuries/km)

The number of fatalities along the route N_{ftl} is calculated as:

$$N_{ftl} = N_{shp} \cdot \sum_{i}^{Nst} P_{ftl,i} \cdot 2 \cdot DIST_i \quad (2\text{-}18)$$

$P_{ftl,i}$ = fatality rate in state i (fatalities/km)

3. INPUT DATA FOR THE INCIDENT-FREE TRANSPORTATION ANALYSIS

3.1 Route Data

Nine routes from waste generator sites to the WIPP facility and five routes from waste generator sites to INL are defined in Attachment B of WIPP Nuclear Waste Partnership, 2020. The route from Hanford to INL coincides with the Hanford to INL segment of the route from Hanford to the WIPP facility. The route from Lawrence Berkley Laboratory (LBL) to INL was closed. Consequently, nine routes from generator sites to the WIPP facility and three routes from generator sites to INL are considered in this TA. The routes are listed in Table 3-1. It is assumed that these routes will remain the same for the duration of the WIPP shipment campaign and no other routes will be introduced. Note that the 2008 TA considered 16 routes. Five of these routes identified in Table 3-1 are no longer in use and the route from Nuclear Radiation Development (NRD), LLC, NY to INL was not used in 2008.

Table 3-1. Transportation Routes to Be Considered in TA.

Route ID	Generator Site
Routes from Generator Sites to the WIPP	
1	Hanford Site (Hanford), WA
2	Idaho National Laboratory (INL), ID
3	Los Alamos National Laboratory (LANL), NM
4	Oak Ridge National Laboratory (ORNL), TN
5	Savannah River Site (SRS), SC
6	Argonne National Laboratory (ANL), IL
7	Bettis Atomic Power Laboratory, (Bettis), PA
8	Sandia National Laboratories (SNL), NM
9	Knolls Atomic Power Laboratory (KAPL), NY
Routes from Generator Sites to INL	
10	Lawrence Livermore National Laboratory (LLNL), CA
11	Nuclear Radiation Development (ND), LLC, NY (West Valley)
12	Nevada National Security Site (NNSS), NV
2008 TA Routes that Are No Longer Used	
	Battelle Memorial Institute, OH
	Brookhaven National Laboratory, NY
	Army Materials Command, VA
	Missouri University Research Reactor, MO
	Rocky Flats Environmental Test Site, CO

The route information was used as an input into the ORNL routing software WebTragis (Peterson, 2018) to obtain the population density within 800 m (2,625 ft) of either side of the highway, population category (rural, suburban, and urban), and travel times and distances along the transportation route. Note that some routes changed since 2008. The old routes are shown along with the new routes when this is the case.

The route data were also used to define the stops. The following types of stops along the route were considered:

- Safety check
- Break
- Refueling
- Border inspection

The safety check and break stops were defined in accordance with the following federal regulations:

a. 49CFR 395(g)(B) requires a 30-minute break after 8 hours of driving

b. 49CFR 392.9(b)(2) requires a safety load and securement check within the first 50 miles

> *(2) Inspect the cargo and the devices used to secure the cargo within the first 50 miles after beginning a trip and cause any adjustments to be made to the cargo or load securement devices as necessary, including adding more securement devices, to ensure that cargo cannot shift on or within, or fall from the commercial motor vehicle; and*

c. 49CFR 392.9(b)(3)(ii)(iii) requires a safety load and securement check after 3 hours or 150 miles

> *(3) Reexamine the commercial motor vehicle's cargo and its load securement devices during the course of transportation and make any necessary adjustment to the cargo or load securement devices, including adding more securement devices, to ensure that cargo cannot shift on or within, or fall from, the commercial motor vehicle. Reexamination and any necessary adjustments must be made whenever—*
>
> *(i) The driver makes a change of his/her duty status; or*
>
> *(ii) The commercial motor vehicle has been driven for 3 hours; or*
>
> *(iii) The commercial motor vehicle has been driven for 150 miles, whichever occurs first.*

Note that the safety check and break stops were not considered in the 2008 TA.

The refueling stops were specified every 845 km (525 mi), the same as in the 2008 TA.

At the present time inspections are required in Colorado (Fort Collins). Per Attachment A of WIPP Nuclear Waste Partnership, 2020, the average time spent at the Wyoming/Colorado border is 5 hours. Inspections are also performed when the WIPP trucks enter New Mexico. No other state border inspections are required. The inspection stops were defined based on this information.

In the 2008 TA the inspection stops were specified in each state crossed by the transportation route.

The route data in the following sections are reported in English units because they were taken directly from the WebTragis output.

3.1.1 Hanford to WIPP Route

The transportation route from Hanford to the WIPP facility is shown in Figure 3-1. The route is the same as in the 2008 TA. The route data from WebTragis is summarized in Table 3-2.

The following stops were defined along the route:

- 12 safety checks
- 3 breaks
- 2 inspection stops

- 4 refueling stops

Table 3-2. Hanford to WIPP Route Data from WebTragis.

State	Rural		Suburban		Urban	
	Population Density (persons/mi^2)	Distance (mi)	Population Density (persons/mi^2)	Distance (mi)	Population Density (persons/mi^2)	Distance (mi)
WA	17.3	29.52	1,631.9	12.99	3,356.3	0.06
OR	37.2	193.34	946	15.2	3,446.4	0.13
ID	35.5	227.01	851.2	46.93	4,370.7	1.45
UT	37.9	116.34	912.3	32.61	3,401.6	0.15
WY	24.5	342.79	651.5	23.86	3,327.3	0.01
CO	45.4	188.31	1,505.3	78.97	5,128.9	31.21
NM	23	448.56	489.9	24.98	0	0

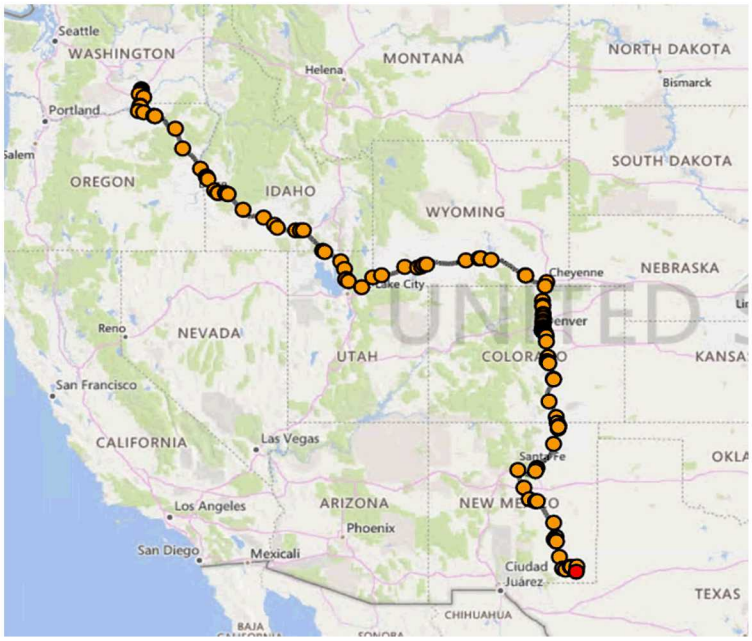

Figure 3-1. Transportation Route from Hanford to the WIPP Facility.

3.1.2 INL to WIPP Route

The transportation route from INL to the WIPP facility is shown in Figure 3-2. The route is the same as in the 2008 TA. The route data from WebTragis are summarized in Table 3-3.

The following stops were defined along the route:

- 9 safety checks
- 2 breaks

- 2 inspection stops
- 2 refueling stops

Table 3-3. INL to WIPP Route Data from WebTragis.

State	Rural		Suburban		Urban	
	Population Density (persons/mi^2)	Distance (mi)	Population Density (persons/mi^2)	Distance (mi)	Population Density (persons/mi^2)	Distance (mi)
ID	29.9	110.16	738.7	19.11	3,947.7	0.7
UT	45.2	95.05	905	33.27	3,401.6	0.15
WY	24.5	342.79	651.5	23.86	3,327.3	0.01
CO	45.4	188.31	1,505.3	78.97	5,128.9	31.21
NM	23	448.56	489.9	24.98	0	0

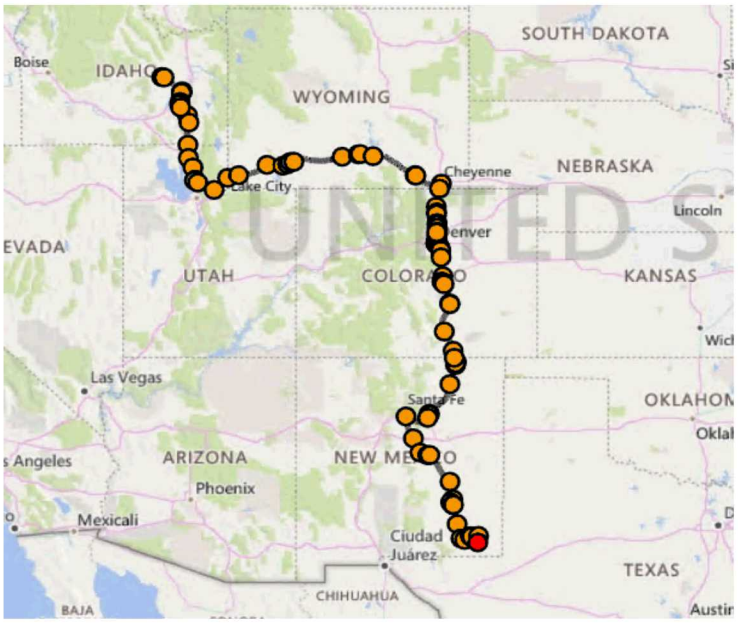

Figure 3-2. Transportation Route from INL to the WIPP facility.

3.1.3 LANL to WIPP Route

The transportation route from LANL to the WIPP facility is shown in Figure 3-3. The route is the same as in the 2008 TA. The route data from WebTragis are summarized in Table 3-4. Three safety check stops were defined along the route. There are no breaks, inspections, or refueling stops because the route is short.

Table 3-4. LANL to WIPP Route Data from WebTragis.

State	Rural		Suburban		Urban	
	Population Density (persons/mi^2)	Distance (mi)	Population Density (persons/mi^2)	Distance (mi)	Population Density (persons/mi^2)	Distance (mi)
NM	37.6	326.3	568.4	38.18	0	0

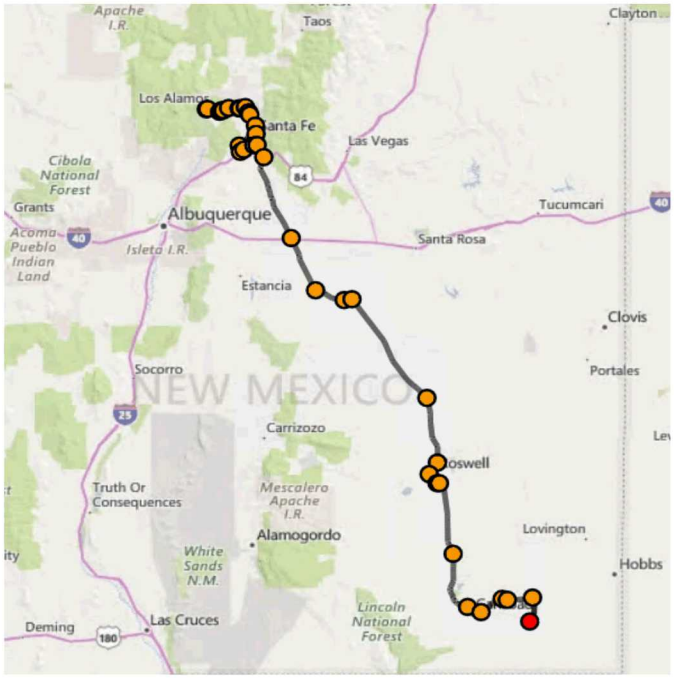

Figure 3-3. Transportation Route from LANL to the WIPP facility.

3.1.4 ORNL to WIPP Route

The transportation route from ORNL to the WIPP facility is shown in Figure 3-4. The route is different from the 2008 TA on the segment from ORNL to Dallas and through West Texas and New Mexico as shown in this figure. The route data from WebTragis are summarized in Table 3-5.

The following stops were defined along the route:

- 10 safety checks
- 3 breaks
- 1 inspection stop
- 2 refueling stops

Table 3-5. ORNL to WIPP Route Data from WebTragis.

State	Rural		Suburban		Urban	
	Population Density (persons/mi^2)	Distance (mi)	Population Density (persons/mi^2)	Distance (mi)	Population Density (persons/mi^2)	Distance (mi)
TN	45.1	63.76	1,018.4	46.1	3,501.7	1.8
GA	62.8	16.64	566.2	6	0	0
AL	52.6	176.06	713.3	65.34	3802	1.78
MS	43.3	105.44	804	48.34	3,671.4	1.08
LA	37.5	128.13	534.7	63.5	3,833.2	1
TX	38.6	487.17	777	1,51.21	4,088.6	10.06
NM	9.1	69.01	1,150.1	5.84	3,580.9	0.34

Figure 3-4. Transportation Route from ORNL to the WIPP facility.

3.1.5 SRS to WIPP Route

The transportation route from SRS to the WIPP facility is shown in Figure 3-5. The route is different from the 2008 TA on the very last segment as shown in this figure. The route data from WebTragis are summarized in Table 3-6.

The following stops were defined along the route:

- 10 safety checks
- 3 breaks
- 1 inspection stop
- 2 refueling stops

Table 3-6. SRS to WIPP Route Data from WebTragis.

State	Rural		Suburban		Urban	
	Population Density (persons/mi^2)	Distance (mi)	Population Density (persons/mi^2)	Distance (mi)	Population Density (persons/mi^2)	Distance (mi)
SC	25.5	18.1	402.9	6.19	0	0
GA	52.1	115.43	1,284.9	103.8	3,543.4	4.12
AL	47.1	141.54	784.2	69.93	3,802	1.78
MS	43.3	105.44	804	48.34	3,671.4	1.08
LA	37.5	128.13	534.7	63.5	3,833.2	1
TX	38.6	487.17	777	151.21	4,088.6	10.06
NM	9.1	69.01	1150.1	5.84	3,580.9	0.34

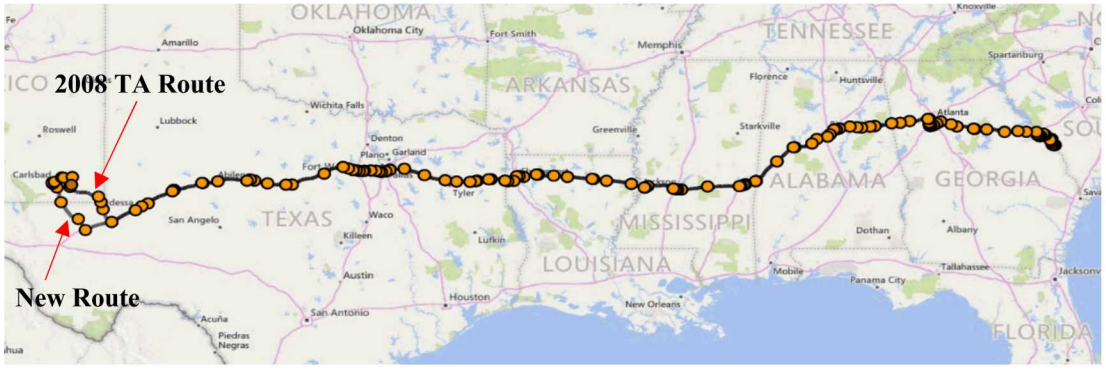

Figure 3-5. Transportation Route from SRS to the WIPP facility.

3.1.6 ANL to WIPP Route

The transportation route from ANL to the WIPP facility is shown in Figure 3-6. The route is completely different from the 2008 TA route as shown in this figure. The route data from WebTragis are summarized in Table 3-7.

The following stops were defined along the route:

- 12 safety checks
- 3 breaks
- 2 inspection stops
- 3 refueling stops

Table 3-7. ANL to WIPP Route Data from WebTragis.

State	Rural		Suburban		Urban	
	Population Density (persons/mi^2)	Distance (mi)	Population Density (persons/mi^2)	Distance (mi)	Population Density (persons/mi^2)	Distance (mi)
IL	44.4	102.8	844.2	47.15	3,364.2	0.3
IA	52.5	231.7	544.4	74.87	3,702.9	1.14
NE	18.7	421.97	804.5	31.29	3,687.3	3.99
WY	12	44.55	715.4	6.76	3,889.2	0.53
CO	45.4	188.31	1,505.3	78.97	5,128.9	31.21
NM	23	448.56	489.9	24.98	0	0

Figure 3-6. Transportation Route from ANL to the WIPP facility.

3.1.7 Bettis to WIPP Route

The transportation route from Bettis to the WIPP facility is shown in Figure 3-7. The route is different from the 2008 TA on the segment from Bettis to Dallas as shown in this figure. The route data from WebTragis are summarized in Table 3-8.

The following stops were defined along the route:

- 14 safety checks
- 4 breaks
- 1 inspection stop
- 4 refueling stops

Table 3-8. Bettis to WIPP Route Data from WebTragis.

State	Rural		Suburban		Urban	
	Population Density (persons/mi^2)	Distance (mi)	Population Density (persons/mi^2)	Distance (mi)	Population Density (persons/mi^2)	Distance (mi)
PA	54.6	46.48	766.9	30.8	0	0
WV	95.8	27.14	639.7	42.1	3,359.5	0.05
MD	53.6	79.88	822.1	27.29	4,716.1	1.22
VA	73.1	179.6	663.4	140.42	4774	3.8
TN	66.8	133.14	998.1	87.15	3,815.9	8.51
GA	62.8	16.64	566.2	6	0	0
AL	52.6	176.06	713.3	65.34	3,802	1.78
MS	43.3	105.44	804	48.34	3,671.4	1.08
LA	37.5	128.13	534.7	63.5	3,833.2	1
TX	38.6	487.17	777	151.21	4,088.6	10.06
NM	9.1	69.01	1,150.1	5.84	3,580.9	0.34

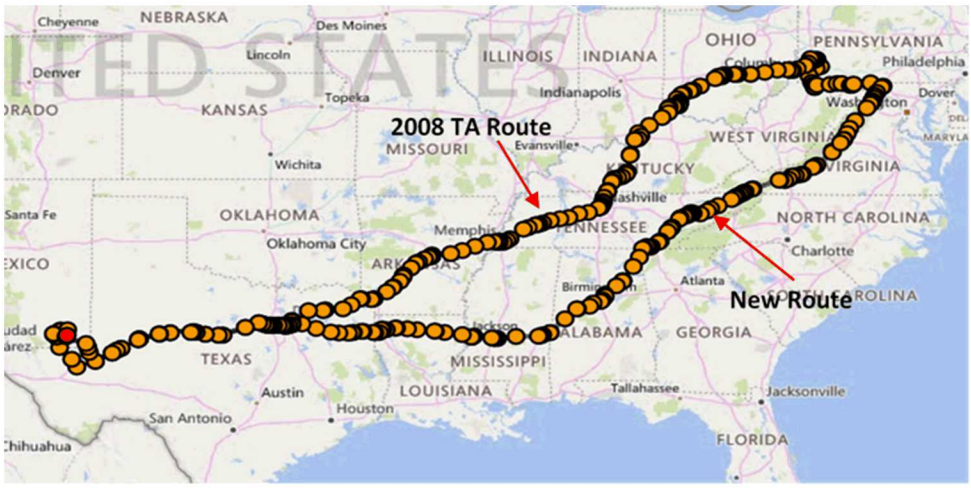

Figure 3-7. Transportation Route from Bettis to the WIPP facility.

3.1.8 SNL to WIPP Route

The transportation route from SNL to the WIPP facility is shown in Figure 3-8. The route is the same as in the 2008 TA. The route data from WebTragis are summarized in Table 3-9. Two safety check stops were defined along the route. There are no breaks, inspections, or refueling stops because the route is short and within NM.

Table 3-9. SNL to WIPP Route Data from WebTragis.

State	Rural		Suburban		Urban	
	Population Density (persons/mi^2)	Distance (mi)	Population Density (persons/mi^2)	Distance (mi)	Population Density (persons/mi^2)	Distance (mi)
NM	21	284.67	639	31.03	4,372.3	2.91

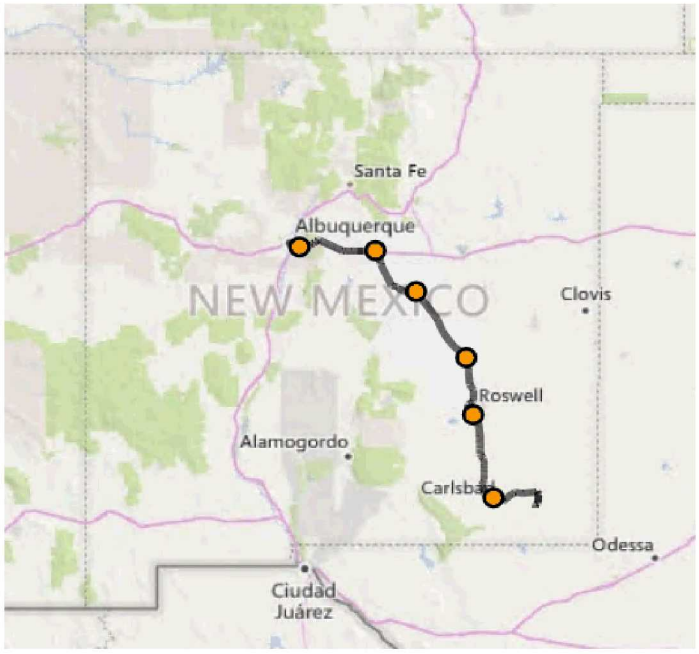

Figure 3-8. Transportation Route from SNL to the WIPP facility.

3.1.9 Knolls to WIPP Route

The transportation route from Knolls to the WIPP facility is shown in Figure 3-9. The route is different from the 2008 TA in the middle part as shown in this figure. The route data from WebTragis are summarized in Table 3-10.

The following stops were defined along the route:

- 15 safety checks
- 5 breaks
- 1 inspection stop
- 4 refueling stops

Table 3-10. Knolls to WIPP Route Data from WebTragis.

State	Rural		Suburban		Urban	
	Population Density (persons/mi^2)	Distance (mi)	Population Density (persons/mi^2)	Distance (mi)	Population Density (persons/mi^2)	Distance (mi)
NY	55.8	86.88	1,241.7	53.39	4,023.7	3.37
PA	63.2	125.07	853.8	105.95	3,622.4	0.79
WV	97.2	3.68	693.8	22.27	3,359.5	0.05
MD	105.9	0.23	1,327.3	11.71	0	0
VA	73.1	179.6	663.4	140.42	4,774	3.8
TN	66.8	133.14	998.1	87.15	3,815.9	8.51
GA	62.8	16.64	566.2	6	0	0
AL	52.6	176.06	713.3	65.34	3,802	1.78
MS	43.3	105.44	804	48.34	3,671.4	1.08
LA	37.5	128.13	534.7	63.5	3,833.2	1
TX	38.6	487.17	777	151.21	4,088.6	10.06
NM	9.1	69.01	1,150.1	5.84	3,580.9	0.34

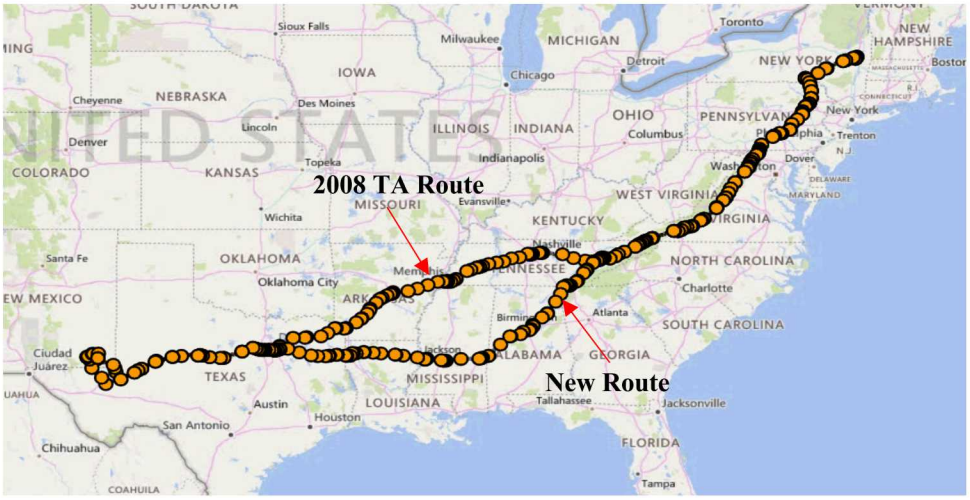

Figure 3-9. Transportation Route from Knolls to the WIPP facility.

3.1.10 LLNL to INL Route

The transportation route from LLNL to INL is shown in Figure 3-10. In the 2008 TA the route from LLNL was different because it was directly to the WIPP facility. The route data from WebTragis are summarized in Table 3-11.

The following stops were defined along the route:

- 6 safety checks
- 2 breaks
- 1 refueling stops

Note that there are no inspections on this route.

Table 3-11. LLNL to INL Route Data from WebTragis.

State	Rural		Suburban		Urban	
	Population Density (persons/mi^2)	Distance (mi)	Population Density (persons/mi^2)	Distance (mi)	Population Density (persons/mi^2)	Distance (mi)
CA	45.6	106.4	1,596.7	64.56	4,836.2	33.72
ID	29.9	110.16	738.7	19.11	3,947.7	0.7
NV	24	366.85	738.6	34.67	5,982.7	8.07
UT	29.9	153.76	1,350.9	44.78	4,262.9	11.94

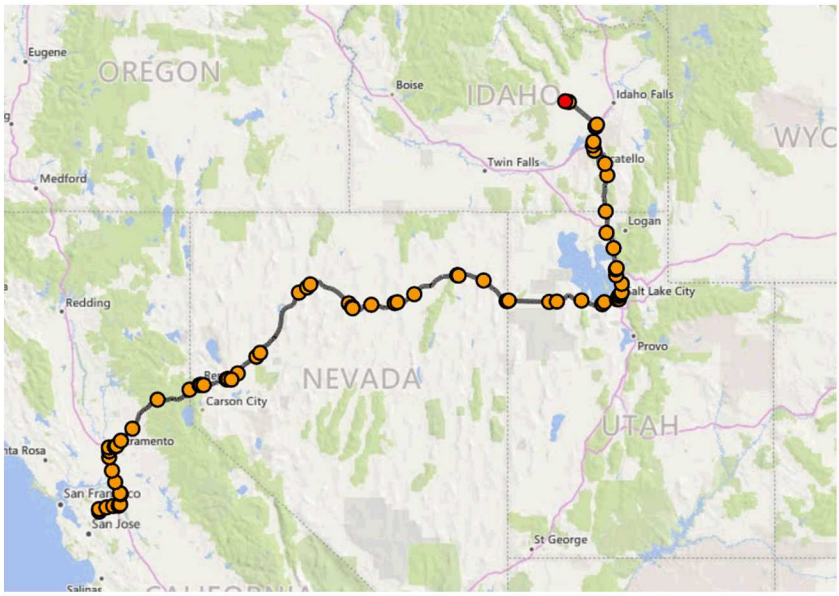

Figure 3-10. Transportation Route from LLNL to INL.

3.1.11 NRD, LLC, NY to INL Route

The transportation route from NRD, LLC, NY to INL is shown in Figure 3-11. This route was not considered in the 2008 TA. The route data from WebTragis are summarized in Table 3-12.

The following stops were defined along the route:

- 16 safety checks
- 5 breaks
- 4 refueling stops

Note that there are no inspections on this route.

Table 3-12. NRD, LLC, NY to INL Route Data from WebTragis.

.State	Rural		Suburban		Urban	
	Population Density (persons/mi^2)	Distance (mi)	Population Density (persons/mi^2)	Distance (mi)	Population Density (persons/mi^2)	Distance (mi)
IA	52.5	231.7	544.4	74.87	3,702.9	1.14
ID	29.9	110.16	738.7	19.11	3,947.7	0.7
IL	49.8	158.65	679.8	58.36	3,961	0.87
IN	45.8	109.42	1,201.8	44.39	4,186.6	13.34
NE	18.7	421.97	804.5	31.29	3,687.3	3.99
NY	43.2	66.53	790.7	16.61	3,868.5	1.51
OH	51.6	126.15	847.2	98.87	3,753.4	5.75
PA	69.8	133.27	813.6	92.92	4,265.2	2.07
UT	45.2	95.05	905	33.27	3,401.6	0.15
WV	73.1	5.37	1,557.2	7.82	0	0
WY	24.6	369.84	735.1	30.44	3,608.2	0.54

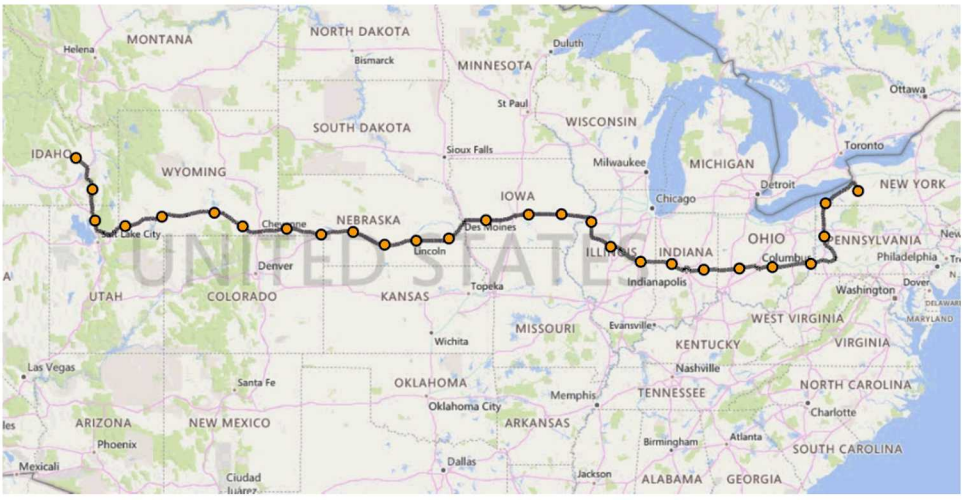

Figure 3-11. Transportation Route from NRD, LLC, NY to INL.

3.1.12 NNSS to INL Route

The transportation route from NNSS to INL is shown in Figure 3-12. In the 2008 TA the route from NNSS was different because it was directly to the WIPP facility. The route data from WebTragis are summarized in Table 3-13.

The following stops were defined along the route:

- 5 safety checks
- 1 break
- 1 refueling stop

Note that there are no inspections on this route.

Table 3-13. NNSS to INL Route Data from WebTragis.

State	Rural		Suburban		Urban	
	Population Density (persons/mi^2)	Distance (mi)	Population Density (persons/mi^2)	Distance (mi)	Population Density (persons/mi^2)	Distance (mi)
ID	29.9	110.16	738.7	19.11	3,947.7	0.7
NV	8.1	415.05	599.7	12.12	0	0
UT	29.9	153.76	1,350.9	44.78	4,262.9	11.94

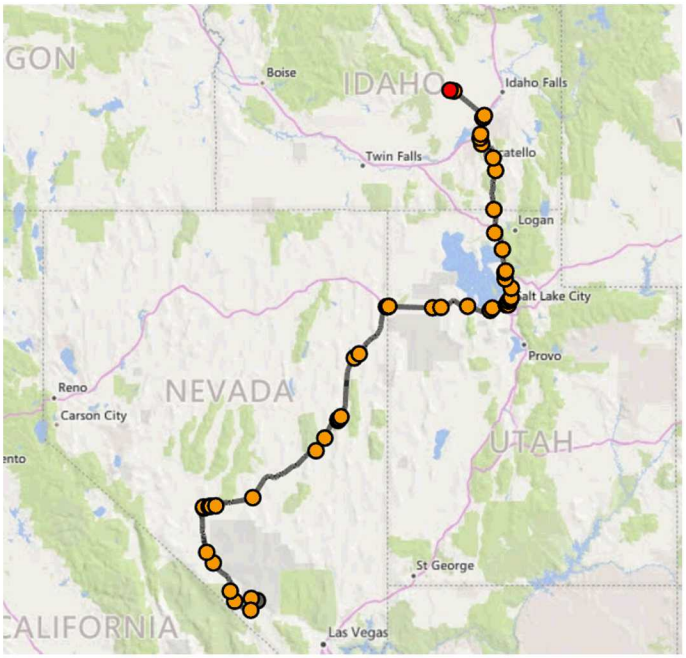

Figure 3-12. Transportation Route from NNSS to INL.

3.1.13 Route Data Summary

Figure 3-13 shows all the transportation routes considered in this TA. The routes were generated as close to the route description in Attachment B of WIPP Nuclear Waste Partnership, 2020 as was possible in WebTragis. The average difference in the total route distance is 1.8 percent (Table 3-14). On average, 79.1 percent of the route was rural, 19.2percent was suburban, and 1.7 percent was urban (Table 3-14). Figure 3-14 shows the route specific distribution of rural, suburban, and urban segments. On average, 91.6 percent of the route was on interstate highways, 0.9 percent was on state highways, and 7.5 percent was on local highways (Table 3-14). Figure 3-15 shows the route specific distribution of interstate, state, and local highways. The calculated average speed was 59.1-mph. Figures 3-16 shows the route specific distribution of the average speed. This provides justification for using non-rush hour speed of 55-mph in calculating radiological impacts from the incident-free transportation. Note that assuming slightly lower speed results in calculating higher doses.

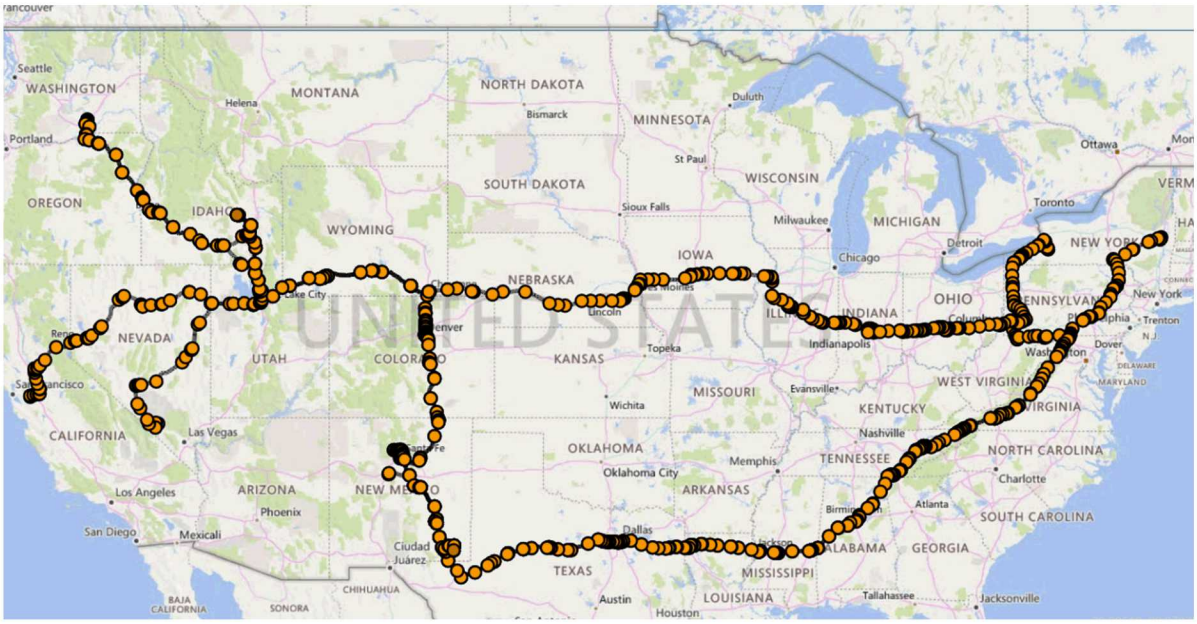

Figure 3-13. Transportation Routes Considered in This TA.

Table 3-14. Route Data Summary.

Route	Total Distance (mi)	Percent Difference (%)	Rural % Total)	Sub-Urban (% Total)	Urban (% Total)	Federal Highway (% Total)	State Highway (% Total)	Local Highway (% Total)	Average Speed (mph)
ANL	1,739	0.58	82.68	15.18	2.14	98.68	0.48	0.83	61.20
Bettis	2,145	2.12	67.55	31.15	1.30	98.56	0.78	0.66	61.13
Hanford	1,814	3.71	85.20	12.98	1.82	98.37	0.24	1.38	61.06
INL	1,397	0.30	84.81	12.90	2.30	98.49	0.00	1.51	61.32
Knolls	2,303	3.50	65.61	33.05	1.34	99.27	0.08	0.65	61.52
LANL	364	2.67	89.52	10.48	0.00	85.33	7.34	7.33	53.21
ORNL	1,449	0.60	72.22	26.67	1.11	98.26	0.34	1.40	59.94
SNL	319	0.43	89.35	9.74	0.91	92.27	0.00	7.73	55.09
SRS	1,532	1.54	69.50	29.30	1.20	97.49	1.25	1.03	60.08
LLNL	955	3.17	77.21	17.09	5.70	95.78	0.00	4.22	59.67
NNSS	768	1.96	88.45	9.90	1.65	39.55	0.00	60.45	53.49
NRD, LLC	2,366	1.08	77.26	21.47	1.27	97.34	0.22	2.44	61.43
Mean		**1.81**	**79.11**	**19.16**	**1.73**	**91.62**	**0.90**	**7.47**	**59.09**

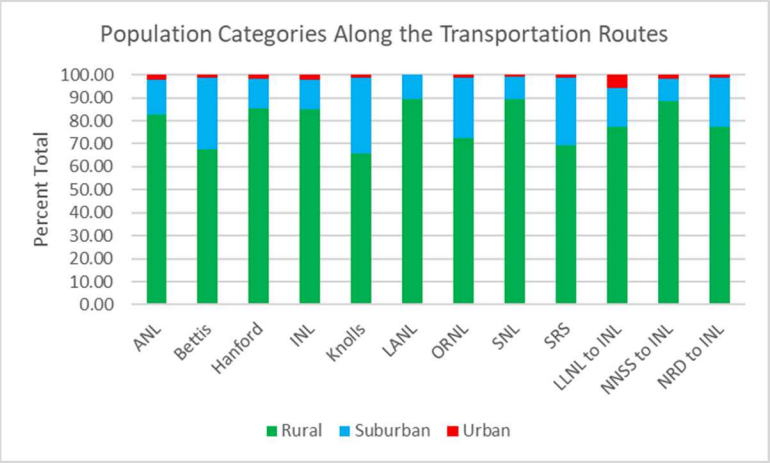

Figure 3-14. Percent Rural, Suburban, and Urban Links along the Transportation Routes.

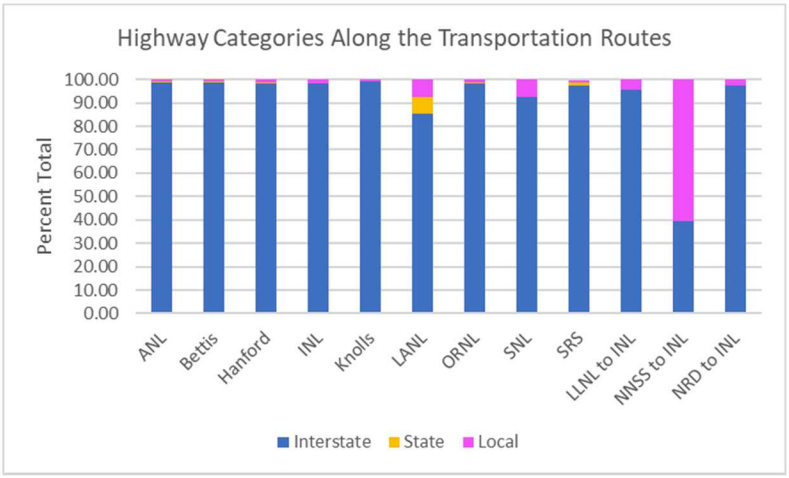

Figure 3-15. Percent Interstate, State, and Local Highways along the Transportation Routes.

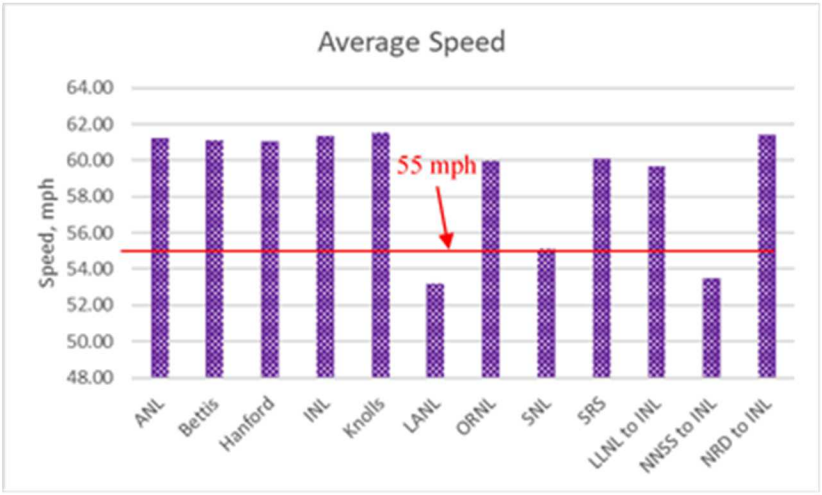

Figure 3-16. Average Speed along the Transportation Routes.

3.2 Population Increase Data

The population data obtained from WebTragis for each route and summarized in Table 3-2 – Table 3-13 are from 2010 Census data. These data needed to be adjusted to reflect the population change since 2010. In the 2008 TA, the 2000 census data were updated using the 2008 percent increase in population for each of the 50 states of the United States (U.S.). These data were used to calculate the population multipliers for states along the WIPP routes. The state-specific multiplier was applied to rural and suburban routes through the state, and the multiplier for the largest metropolitan area in that state was applied to the urban routes. This TA uses a similar approach (state-specific multipliers) to update the 2010 census data. In addition, change in population multipliers were developed for 2030 and 2040 to be considered in the sensitivity analysis. The projection beyond 20 years in the future are considered to be not defensible.

The data on the percent change in population from 2010 to 2018 (the most recent data available) are available from the Bureau of Census website:
https://www2.census.gov/programs-surveys/popest/tables/2010-2018/national/totals/.

The data used in this analysis are from:

- Table 1, Annual Estimates of the Resident Population for the United States, Regions, States, and Puerto Rico, April 1, 2010 to July 1, 2018 (NST-EST2018-01), U.S. Census Bureau, Population Division (Release Date: December 2018).
- Table 2, Cumulative Estimates of Resident Population Change for the United States, Regions, States, and Puerto Rico and Region and State Rankings, April 1, 2010 to July 1, 2018 (NST-EST2018-02), U.S. Census Bureau, Population Division (Release Date: December 2018)

The 1999 population data are from the Bureau of Census website:
https://www2.census.gov/programs-surveys/popest/tables/1990-2000/state/totals/st-99-01.txt. The 1999 and 2010-2018 data are used in generating the future projections.

Figure 3-17 shows percent population change from 2010 to 2018 for the states crossed by the WIPP transportation routes. During this period, the population decreased in Illinois and West Virginia. The states with the fastest growing population (percent increase 10 percent or greater) are: Utah, Texas, Colorado, Nevada, Washington, and Idaho.

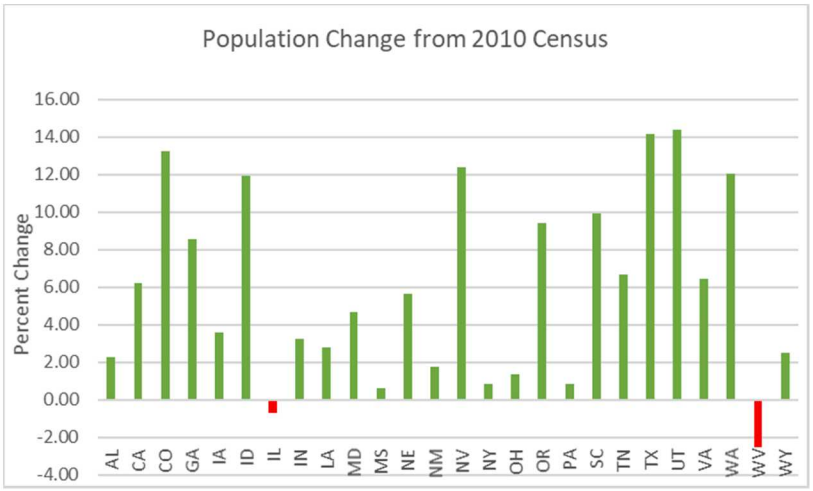

Figure 3-17. Percent Population Change from 2010 to 2018.

Figure 3-18 shows the population in the six fastest growing states using 1999 Bureau of Census data and 2010-2018 data from the Bureau of Census Table 1. In all six states, the growth follows a linear trend. It was assumed that the linear trend can be used to project the population changes into 2030 and 2040.

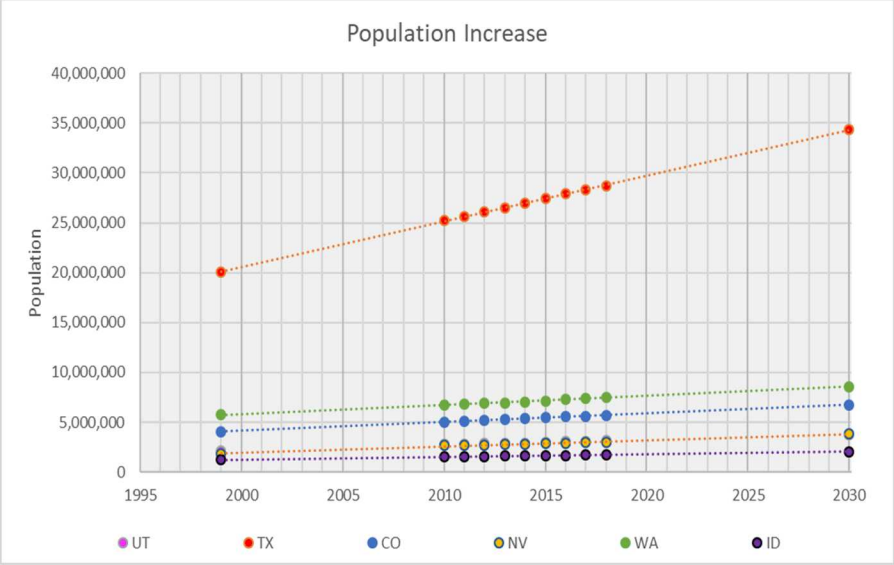

Figure 3-18. Projection of the Population Increase in the Fastest Growing States.

Table 3-15 summarizes the percent population change by state from 2010 census to 2018 using the data from Table 2 from the U.S. Census Bureau and the projection of these changes to 2030 and 2040.

Table 3-15. Percent Population Change by State from 2010 Census.

State	Actual	Projected	
	2018	2030	2040
Alabama	2.25	10.03	15.68
California	6.2	17.97	27.19
Colorado	13.25	33.57	50.64
Georgia	8.57	27.16	41.78
Iowa	3.59	9.71	14.68
Idaho	11.90	30.45	46.59
Illinois	-0.71	4.08	6.71
Indiana	3.20	10.99	16.97
Louisiana	2.79	7.78	11.48
Maryland	4.66	15.37	23.43
Mississippi	0.62	6.56	10.44
Nebraska	5.64	14.81	22.39
New Mexico	1.76	15.13	24.10
Nevada	12.40	41.83	65.02
New York	0.85	6.95	10.81
Ohio	1.30	3.59	5.51
Oregon	9.39	22.90	34.67
Pennsylvania	0.82	5.68	9.00
South Carolina	9.92	25.88	39.31
Tennessee	6.68	19.73	30.20
Texas	14.14	35.94	54.09
Utah	14.37	36.96	56.14
Virginia	6.46	20.52	31.34
Washington	12.06	27.13	40.76
West Virginia	-2.55	-0.62	-0.45
Wyoming	2.48	17.52	27.18

3.3 Traffic Count Data

The traffic count data (average number of vehicles per hour in all lanes) is an input parameter for calculating the radiological impacts to the people sharing the road with the truck carrying the TRU waste package (Eq. 2-2). The average traffic count varies from state to state and it also depends on the segment type – rural, suburban, or urban. Note that the collective external dose the people sharing the road receive is proportional to the traffic count data. Because the traffic count data could have changed from 2008, new data were collected.

It should be noted that the traffic count data are not readily available and cannot be found in a single source. The state specific traffic count was calculated from the Annual Average Daily Traffic (AADT) metric. The AADT metric indicates a measure of the total traffic volume on a given road or highway over the period of a year divided by 365. Its accuracy is relied on by Federal, State and Metropolitan planning organizations, as well as by cities and local agencies. Annual Average Daily Traffic information is collected in several

different ways. There are many permanent traffic count stations that collect data over the entire year, producing a highly accurate AADT. On roads that are not feasible for maintaining a permanent traffic count station the use of temporary counters is employed. A temporary counter may be active for between a few hours to a week, after which hourly traffic volume is extrapolated to form an estimate of the roads AADT. Some areas will perform traffic counts on a yearly basis, while others perform counts every other year, every third year, or every sixth year. Reports from the Federal Highway Administration conclude that the bias error in AADT calculation and extrapolation is "consistent and small", with high accuracy in AADT measurement.

The collected data are from a variety of sources. State-specific data were primarily obtained from state department of transportation sites. These sources are summarized in Table 3-16. For states that did not offer this data, data were obtained from an Environmental Systems Research Institute dataset of traffic counts in the US:
https://www.arcgis.com/home/item.html?id=70507a8779a2470b89c6a8c90394d68e

Figure 3-19 shows the averaged value of AADT values per state with data labels indicating the year of collection. For states with very little available data, year of collection was confined to years after 2008.

Table 3-16. State-Supplied AADT Data Sources.

State	Data Source
Alabama	https://aldotgis.dot.state.al.us/atd/default.aspx#
California	https://dot.ca.gov/programs/traffic-operations/census
Colorado	https://data.colorado.gov/Transportation/Road-Traffic-Counts-in-Colorado-2017/uzf4-3qtt
Georgia	https://gdottrafficdata.drakewell.com/publicmultinodemap.asp
Idaho	https://iplan.maps.arcgis.com/apps/webappviewer/index.html?id=e8b58a3466e74f249cca6aad30e83ba2
Illinois	http://www.idot.illinois.gov/Assets/uploads/files/Transportation-System/Reports/OP&P/Travel-Stats/2018_ITS.pdf
Indiana	https://www.in.gov/indot/2469.htm
Maryland	https://data.imap.maryland.gov/datasets/maryland-annual-average-daily-traffic-annual-average-daily-traffic-sha-statewide-aadt-lines/data
Nebraska	https://gis.ne.gov/portal/apps/webappviewer/index.html?id=bb00781d6653474d945d51f49e1e7c34
Nevada	https://www.nevadadot.com/doing-business/about-ndot/ndot-divisions/planning/traffic-information/-folder-401
New York	https://www.dot.ny.gov/divisions/engineering/technical-services/highway-data-services/hdsb
South Carolina	https://www.scdot.org/travel/travel-trafficdata.aspx
Tennessee	https://www.arcgis.com/apps/webappviewer/index.html?id=075987cdae37474b88fa400d65681354
Texas	http://txdot.maps.arcgis.com/apps/webappviewer/index.html?id=75e148d784554d99bea6e8602986bfd2
Utah	https://www.udot.utah.gov/main/f?p=100:pg:0::::V,T:,529
Virginia	https://www.virginiadot.org/info/2018_traffic_data.asp
Washington	https://www.wsdot.wa.gov/mapsdata/tools/trafficplanningtrends.htm
West Virginia	http://data-wvdot.opendata.arcgis.com/datasets/aadt-traffic-count-2017/data?orderBy=LRS_Measu&orderByAsc=false

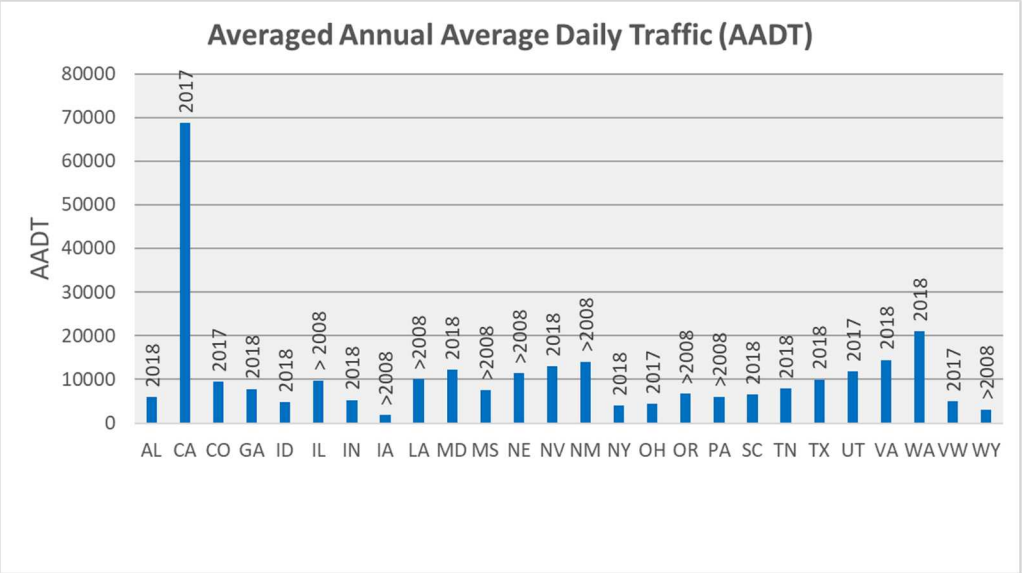

Figure 3-19. Annual Average Daily Traffic (AADT) by State.

The following method was used to convert the AADT data into the traffic count measured in vehicles per hour. The AADT for each state was expressed as a percent of the national average AADT. The state specific traffic count in vehicles per hour was calculated as the state specific AADT times the national average of vehicle per hour (3,020 vehicles/hr). The national average vehicles per hour is from the 2008 TA. The national average AADT did not significantly change from 2008. It was 8,967 in 2008 and 9,070 in 2018 (https://livingatlas.arcgis.com/en/browse/#d=2&q=%222019%20USA%20Traffic%20Counts%22). Table 3-17 summarizes the traffic count data.

Table 3-17. Traffic Count by State

State	Vehicles/hr	State	Vehicles/hr
AL	1,962	NM	4,692
CA	22,901	NY	1,326
CO	3,162	OH	1,455
GA	2,598	OR	2,239
IA	610	PA	2,016
ID	1,575	SC	2,156
IL	3,234	TN	2,613
IN	1,744	TX	3,302
LA	3,330	UT	3,944
MD	4,048	VA	4,818
MS	2,541	WA	6,998
NE	3,797	WV	1,671
NV	4,320	WY	1,030

In the 2008 TA rural, suburban, and urban vehicles per hour values were defined for each state. The source of these values is unclear. These data were used to calculate the state specific average number of vehicles/hr. Figure 3-20 shows the ratio of the latest traffic count values (Table 3-20) and the values from the 2008 TA.

The values that are higher than in the 2008 TA are shown in red, those that are smaller are shown in blue, and similar values are shown in green.

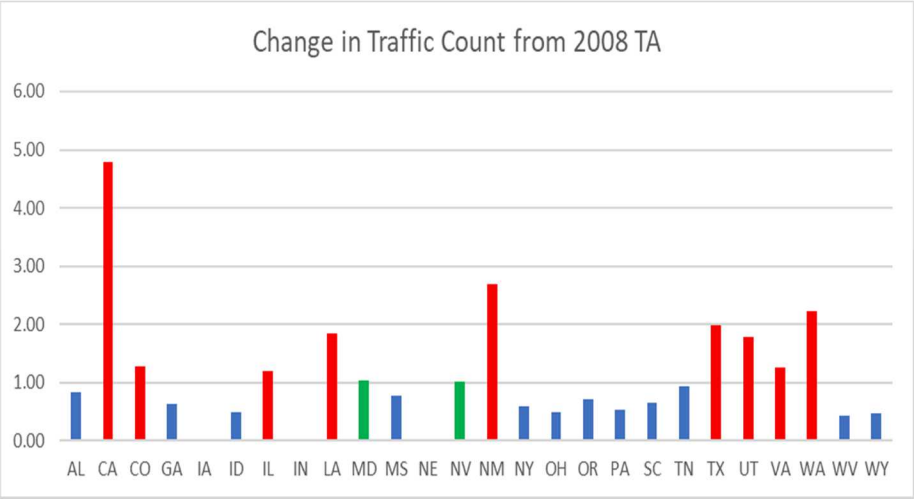

Figure 3-20. The Ratio of the Latest Traffic Count and the 2008 TA Values.

In general, the change in traffic count is loosely correlated with the changes in the population as indicated in Figure 3-21.

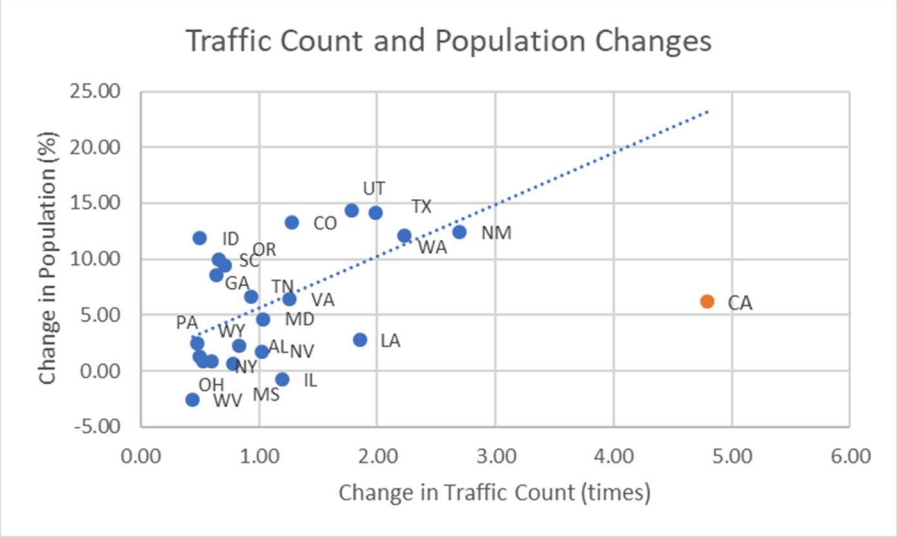

Figure 3-21. Traffic Count and Population Changes from 2008 by State.

The traffic count values shown in Table 3-20 are the average for the state. To obtain the state specific rural, suburban, and urban traffic count, the state average values are multiplied by the following coefficients: 0.44 (rural), 0.9 (suburban), and 1.67 (urban). These coefficients represent percent of the average calculated from the 2008 data.

3.4 Accident Data

Accident data (accidents per vehicle-km) is an input parameter for calculating the radiological impacts from the transportation accidents (Eq. 2-14 and 2-15) and for calculating non radiological impacts (Eq. 2-16). The injuries and fatalities rates (injuries/vehicle-km and fatalities/vehicle-km) are input for calculating non radiological impacts (Eq. 2-17 and 2-18).

The accident data from 2018 were gathered from the Federal Motor Carrier Safety Administration's (FMCSA) A&I online crash statistics database (https://ai.fmcsa.dot.gov/CrashStatistics/Default.aspx). Note that the units are the number of accidents, injuries, or fatalities per year. To access the data directly one must navigate from the homepage to the crash query tool, in which the summary report tool can be used. The summary report tool allows for filtering crash data by carrier domicile (USA, Mexico, or Canada), vehicle type (larger trucks and buses, large trucks, buses), time period (options offered on a yearly basis from 2015 onward), and data source (Motor Carrier Management Information System (MCMIS) , Fatality Analysis Reporting System (FARS)). For the purposes of this report, the year selected was 2018, data source was MCMIS, carrier domicile was USA, and vehicle type was large trucks. MCMIS was chosen over FARS as it is comprehensive for motor vehicle accidents, whereas FARS only handles crash data related to fatalities.

In order to obtain the accident, injuries, and fatalities rates per vehicle-km, the vehicle miles traveled (VMT) data are needed. The VMT data were gathered from the Federal Highway Administration's annual Highway Statistics report (https://www.fhwa.dot.gov/policyinformation/statistics/2018/). The state-by-state annual vehicle miles traveled for combination trucks was calculated using table VM-2 and table VM-4 of the report.

Table VM-2 contains state annual VMT by road type (or functional system as it is referred to in the table) for all vehicles. Table VM-4 contains percentages of total state vehicle miles traveled per road type by different vehicle classifications (for example the table gives the percentage of Alabama's total interstate VMT that was traveled by combination trucks).

Table VM-2 provides total state VMT in two categories: rural and urban roadways. Within each of those two categories there are 7 sub-categories: interstate, other freeways and expressways, other principal arterial, minor arterial, major collector, minor collector, and local.

Table VM-4 provides state roadway vehicle mile percentages in three categories: interstate system, other arterials, and other. Within each of those categories are six sub-categories: motorcycles, passenger cars, light trucks, buses, single unit trucks, and combination trucks.

To fit the style in which percentages are presented in table VM-4, the table VM-2 data were combined into the same three categories as shown in Table 3.18.

Table 3-18. Category Considered in Calculating VMT.

Table VM-4 category	Corresponding Table VM-2 categories
Interstate system	Interstate, other freeways and expressways
Other arterials	Other principal arterial, minor arterial
Other	Major collector, minor collector, local

Once the VM-2 data were combined into the VM-4 categories, the VM-2 VMT data were multiplied by the corresponding VM-4 combination truck percentages and divided by 100 to give the combination truck VMT.

The combination truck VMTs for a state were then added together to get the total state combination truck VMT. The state accident injury and fatality counts were then divided by the VMT to give the annual rates.

With the calculated state VMTs and the state injury fatality and accident data, the state injury fatality and accident rates can be calculated. To do so, the injury, fatality, and accident numbers for each respective state were divided by their respective VMT, giving rates in the form of incidents/million miles. The rates were converted then into incidents/km. Table 3-19 summarized the accident for the states crossed by the WIPP transportation routes.

Table 3-19. 2018 Fatality, Injury and Accident Rates for Large Trucks.

State	Fatalities/km	Injuries/km	Accidents/km
AL	1.75E-08	2.72E-07	5.74E-07
CA	6.21E-09	6.21E-08	6.21E-07
CO	2.90E-09	2.23E-08	5.17E-07
GA	1.30E-08	2.31E-07	4.36E-07
IA	2.07E-09	1.12E-08	3.98E-07
ID	1.02E-09	7.07E-09	3.78E-07
IL	1.03E-08	6.00E-08	5.05E-07
IN	6.21E-09	6.21E-08	6.21E-07
LA	1.32E-08	4.02E-07	4.72E-07
MD	6.79E-09	1.53E-07	9.40E-07
MS	2.25E-08	2.15E-07	3.89E-07
NE	1.51E-09	2.33E-08	4.30E-07
NM	1.69E-08	1.84E-07	3.42E-07
NV	6.21E-09	6.21E-08	6.21E-07
NY	1.00E-08	4.00E-07	8.12E-07
OH	6.21E-09	6.21E-08	6.21E-07
OR	1.39E-08	1.37E-07	3.50E-07
PA	1.68E-08	3.86E-07	7.52E-07
SC	2.57E-08	5.63E-07	8.62E-07
TN	3.08E-09	5.23E-08	3.62E-07
TX	1.78E-08	2.54E-07	4.45E-07
UT	3.67E-10	3.97E-09	3.21E-07
VA	1.43E-08	2.52E-07	5.55E-07
WA	1.39E-09	6.65E-09	3.57E-07
WV	2.40E-08	1.93E-07	4.20E-07
WY	1.73E-09	1.90E-08	3.43E-07

A detailed study of accidents, injuries and fatalities was conducted in late 90's and reported in C.L. Saricks and M.M. Tompkins (1999). The data considered in this report are for the 1994-1999 period. This study is still used as a source of accident data. Usually the accident data are multiplied by a coefficient (~1.6) to reflect the increase in the corresponding incidents since 1999.

Table 3-20 and Figure 3-22 compare the ratio of 2018 and 1999 incidents for the states crossed by the WIPP transportation routes. On average, since 1999 the accident rate (accident/vehicle-mi) increased 2.1 times, the injury rate increased 1.26 times, and the fatality rate increased 1.47 times. The higher rate of accidents

is related to higher traffic. The injuries and fatality increase are noticeably smaller which is probably due to the improvements in car safety since 1999. The number of fatalities per accident decreased 1.35 times since 1999 (2018 to 1999 ratio of 0.74).

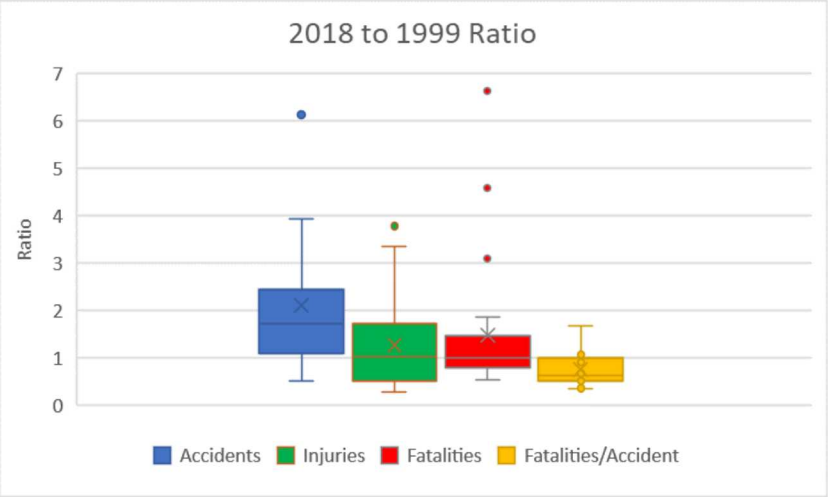

Figure 3-22. Comparison of the 1999 and 2018 Incident Data for the States Crossed by WIPP Routes.

Table 3-20. Comparison of 2018 and 1999 Incident Data for the States Crossed by WIPP Routes.

Statistic	2018 Incidents per vehicle-mi/1999 Incidents per vehicle-mi			
	Accidents	Injuries	Fatalities	Fatalities/Accident
Minimum	0.51	0.28	0.52	0.34
Maximum	6.17	3.77	6.63	1.67
Average	2.10	1.26	1.47	0.74

In the 2008 TA, state specific accident rates were defined. The fatalities per accident was set equal to 3.53×10^{-3}. The same value was used for all the states. The source of the accident rate data is unclear. The 2008 data are compared to 1999 and 2018 data in Figures 3-23 and 3-24.

As evident from these figures, the accident rates used in 2008 TA are noticeably higher than the 1999 and 2018 data and the fatalities per accident are noticeably lower. The input into this analysis is the data in Table 3-19.

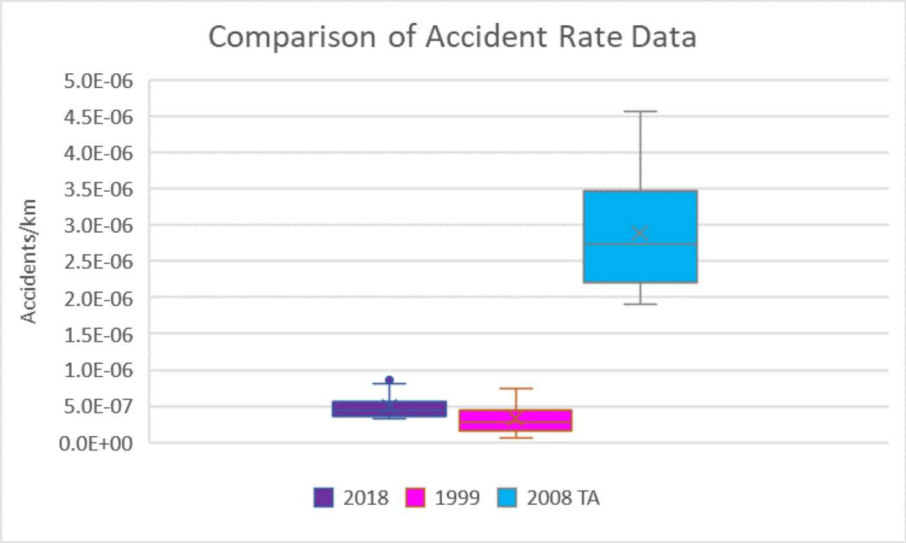

Figure 3-23. Comparison of the Accident Rate Data.

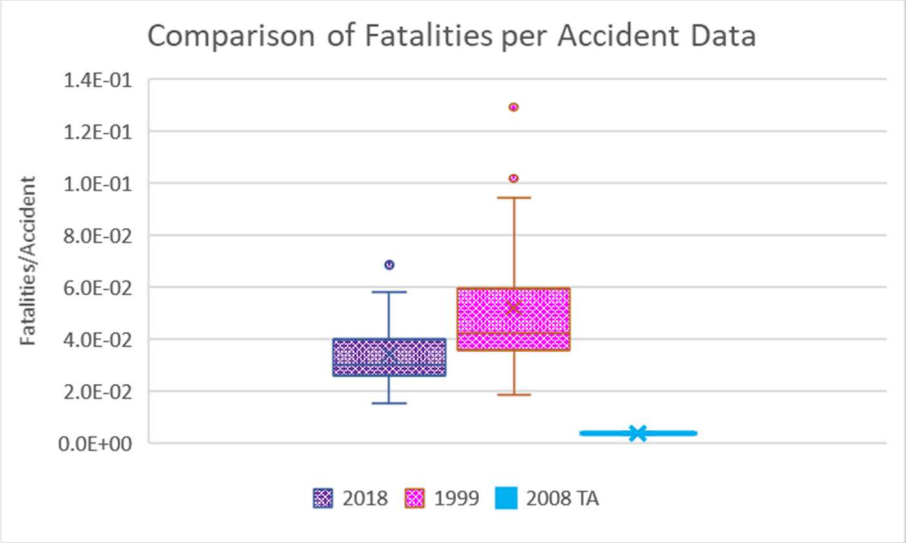

Figure 3-24. Comparison of the Fatalities per Accident Data.

3.5 Shipment Data

The data on the number of shipments and shipment types are needed for each generator site. These data are used in both, radiological and non-radiological impact calculations. The different package types have different transportation indexes (TIs) and inventory which affects the per shipment radiological impacts from the incident-free (TIs) and transportation accident (inventory). The number of shipments is needed for campaign non-radiological and radiological impact calculations.

The number of shipments was estimated based on the estimates of the type of waste (CH, RH), the waste volume, waste mass, container type, and other waste stream specific information. Note that specific restrictions apply to the number of containers per different package types and maximum gross weight of different container types.

The annual number of shipments by package type was estimated for each generator site. This information is provided in Attachments D and E of WIPP Nuclear Waste Partnership, 2020. These data were used to calculate the number of shipments during the transportation campaign shown in Table 3-21. Note that the shipments from the generator sites to INL were added to the shipments from INL to the WIPP facility.

Table 3-21. Number of Shipments by Shipment Type.

Site	1 HalfPACT and 2 TRUPACT-II	3 HalfPACT with SCA*	3 TRUPACT-II with CCO*	1 RH-TRU 72-B	1 TRUPACT-III
ANL	28	79		136	
Bettis				12	
Hanford	5,903	1,669		362	281
INL	3,212			591	91
Knolls	31			26	
LANL	5,160			90	408
ORNL	2,997			1,968	
SNL	8	10		5	
SRS	505	9	3,877	66	7
LLNL	209				40
NRD, LLC	1				
NNSS	34				
Total	**18,088**	**1,767**	**3,877**	**3,256**	**827**

*SCA = shielded container assembly; CCO = criticality control overpack

Figure 3-25 shows the number of shipments of CH-TRU and RH-TRU waste by generator site.

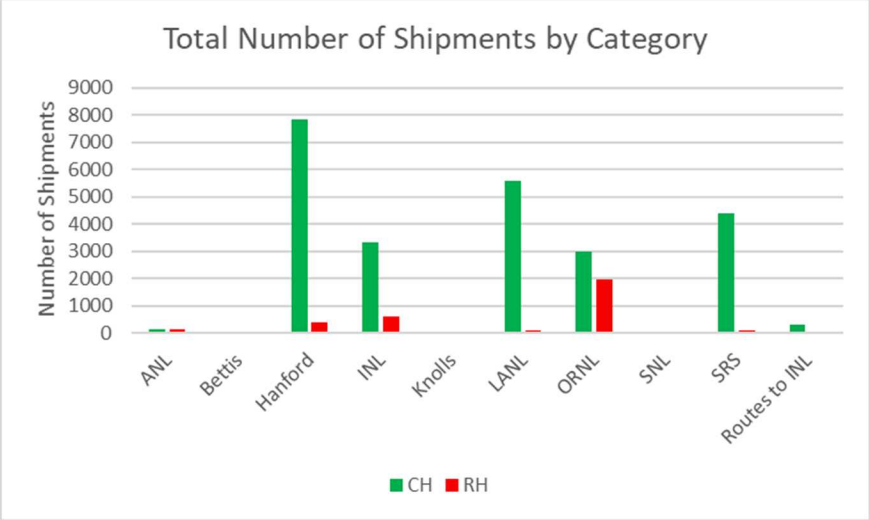

Figure 3-25. Number of Shipments of CH-TRU and RH-TRU Waste.

The total number of shipments by site is compared to the 2008 TA values in Figure 3-26. More shipments are expected from Hanford, LANL, ORNL, and SRS than was assumed in the 2008 TA and fewer shipments are expected from INL. The difference in the number of shipments may affect the campaign total radiological and non-radiological impacts for the site compared to the 2008 TA.

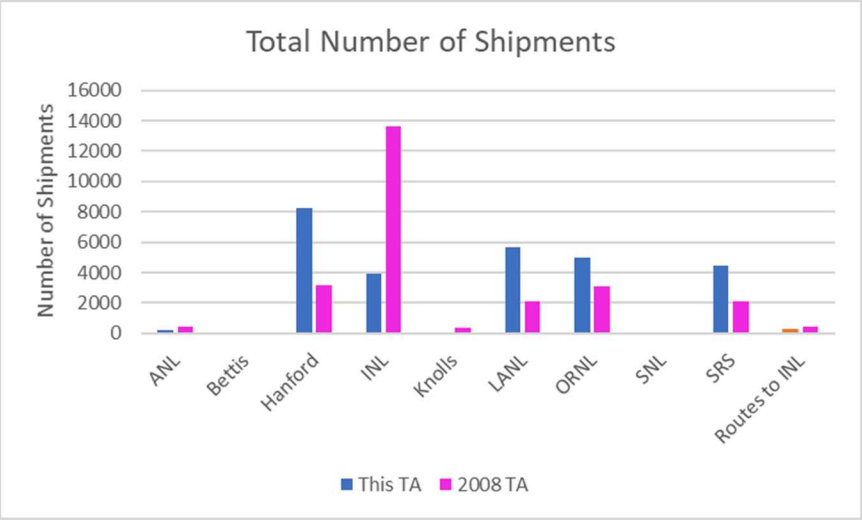

Figure 3-26. Comparison of the Total Number of Shipments.

3.6 Transportation Index (TI)

3.6.1 TI Data Analysis

The major parameters required for the assessment of the radiological impacts due to the external radiation during the routine transportation and transportation accidents without release of radioactive materials are transportation index (TI) and external radiation gamma and neutron fractions. This information is required for each package. The TI represents the radiation dose rate at 3.3 ft (1 m) from the surface of the package. It is a function of the waste density, radionuclide inventory, and self-shielding provided by the waste and by the package.

In the 2008 TA the TI values were calculated using MICROSHIELD (Version 7.0). Packages with surplus plutonium were not considered in the 2008 TA.

In this TA the TIs were derived based on the actual data (measured TIs) of the WIPP shipments from the beginning of the transportation campaign through October 4, 2019 (except for surplus plutonium none of which has been shipped). The measured dose rate data were provided in Attachment C of WIPP Nuclear Waste Partnership, 2020.

The statistics of the measured TI data are summarized in Table 3-22 for the different package types. Note that this includes the TIs of TRUPACT-II and HalfPACT with pipe overpack containers (POCs). There are 232 measurements for TRUPACT-III. The measured TIs are equal to 0.5 mrem/hr in 226 cases and greater than 0.5 mrem/hr in 6 cases with maximum of 5.3 mrem/hr.

The surplus plutonium will be shipped in criticality control overpacks (CCOs). Fourteen CCOs will be loaded in each TRUPACT-II. There is no data on the actual TI of TRUPACT-II with CCOs because none of them was shipped.

Table 3-23 summarizes the TIs values used in the 2008 TA and SEIS-II. The percentiles were obtained by placing the 2008 TA and SEIS-II values on the corresponding measured TIs frequency curves (Figures 3-27, 3-28, and 3-31).

Table 3-22. Dose Rates at 1 m (TIs) for Different Packages.

Package	Number of Measurements	Dose Rate (mrem/hr)			
		25th	50th	75th	95th
TRUPACT-II	29,709	0.2	0.2	0.5	0.7
HalfPACT (CH)	2,886	0.2	0.2	0.2	0.6
HalfPACT (SCA)	15	0.9825	1.8	2.3	2.85
TRUPACT-III	232	0.5	0.5	0.5	0.5
RH-TRU 72-B	719	0.4445	1.1	1.1	4

Table 3-23. Dose Rates (TIs) Used in the 2008 TA and SEIS-II.

Package	2008 TA		SEIS II	
	Dose Rate (mrem/hr)	Percentile	Dose Rate (mrem/hr)	Percentile
TRUPACT-II	0.5	0.80	4	0.995
HalfPACT (CH)	0.312	0.85	N/A	N/A
HalfPACT (SCA)	N/A	N/A	N/A	N/A
RH-TRU 72-B	2.5	0.915	10	0.975

Figure 3-27 shows the cumulative frequency distribution of the measured TIs for TRUPACT-II. The values used in the 2008 TA and SEIS-II when placed on this curve corresponds to 80th percentile (2008 TA) and 99.5th percentile (SEIS-II). The TI value corresponding to the 95th percentile is 0.7 mrem/hr. The curve has a very long tail that represents a few values with TIs higher than 1 mrem/hr.

Figure 3-28 shows the cumulative frequency distribution of the measured TIs for HalfPACT with CH-TRU waste. The value used in the 2008 TA when placed on this curve corresponds to 85th percentile. HalfPACTs did not exist at the time of SEIS-II. The TI value corresponding to the 95th percentile is 0.6 mrem/hr. The curve has a very long tail that represents a few values with TIs higher than 1 mrem/hr.

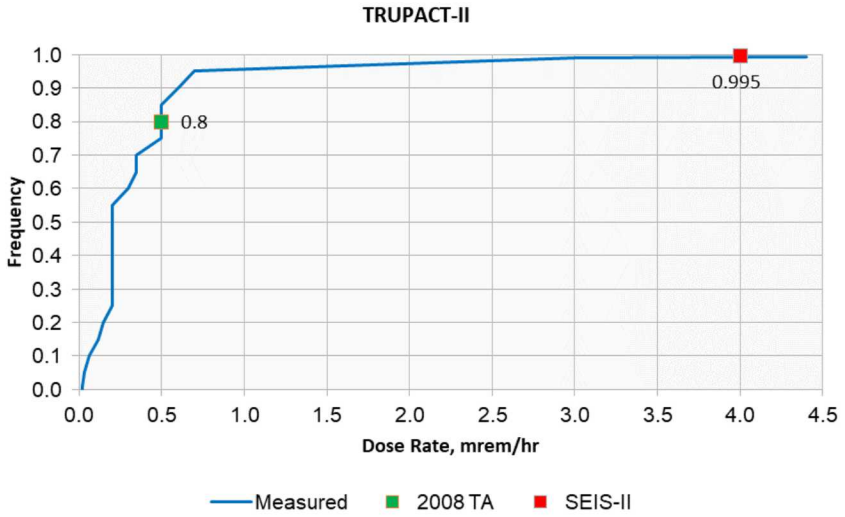

Figure 3-27. Cumulative Frequency of the Measured TIs of TRUPACT-II Packages.

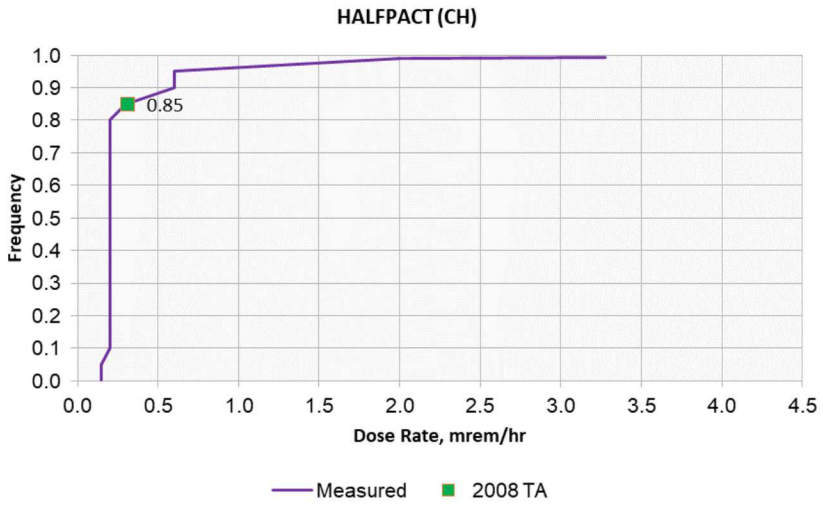

Figure 3-28. Cumulative Frequency of the Measured TIs of HalfPACT Packages with CH-TRU Waste.

Figure 3-29 compares TRUPACT-II and HalfPACT TIs. The curves are very similar. Differences around 75th percentile are most likely due to fewer measurements available for HalfPACT which lead to smaller variability in the TI values. As evident from Figure 3-29, the TRUPACT-II TIs are bounding for the HalfPACT TIs, except for a few very low TI values.

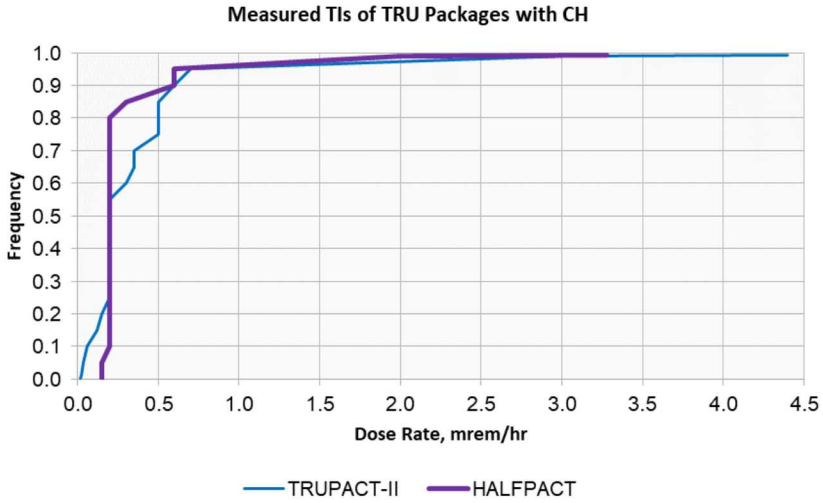

Figure 3-29. Comparison between TRUPACT-II and HalfPACT (CH) TIs.

Figure 3-30 compares the TIs distributions of TRUPACT-II and HalfPACT packages with and without POCs. The HalfPACT curves with and without POCs are virtually identical partially because only 6 HalfPACTs with POCs were shipped. The TRUPACT-II curves with and without POCs are very similar even though 1,988 TRUPACT-II with POCs were shipped. Based on this comparison it can be concluded that there is no reason to consider different TIs for the TRUPACT-II and HalfPACT with POCs.

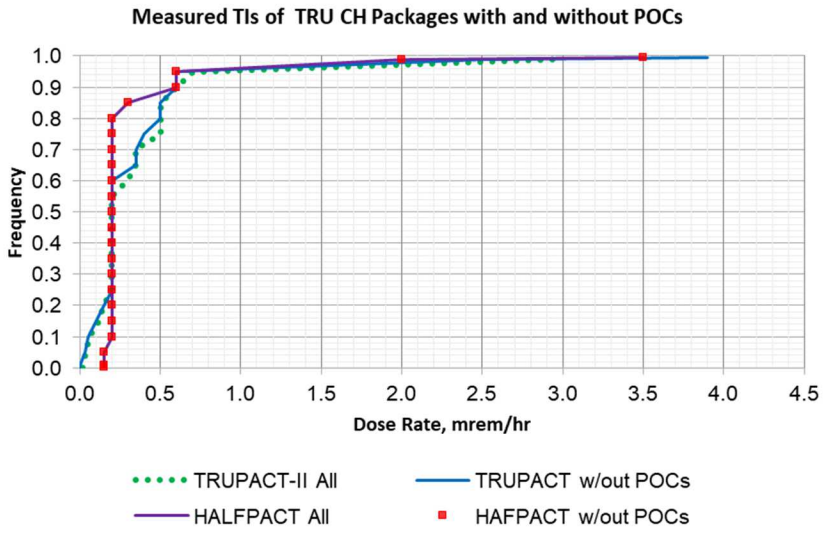

Figure 3-30. Comparison between TRUPACT-II and HalfPACT (CH) TIs with and without POCs.

Figure 3-31 shows the cumulative frequency distribution of the measured TIs for RH-TRU 72-B. The values used in the 2008 TA and SEIS-II when placed on this curve corresponds to 91.5th percentile (2008 TA) and 97.5th percentile (SEIS-II). The TI value corresponding to the 95th percentile is 4 mrem/hr. The curve has a very long tail that represents a few values with TIs higher than 6 mrem/hr.

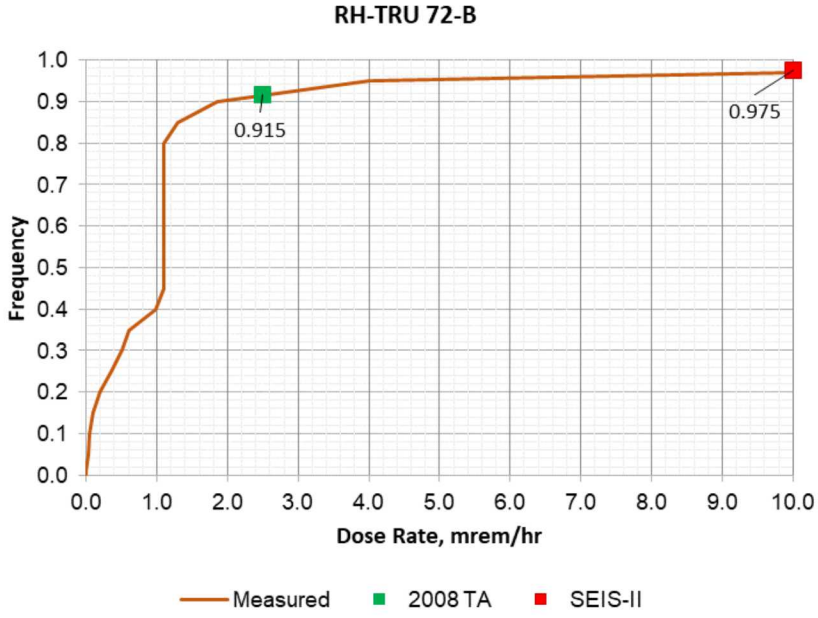

Figure 3-31. Cumulative Frequency of the Measured TIs of RH-TRU 72-B.

Figure 3-32 shows the cumulative frequency distribution of the measured TIs for HalfPACT with SCA. The TIs for HalfPACT with SCA was not reported in the 2008 TA. HalfPACTs did not exist at the time of SEIS-II. The TI value corresponding to the 95th percentile is 2.85 mrem/hr. There were not enough measurements for the tail of the distribution to be captured.

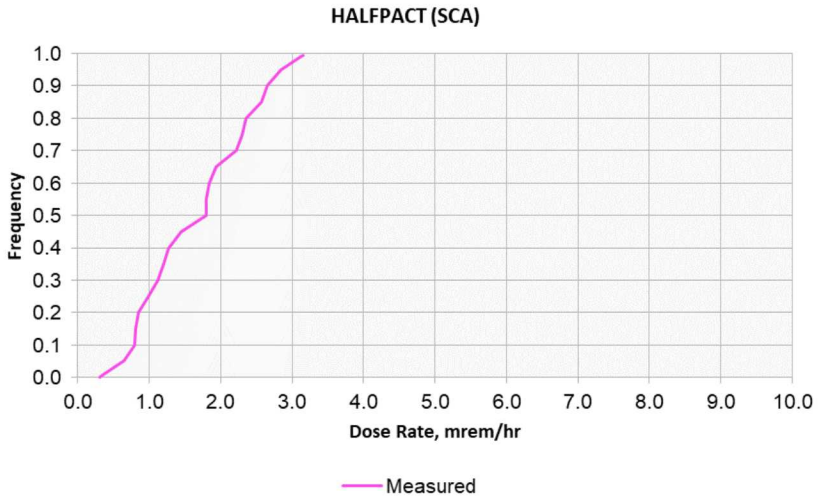

Figure 3-32. Cumulative Frequency of the Measured TIs of HalfPACT Packages with SCA.

Figure 3-33 compares RH-TRU 72-B and HalfPACT with SCA TIs. Note that there are significantly less measurements for HalfPACT with SCA than for RH-TRU 72-B. This affects especially the distribution tail. HalfPACT with SCA has higher 50th and 75th percentiles TIs. If more data were available, the distribution tail would probably have extended in a similar way as the RH-TRU 72-B distribution.

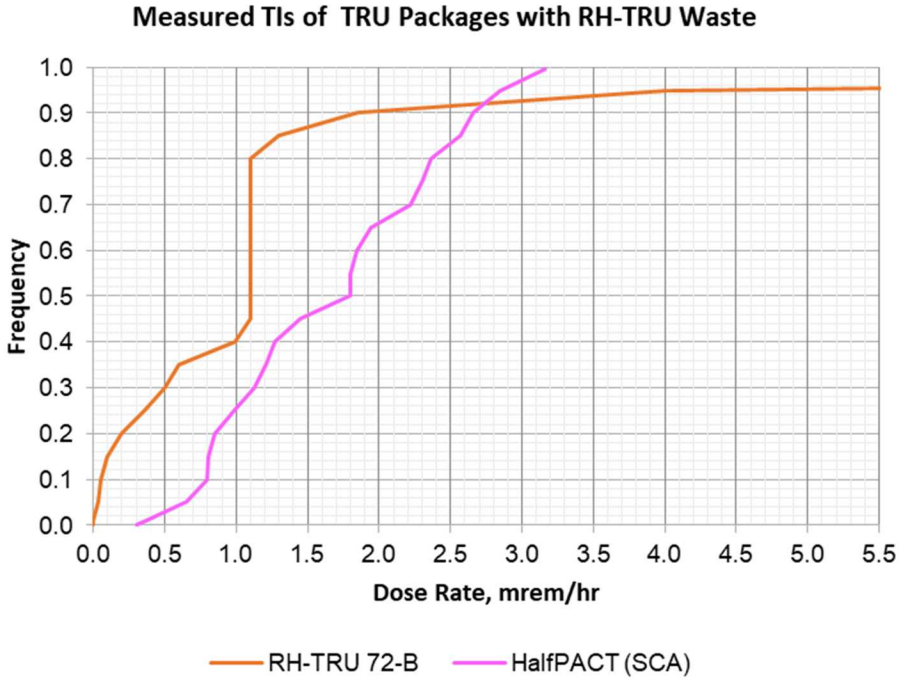

Figure 3-33. Comparison between RH-TRU 72-B and HalfPACT with SCA TIs.

3.6.2 Recommended TIs for the Incident-Free Analysis

The recommended TIs for the incident-free analysis are summarized in Table 3-24 for the different shipment types. The content of HalfPACT and TRUPACT-II in shipment "One HalfPACT and Two TRUPACT-II" may include 55-gal drums, 100-gal drums, ten drum overpacks (TDOPs), standard waste

boxes (SWBs), and POCs. The 95th percentile TIs represent the base case considered in Section 4.2. The 50th and 75th percentiles of the recommended TIs are considered in the sensitivity analysis.

Table 3-24. Shipment TIs Recommended for Use in the Incident-Free Analysis.

Shipment Type	Shipment ID	Dose Rate at 1 m (mrem/hr)		
		50th	75th	95th
One HalfPACT and Two TRUPACT-II	1	0.2	0.5	0.7
Three HalfPACT (SCA)		1.8	2.3	2.85
Three TRUPACT-II (CCO)		4	4	4
One TRUPACT-III	2	0.5	0.5	0.5
One RH-TRU 72-B	3	1.1	1.1	4

4. RADIOLOGICAL IMPACTS FROM INCIDENT FREE TRANSPORTATON

4.1 Unit Risk Factors for Incident-Free Transport

The collective external non-occupational doses are calculated for the following receptors:

- Residents along the route (also called Off-Link exposure in RADTRAN 6.02)
- Occupants of vehicles sharing the route (also called On-Link exposure in RADTRAN 6.02)
- Residents near refueling stops
- People at the refueling stops
- Person in a traffic jam next to the WIPP truck with the TRU waste package(s)

The equations used in these calculations and the input parameters, except the unit risk factors, are defined in Section 2.1.1. This section describes the unit risk factors.

The unit risk factors were calculated using RADTRAN 6.02 for each shipment ID. The shipment IDs are provided in Table 4-1 for the different shipment types. The shipment ID equal to 1 is the same for the first three shipment types in Table 4-1 because the critical dimensions of these shipments are the same. Note that the critical dimensions are different for the crew as described later in this section.

Table 4-1. Shipment Critical Dimensions for All Receptors Except the Crew.

Shipment Type	Shipment Critical Dimension (m)	Shipment ID
One HalfPACT and Two TRUPACT-II	7.4	1a
Three HalfPACT (SCA)	7.4	1b
Three TRUPACT-II (CCO)	7.4	1c
One TRUPACT-III	6.1	2
One RH-TRU 72-B	3.7	3

The package critical dimension is the RADTRAN 6.02 parameter that is an input into the exposure calculations for incident free transport. The critical dimension is the largest dimension of the package facing the potentially exposed people/person. The name comes from RADTRAN literature in which, for historical reasons, this dimension is called the “critical dimension”. It is not related to criticality.

The package critical dimensions assumed in the 2008 TA were:

- HalfPACT (3 per shipment) – 7.4 m (24.3 ft)
- TRUPACT-II (3 per shipment) – 7.4 m (24.3 ft)
- TRUPACT-III (1 per shipment) – 6.1 m (20 ft)
- RH-TRU 72-B (1 per shipment) – 3.7 m (12 ft)

The critical dimensions in the 2008 TA were defined assuming that three TRUPACT-II containers in one shipment can be modeled as one package. The TRUPACT-II and HalfPACT are 2.44 m (8 ft) in diameter. The critical dimension is then the length (three diameters) ~7.4 m (24.3 ft). The critical dimension for the RH-TRU 72-B was calculated assuming one container per shipment. The largest dimension is then the length, which is 3.7 m (12 ft) (3.6 m was assumed in the 2008 TA). The critical dimension for TRUPACT-III was calculated assuming one container per shipment. The largest dimension is then the length, which is

6.1 m (20 ft). The same approach was used in this TA. Note that the critical dimension of the TRUPACT-II shipment in the 2008 TA report is shown as 7.4 m and in the 2008 TA RADTRAN input file it is 8.4 m.

The unit risk factor for the residents along the transportation route was calculated for each shipment ID assuming the corresponding shipment critical dimension (Table 4-1), shipment TI equal to 1 mrem/hr, shielding factor equal to 1 (no shielding), link distance equal to 1 km, population density equal to 1 person/km^2, and vehicle speed equal to 1 km/hr.

The unit risk factor for the occupants of vehicles sharing the transportation route was calculated for each shipment ID assuming the corresponding shipment critical dimension, shipment TI equal to 1 mrem/hr, link distance equal to 1 km, vehicle occupancy equal to 1 person, and vehicle speed equal to 88.51 km/hr (55-mph) for non-rush hour and 44.26 km/hr (27.5-mph) for rush hour.

The unit risk factor for residents near the refueling stop was calculated for each shipment ID assuming the corresponding shipment critical dimension, shipment TI equal to 1 mrem/hr, shielding factor equal to 1, population density equal to 1 person/km^2, and the stop time equal to 1 hr. The residents were assumed to be at a radial distance from 30 m to 800 m from the truck. The same assumption about the radial distance was used in the 2008 TA.

The unit risk factor for people at the refueling stop was calculated for each shipment ID assuming the corresponding shipment critical dimension, shipment TI equal to 1 mrem/hr, shielding factor equal to 1, population density equal to 1 person/km^2, and the stop time equal to 1 hr. The people were assumed to be at the radial distance from 1 m to 15 m from the truck. The same assumption about the radial distance was used in the 2008 TA.

The unit risk factor for a person in a traffic jam next to the WIPP truck with the TRU package(s) was calculated for each shipment ID assuming the corresponding shipment critical dimension, shipment TI equal to 1 mrem/hr, shielding factor equal to 1, the time in the traffic jam equal to 1 hr, and the exposure distance equal to 2 m. The same assumption about the distance between a person in a traffic jam and the cargo was used in the 2008 TA.

The collective external occupational doses are calculated for the following receptors:

- Inspector at the generator site inspecting the shipment leaving the site or inspector at the state border
- Refueling stop employee
- Truck crew while driving and while at stops

The unit risk factor for an inspector at the generator site or at the state border was calculated for each shipment ID assuming the corresponding shipment critical dimension, shipment TI equal to 1 mrem/hr, shielding factor equal to 1, inspection time equal to 1 hr, and the distance from the cargo equal to 1 m. The same assumption about the distance between the inspector and the cargo was used in the 2008 TA.

The unit risk factor for an employee at a refueling stop was calculated for each shipment ID assuming the corresponding shipment critical dimension, shipment TI equal to 1 mrem/hr, shielding factor equal to 1, population density equal to 1 person/km^2, and the stop time equal to 1 hr. The employee was assumed to be at the radial distance from 1 m to 15 m from the truck. The same assumption about the radial distance was used in the 2008 TA. Note that the unit risk factors for an employee at a refueling stop are the same as the unit risk factors for the people at the refueling stop because the same assumptions apply.

The unit risk factor for one crew person at stops (refueling and others) was calculated for each shipment ID assuming the corresponding shipment critical dimension, shipment TI equal to 1 mrem/hr, shielding factor

equal to 1, stop time equal to 1 hr, and the distance from the cargo equal to 1 m. The same assumption about the distance between the crew and the cargo at stops was used in the 2008 TA. Note that the unit risk factors for the crew member at a stop are the same as the unit risk factors for the inspector because the same assumptions apply.

The unit risk factor for the crew while driving was calculated for each shipment ID using the critical dimensions defined in Table 4-2. These dimensions are different from the ones in Table 4-1 because the critical dimension for the crew is the largest dimension of the cargo that faces toward the crew. In the case of a shipment of one HalfPACT and two TRUPACT-II and three TRUPACT-II, the largest dimension is the height of the TRUPACT-II (3.05 m). In the case of a shipment of three HalfPACTs, the largest dimension is the diameter (2.44 m). In the case of a shipment of one TRUPACT-III, the largest dimension is the height (2.65 m). In the case of a shipment of one RH-TRU 72-B, the largest dimension is the diameter (1.07 m).

Table 4-2. Shipment Critical Dimensions for Crew.

Shipment Type	Shipment Critical Dimension (m)	Shipment ID
One HalfPACT and Two TRUPACT-II	3.05	1a
Three HalfPACT (SCA)	2.44	1b
Three TRUPACT-II (CCO)	3.05	1a
One TRUPACT-III	2.65	2
One RH-TRU 72-B	1.07	3

The unit risk factor for the crew of 2 people was calculated for each shipment ID assuming the corresponding shipment critical dimension (Table 4-2), shipment TI equal to 1 mrem/hr, shielding factor equal to 1, link distance equal to 1 km, vehicle speed equal to 1 km/hr, and the distance from the cargo equal to 4 m. The same assumption about the distance between the crew and the cargo was used in the 2008 TA. The non-occupational and occupational unit risk factors for the incident-free transport are summarized in Table 4-3.

Table 4-3. Unit Risk Factors for Incident-Free Transport.

Unit Risk Factor	Notation	Units	Speed, km/hr	Shipment ID		
				1	2	3
Receptor	**Non-Occupational**					
Residents along the route (Off Link)	URF_{off}	km^2	1	3.19E-07	2.67E-07	1.69E-07
People sharing the route (On Link), non -rush hour	URF_{on}	hr^2/km	88.51	9.38E-10	7.83E-10	4.96E-10
People sharing the route (On Link), rush hour		hr^2/km	44.26	3.91E-09	3.26E-09	2.07E-09
Resident near refueling stop	URF_{st}	km^2	N/A	3.17E-07	2.64E-07	1.68E-07
People at the refueling stop	URF_{pst}	km^2	N/A	2.61E-07	2.18E-07	1.38E-07
Person in a traffic jam	URF_{ptrf}	unitless	N/A	1.96E-03	1.79E-03	1.43E-03
Receptor	**Occupational**					
Inspector	URF_{ins}	unitless	N/A	3.92E-03	3.58E-03	2.85E-03
Refueling stop employee	URF_{emp}	unitless	N/A	2.61E-07	2.18E-07	1.38E-07

Unit Risk Factor	Notation	Units	Speed, km/hr	Shipment ID		
				1	2	3
Crew while driving	URF_{crdr}	unitless	1	8.03E-04 (a) 6.21E-04 (b)	6.81E-04	2.97E-04
Crew at stops	URF_{crst}	unitless	N/A	3.92E-03	3.58E-03	2.85E-03

Note: (a) and (b) refer to shipment IDs 1a and 1b in Table 4-2.

4.2 Results

The radiological impacts from incident-free transport are expressed in terms of collective doses or individual doses. The methods used to calculate the collective and individual doses are described in Section 2. Equations 2-1 – 2.15 were used. The input data required for these calculations are described in Section 3. The calculations are based on the unit risk factor approach. The calculations of the unit risk factors are described in Section 4.1.

The following sections provide the results of the non-occupational and occupational radiological impacts. The results are presented for each receptor considered in the analysis.

The results in this section are often displayed using a box and whisker plot. The ends of the box represent the upper and lower quartiles. The median is marked by a vertical line inside the box and the whiskers extend to the highest and lowest values of observations.

4.2.1 Residents along the Transportation Routes

The per shipment and per campaign collective doses to the residents along the transportation routes are summarized in Table 4-4 for each type of shipment. The per shipment collective doses are shown in Figure 4-1 and per campaign collective doses are shown in Figure 4-2.

The collective doses were calculated using the following scenario parameters:

- 95^{th} percentile TI for each shipment type
- Population along the route adjusted to account for population increase from 2010 to 2018.
- Vehicle speed of 55-mph during non-rush hour and 27.5-mph during rush hour.
- The percent of urban and suburban areas affected by rush hour of 20 percent.

The collective doses per shipment of 1xTRUPACT-III are lower (maximum of 4.5E-04 person-rem) and the collective doses per shipment of 3xTRUPACT-II with CCOs are higher (maximum of 4.3E-03 person-rem) compared to the other shipments. The per campaign collective doses are very similar for 1x HalfPACT and 2xTRUPACT-II, 3xHalfPACT (SCA), and 1xRH-TRU 72-B shipments because the number of 1xHalfPACT and 2xTRUPACT-II shipments is significantly higher. The per campaign collective dose per shipment of 3xTRUPACT-II with CCOs is somewhat higher than the other shipments.

Table 4-4. Collective Doses for the Resident Along the Route (Off Link Doses).

Route	Shipment Type	Collective Dose (person-rem)					
		CH				RH	Route Total
		1xHalfPACT 2xTRUPACT_II	3xHalfPACT (SCA)	3xTRUPACT-II (CCO)	1x-TRUPACT-III	1xRH-TRU 72-B	
ANL	Number of Shipments	28	79			136	
	Per shipment	5.05E-04	2.06E-03			1.53E-03	
	Campaign Total	1.42E-02	1.63E-01			2.08E-01	0.39
Bettis	Number of Shipments					12	
	Per shipment					3.00E-03	
	Campaign Total					3.61E-02	0.04
Hanford	Number of Shipments	5,903	1,669		281	362	
	Per shipment	5.47E-04	2.23E-03		3.27E-04	1.66E-03	
	Campaign Total	3.23E+00	3.72E+00		9.19E-02	5.99E-01	7.64
INL	Number of Shipments	3,212			91	591	
	Per shipment	4.14E-04			2.47E-04	1.25E-03	
	Campaign Total	1.33E+00			2.25E-02	7.40E-01	2.09
Knolls	Number of Shipments	31				26	
	Per shipment	1.19E-03				3.60E-03	
	Campaign Total	3.68E-02				9.35E-02	0.13
LANL	Number of Shipments	5,160			408	90	
	Per shipment	5.57E-05			3.33E-05	1.69E-04	
	Campaign Total	2.87E-01			1.36E-02	1.52E-02	0.32
ORNL	Number of Shipments	2,997				1,968	
	Per shipment	5.91E-04				1.79E-03	

Route	Shipment Type	Collective Dose (person-rem)					
		CH				RH	Route Total
		1xHalfPACT 2xTRUPACT_II	3xHalfPACT (SCA)	3xTRUPACT-II (CCO)	1x-TRUPACT-III	1xRH-TRU 72-B	
	Campaign Total	1.77E+00				3.52E+00	5.29
SNL	Number of Shipments	8	10			5	
	Per shipment	4.30E-05	1.75E-04			1.30E-04	
	Campaign Total	3.44E-04	1.75E-03			6.51E-04	0.003
SRS	Number of Shipments	505	9	3,877	7	66	
	Per shipment	7.59E-04	3.09E-03	4.34E-03	4.54E-04	2.30E-03	
	Campaign Total	3.83E-01	2.78E-02	1.68E+01	3.18E-03	1.52E-01	17.37
LLNL	Number of Shipments	209			40		
	Per shipment	4.13E-04			2.47E-04		
	Campaign Total	8.62E-02			9.87E-03		0.096
NNSS	Number of Shipments	34					
	Per shipment	1.74E-04					
	Campaign Total	5.93E-03					0.006
NRD	Number of Shipments	1					
	Per shipment	8.07E-04					
	Campaign Total	8.07E-04					0.001
Total	**All Shipments**	**7.15**	**3.91**	**16.80**	**0.14**	**5.36**	**33.36**

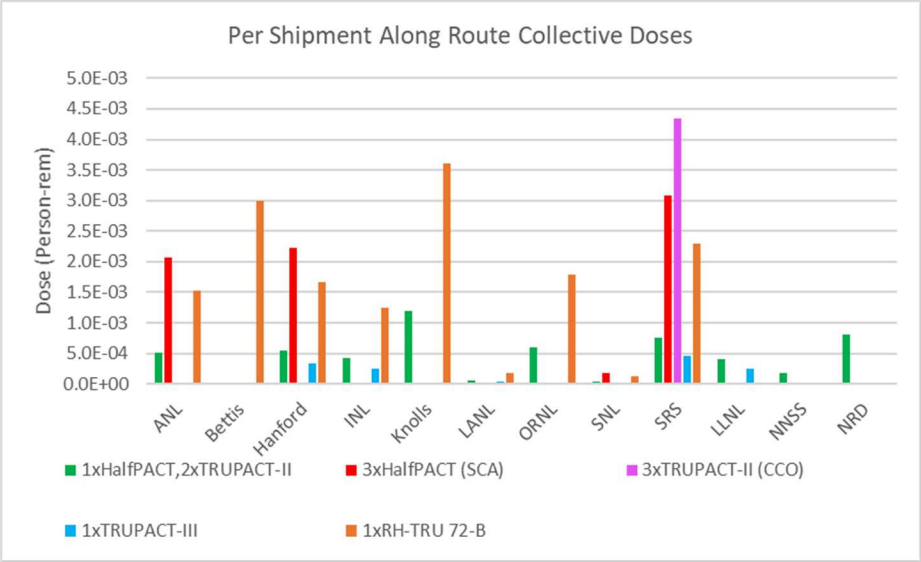

Figure 4-1. Per Shipment Collective Doses for the Resident Along the Route (Off Link Doses).

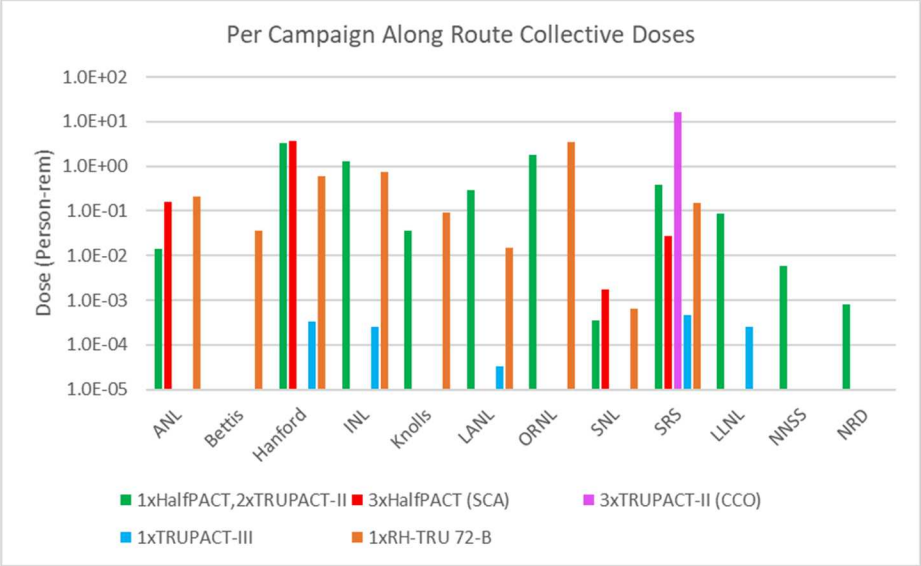

Figure 4-2. Per Campaign Collective Doses for the Resident Along the Route (Off Link Doses).

The per shipment collective dose to the residents along the transportation route is the sum of the doses along the rural, suburban, and urban segments of the route. Table 4-4 summarized the contributions from different segments to the total dose. Figure 4-3 shows the contributions for the CH shipments and Figure 4-4 shows the contributions for the RH shipments. In all the cases, the major contribution is from the suburban segment of the route (82-90 percent). The contribution from the rural segment is from 9 to 17 percent and the contribution from the urban segment is less than 1.1 percent. Note that the distance traveled in rural areas is larger than in suburban areas. The shielding factor in suburban areas (0.87) is slightly smaller than in the rural areas (1.0). However, the population density is significantly higher which results in higher contribution. The shielding factor in urban areas is significantly lower (0.018) and the distance traveled is small (Section 3.13) resulting in a small contribution to the total collective dose.

Table 4-5. Contributions to the Total Residents Along the Route Collective Doses.

Population Area	Percent Contribution to Total Along the Route Dose				
	1xHalfPACT and 2xTRUPACT-II	3xHalfPACT (SCA)	3xTRUPACT-II (CCO)	1xRH-TRU 72-B	1xTRUPACT-III
Rural	15.15%	15.15%	9.40%	16.02%	16.50%
Suburban	83.90%	83.87%	90.25%	83.24%	82.42%
Urban	0.93%	0.98%	0.35%	0.74%	1.08%

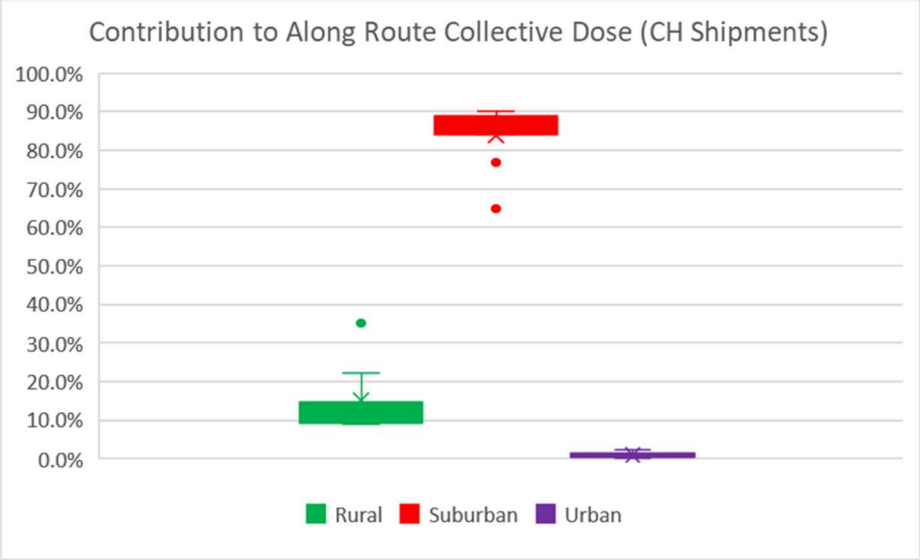

Figure 4-3. Contributions to Residents Along the Route Collective Dose for CH Shipments.

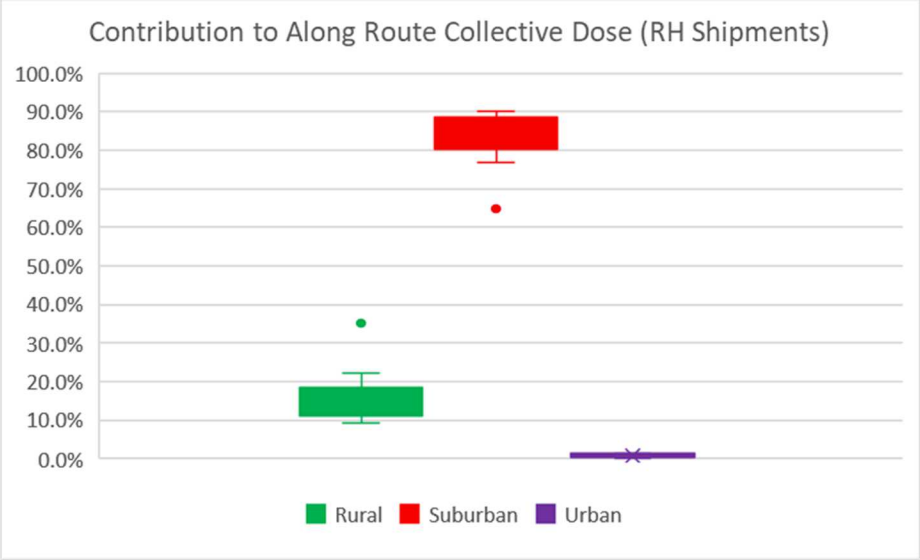

Figure 4-4. Contributions to Residents Along the Route Collective Dose for RH Shipments.

Figure 4-5 shows the collective doses versus the total route distance for the CH and RH shipments. In both cases, the longer the route, the higher the collective dose to the residents along the route.

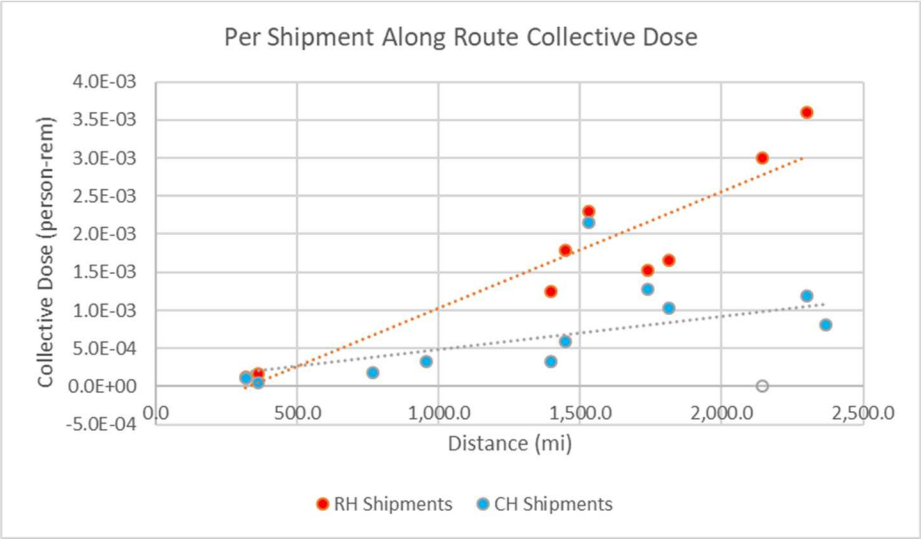

Figure 4-5. Residents Along the Route Collective Dose versus Route Total Distance.

Figure 4-6 compares the per CH shipment collective doses to the residents along the route calculated in this TA and in the 2008 TA. The doses used in this comparison were calculated using the same TIs for CH shipments as in the 2008 TA. The median dose in this TA is slightly higher (~12 percent) and the range is larger than in the 2008 TA. This was expected taking in account the differences in routes and increase in population since 2008.

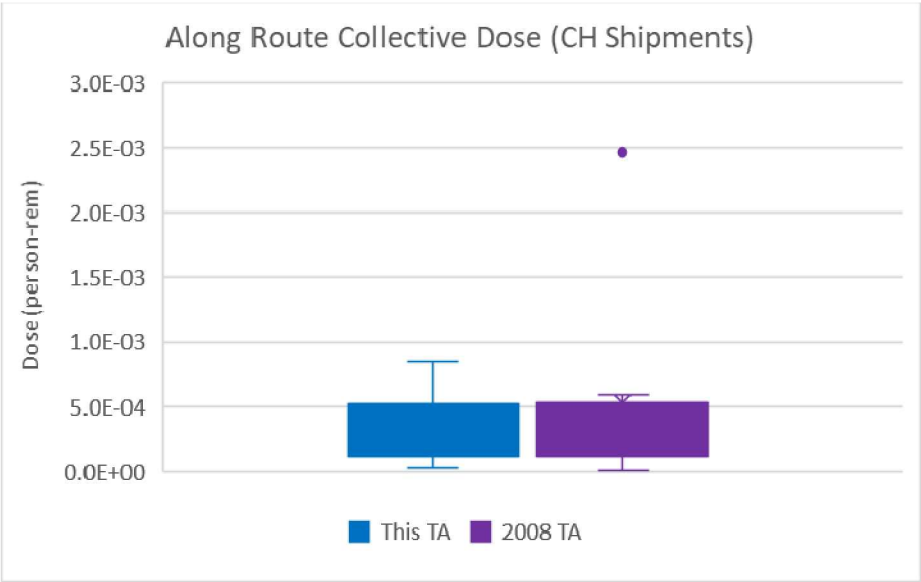

Figure 4-6. Comparison between the Residents Along the Route Collective Doses for CH Shipments.

4.2.2 People Sharing the Transportation Route

The per shipment and per campaign collective doses to the people sharing the transportation routes are summarized in Table 4-6 for each type of shipment. The per shipment collective doses are shown in Figure 4-7 and per campaign collective doses are shown in Figure 4-8.
The collective doses were calculated using the same scenario parameters as the ones discussed in Section 4.2.1. The additional scenario parameter for this receptor is the traffic count multiplier during the rush hour. The multiplier was set equal to 2 (2 times more vehicles per hour during rush hour).

The collective doses per shipment of 1xTRUPACT-III are lower (maximum of 1.2E-02 person-rem) and the collective doses per shipment of 3xTRUPACT-II with CCOs are higher (maximum of 5.4E-02 person-rem) compared to the other shipments. The per campaign collective doses are similar for 1x HalfPACT and 2xTRUPACT-II, 3xHalfPACT (SCA), and 1xRH-TRU 72-B shipments because the number of 1xHalfPACT and 2xTRUPACT-II shipments is significantly higher. The per campaign collective dose per shipment of 3xTRUPACT-II with CCOs is somewhat higher than the other shipments.

Table 4-6. Collective Doses for the Resident Sharing the Route (On Link Doses).

Route	Shipment Type	Collective Dose (person-rem)					
		CH				RH	Route Total
		1xHalfPACT 2xTRUPACT_II	3xHalfPACT (SCA)	3xTRUPACT-II (CCO)	1x TRUPACT-III	1xRH-TRU 72-B	
ANL	Number of Shipments	28	79			136	
	Total per shipment	8.74E-03	3.56E-02			2.64E-02	
	Campaign Total	2.45E-01	2.81E+00			3.59E+00	6.65
Bettis	Number of Shipments					12	
	Total per shipment					4.61E-02	
	Campaign Total					5.53E-01	0.55
Hanford	Number of Shipments	5,903	1,669		281	362	
	Total per shipment	8.46E-03	3.44E-02		5.04E-03	2.56E-02	
	Campaign Total	4.99E+01	5.75E+01		1.42E+00	9.25E+00	118.07
INL	Number of Shipments	3,212			91	591	
	Total per shipment	6.82E-03			4.06E-03	2.06E-02	
	Campaign Total	2.19E+01			3.70E-01	1.22E+01	34.47
Knolls	Number of Shipments	31				26	
	Total per shipment	1.58E-02				4.77E-02	
	Campaign Total	4.89E-01				1.24E+00	1.73
LANL	Number of Shipments	5,160			408	90	
	Total per shipment	2.26E-03			1.35E-03	6.84E-03	
	Campaign Total	1.17E+01			5.51E-01	6.16E-01	12.87
ORNL	Number of Shipments	2,997				1,968	
	Total per shipment	8.67E-03				2.62E-02	
	Campaign Total	2.60E+01				5.16E+01	77.60
SNL	Number of Shipments	8	10			5	
	Total per shipment	2.04E-03	8.32E-03			6.18E-03	
	Campaign Total	1.64E-02	8.32E-02			3.09E-02	0.13
SRS	Number of Shipments	505	9	3877	7	66	

Route	Shipment Type	Collective Dose (person-rem)					
		CH				RH	Route Total
		1xHalfPACT 2xTRUPACT_II	3xHalfPACT (SCA)	3xTRUPACT-II (CCO)	1x TRUPACT-III	1xRH-TRU 72-B	
	Total per shipment	9.51E-03	3.87E-02	5.43E-02	5.67E-03	2.87E-02	
	Campaign Total	4.80E+00	3.48E-01	2.11E+02	3.97E-02	1.90E+00	218.09
LLNL	Number of Shipments	209			40		
	Total per shipment	2.05E-02			1.22E-02		
	Campaign Total	4.29E+00			4.89E-01		4.78
NNSS	Number of Shipments	34					
	Total per shipment	4.03E-03					
	Campaign Total	1.37E-01					0.14
NRD	Number of Shipments	1					
	Total per shipment	8.81E-03					
	Campaign Total	8.81E-03					0.01
Total	**All Shipments**	**119.49**	**60.74**	**211.00**	**2.87**	**80.98**	**475.08**

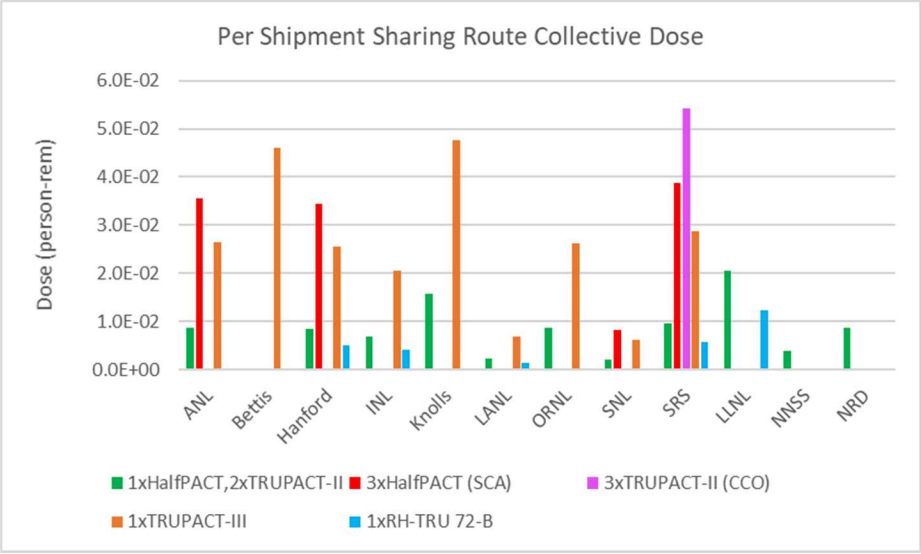

Figure 4-7. Per Shipment Collective Doses for the People Sharing the Route (On Link Doses).

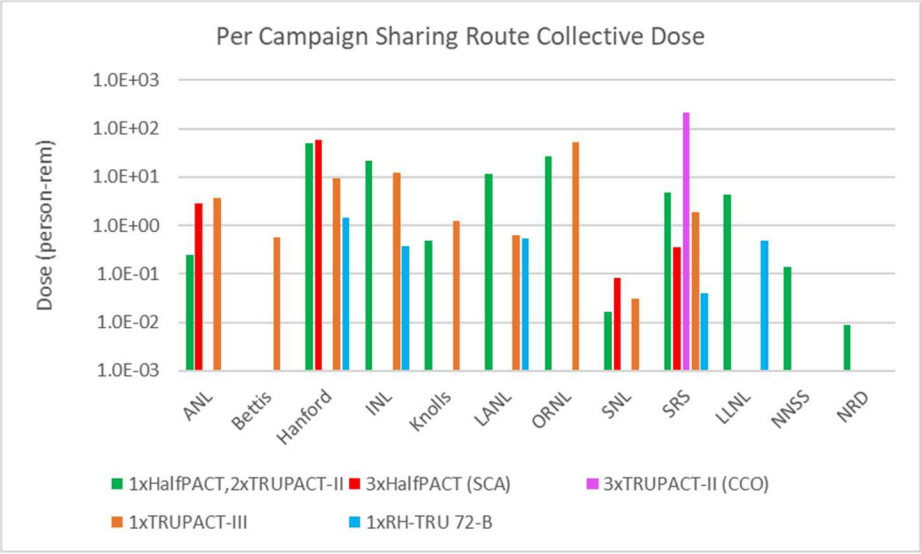

Figure 4-8. Per Campaign Collective Doses for the People Sharing the Route (On Link Doses).

The per shipment collective dose to the people sharing the route is the sum of the doses from the segment with rush hour speed (27.5-mph) and the segment with non-rush hour speed (55-mph). Table 4-7 summarized the contributions from these segments to the total dose. Figure 4-9 shows the contributions for the CH shipments and Figure 4-10 shows the contributions for the RH shipments. In all the cases, the contribution from the segment with 27.5-mph is from 54 to 65 percent even though the rush hour speed was assigned to 20 percent of the urban and suburban segments. This is because the dose is inversely proportional to the squared vehicle speed.

Table 4-7. Contributions to the Total People Sharing the Route Collective Doses.

Speed	Percent Contribution to Total Sharing the Route Dose				
	1xHalfPACT and 2xTRUPACT-II	3xHalfPACT (SCA)	3xTRUPACT-II (CCO)	1xRH-TRU 72-B	1xTRUPACT-III
27.5mph	62.48%	65.09%	53.86%	62.08%	61.51%
55mph	37.52%	34.91%	46.14%	37.92%	38.49%

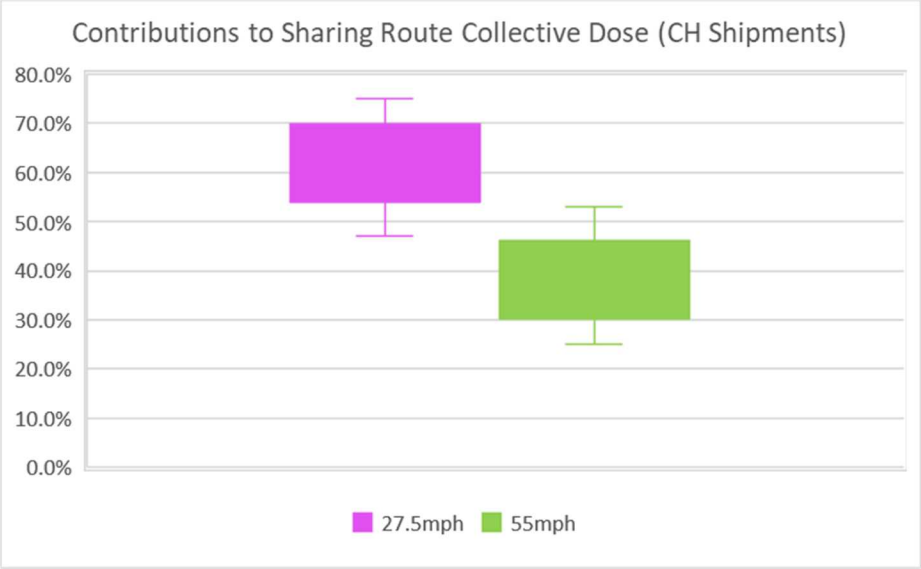

Figure 4-9. Contributions to People Sharing the Route Collective Dose for CH Shipments.

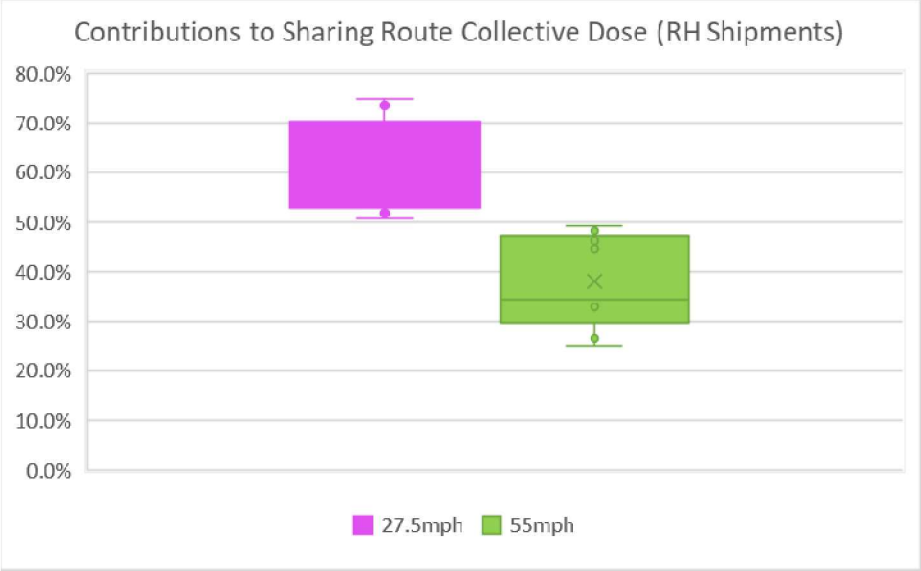

Figure 4-10. Contributions to People Sharing the Route Collective Dose for RH Shipments.

Figure 4-11 shows the collective doses versus the total route distance for the CH and RH shipments. In both cases, the longer the route, the higher the collective dose to the people sharing the route.

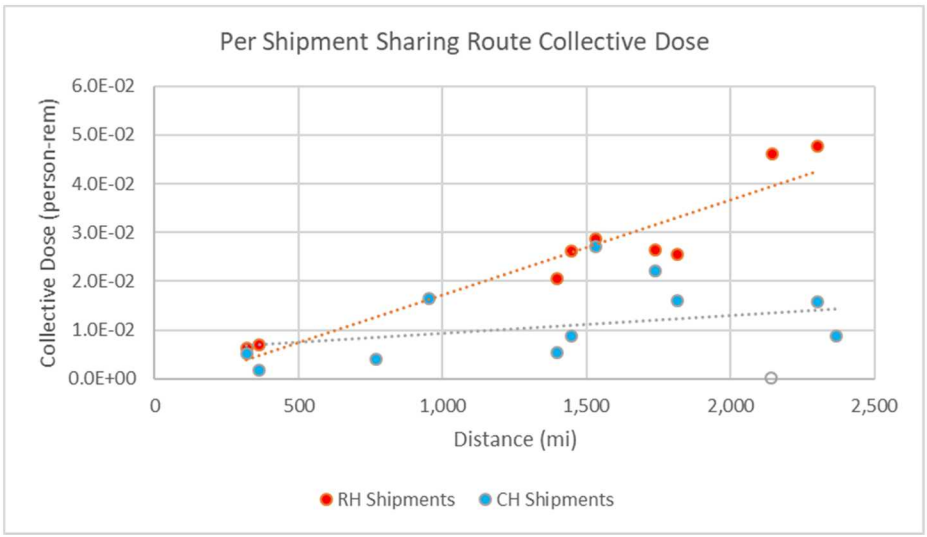

Figure 4-11. People Sharing the Route Collective Dose versus Route Total Distance.

Figures 4-12 and 4-13 compare the per CH shipment and per RH shipment collective doses to the people sharing the route calculated in this TA and in the 2008 TA. The doses used in this comparison were calculated using the same TIs for CH and RH shipments as in the 2008 TA. In both cases, the median doses in this TA are slightly higher than in 2008 TA, but the range is narrower. This is the result of the differences in routes and state specific traffic counts (Section 3.3).

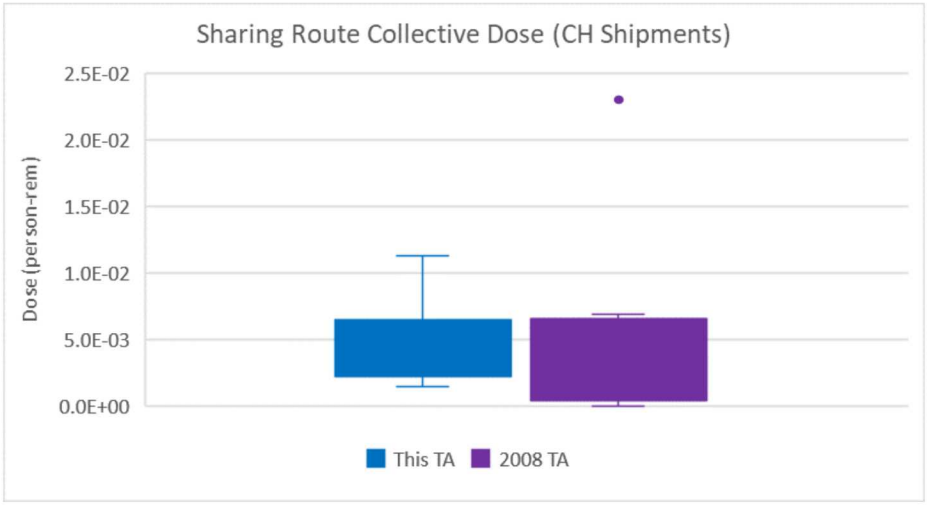

Figure 4-12. Comparison between the People Sharing the Route Collective Doses for CH Shipments.

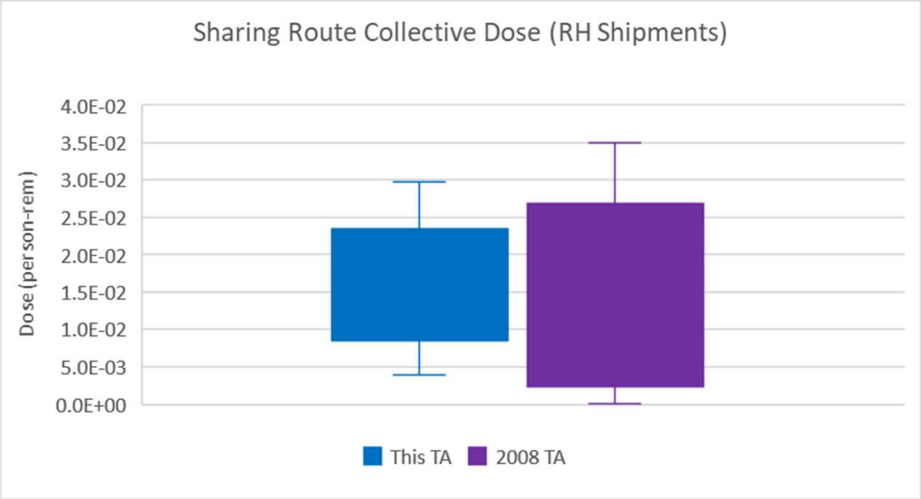

Figure 4-13. Comparison between the People Sharing the Route Collective Doses for RH Shipments.

Figures 4-14 and 4-15 compare the collective dose to residents along the routes and to people sharing the routes for the CH and RH shipments respectively. In both cases the collective doses to people sharing the route are more than an order of magnitude higher than the collective doses to residents along the route.

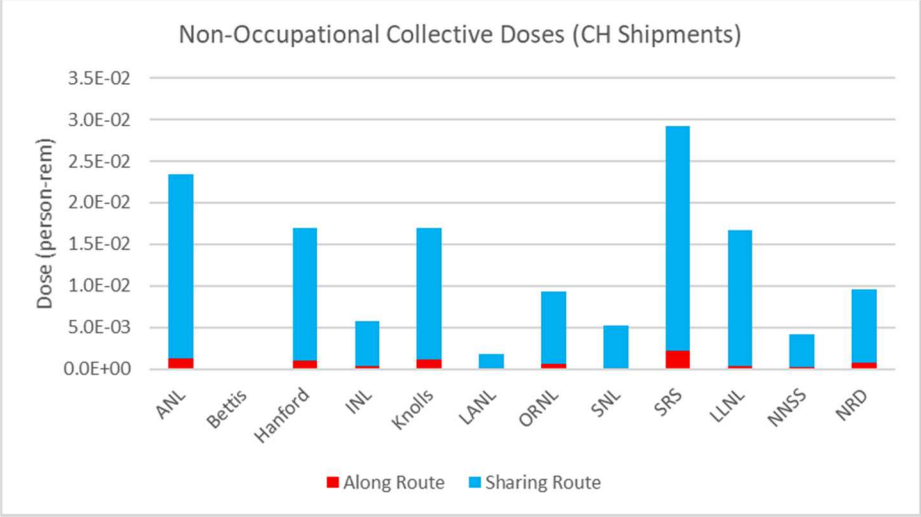

Figure 4-14. Route Specific Non-Occupational Collective Doses for CH Shipments.

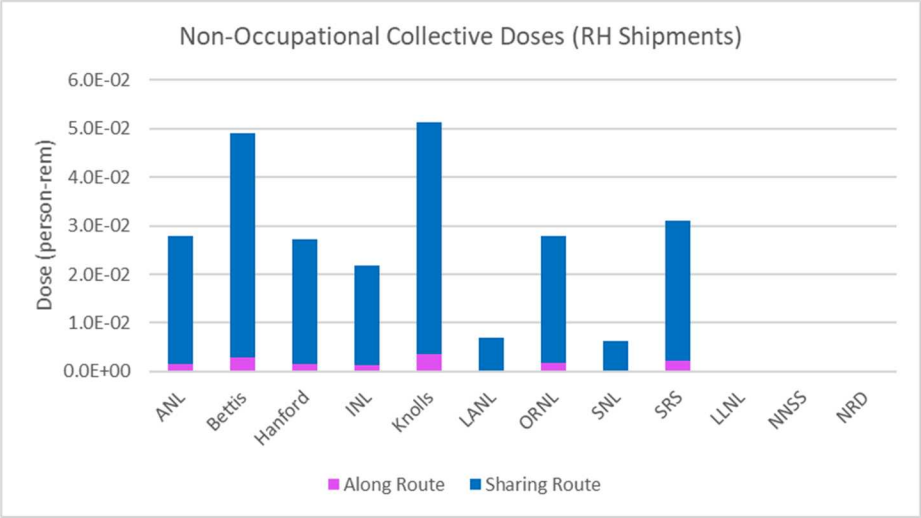

Figure 4-15. Route Specific Non-Occupational Collective Doses for RH Shipments.

Figure 4-16 shows the collective doses to the residents along the route versus the collective doses to the people sharing the route for the CH and RH shipments. In both cases the higher doses to residents along the route correspond to the higher doses to the people sharing the route.

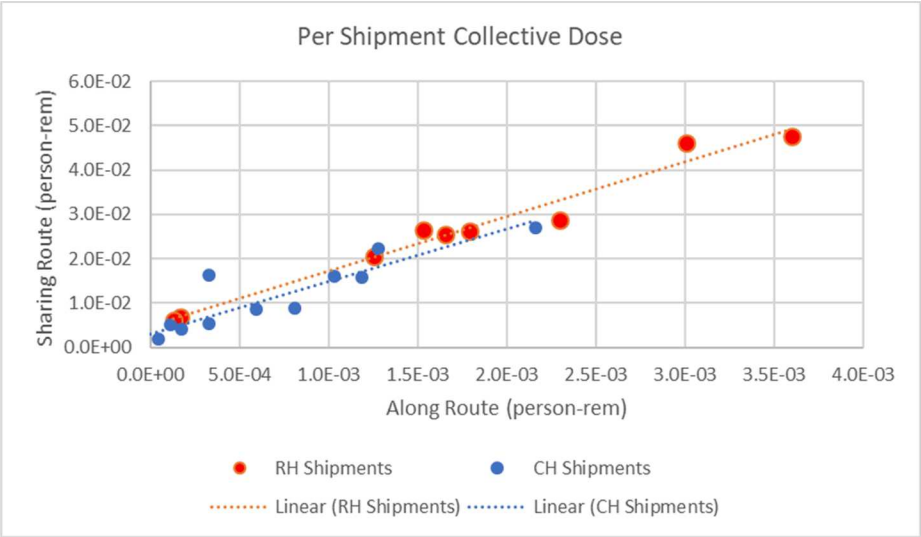

Figure 4-16. Along the Route and Sharing the Route Collective Doses.

4.2.3 Vehicle Crew

The collective doses to the crew were calculated using the following additional scenario parameters:

- Two crew members
- The distance from the crew to the cargo while driving is 4 m
- During the stops, each crew member spends half the time next to the truck at a distance of 1 m.
- The crew stay away from the truck during the inspections at the state borders.

Note that the crew is facing the cargo differently while driving. Consequently, the critical dimensions of the cargo are different during driving and while at stops. The details are discussed in Section 4.1.

The per shipment collective doses to the crew are summarized in Table 4-8 for each type of shipment. The per campaign collective doses are not provided because the crew will change over the years of the transportation campaign. Also, the crew members are monitored with radiation dosimeters. Any crew member who receives a radiation dose close to the administrative limit for occupational doses (2 rem) in any given year is transferred to another activity not involving radiation exposure. Based on the collective doses in Table 4-8, the number of CH shipments resulting in a total dose to a crew member of 2 rem in any given year would be from 25 to 1,250 depending on the shipment type and the route. The number of RH-TRU 72-B shipments resulting in a total dose to a crew member of 2 rem would be between 31 to 369 depending on the route.

Table 4-8. Occupational Collective Doses (Crew) per Shipment.

Route	Shipment Type	Collective Dose for 2 crew members (person-rem)				
		CH				RH
		1xHalfPACT 2xTRUPACT_II	3xHalfPACT (SCA)	3xTRUPACT-II (CCO)	1x TRUPACT-III	1xRH-TRU 72-B
ANL	Total per shipment	3.07E-02	1.08E-01			9.02E-02
Bettis	Total per shipment					1.14E-01
Hanford	Total per shipment	3.24E-02	1.14E-01		2.02E-02	9.55E-02
INL	Total per shipment	2.34E-02			1.46E-02	6.72E-02
Knolls	Total per shipment	4.25E-02			0.00E+00	1.25E-01
LANL	Total per shipment	5.18E-03			3.20E-03	1.37E-02
ORNL	Total per shipment	2.61E-02			0.00E+00	7.67E-02
SNL	Total per shipment	4.24E-03	1.42E-02		0.00E+00	1.08E-02
SRS	Total per shipment	2.71E-02	9.51E-02	1.55E-01	1.69E-02	7.88E-02
LLNL	Total per shipment	1.66E-02			1.04E-02	
NNSS	Total per shipment	1.26E-02				
NRD	Total per shipment	4.31E-02				

The per shipment collective doses are shown in Figure 4-17. The dose is collective because it is a dose to the crew, not to one crew member. The collective doses per shipment of 1xTRUPACT-III are lower (maximum of 2.0E-02 person-rem) and the collective doses per shipment of 3xTRUPACT-II (CCO) are higher (maximum of 1.55E-01 person-rem) compared to the other shipments.

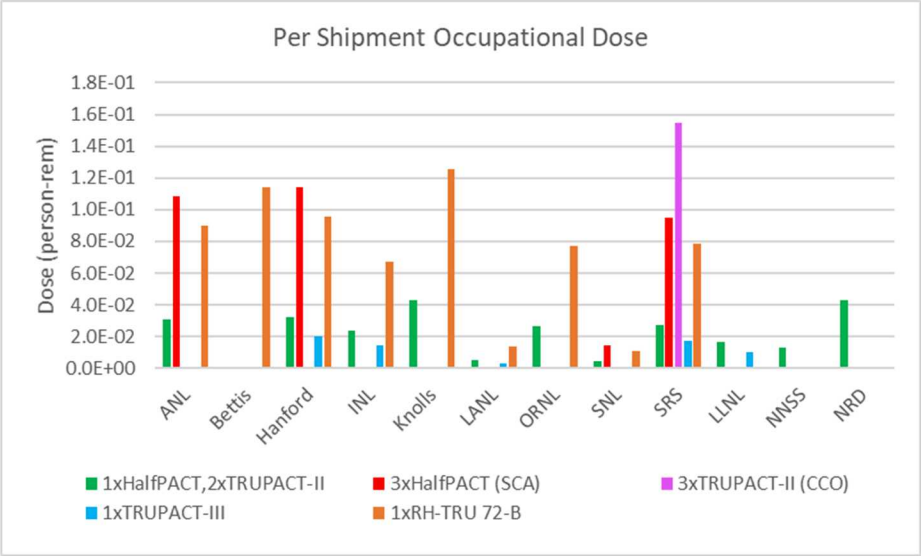

Figure 4-17. Per Shipment Occupational Collective Doses (Crew).

The per shipment collective dose to the crew is the sum of the doses while the crew is driving and while the truck is at stops. Table 4-9 summarizes the contributions from these two components to the total dose. Figure 4-18 shows the contributions for the CH shipments and Figure 4-19 shows the contributions for the RH shipments. The contributions of the doses while driving range from 59 percent to 63 percent, except for the RH-TRU 72-B shipment for which this contribution is 47.6 percent.

Table 4-9. Contributions to the Total Occupational Doses.

Speed	Percent Contribution to Total Occupational Dose				
	1xHalfPACT and 2xTRUPACT-II	3xHalfPACT (SCA)	3xTRUPACT-II (CCO)	1xRH-TRU 72-B	1xTRUPACT-III
Stops	36.59%	41.26%	38.77%	52.40%	38.10%
Driving	63.41%	58.74%	61.23%	47.60%	61.90%

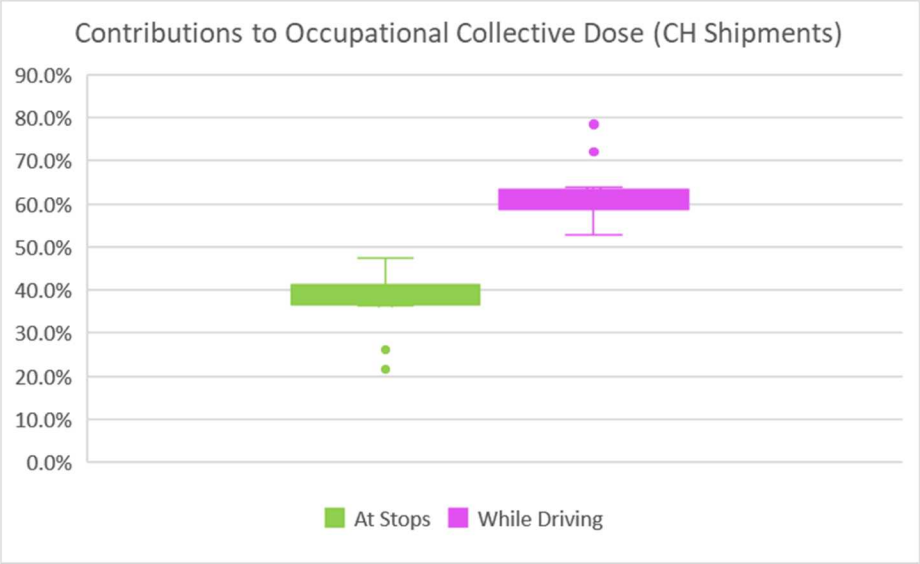

Figure 4-18. Contributions to Occupational Collective Dose for CH Shipments.

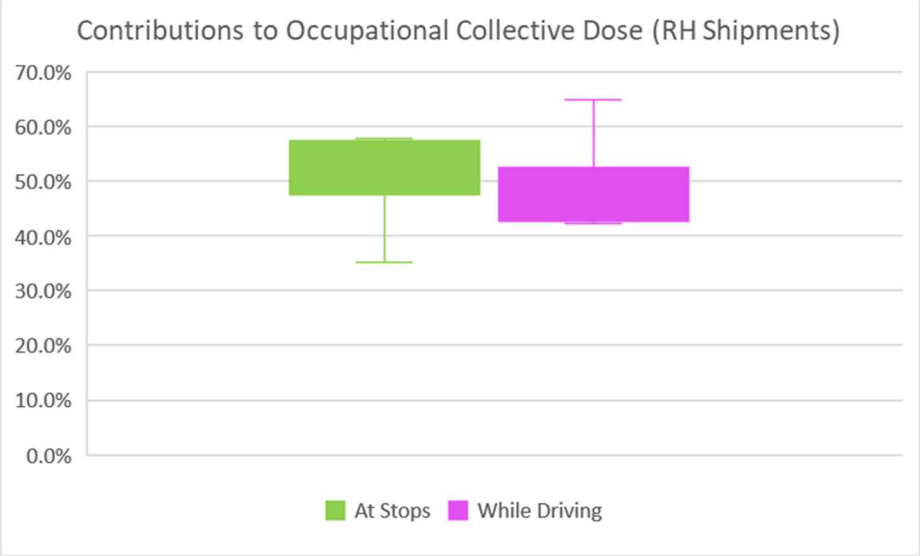

Figure 4-19. Contributions to Occupational Collective Dose for RH Shipments.

Figure 4-20 shows the collective doses to the crew versus the total route distance for the CH and RH shipments. In both cases, the longer the route, the higher the collective dose to the crew.

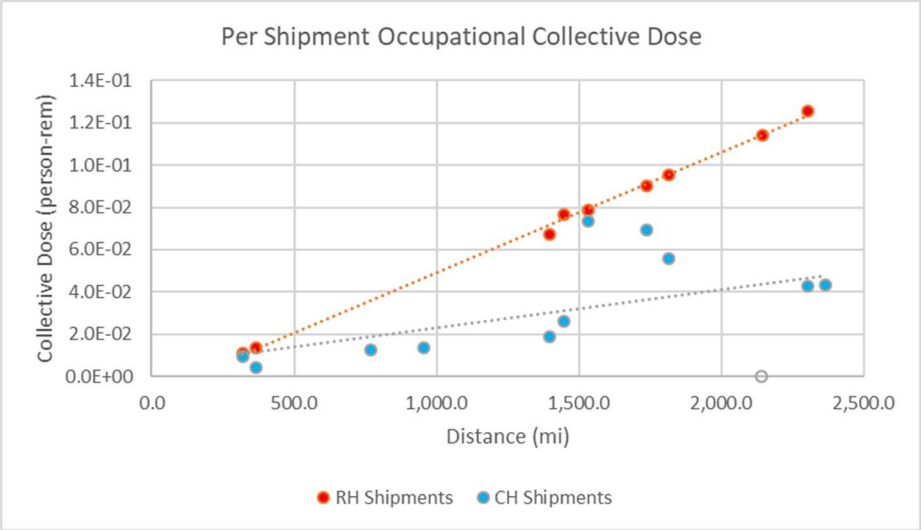

Figure 4-20. Occupational Collective Dose versus Route Total Distance.

Figures 4-21 and 4-22 compare the per CH shipment and per RH shipment collective doses to the crew calculated in this TA and in the 2008 TA. The doses used in this comparison were calculated using the same TIs for CH and RH shipments as in the 2008 TA. The median doses to crew per CH shipment in this TA (1.63E-02 persons-rem) are slightly higher than in the 2008 TA (1.26E-02 persons-rem) and the range is larger. This is the result of the differences in the routes and the additional stops considered in this TA as discussed in Section 3.1. The median doses to crew per RH shipment in this TA (4.67E-02 persons-rem) are somewhat higher than in 2008 TA (1.88E-02 persons-rem). This is because in the case of RH-TRU 72-B shipment the contribution from the stops to the crew dose is higher than the contribution to the dose while driving (Figure 4-19). As a result, the contribution from the additional stops considered in this TA is noticeable. There is one value in the 2008 TA that is significantly higher than the others and significantly higher than the values in this TA. This appears to have been a typographical error.

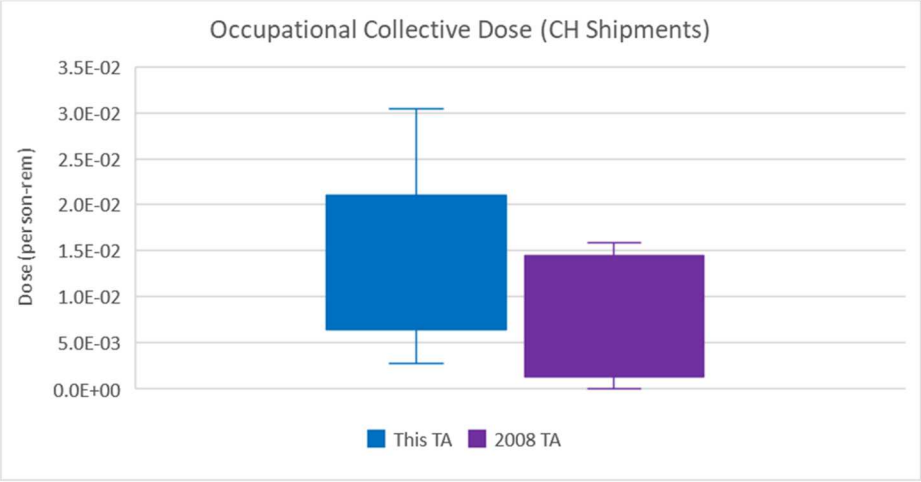

Figure 4-21. Comparison between the Occupational Collective Doses for CH Shipments.

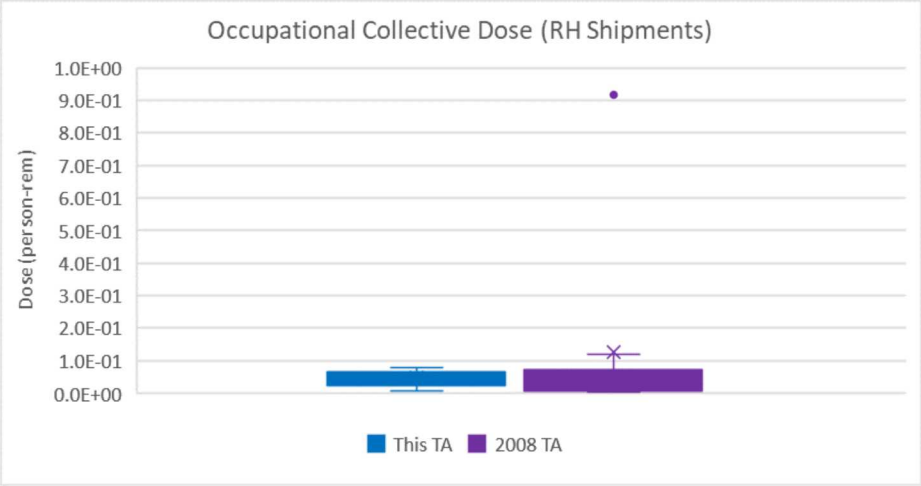

Figure 4-22. Comparison between the Occupational Collective Doses for RH Shipments.

Figure 4-23 compares the route specific collective doses to the crew for CH and RH shipments. The collective doses to the crew are higher for RH shipments. Figures 4-24 and 4-25 compare the per CH and per RH shipment collective doses to the people along the route, to the people sharing the route, and to the crew. The collective doses to the crew are higher and the range is larger, especially per RH shipment, compared to the non-occupational doses.

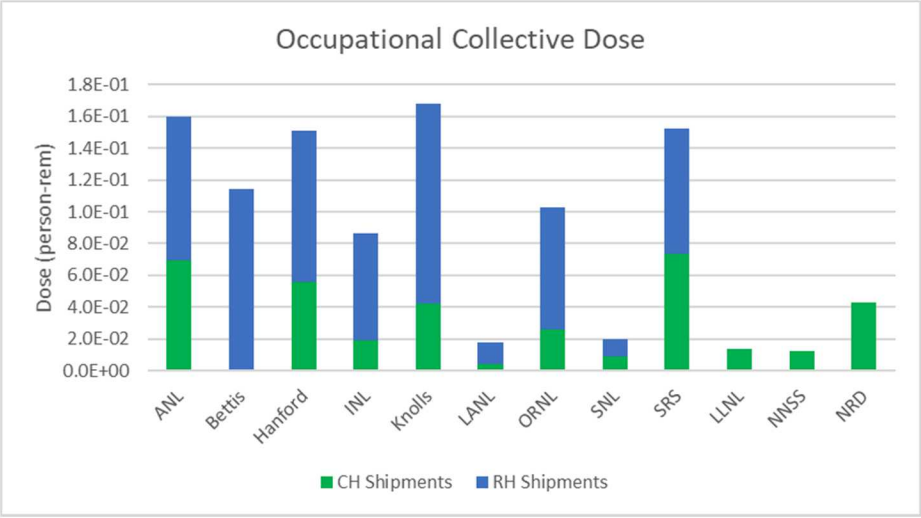

Figure 4-23. Route Specific per Shipment CH and RH Occupational Collective Doses.

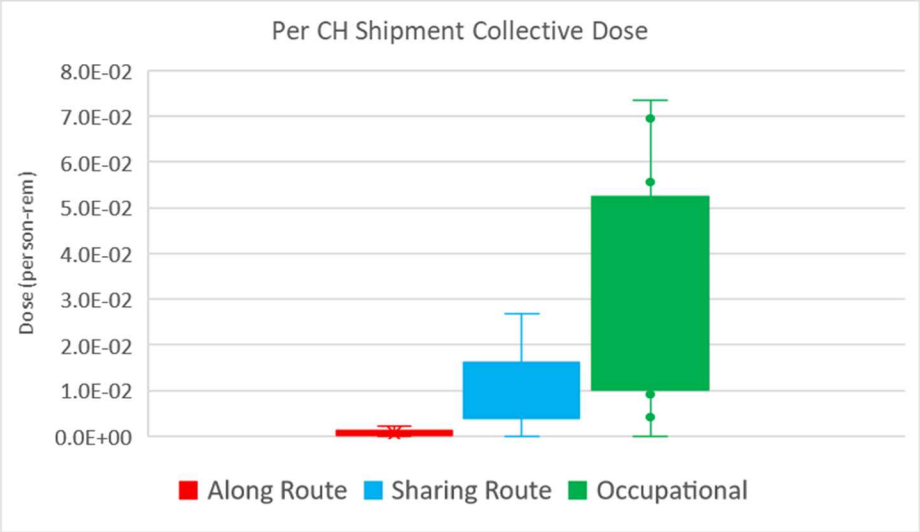

Figure 4-24. Comparison between Non-Occupational and Occupational Collective Doses for CH Shipments.

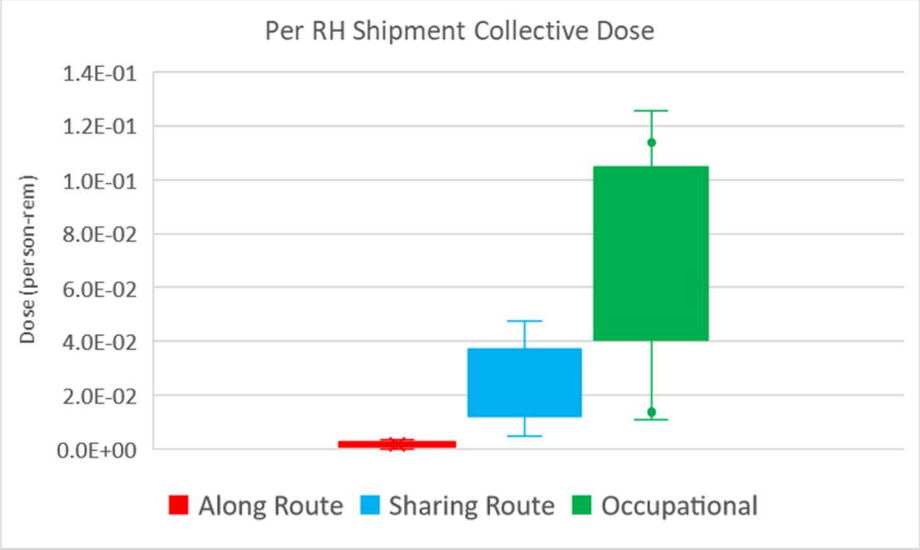

Figure 4-25. Comparison between Non-Occupational and Occupational Collective Doses for RH Shipments.

Figures 4-26 – 4-28 compare non-occupational and occupational collective doses for the CH shipments and the RH shipments.

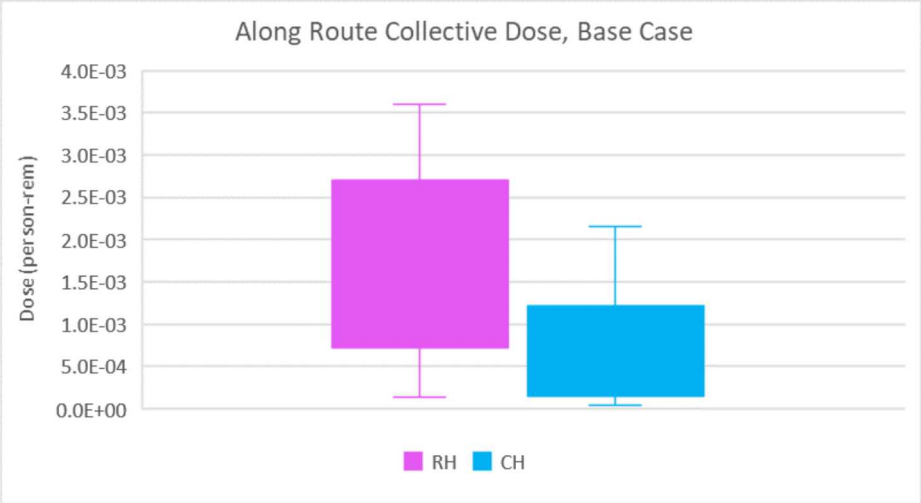

Figure 4-26. Along Route CH and RH Shipment Collective Doses.

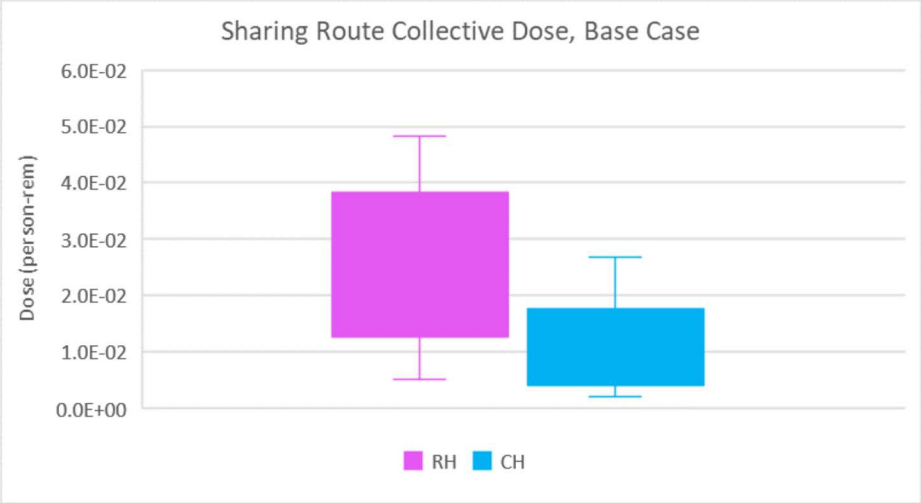

Figure 4-27. Sharing Route CH and RH Shipment Collective Doses.

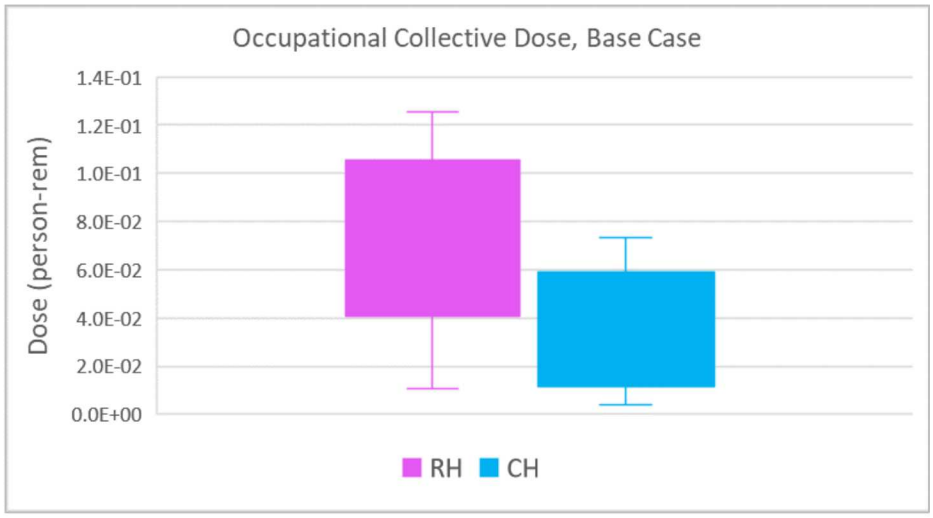

Figure 4-28. Occupational CH and RH Shipment Collective Doses.

Table 4-10 summarizes non-occupational and occupational collective doses. The per CH values are the average values of the different CH shipments. The RH value is the value calculated for RH-TRU 72-B. Table 4-11 provides the corresponding Latent Cancer Fatality (LCF) risks. The risk factor used in these calculations was $6x10^{-4}$ LCF/rem (ISCORS, 2002), the same as in the 2008 TA.

Table 4-10. Per Shipment Collective Doses from Routine Transport.

Route	Per Shipment Collective Dose (person-rem)					
	CH			RH		
	Occupational	Along Route	Sharing Route	Occupational	Along Route	Sharing Route
ANL	6.95E-02	1.28E-03	2.22E-02	9.02E-02	1.53E-03	2.64E-02
Bettis				1.14E-01	3.00E-03	4.61E-02
Hanford	5.56E-02	1.03E-03	1.60E-02	9.55E-02	1.66E-03	2.56E-02
INL	1.90E-02	3.31E-04	5.44E-03	6.72E-02	1.25E-03	2.06E-02
Knolls	4.25E-02	1.19E-03	1.58E-02	1.25E-01	3.60E-03	4.77E-02
LANL	4.19E-03	4.45E-05	1.81E-03	1.37E-02	1.69E-04	6.84E-03
ORNL	2.61E-02	5.91E-04	8.67E-03	7.67E-02	1.79E-03	2.62E-02
SNL	9.22E-03	1.09E-04	5.18E-03	1.08E-02	1.30E-04	6.18E-03
SRS	7.36E-02	2.16E-03	2.71E-02	7.88E-02	2.30E-03	2.87E-02
LLNL	1.35E-02	3.30E-04	1.64E-02			
NNSS	1.26E-02	1.74E-04	4.03E-03			
NRD	4.31E-02	8.07E-04	8.81E-03			

Table 4-11. Per Shipment LCF Risk from Routine Transport.

Route	Per Shipment LCF Risk					
	CH			RH		
	Occupational	Along Route	Sharing Route	Occupational	Along Route	Sharing Route
ANL	4.17E-05	7.69E-07	1.33E-05	5.41E-05	9.18E-07	1.58E-05
Bettis				6.84E-05	1.8E-06	2.77E-05
Hanford	3.33E-05	6.20E-07	9.59E-06	5.73E-05	9.94E-07	1.53E-05
INL	1.14E-05	1.98E-07	3.26E-06	4.03E-05	7.52E-07	1.24E-05
Knolls	2.55E-05	7.13E-07	9.46E-06	7.52E-05	2.16E-06	2.86E-05
LANL	2.51E-06	2.67E-08	1.08E-06	8.24E-06	1.01E-07	4.11E-06
ORNL	1.57E-05	3.55E-07	5.20E-06	4.6E-05	1.07E-06	1.57E-05
SNL	5.53E-06	6.54E-08	3.11E-06	6.5E-06	7.81E-08	3.71E-06
SRS	4.41E-05	1.30E-06	1.62E-05	4.73E-05	1.38E-06	1.72E-05
LLNL	8.09E-06	1.98E-07	9.83E-06			
NNSS	7.56E-06	1.05E-07	2.42E-06			
NRD	2.59E-05	4.84E-07	5.28E-06			

4.2.4 Sensitivity Analysis

The base case assumptions used to calculate the non-occupational and occupational collective doses in Sections 4.2.1 - 4.2.3 were modified as described below to evaluate their potential impacts on the results. The base case population increase corresponded to increase from 2010 (census) to 2018 (most recent data available). The projection of the future population increase was developed in Section 3.2. The projection considered the population increase from 2010 to 2030 and from 2010 to 2040. The population increase affects the collective dose to the people along the route and has no impact on the people sharing the route and the crew assuming no changes in the traffic count. Note that there is not sufficient data for projecting the traffic count changes as a function of the population changes. The effects of traffic count changes are considered independently from the population changes.

Figures 4-29 and 4-30 show the impacts from the projected future population increase on the collective doses to the residents along the route from CH and RH shipments. Using projected population increase results in a 12 percent (2030) and a 23 percent (2040) average increase in the collective doses.

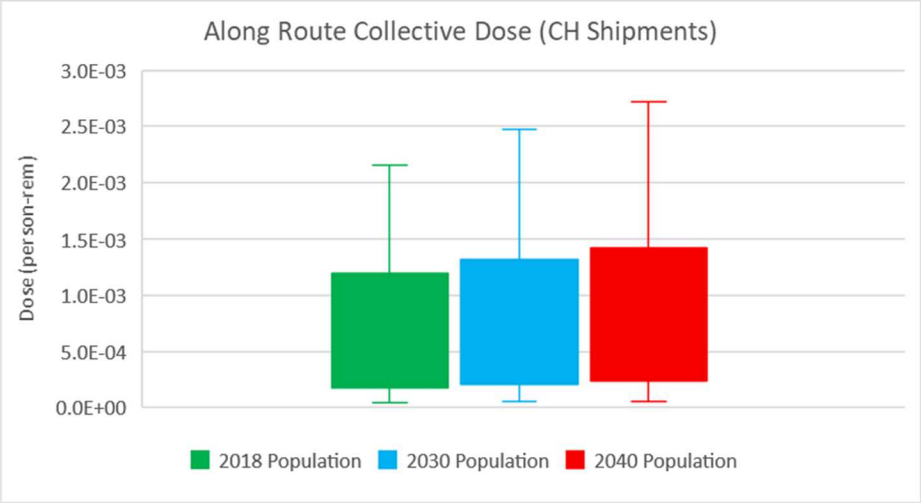

Figure 4-29. Impacts from Population Increase on Along the Route Collective Dose for CH Shipments.

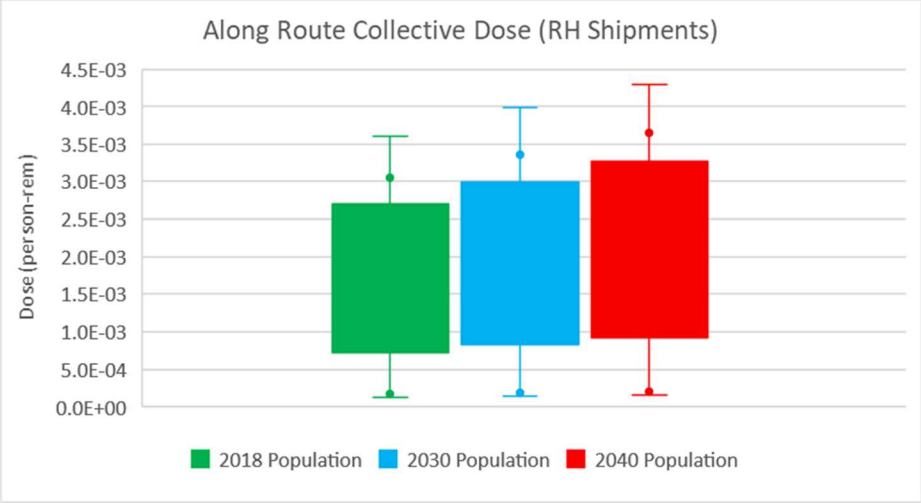

Figure 4-30. Impacts from Population Increase on Along the Route Collective Dose for RH Shipments.

In the base case scenario, the traffic count (vehicle per hour) within 20 percent of the suburban and urban segments of the route was doubled to account for rush hour. The traffic count affects the collective doses to the people sharing the route and has no impact on the residents along the route and the crew.

Figures 4-31 and 4-32 compare the per CH and per RH shipment collective doses to the people sharing the route for the base case and the case in which the rush hour traffic count was 2 times the base case values (4 times the non-rush hour traffic count). The average increase in the collective dose is 38 percent.

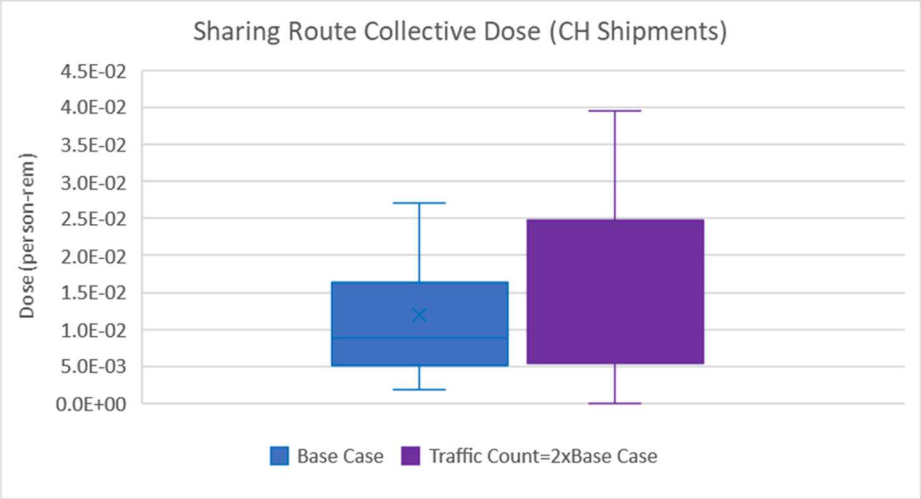

Figure 4-31. Impacts from Rush Hour Traffic on Sharing the Route Collective Dose for CH Shipments.

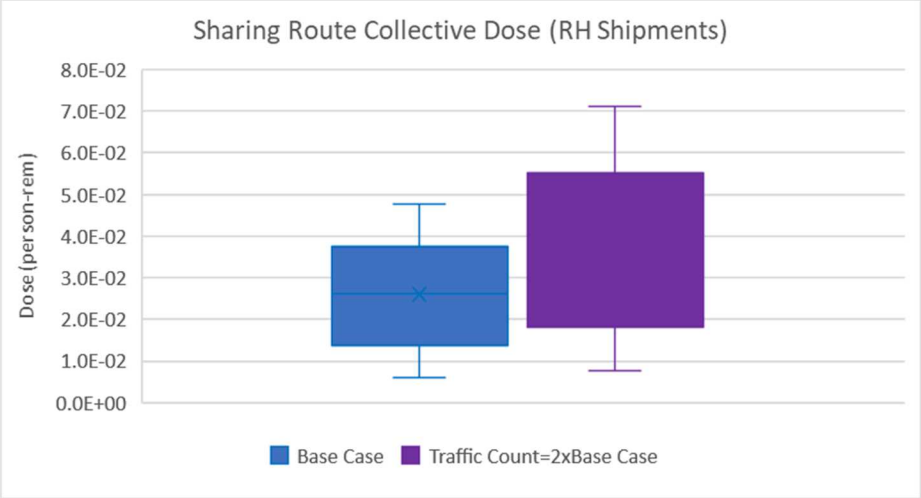

Figure 4-32. Impacts from Rush Hour Traffic on Sharing the Route Collective Dose for RH Shipments.

In the base case scenario, the area affected by the rush hour was set equal to 20 percent of the suburban and urban segments of the route. This parameter affects non-occupational and occupational collective doses because they all are a function of the vehicle speed.

Figures 4-33 and 4-34 compare the per CH and per RH shipment collective doses for the base case and the case in which the rush hour area is 40 percent of the suburban and urban areas. The average increase in the collective doses to the crew is only 1.6 percent. The average increase in the collective doses to the residents along the route is 12 percent. The highest average increase in dose (33 percent) is to the people sharing the route. This is because this dose to the people sharing the route is inversely proportional to the square of the vehicle speed while the other doses are inversely proportional to the speed.

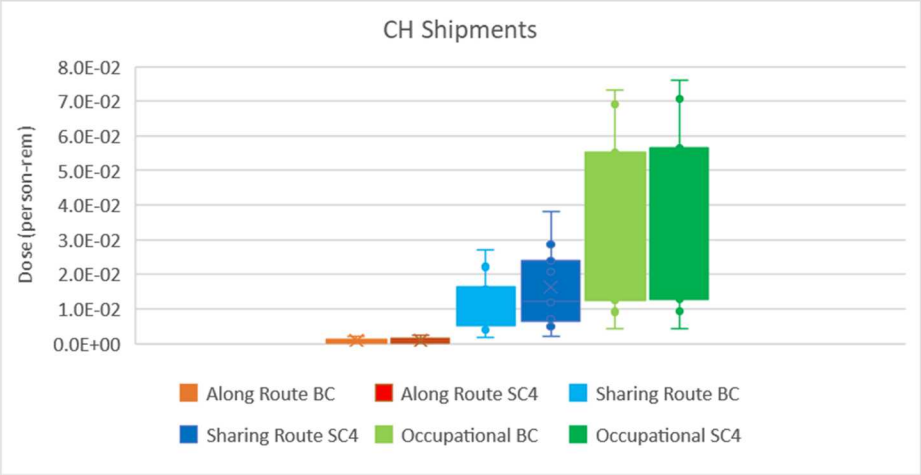

Figure 4-33. Impacts from Rush Hour Distance Traveled on Collective Doses for CH Shipments.

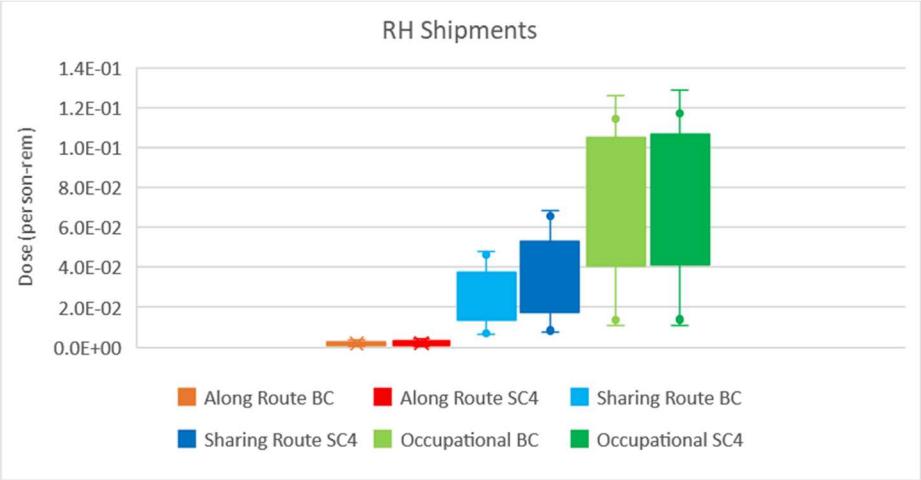

Figure 4-34. Impacts from Rush Hour Distance Traveled on Collective Doses for RH Shipments.

The collective doses are directly proportional to the package TIs. The base case considered the 95th percentile TIs. Figures 4-35 - 4-37 compare collective doses per CH shipment for the base case and for the 50th and 75th percentile cases. Using 75th percentile TIs for the CH shipments results in 21-23 percent decrease in the collective doses. Using 50th percentile TIs for the CH shipments results in 51-52 percent decrease in the collective doses. Figures 4-38 - 4-40 compare collective doses per RH shipment for the base case and for the 75th percentile case. The collective doses per RH shipment decrease by 73-86 percent. Note that the 75th and 50th percentiles TI of the RH shipment are the same (Section 3.6). Consequently, the decrease in the collective doses would be the same as well.

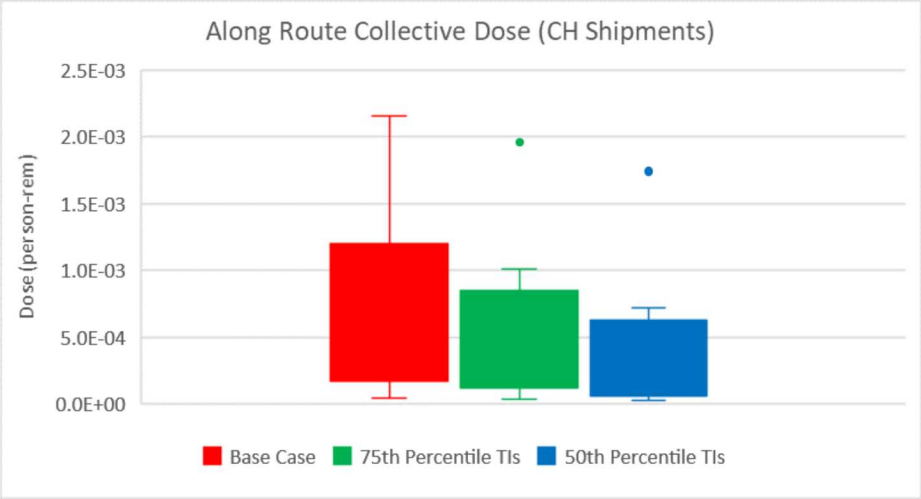

Figure 4-35. Along the Route Collective Doses for 95th, 75th, and 50th Percentile TIs, CH Shipments.

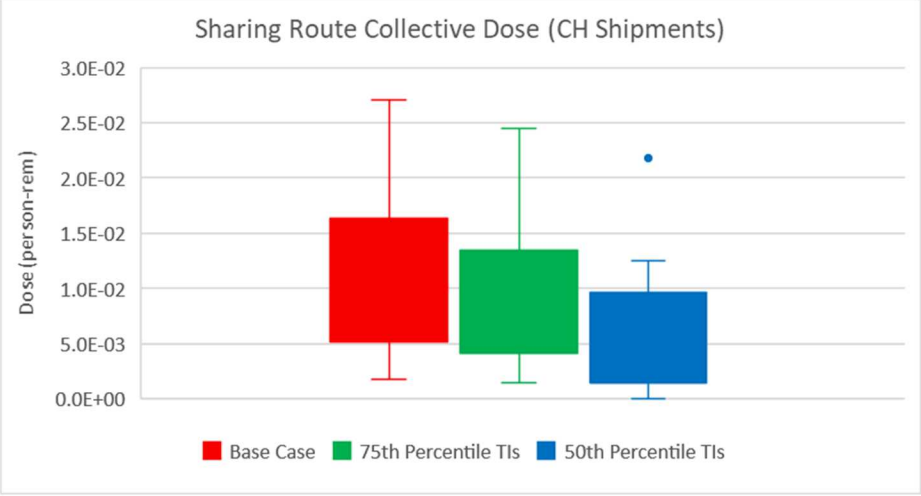

Figure 4-36. Sharing the Route Collective Doses for 95th, 75th, and 50th Percentile TIs, CH Shipments.

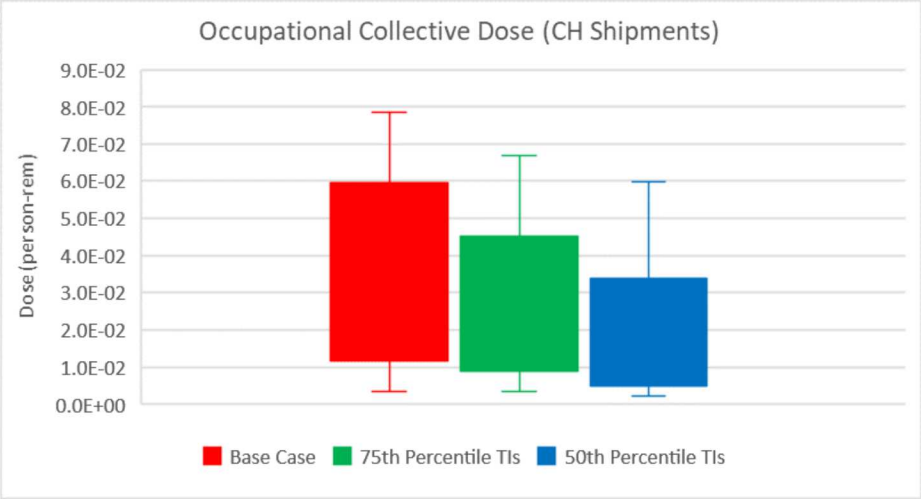

Figure 4-37. Occupational Collective Doses for 95th, 75th, and 50th Percentile TIs, CH Shipments.

Figure 4-38. Along the Route Collective Doses for 95th, 75th, and 50th Percentile TIs, RH Shipments.

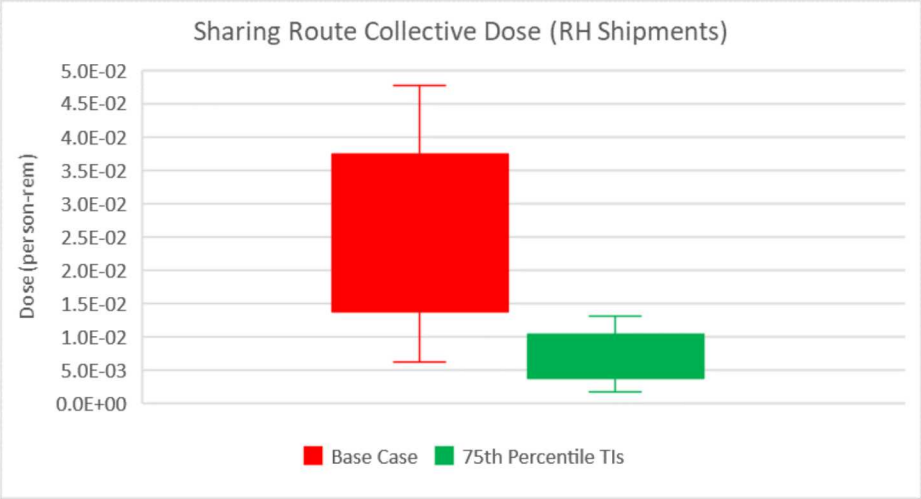

Figure 4-39. Sharing the Route Collective Doses for 95th, 75th, and 50th Percentile TIs, RH Shipments.

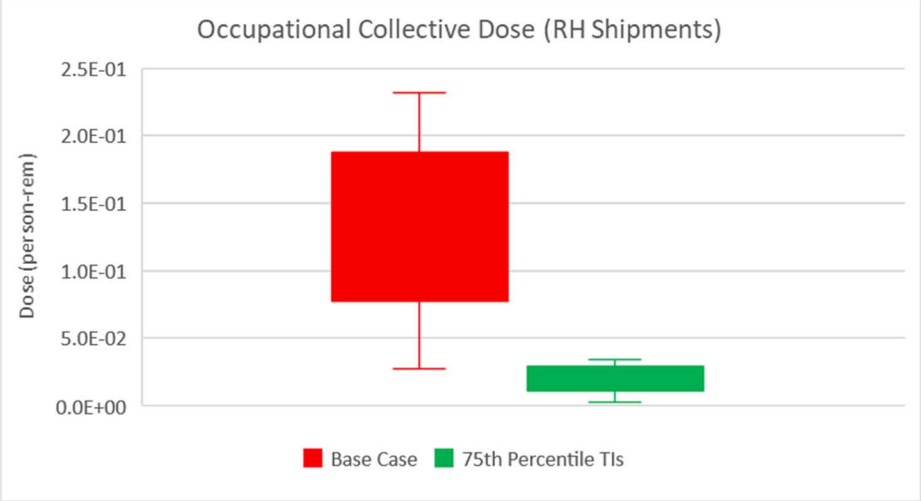

Figure 4-40. Occupational Collective Doses for 95th, 75th, and 50th Percentile TIs, RH Shipments.

Figure 4-41 and 4-42 compare the base case (BC) collective doses per CH and per RH shipment to the bounding case (SC7). The bounding case considered the 2040 population increase, two times higher traffic density during rush hour than in base case, and 40 percent of the suburban and urban segments of the route affected by the rush hour traffic. The collective doses to the crew are not plotted because they are the same as in Figures 4-33 and 4-34. The increase in the collective doses to the residents along the route is 41 percent. The increase in the collective doses to the people sharing the route is 109 percent. Table 4-12 summarizes the results of the cases considered above.

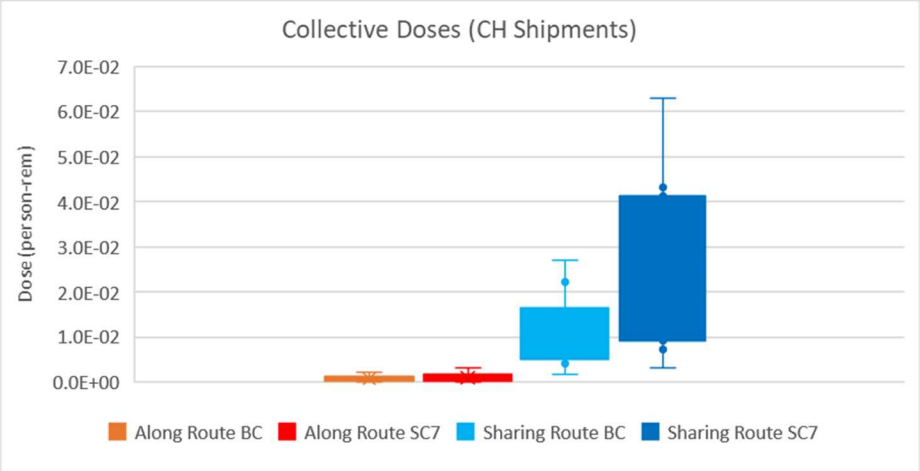

Figure 4-41. Impacts from Bounding Case on Collective Doses for CH Shipments.

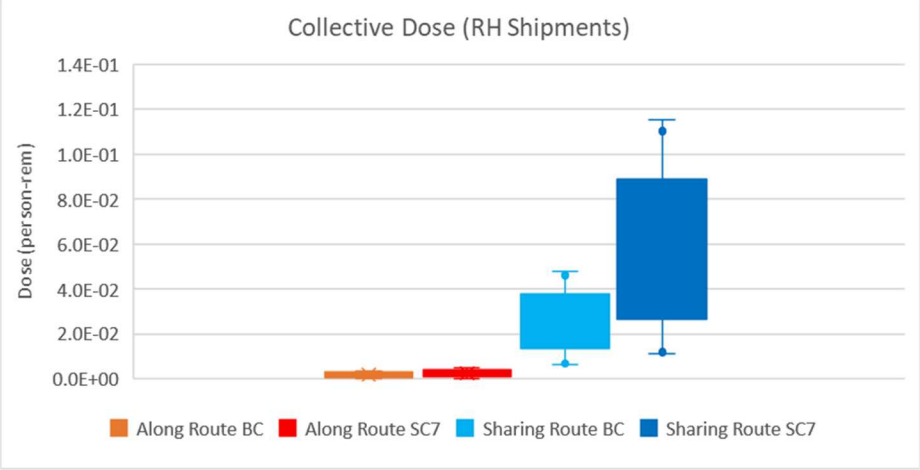

Figure 4-42. Impacts from Bounding Case on Collective Doses for RH Shipments.

Table 4-12. Percent Change in Collective Doses.

Sensitivity Case		Along Route		Sharing Route		Occupational (Crew)	
		CH	RH	CH	RH	CH	RH
Case 1	2030 Population	12.3%	11.9%	0.0%	0.0%	0.0%	0.0%
Case 2	2040 Population	23.2%	22.3%	0.0%	0.0%	0.0%	0.0%
Case 3	2xRush Hour Traffic Multiplier	0.0%	0.0%	37.5%	37.9%	0.0%	0.0%
Case 4	2xPercent Rush Hour	12.4%	12.2%	33.0%	33.4%	2.9%	1.5%
Case 5	75th Percentile TI	-22.8%	-72.9%	-21.7%	-72.5%	-20.9%	-86.0%
Case 6	50th Percentile TI	-52.1%	-72.9%	-51.4%	-72.5%	-51.0%	-86.0%
Case 7	Bounding Case	40.7%	39.4%	108.0%	109.2%	2.9%	1.5%

4.2.5 Residents near stop and people at the stops

Collective doses to the residents near stops were calculated for each stop including safety check stops, refueling stops, rest stops, and border inspections. The locations of the stops and the stop durations were defined for each route as described in Section 3.1. The truck stops were either in suburban or rural areas. The population density near each stop was obtained from WebTragis and then adjusted to account for the population increase since 2010. It was assumed that the residents are from 30 to 800 m from the location of the truck.

The collective doses to the people at the stops were calculated for the refueling stops only. It was assumed that there are 7 people at the refueling stop and they are from 1 m to 15 m from the truck. Table 4-13 summarizes per shipment and per campaign collective doses to the residents near stops for the different types of shipments. Table 4-14 summarizes per shipment and per campaign collective doses to the people at the refueling stops.

Figures 4-43 and 4-44 show the per shipment and per campaign collective doses to the residents near stops. Figures 4-45 and 4-46 show the per shipment and per campaign collective doses to the people at refueling stops.

The collective doses to the residents near stops per shipment of 3xHalfPACT with SCA and 1xRH-TRU 72-B shipments have higher collective doses than the other shipments. The per campaign collective doses are similar for 1xHalfPACT and 2xTRUPACT-II, 3xHalfPACT (SCA), 1xRH-TRU 72-B, and 3xTRUPACT-II with CCOs shipments. The collective doses per campaign are dominated by the number of shipments.

The collective doses to people at stops per shipment of 1xTRUPACT-III are lower (maximum of 1.5E-03 person-rem) and the collective doses per shipment of 3xHalfPACT (SCA) are higher (maximum of 9.9E-03 person-rem) compared to the other shipments. The per campaign collective doses are similar for 1x HalfPACT and 2xTRUPACT-II and 3xHalfPACT (SCA) shipments because the number of 1xHalfPACT and 2xTRUPACT-II shipments is significantly higher. The per campaign collective dose per shipment of 3xTRUPACT-II with CCOs is somewhat higher than the other shipments.

Table 4-13. Collective Doses to the Residents Near Stops.

Route	Shipment Type	Collective Dose (person-rem)					
		CH				RH	Total
		1xHalfPACT 2xTRUPACT_II	3xHalfPACT (SCA)	3xTRUPACT-II (CCO)	1x TRUPACT-III	1xRH-TRU 72-B	
ANL	Number of Shipments	28	79			136	
	Per shipment	5.69E-04	2.32E-03			1.72E-03	
	Per Campaign	1.59E-02	1.83E-01			2.34E-01	0.43
Bettis	Number of Shipments					12	
	Per shipment					1.08E-03	
	Per Campaign					1.30E-02	0.01
Hanford	Number of Shipments	5903	1669		281	362	
	Per shipment	5.53E-04	2.25E-03		3.29E-04	1.67E-03	
	Per Campaign	3.26E+00	3.76E+00		9.24E-02	6.06E-01	7.72
INL	Number of Shipments	3212			91	591	
	Per shipment	5.26E-04			3.13E-04	1.59E-03	
	Per Campaign	1.69E+00			2.85E-02	9.41E-01	2.66
Knolls	Number of Shipments	31				26	
	Per shipment	3.87E-04				1.17E-03	
	Per Campaign	1.20E-02				3.05E-02	0.04
LANL	Number of Shipments	5160			408	90	
	Per shipment	8.84E-06			5.26E-06	2.68E-05	
	Per Campaign	4.56E-02			2.15E-03	2.41E-03	0.05
ORNL	Number of Shipments	2997				1968	
	Per shipment	1.91E-04				5.77E-04	
	Per Campaign	5.71E-01				1.14E+00	1.71
SNL	Number of Shipments	8	10			5	
	Per shipment	6.80E-06	2.77E-05			2.06E-05	
	Per Campaign	5.44E-05	2.77E-04			1.03E-04	0.00

SRS	Number of Shipments	505	9	3877	7	66	
	Per shipment	2.04E-04	8.31E-04	1.17E-03	1.21E-04	6.18E-04	
	Per Campaign	1.03E-01	7.48E-03	4.52E+00	8.50E-04	4.08E-02	4.67
LLNL	Number of Shipments	209			40		
	Per shipment	1.80E-04			1.11E-04		
	Per Campaign	3.76E-02			4.46E-03		0.04
NNSS	Number of Shipments	34					
	Per shipment	7.74E-05					
	Per Campaign	2.63E-03					0.003
NRD	Number of Shipments	1					
	Per shipment	4.92E-04					
	Per Campaign	4.92E-04					0.0005
Total	**All Shipments**	**5.74**	**3.95**	**4.52**	**0.13**	**3.01**	**17.35**

Table 4-14. Collective Doses to People at Stops.

Route	Shipment Type	Collective Dose (person-rem)					
		CH				RH	Total
		1xHalfPACT 2xTRUPACT_II	3xHalfPACT (SCA)	3xTRUPACT-II (CCO)	1 TRUPACT-III	1xRH 72-B	
ANL	Number of Shipments	28	79			136	
	Per shipment	1.82E-03	7.40E-03			5.49E-03	
	Per Campaign	5.09E-02	5.85E-01			7.47E-01	1.38
Bettis	Number of Shipments					12	
	Per shipment					7.32E-03	
	Per Campaign					8.79E-02	0.09
Hanford	Number of Shipments	5903	1669		281	362	
	Per shipment	2.42E-03	9.87E-03		1.45E-03	7.32E-03	
	Per Campaign	1.43E+01	1.65E+01		4.06E-01	2.65E+00	33.86
INL	Number of Shipments	3212			91	591	
	Per shipment	1.21E-03			7.23E-04	3.66E-03	
	Per Campaign	3.89E+00			6.58E-02	2.16E+00	6.12
Knolls	Number of Shipments	31				26	
	Per shipment	2.42E-03				7.32E-03	
	Per Campaign	7.51E-02				1.90E-01	0.27
LANL	Number of Shipments	5160			408	90	
	Per shipment	0.00			0.00	0.00	
	Per Campaign	0.00			0.00	0.00	0.00
ORNL	Number of Shipments	2997				1968	
	Per shipment	1.21E-03				3.66E-03	
	Per Campaign	3.63E+00				7.20E+00	10.83
SNL	Number of Shipments	8	10			5	
	Per shipment	0.00	0.00			0.00	
	Per Campaign	0.00	0.00			0.00	0.00

Route	Shipment Type	Collective Dose (person-rem)					
		CH				RH	Total
		1xHalfPACT 2xTRUPACT_II	3xHalfPACT (SCA)	3xTRUPACT-II (CCO)	1 TRUPACT-III	1xRH 72-B	
SRS	Number of Shipments	505	9	3877	7	66	
	Per shipment	1.21E-03	4.93E-03	6.92E-03	7.23E-04	3.66E-03	
	Per Campaign	6.12E-01	4.44E-02	2.68E+01	5.06E-03	2.42E-01	27.70
LLNL	Number of Shipments	209			40		
	Per shipment	6.06E-04			3.61E-04		
	Per Campaign	1.27E-01			1.45E-02		0.14
NNSS	Number of Shipments	34					
	Per shipment	6.06E-04					
	Per Campaign	2.06E-02					0.02
NRD	Number of Shipments	1					
	Per shipment	2.42E-03					
	Per Campaign	2.42E-03					0.002
Total	**All Shipments**	**22.71**	**17.13**	**26.80**	**0.49**	**13.28**	**80.41**

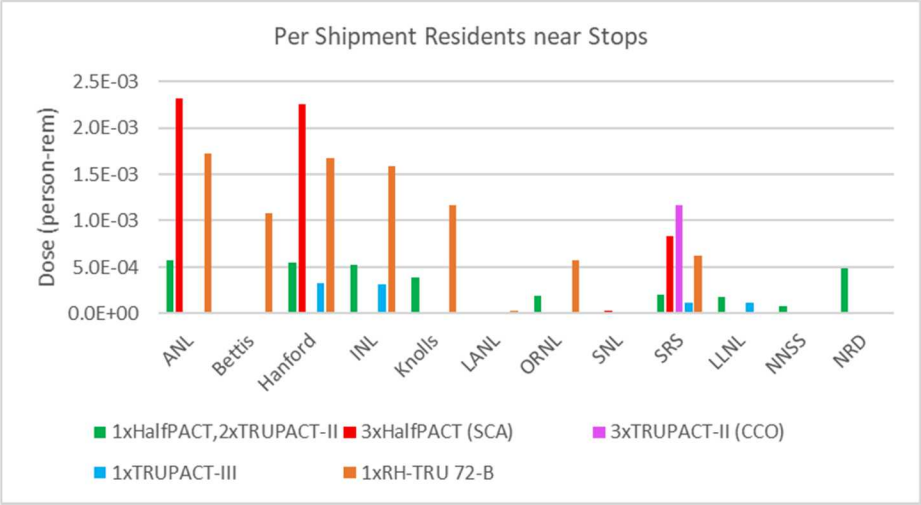

Figure 4-43. Per Shipment Collective Doses to the Residents Near Stops.

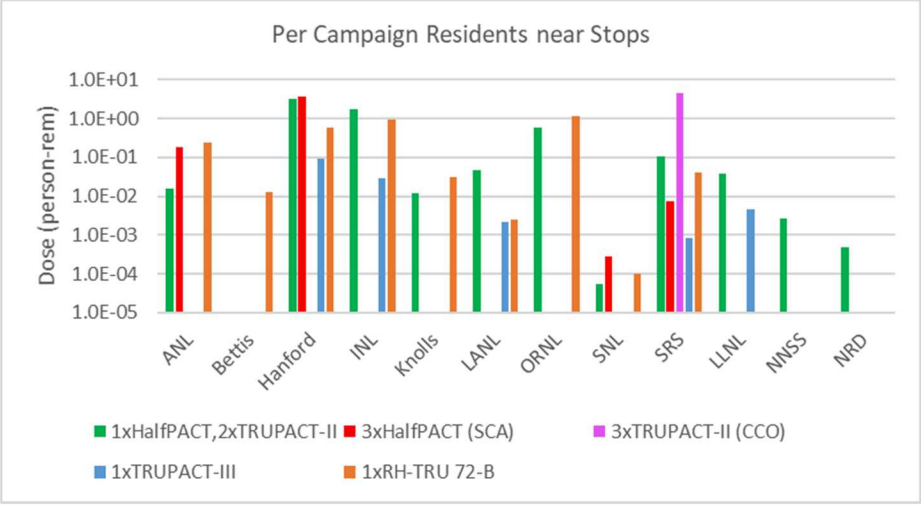

Figure 4-44. Per Campaign Collective Doses to the Residents Near Stops.

Figure 4-45. Per Shipment Collective Doses to People at Stops.

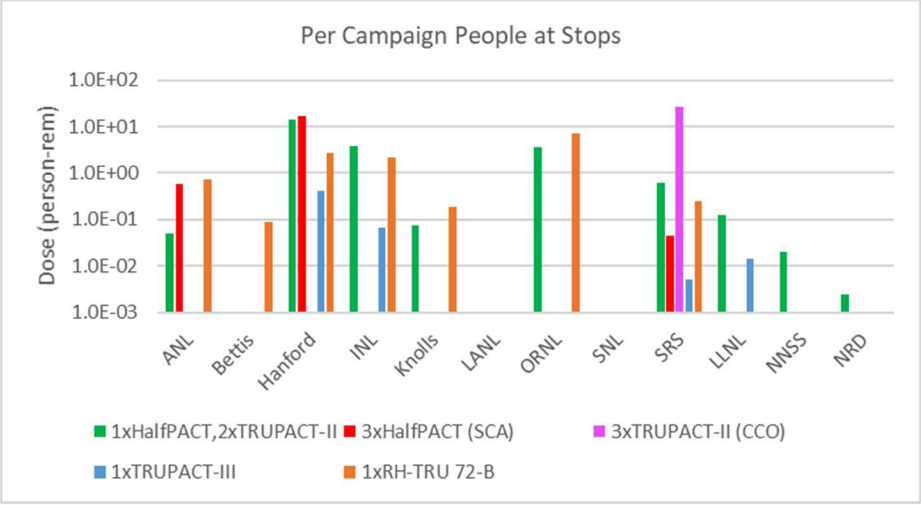

Figure 4-46. Per Campaign Collective Doses to People at Stops.

Figures 4-47 and 4-48 compare the collective doses to the residents at refueling stops to the doses at all the other stops per CH and RH shipments. In both cases, the collective doses at the refueling stops are lower than at the other stops. This is because the total time spent at the other stops is greater than the total time spent at the refueling stops.

Figure 4-49 compares the collective doses to the residents near stops and to the people at stops per CH and RH shipments. The collective doses to the residents near stops are similar for CH and RH shipments. The collective doses to the people at stops are noticeably lower for CH shipments. The collective doses to the people at the stops are higher than the collective doses to the residents near the stops for both, CH and RH shipments. This is because people at stops are significantly closer (1 to 15 m) to the WIPP truck than the residents (30 to 800 m from the truck).

Figure 4-47. Collective Doses to Residents near Stops (CH Shipments).

Figure 4-48. Collective Doses to Residents near Stops (RH Shipments).

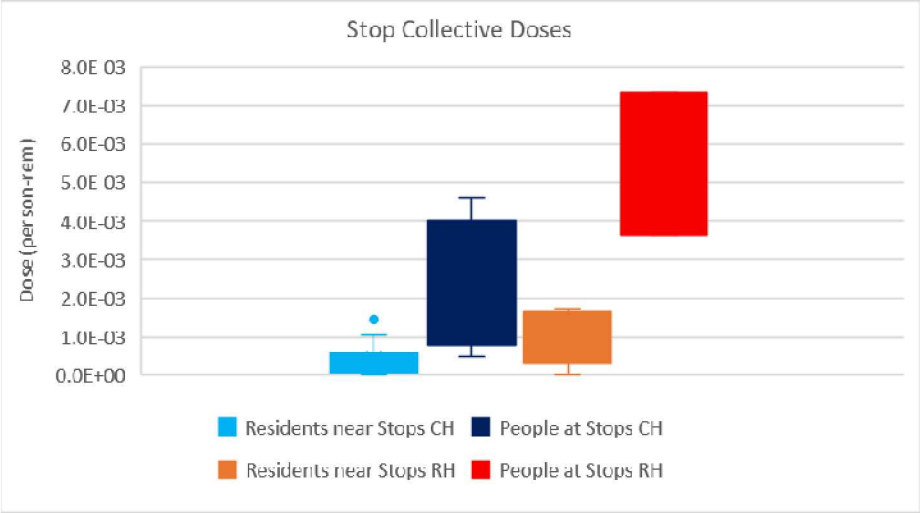

Figure 4-49. Collective Doses to Residents near Stops and People at Stops.

Figure 4-50 compares the per CH shipment collective doses to the residents near refueling stops calculated in this TA and in the 2008 TA. Figure 4-51 compares the per RH shipment collective doses to the people at the refueling stops calculated in this TA and in the 2008 TA. The doses used in this comparison were calculated using the same TIs for CH and RH shipments as in the 2008 TA. In both cases, the median doses in this TA are slightly higher than in 2008 TA. This is the result of the differences in routes and the number of stops as well as the population increase.

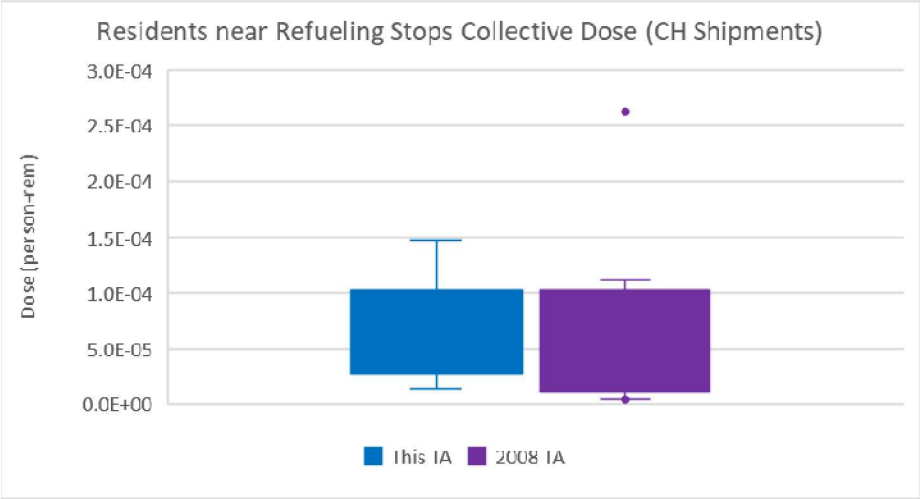

Figure 4-50. Comparison between the Collective Doses to Residents Near Stops (CH Shipments).

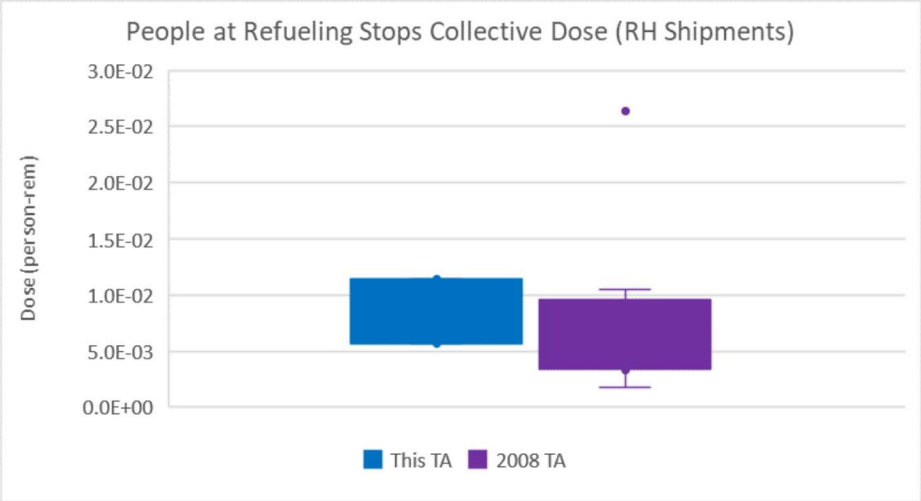

Figure 4-51. Comparison between the Collective Doses to People at Stops (RH Shipments).

Table 4-15 summarizes per shipment collective doses for stops. The per CH values are the average values of the different CH shipments. The RH value is the value calculated for RH-TRU 72-B shipments. Table 4-16 provides the corresponding LCF risks.

Table 4-15. Per Shipment Collective Doses for Stops.

Route	Per Shipment Collective Dose (person-rem)			
	CH Shipments		RH Shipments	
	Residents near Stops	People at Stops	Residents near Stops	People at Stops
ANL	1.44E-03	4.61E-03	1.72E-03	5.49E-03
Bettis			1.08E-03	7.32E-03
Hanford	1.04E-03	4.58E-03	1.67E-03	7.32E-03
INL	4.19E-04	9.67E-04	1.59E-03	3.66E-03
Knolls	3.87E-04	2.42E-03	1.17E-03	7.32E-03
LANL	7.05E-06		2.68E-05	
ORNL	1.91E-04	1.21E-03	5.77E-04	3.66E-03
SNL	1.73E-05		2.06E-05	
SRS	5.81E-04	3.45E-03	6.18E-04	3.66E-03
LLNL	1.46E-04	4.84E-04		
NNSS	7.74E-05	6.06E-04		
NRD	4.92E-04	2.42E-03		

Table 4-16. Per Shipment LCF Risks for Stops.

Route	Per Shipment LCF			
	CH		RH	
	Residents near Stops	People at Stops	Residents near Stops	People at Stops
ANL	8.66E-07	2.76E-06	1.03E-06	3.29E-06
Bettis			6.50E-07	4.39E-06
Hanford	6.26E-07	2.75E-06	1.00E-06	4.39E-06
INL	2.52E-07	5.80E-07	9.56E-07	2.20E-06
Knolls	2.32E-07	1.45E-06	7.03E-07	4.39E-06
LANL	4.23E-09		1.61E-08	
ORNL	1.14E-07	7.27E-07	3.46E-07	2.20E-06
SNL	1.04E-08		1.24E-08	
SRS	3.49E-07	2.07E-06	3.71E-07	2.20E-06
LLNL	8.74E-08	2.90E-07		
NNSS	4.65E-08	3.63E-07		
NRD	2.95E-07	1.45E-06		

The collective doses to the residents near stops depend on the population density near the stops. Figures 4-52 and 4-53 show the impacts from the projected future population increase on the collective doses to the residents near stops from CH and RH shipments. Using projected population increase results in 14 (CH) - 15 (RH) percent (2030) and 25 (RH) – 28 (CH) percent (2040) average increase in the collective doses.

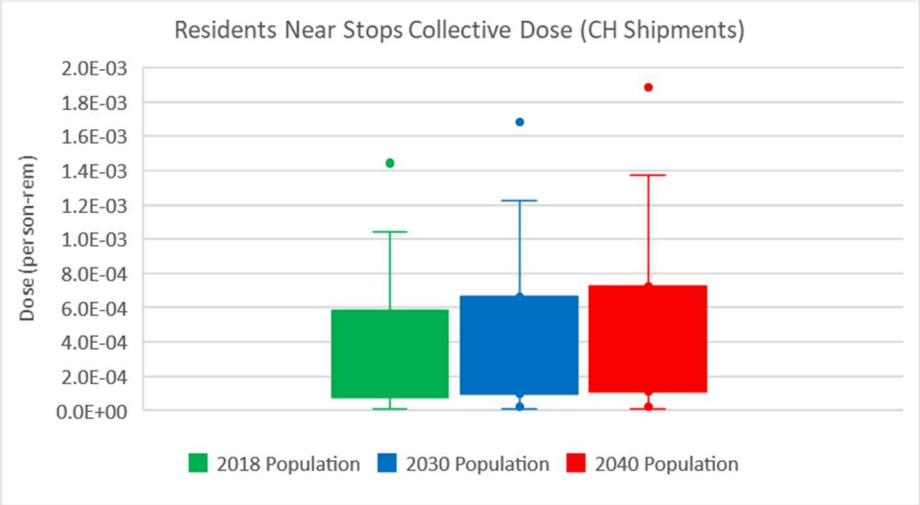

Figure 4-52. Impacts from Population Increase on Residents Near the Stops Collective Dose for CH Shipments.

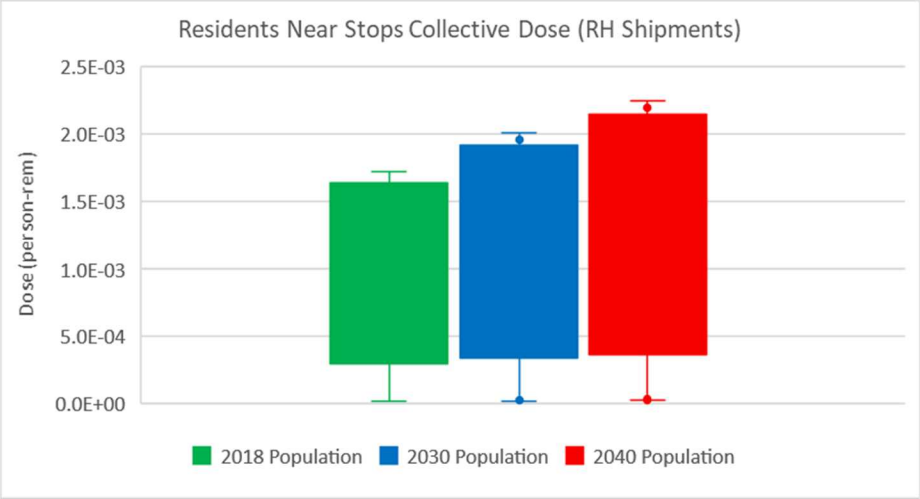

Figure 4-53. Impacts from Population Increase on Residents Near the Stops Collective Dose for RH Shipments.

The base case assumed 7 people at a refueling stop. The collective doses to the people at stops are directly proportional to the number of people at the stops. Doubling the number of people will result in doubling the doses as shown in Figures 4-54 and 4-55 for the CH and RH shipments.

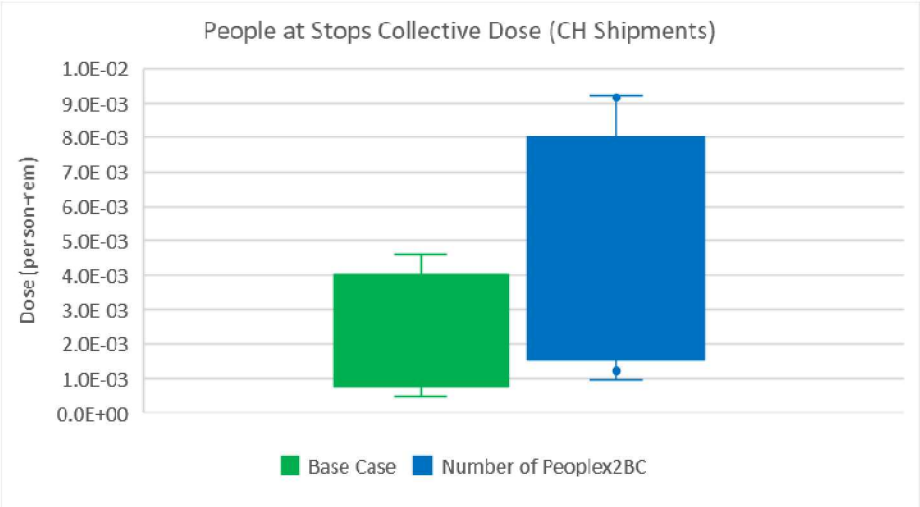

Figure 4-54. Impacts from Number of People at Stops on People at Stops Collective Dose for CH Shipments.

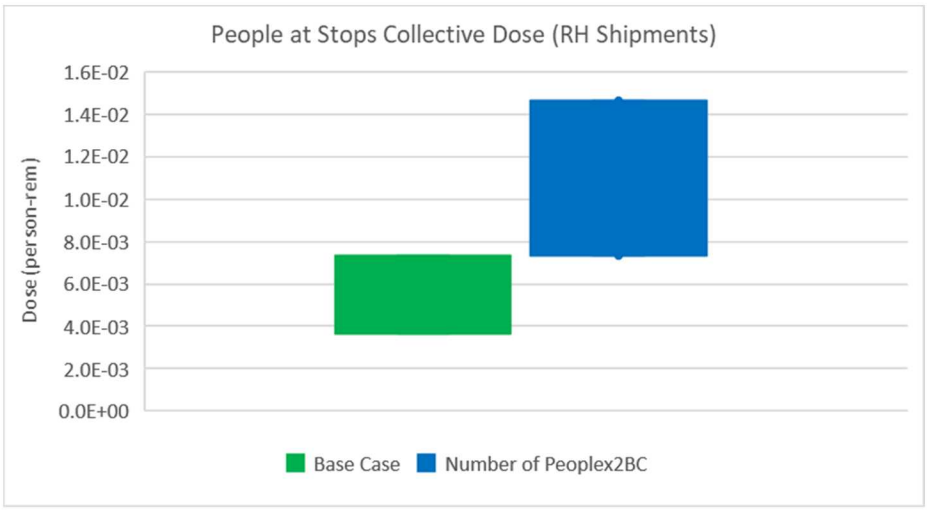

Figure 4-55. Impacts from Number at Stops on People at Stops Collective Dose for RH Shipments.

4.2.6 Refueling Station Employee

The dose to the refueling station employee was calculated assuming that the individual will be exposed to approximately 20 percent of all shipments over a 10-year period. This assumption is made on the basis that all trucks stop at the same location, an individual works for 10 years at the truck stop, and there are 3 shifts per day at the truck stop. The assumed stop duration was 20 minutes. These are the same assumptions as in the 2008 TA.

Table 4-17 summarizes the doses and LCF risks to the refueling station employee for a 20 min stop (base case) and for a 50 min stop. The annual doses to the employee were divided by an average background radiation dose of 0.31 rem/yr (NCRP No. 160) and are shown in this table as percent background. Note that the background radiation dose used in the 2008 TA was 0.36 rem/yr.

Figure 4-56 shows the route specific refueling station employee doses for 20 min and 50 min stops. The doses to employee are directly proportional to the duration of the stop that defines the exposure time. The maximum dose is 0.19 rem for the 20 min stop and 0.47 rem for the 50 min stop. The doses are very small for the routes with fewer shipments. For example, the dose to the refueling station employee on the NRD route is 1.3E-05 rem.

Using the same TIs as in the 2008 TA results in the average dose to the employee (across all routes) of 0.1 rem. The average dose to the refueling station employee in the 2008 TA was 0.18 rem. Note that the number of shipments is the major parameter in these calculations. The differences in the number of shipments along the different routes result in the different route specific doses to the employee and affect the mean value across all the routes.

Table 4-17. Doses and LCF Risks to a Refueling Stop Employee.

Route	20 min Stop				50 min Stop			
	Total Dose (rem)	10-Year Dose (rem)	Percent Background	LCF Risk	Total Dose (rem)	10-Year Dose (rem)	Percent Background	LCF Risk
ANL	3.95E-02	7.59E-03	0.24%	4.56E-06	9.87E-02	1.90E-02	0.61%	1.14E-05
Bettis	2.51E-03	4.83E-04	0.02%	2.90E-07	6.28E-03	1.21E-03	0.04%	7.24E-07
Hanford	9.66E-01	1.86E-01	6.00%	1.12E-04	2.42E+00	4.65E-01	14.99%	2.79E-04
INL	1.75E-01	3.36E-02	1.08%	2.02E-05	4.37E-01	8.41E-02	2.71%	5.04E-05
Knolls	7.58E-03	1.46E-03	0.05%	8.75E-07	1.90E-02	3.65E-03	0.12%	2.19E-06
LANL								
ORNL	3.10E-01	5.95E-02	1.92%	3.57E-05	7.74E-01	1.49E-01	4.80%	8.93E-05
SNL								
SRS	7.93E-01	1.52E-01	4.92%	9.15E-05	1.98E+00	3.81E-01	12.29%	2.29E-04
LLNL	4.03E-03	7.75E-04	0.03%	4.65E-07	1.01E-02	1.94E-03	0.06%	1.16E-06
NNSS	5.88E-04	1.13E-04	0.004%	6.79E-08	1.47E-03	2.83E-04	0.01%	1.70E-07
NRD	6.92E-05	1.33E-05	0.0004%	7.99E-09	1.73E-04	3.33E-05	0.001%	2.00E-08

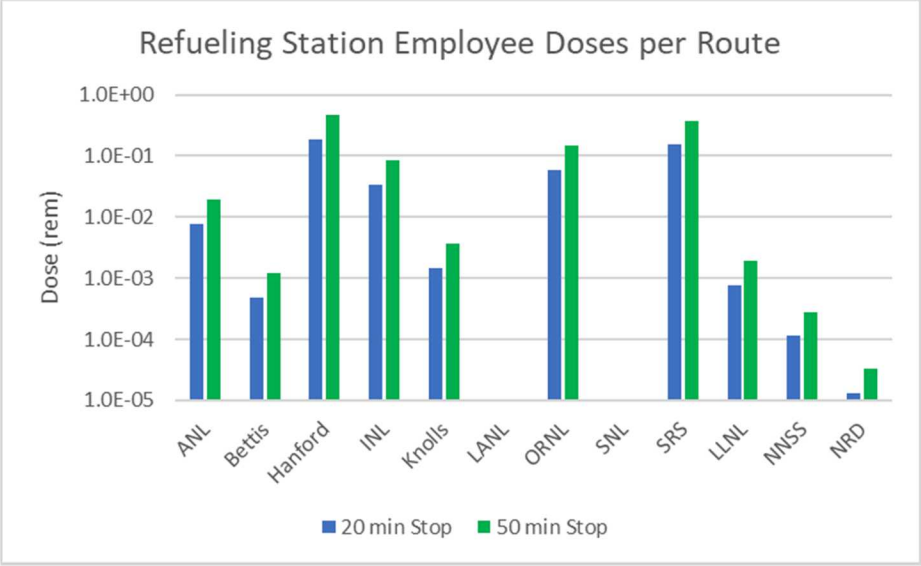

Figure 4-56. Route Specific Refueling Station Employee Doses.

Figure 4-57 compares the base case scenario to a few different scenarios. These scenarios are:

- The employee exposure to 40 percent (2 times base case) of all the shipments along the route
- 50 min stop
- 50 min stop and the employee exposure to 40 percent (2 times base case) of all the shipments along the route.
- 50th percentile TIs

The dose to the employee is directly proportional to the number of shipments to which the employee is exposed, to the duration of the stop, and to the TIs. The 50 min stop and exposure to 40 percent of shipments bring the maximum employee dose to 0.93 rem, 5 times higher than in base case. However, considering the 50th percentile TIs instead of 95th percentile used in base case results in significant reduction in the dose to the employee.

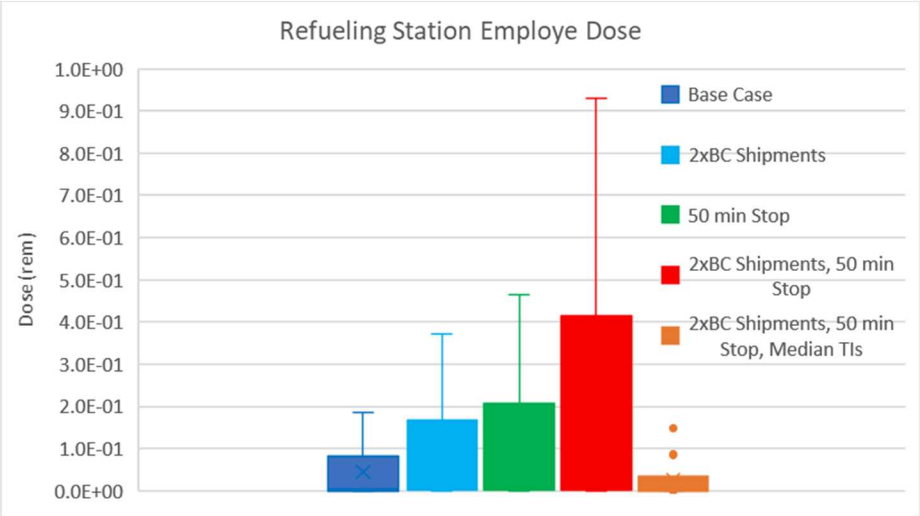

Figure 4-57. Refueling Station Employee Doses for Different Scenario Parameters.

4.2.7 State Inspector

The doses to the state inspector were calculated for an inspector at the CO/NM border and an inspector at the TX/NM border. Note that the dose to an inspector at the WY/CO border (conducted at Fort Collins, CO) will be the same as the dose to an inspector at the CO/NM border because the number of shipments is the same. Per Attachment A of WIPP Nuclear Waste Partnership (2020), the inspections are performed when the WIPP trucks enter NM. The port of entry is Raton for shipments traveling south and Eunice (NM) for shipments from the southern routes. The inspections are not required at the other state borders. Note that in the 2008 TA the inspections were done at each state border crossed by the transportation route.

The doses to the state border inspectors were calculated assuming that the state border inspector would be involved in 20 percent of the inspection over a 10-year period with an average exposure distance of approximately 1 meter and inspection time of 1 hr. These are the same assumptions as in the 2008 TA.

Table 4-18 summarizes the doses to the state inspectors. The annual dose to the inspector was divided by an average background radiation dose (0.31 rem/yr) and is shown in this table as percent background.

Table 4-18. Doses and LCF Risks to State Inspectors.

Border	Number of CH Shipments	Number of RH Shipments	Dose (rem)	LCF Risk	Percent Background Dose
Fort Collins (CO)	11,263	1,089	2.22	1.33E-03	71.59%
CO/NM	11,263	1,089	3.62	2.17E-03	116.90%
TX/NM	7,426	2,072	2.22	1.33E-03	71.59%

The 2008 TA assumed one location on the NM border, 22,888 (CH) and 5,691 (RH) shipments. The calculated inspector dose was 5.2 rem. Note that the number of shipments is the major parameter in these calculations. The differences in the number of shipments results in the difference in the doses.

Figure 4-58 shows the doses to the state inspectors for 50th, 75th, and 95th percentile TIs. The doses calculated using the 50th percentile TIs are 1.3 times lower for the TX/NM border inspector and 2.5 times lower for the CO/NM border inspector.

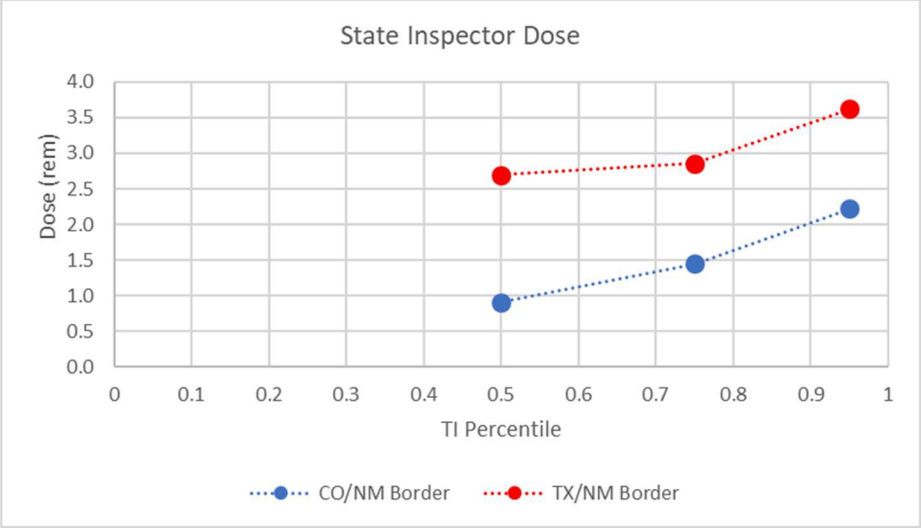

Figure 4-58. State Inspector Dose for 50th, 75th, and 95th Percentiles TIs.

4.2.8 Origin Site Inspectors

The doses to the inspector at the generator site were calculated using the following assumptions. The exposure distance was assumed to be 1 meter and the exposure duration (inspection time) was assumed to be one hour. The inspector was assumed to be working at the same job for 10 years with two shifts working the same job. These are the same assumptions as in the 2008 TA.

Table 4-19 summarizes the doses and LCF risks to the on-site inspectors. The annual doses to the inspectors were divided by an average background radiation dose (0.31 rem/yr) and are shown in this table as percent background. Figure 4-59 shows the route specific doses to the on-site inspectors for the CH and RH shipments. The maximum 10-year dose is 6 rem (SRS route). The majority of the doses are below 2 rem.

Table 4-19. Doses and LCF Risks to On Site Inspectors.

Site	10-yr Dose (rem)		Total 10- yr Dose (rem)	LCF Risk	%Background Dose
	CH Shipments	RH Shipments			
ANL	7.39E-03	2.34E-01	2.41E-01	1.45E-04	7.78%
Bettis	0.00E+00	1.32E-02	1.32E-02	7.89E-06	0.42%
Hanford	1.61E+00	2.19E+00	3.80E+00	2.28E-03	122.44%
INL	8.63E-01	6.48E-01	1.51E+00	9.07E-04	48.74%
Knolls	8.18E-03	2.85E-02	3.67E-02	2.20E-05	1.18%
LANL	1.43E+00	9.87E-02	1.53E+00	9.18E-04	49.37%
ORNL	7.91E-01	2.16E+00	2.95E+00	1.77E-03	95.10%
SNL	2.11E-03	1.62E-02	1.83E-02	1.10E-05	0.59%
SRS	5.98E+00	8.20E-02	6.06E+00	3.64E-03	195.54%
LLNL	6.20E-02	0.00E+00	6.20E-02	3.72E-05	2.00%
NNSS	8.97E-03	0.00E+00	8.97E-03	5.38E-06	0.29%
NRD	2.64E-04	0.00E+00	2.64E-04	1.58E-07	0.01%

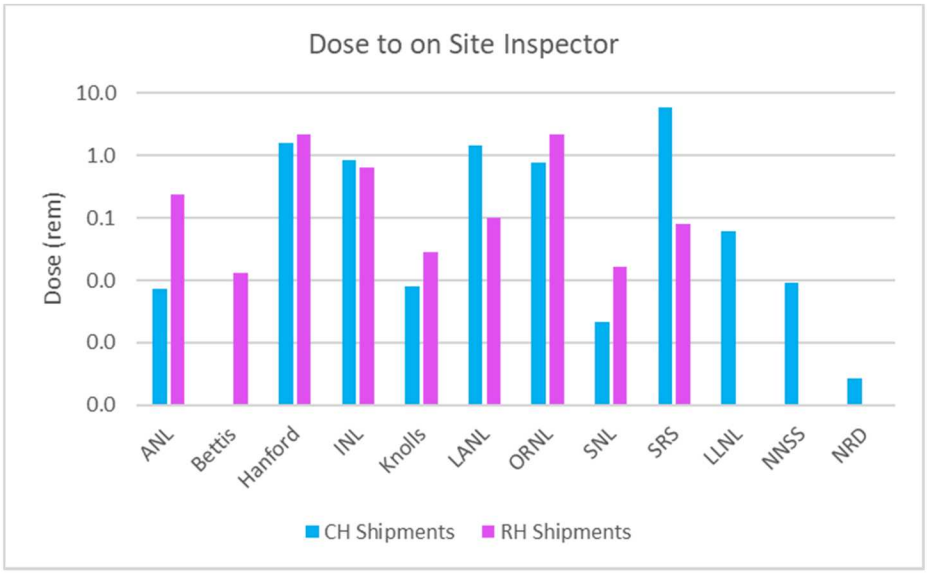

Figure 4-59. Doses to On-Site Inspectors from CH and RH Shipments.

Figure 4-60 compares the doses to the on-site inspectors from all the shipments (CH and RH) to the corresponding 2008 TA doses. The doses used in this comparison were calculated using the same TIs for CH and RH shipments as in the 2008 TA. The ranges are similar, except one value in the 2008 TA is significantly higher than all the others. Note that the number of shipments generated at each site impacts the dose to the on-site inspector. The different number of shipments in this TA and in the 2008 TA contributes to the differences in the calculated doses.

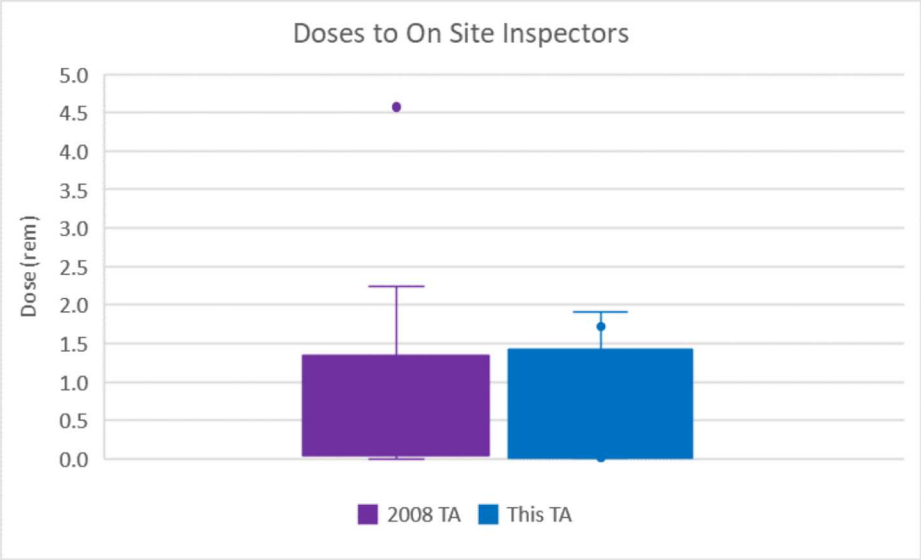

Figure 4-60. Comparison between the Total 10-Year Doses to the On-Site Inspectors.

Figure 4-61 shows the doses to the on-site inspectors for the 50th, 75th, and 90th percentile of TIs. Note that the TI of 3xTRUPACT-II with CCOs is constant and equal to 4 mrem/hr. Consequently, the maximum doses to the inspector at the SRS site don't change. The doses to the inspectors at the other sites are noticeably smaller for the 75th and 50th percentile TIs.

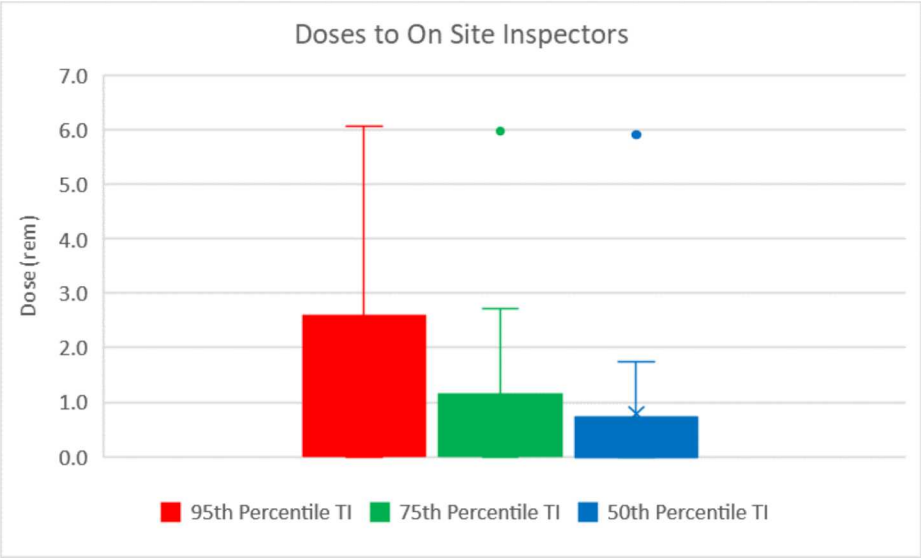

Figure 4-61. Doses to the On-Site Inspectors for 50th, 75th, and 95th Percentiles TIs.

4.2.9 Person in a Traffic Jam

The dose to a person in a traffic jam was calculated assuming an individual in a traffic jam 2 meters laterally from a WIPP-bound truck. The traffic jam lasts for 30 minutes and the person is not shielded by the vehicle he or she is occupying. Note that this is a one-time exposure. These are the same assumptions as in the 2008 TA.

Table 4-20 summarizes the doses to the person in a traffic jam for the different types of shipments. The values are provided for the 95th (base case), 75th, and 50th percentile TIs. Figure 4-62 shows the dose to the person in a traffic jam for the CH and RH shipments. The maximum dose is 2.9E-03 rem for a RH shipment assuming 95th percentile TI.

Using the same TIs as in the 2008 TA results in 4.8E-04 rem for a CH shipment and 1.8E-03 rem for a RH shipment. The corresponding values in the 2008 TA were 5.2E-04 rem (CH shipment) and 1.2E-03 rem (RH shipment). Slight difference might be related to the differences in the critical dimension of the CH and RH shipment as pointed out in Section 4.1.

Table 4-20. Doses to a Person in a Traffic Jam.

Shipment Type	Dose (rem)		
	TI Percentile		
	95th	75th	50th
1xHalfPACT&2xTRUPACT-II	6.85E-04	4.90E-04	1.96E-04
3xHalfPACT (RH)	2.79E-03	2.25E-03	1.76E-03
3xTRUPACT-II (CCO)	3.92E-03	3.92E-03	3.92E-03
1xTRUPACT-III	4.47E-04	4.47E-04	4.47E-04
1xRH-TRU 72-B	2.86E-03	7.87E-04	7.87E-04

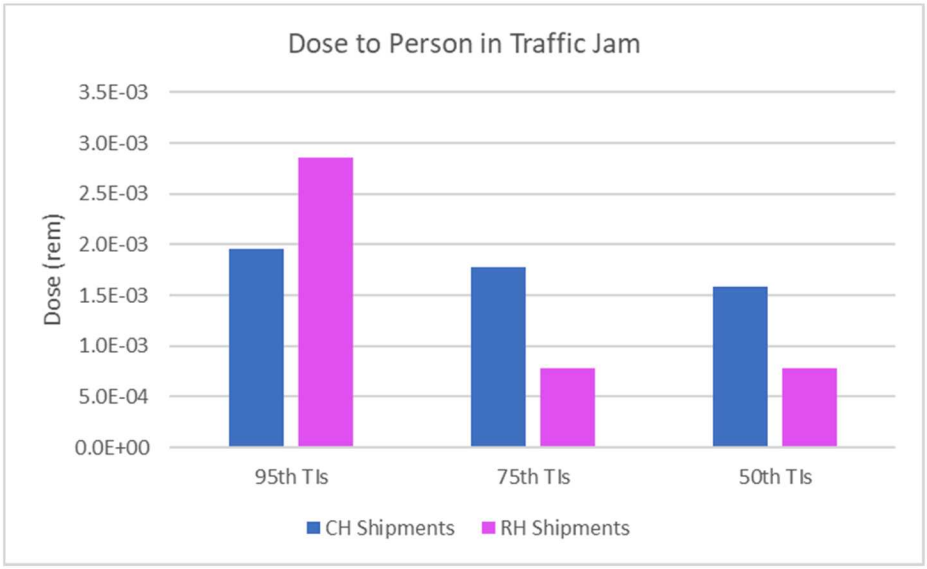

Figure 4-62. Doses to a Person in a Traffic Jam from CH and RH Shipments.

5. NON-RADIOLOGICAL IMPACTS

The inputs into the non-radiological impact calculations are:

- Total distance along each route, Table 3-14.
- Number of shipments along each route, Table 3-20.
- Accident, injury, and fatality rates for the states crossed by the WIPP routes, Table 3-19.

The non-radiological impacts per shipment and per campaign for each route were calculated using Eq. 2-16 – 2-18. They are expressed in the form of an aggregate number of accidents, injuries, and fatalities likely to occur as a result of transporting the TRU waste packages round trip between the generator sites and the WIPP facility and between the generator sites and INL.

The results of non-radiological impacts are summarized in Table 5-1. Also provided in Table 5-1 are the campaign total accidents, fatalities, and number of shipments from the 2008 TA. The routes that changed since 2008 as described in Section 3.1 are shown in red font in this table. The route that was not considered in 2008 is shown in purple font.

Table 5-1. Summary of Non-Radiological Impacts.

Route	Per Shipment			Per Campaign			Number of Shipments	Shipment mi
	Accidents	Injuries	Fatalities	Accidents	Injuries	Fatalities		
ANL	2.35E-03	3.80E-04	3.81E-05	5.70E-01	9.23E-02	9.26E-03	243	1,739
Bettis	3.43E-03	1.65E-03	1.04E-04	4.12E-02	1.99E-02	1.25E-03	12	2,145
Hanford	2.20E-03	4.26E-04	4.12E-05	1.80E+01	3.50E+00	3.39E-01	8,215	1,814
INL	1.72E-03	3.29E-04	3.12E-05	6.68E+00	1.28E+00	1.21E-01	3,894	1,397
Knolls	3.83E-03	1.96E-03	1.12E-04	2.18E-01	1.12E-01	6.38E-03	57	2,303
LANL	4.02E-04	2.16E-04	1.99E-05	2.27E+00	1.22E+00	1.12E-01	5,658	364
ORNL	2.11E-03	1.18E-03	7.64E-05	1.05E+01	5.86E+00	3.79E-01	4,965	1,449
SNL	3.51E-04	1.89E-04	1.74E-05	8.07E-03	4.35E-03	3.99E-04	23	319
SRS	2.27E-03	1.33E-03	8.40E-05	1.01E+01	5.93E+00	3.75E-01	4,464	1,532
LLNL	1.60E-03	1.28E-04	1.30E-05	3.99E-01	3.20E-02	3.23E-03	249	955
NNSS	1.23E-03	9.11E-05	9.22E-06	4.18E-02	3.10E-03	3.13E-04	34	768
NRD, LLC	3.70E-03	5.97E-04	3.83E-05	3.70E-03	5.97E-04	3.83E-05	1	2,366
Total annual (this TA)				**0.94**	**0.35**	**0.03**		
Total (this TA)				**48.90**	**18.05**	**1.35**	**27,815**	**17,150**
Total 2008 TA				**365.71**	**N/A**	**1.37**	**27,579**	

NOTE: Routes that changed since 2008 are shown in red font.

This TA used the same approach and assumptions to non-radiological impact assessment as the 2008 TA. It was assumed that the carrier drivers of TRU waste would not be more careful than other truck drivers on the nation's roads. The impacts were calculated for roundtrip because this analysis is not dependent on whether a truck is transporting full or empty TRU waste packages.

The differences in the results are largely due to the differences in the accident and fatality rates. As discussed in Section 3.4, the 2018 accident rates (accident/km) are significantly smaller than the assumed 2008 accident rates. In the 2008 TA same fatalities per accident value was assumed for all states. The 2018 fatalities rates (fatalities/km) were state specific and generally higher than 2008 fatality rates. Note that the

total number of shipments is comparable. Some differences (though they are smaller) are also due to the changes in the routes. The total fatalities per campaign (1.35) is very close to the 2008 TA (1.37). However, the campaign duration assumed in the 2008 TA was different (35 years).

Figure 5-1 and 5-2 compare the accidents per shipment and fatalities per shipment to the 2008 TA values. The number of accidents per shipment is lower than in 2008 and the number of fatalities per shipment is higher. The spread in the fatalities per shipment is larger because the number of fatalities per accident is state specific compared to a constant value used in the 2008 TA.

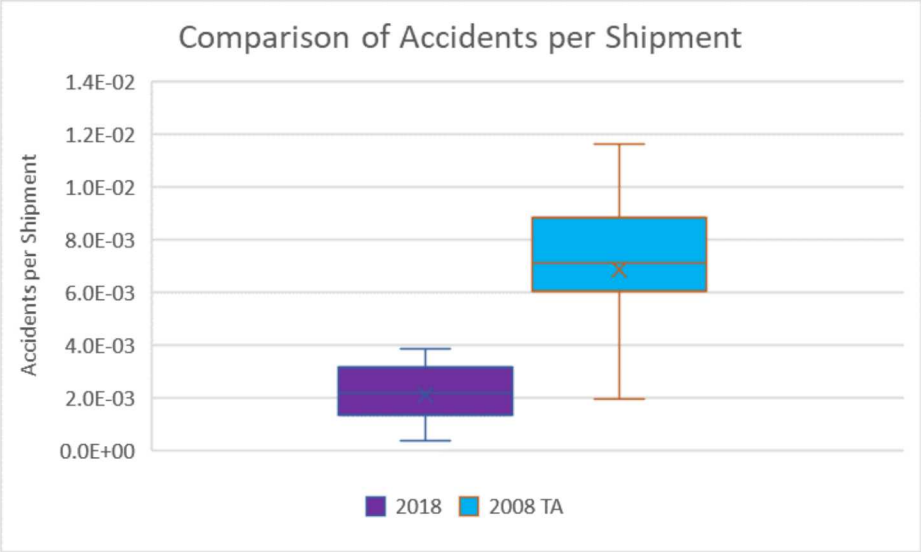

Figure 5-1. Accidents per Shipment Compared to 2008 TA.

Figure 5-2. Fatalities per Shipment Compared to 2008 TA.

The actual number of accidents from 1999 (beginning of WIPP transportation campaign) to October 2019 is 21 over 12,603 shipments, Attachment C of WIPP Nuclear Waste Partnership (2020). There have been

no injuries or fatalities as of June 2020. Excluding the three-year interruption in the WIPP transportation campaign, the number of accidents per year is 1.17.
Figures 5-3 – 5-5 show the non-radiological impact for each route. The number of accidents per year calculated in this TA is 0.94 assuming a campaign duration of 52 years. This estimate is very close to the observed value of 1.17 accidents per year. The number of accidents per year calculated in the 2008 TA is 10.44, which is significantly higher due to the higher assumed accident rates as discussed above. The expected number of fatalities calculated during the WIPP campaign to date (18 years) using the method of this TA is 0.47 meaning that no fatalities should have occurred. This is consistent with the observations.

Figure 5-3 to 5-5 compares the transportation routes with regard to the number of accidents, injuries, and fatalities per shipment.

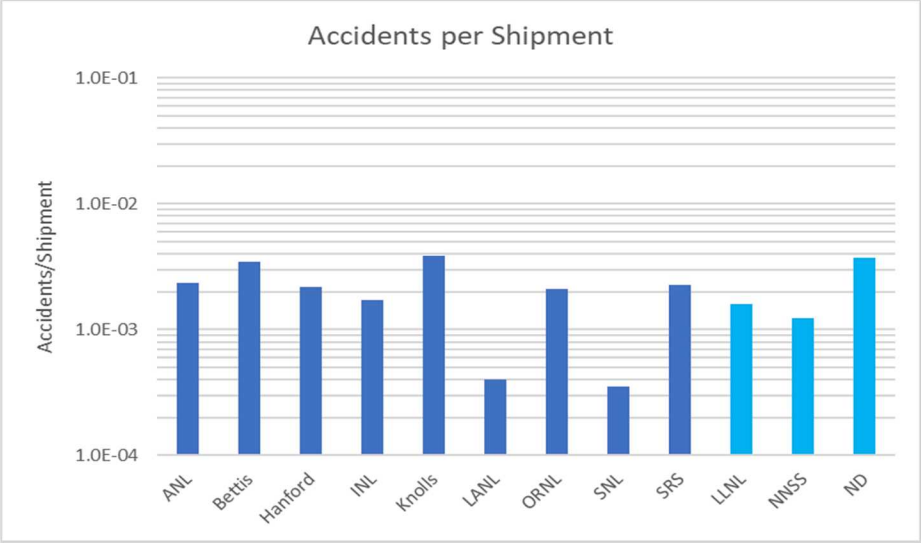

Note: The indirect routes (generator sites to INL) are shown in light blue.

Figure 5-3. Route Specific Number of Accidents per Shipment.

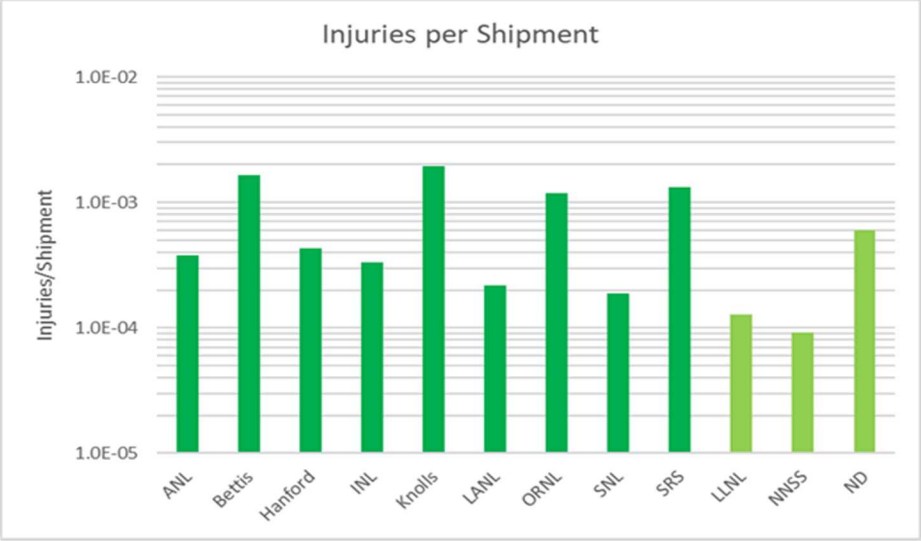

Note: The indirect routes (generator sites to INL) are shown in light green.

Figure 5-4. Route Specific Number of Injuries per Shipment.

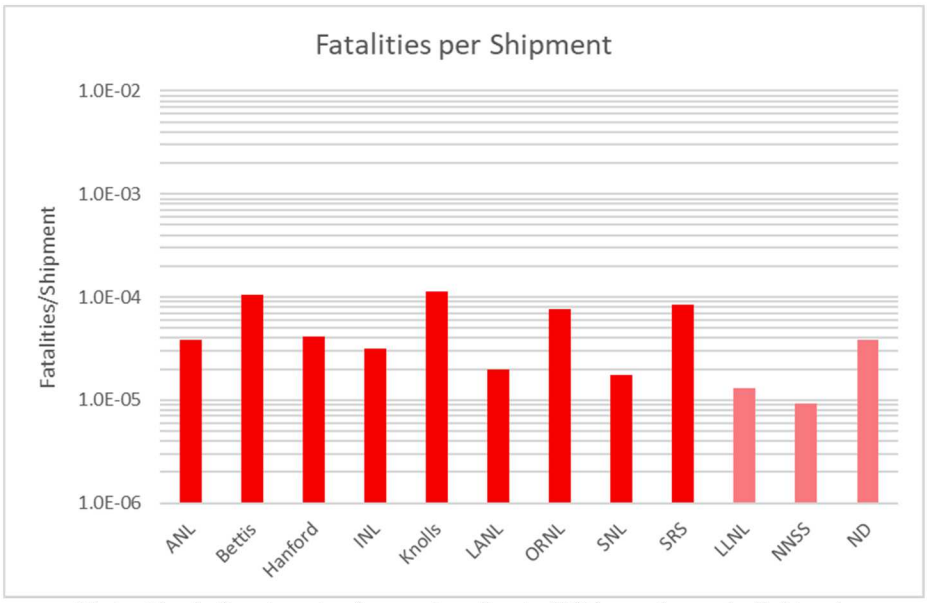

Note: The indirect routes (generator sites to INL) are shown in light red.

Figure 5-5. Route Specific Number of Fatalities per Shipment.

In general, the longer routes have more accidents, injuries and fatalities per shipment. This is evident from Figure 5-6. The correlation between the number of accidents along the route and the route distance is 0.975. The variability is due to the variation in the accident rates that are state specific.

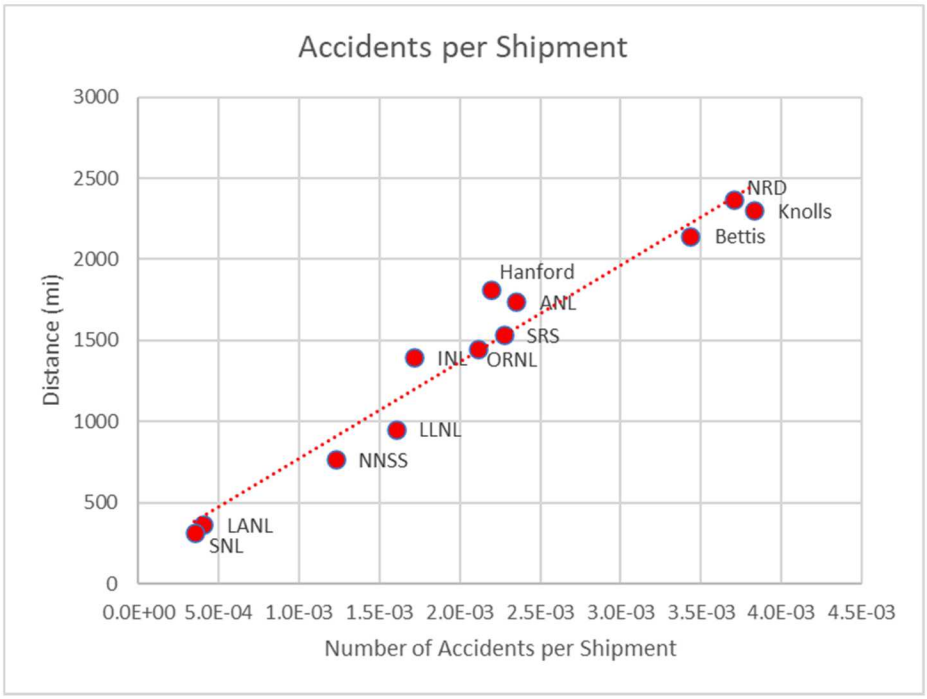

Figure 5-6. Number of Accidents per Shipment versus the Total Route Distance.

6. INPUT DATA FOR THE TRANSPORTATION ACCIDENT ANALYSIS

This section describes the development of the parameters required for the analysis of transportation accidents with release of radioactive materials. The release of radioactive materials (if any) may only occur in the case of an extra-regulatory accident, a very low probability event. This is because the extra-regulatory accident scenarios extend beyond the HAC defined for regulatory accidents in 10 CFR Part 71, for which the packages are demonstrated to remain leak-tight. Consideration of low probability extra-regulatory accidents (probability-based analysis) are included per Department of Energy (DOE) National Environmental Policy Act (NEPA) accident analysis guidance (DOE, 2002).

The intent of the regulatory HAC is to assure that the package will maintain containment in most, but not all, accidents. The fact that the TRUPACT-II may experiences strain levels that could indicate a failure in some analyses of events that are above the regulatory threshold does not mean the package is inadequate. Overall transportation safety is a combination of radiological safety during routine transport, maintaining containment during accidents, and reducing casualties that are the result of accidents that are independent of the cargo being transported. While it would be possible to design a package that maintains containment in a higher percentage of accidents than the TRUPACT-II does, such a package would necessarily be heavier or have a lower payload, leading to an increase in the number of shipments. Since the safety during routine transport and casualties due to non-radiological factors are proportional to the number of shipments, decreasing the already small risk due to release of radioactive material would result in a much larger increase in risk from routine transport and non-radiological factors.

Section 6.1 describes the development of the bounding inventories for CH-TRU and RH-TRU waste. Section 6.2 describes structural finite element analyses of the TRUPACT-II package that impacts an unyielding surface at extra-regulatory velocities and evaluates the consequences for the TRUPACT-II integrity. Section 6.3 describes how the modeling results were used to represent the actual (yielding) impact surfaces (soil, rock and other). Section 6.4 describes thermal analyses of a large engulfing fire during truck transport. The duration of fire was one hour, which is the maximum fire duration reported in NUREG-2125 (NRC, 2014) for truck accidents. Section 6.5 describe how the truck accident event tree (Mills et al. 2006) was modified based on the modeling results and how the corresponding release fractions were developed.

6.1 TRU Waste Source Term Analysis

6.1.1 Introduction

The major parameter required for the assessment of the radiological impacts related to accidents that are severe enough to breach the waste package and to release some of the radioactive materials is the radionuclide source term. In the 2008 TA the source term was defined based on the inventory data in DOE (2008) which represented the waste inventory as it existed on December 31, 2006. The 2008 TA also evaluated the impacts of RH-TRU waste being shipped in SCAs. This 2020 TA covers a similar analysis compared to what was analyzed in the 2008 TA. The 2020 TA uses updated inventory information as of December 31, 2018, which includes ~6MT of surplus plutonium TRU waste (Van Soest, G.D., 2019). The radionuclide activities in this data query have been decay□corrected thru CY 2025 and projected estimates extend thru CY 2062. Only the WIPP-bound waste streams were considered. In addition, ~42.2MT of surplus plutonium TRU waste is included in this TA. In the supplemental information on the 42.2MT surplus plutonium, the radionuclide activities provided are as of CY2020. Note that as of January 2020 no final National Environmental Policy Act (NEPA) decision has been made on the proposed action related to the 42.2MT of surplus plutonium. However, the estimated inventory for surplus plutonium TRU waste was evaluated in the source term analysis.

The source term analysis is based on the TRU waste inventory (stored and projected estimates as reported by the TRU waste generator sites as of December 31, 2018). The data are from the *Comprehensive Inventory Database, data version D.18.00*, August 26, 2019 and September 24, 2019 (Van Soest, G.D., 2019). The major goal of the analysis was to develop the bounding source term for the CH and RH TRU waste to be used in the transportation accident analysis (Section 7).

To develop the bounding source term, both the Ci and A_2 contents of the different waste streams were analyzed. The A_2 value for each radionuclide was taken from 10 CFR Part 71 Appendix A. "For a given radionuclide, the A_1 or A_2 value is defined as the maximum activity permitted in a Type A package. The A_1 value applies for special form radioactive material, while the A_2 value applies for radioactive material in other than special form." The A_2 values include the contribution from short-lived progeny radionuclides, e.g., Cs-137, Ba-137m, Sr-90 and Y-90. Appendix A provides the A_2 values for each radionuclide in the data base query. Note that some radionuclides do not have the associated A_2 values (A_2 is infinite and radionuclide quantity is unlimited).

The A_2 values are commonly used to identify the radionuclides that are major contributors to the radiation dose to a receptor in radiological impact analyses. This method has been traditionally used in RADTRAN, including the Spent Fuel Transportation Risk Assessment – Final Report (NUREG 2125, NRC 2014).

6.1.2 CH TRU Waste

There are 245 WIPP-bound CH-TRU waste streams with associated radionuclide activity reported in the database query (Van Soest, G.D., 2019). The radionuclide composition of the CH waste is reported for each waste stream in terms of Ci of each of 167 radionuclides. Waste stream information includes stored and projected container types and estimated numbers of stored and projected containers. Some waste streams can be loaded into as many as three different container types. The list of container types is provided in Table 6-1.

In this 2020 TA, a shipping package refers to the contents of the shipping container (i.e., TRUPACT-II, HalfPACT, TRUPACT-III). Figure 6-1 shows the distribution of different container types that will make up a shipping package. Seventy percent of the shipping packages will contain 55-gal drums and/or standard waste boxes (SWBs). The TRUPACT-II with CCOs constitutes 8.5 percent of shipping packages. The other shipping packages combined represent 21.6 percent.

Table 6-1. Containers Designated for the CH-TRU Waste.

Container Type
100-gal Drum Direct Load with Liner
100-gal Drum Direct Load without Liner
55-gal CCO with Liner
55-gal Drum Direct Load with Liner
55-gal Drum Direct Load without Liner
55-gal POC - 12" with Liner
55-gal POC - 6" with Liner
SLB2 Direct Load
SWB Direct Load with Liner
SWB Direct Load without Liner
SWB with 4 - 55-gal Drums with Liners
TDOP Direct Load

Container Type
TDOP with 10 - 55-gal Drums with Liners
Notes: CCO = criticality control overpack POC = pipe overpack container SLB2 = standard large box 2 SWB = standard waste box TDOP = ten-drum overpack

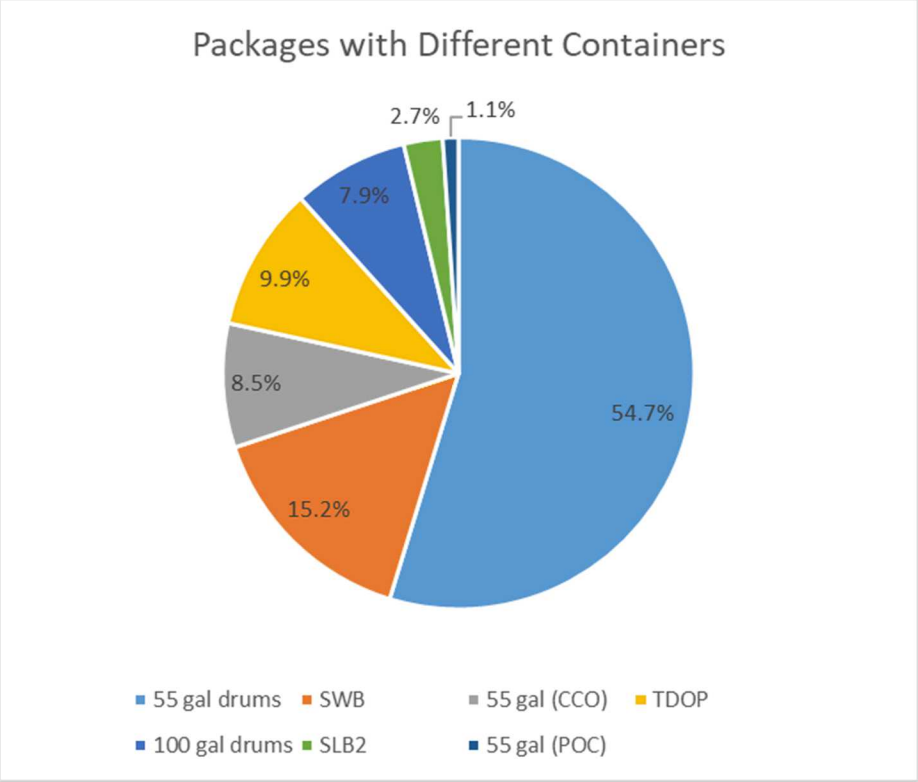

Figure 6-1. Container Types that Will Make Up a Shipping Package.

The shipping package specific payloads are from CH-TRAMPAC Rev. 4, March 2013.
In this analysis the radionuclide composition of 55-gal drums, SWB, SLB2, POCs, and CCOs was analyzed. The total activity of the radionuclides in the package expressed in Curies (Ci) is referred to as the Ci content. The total A_2 of the radionuclides in the package is referred to as the A_2 content. The analysis included the following steps:

1. The waste streams were grouped by the container type and the total number of containers was calculated for each waste stream in the group based on the number of stored and projected containers in the data base query.
2. The number of A_2 values were calculated for each radionuclide in the waste stream. Note that the radionuclide-specific Ci per A_2 values are available for 106 radionuclides out of 167 that are present in the CH-TRU waste. For the remaining radionuclides, the A_2 values were set to 0.
3. The total Ci per container and the total A_2 per container were calculated for each waste stream. For waste streams with multiple container types, Ci and A_2 per container were calculated based on the total number of containers (stored and projected) and their internal (waste) volumes. The internal volumes are provided for the different container types in the following sections.

4. The total Ci and the total A_2 per TRUPACT-II with 55-gal drums, SWB, 55-gal drums with POCs and 55-gal drums with CCOs were calculated for each applicable waste stream using Ci and A_2 per container values.
5. Ci and A_2 per TRUPACT-III with SLB2 were calculated for each applicable waste stream using Ci and A_2 per container values.
6. The cumulative frequency functions of the package Ci and A_2 were generated for TRUPACT-II with 55-gal drums, SWB, POCs, and CCOs and for TRUPACT-III with SLB2.
7. For each waste stream group, the average and maximum Ci values were calculated for each radionuclide. The radionuclides that contribute more than 99 percent to the total A_2 were identified for each waste stream group.
8. The sums of Ci and A_2 values for the major contributing radionuclides were calculated and compared to the total waste stream Ci and A_2 values to confirm that the A_2 contribution of the major radionuclides was 99 percent or greater for the waste streams.
9. The waste stream corresponding to the 95^{th} percentile or greater was selected for each waste stream group. The radionuclide composition of this waste was compared to the corresponding radionuclide composition used in SEIS-II and the 2008 TA when available.
10. The bounding waste stream groups were compared to develop the bounding composition of the CH-TRU waste.

The analysis results are presented below for each waste stream group. The bounding composition is discussed in Section 6.1.2.6.

6.1.2.1 55-gal Drums

According to the inventory, 208 WIPP-bound waste streams with associated radionuclide activity reported in the database are either stored or projected to be generated in 55-gal drums. The major radionuclides for these waste streams were identified as described in Step 7. The contribution of the major radionuclides to the total Ci and A_2 content are shown in Figures 6-2 and 6-3. The combined major radionuclides contribution to the total A_2 is 99.5 percent (average A_2) and 99.7 percent (maximum A_2). The combined major radionuclides contribution to the total Ci is 69.1 percent (average Ci content) and 91.9 percent (maximum Ci content). In the case of the average Ci content the remaining contribution to the total Ci content is primarily from tritium which has a very small contribution to the total A_2 value.

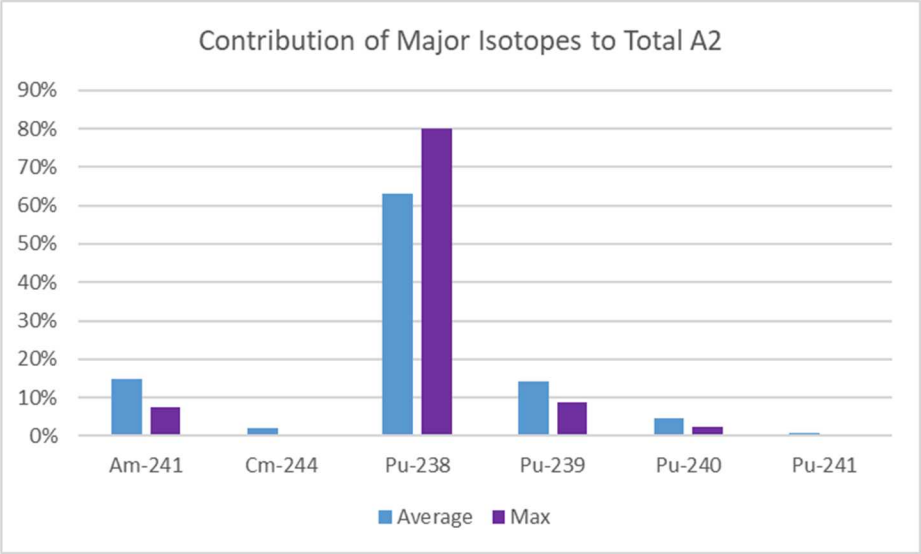

Figure 6-2. Contributions of the Major Radionuclides in Waste Streams Associated with 55-gal Drums.

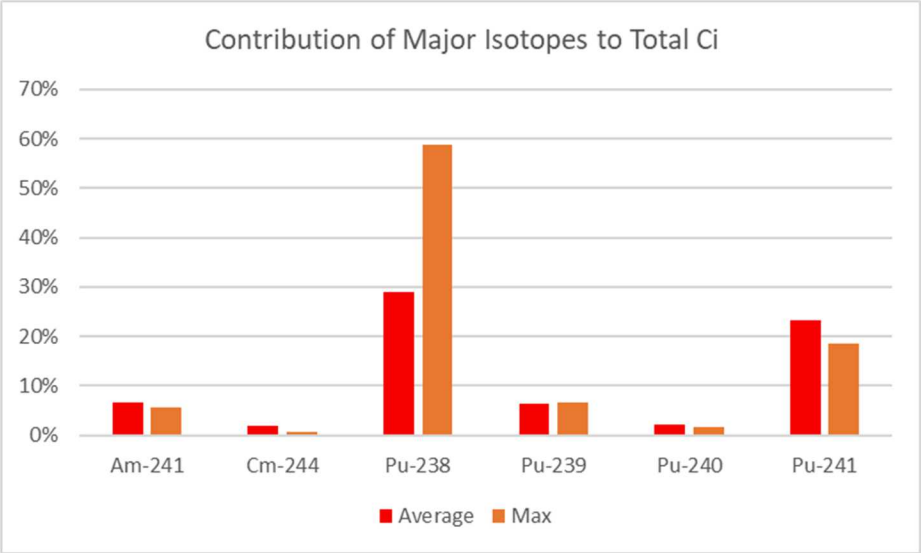

Figure 6-3. Ci Contributions of the Major Radionuclides in Waste Streams Associated with 55-gal Drums.

Figures 6-4 and 6-5 show the cumulative frequency distributions for A_2 and Ci of these waste streams assuming that 14 drums will be placed in a TRUPACT-II. The volume of waste used to calculate A_2 and Ci per 55-gal drum was 0.21 m^3. The fraction of the total waste stream going into the 55-gal drums was calculated as the total number of the 55-gal drums designated for this waste stream times the 55-gal drum volume divided by the total waste volume of the waste stream.

Also shown in Figures 6-4 and 6-5 are the total A_2 and Ci values from SEIS-II and waste stream SR-LA-PAD1. The SR-LA-PAD1 was chosen because it corresponds to 99.5 percentile (A2) and 99.0 percentile Ci. The SEIS-II values, if placed on the measured (projected) frequency curves correspond to 99.2 percentile A_2 and 99.2 percentile Ci. The A_2 (328,431) and Ci (10,582) values used in 2008 TA are greater than the maximum measured (projected) A_2 and Ci content and are not plotted in Figures 6-4 and 6-5. As

stated in 2008 TA, the bounding CH-TRU waste radionuclide composition was based on the SR waste stream with the maximum Ci content. The waste stream ID was not provided in the 2008 TA.

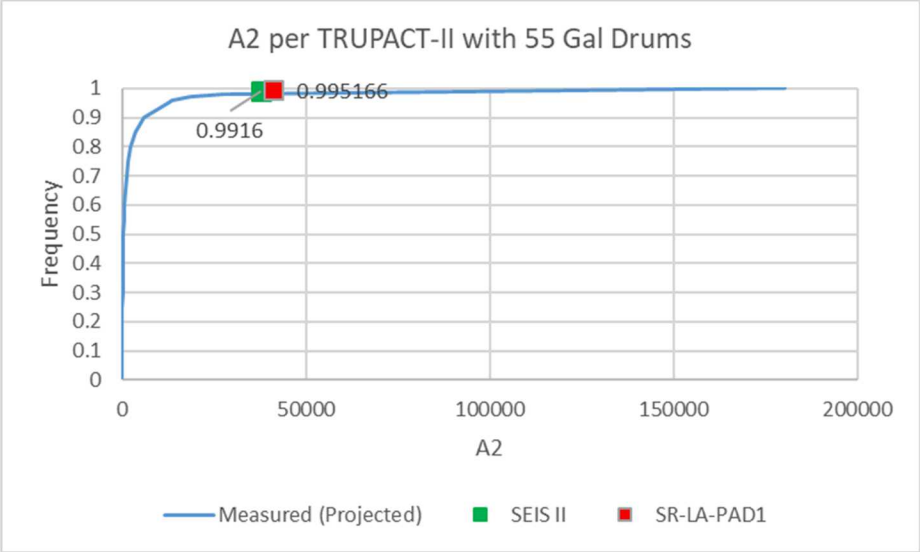

Figure 6-4. Estimated Total A_2 Content per TRUPACT-II with 55-gal Drums.

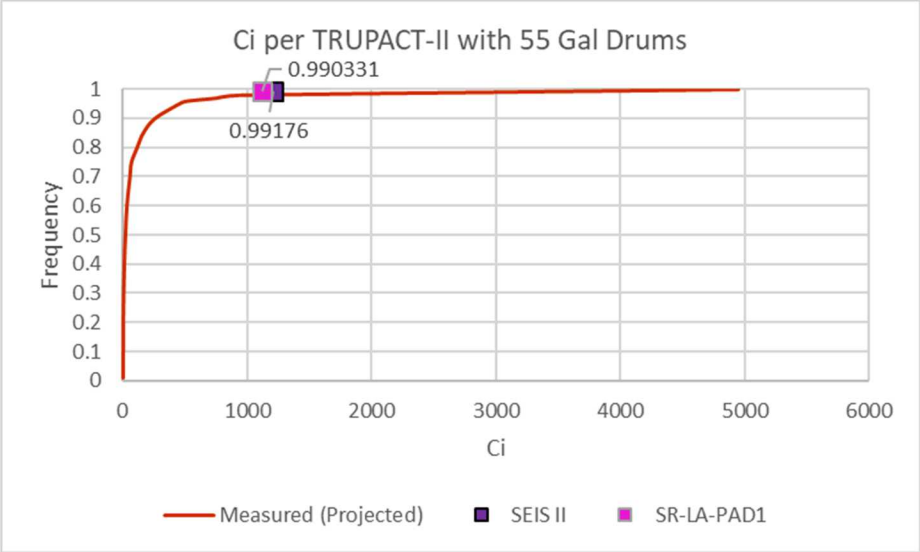

Figure 6-5. Estimated Total Ci Content per TRUPACT-II with 55-gal Drums.

Table 6-2 and Figures 6-6 and 6-7 compare the radionuclide composition assumed in SEIS-II and 2008 TA and radionuclide composition of the waste stream SR-LA-PAD1. The radionuclide content assumed in SEIS-II is similar to the radionuclide content of the waste stream SR-LA-PAD1, except Co-60, Cs-137, and Sr-90 are present in SR-LA-PAD1 in very small amounts and their contributions to the total Ci and A2 are negligible. The 2008 TA radionuclide specific A_2 and Ci values are higher than in SEIS-II and in SR-LA-PAD1.

Table 6-2. CH-TRU Waste Radionuclide Composition Comparison.

Radionuclide	SEIS II		2008 TA		SR-LA-PAD1		SR-MD-PAD1	
	C	A_2	C	A_2	C	A_2	C	A_2
Am-241	3.6	133.3	31.4	1,162.96	2.85	105.49	2.18	80.80
Co-60	6.40E-04	5.82E-05	5.58E-03	5.07E-04	7.76E-10	7.05E-11	6.64E-08	6.04E-09
Cs-137	0.01	6.25E-04	0.087	0.005438	5.93E-06	3.71E-07	8.00E-03	5.00E-04
Pu-238	990	3.67E04	8,630.7	3.2E05	1,105.41	40,941.3	958.58	35,502.90
Pu-239	16	592.6	139.5	5,166.7	1.38	50.95	1.24	45.99
Pu-240	4.2	155.6	36.6	1,355.6	2.18	80.56	1.69	62.50
Pu-241	200	125	1,743.6	1,089.8	12.98	8.11	10.43	6.52
Pu-242	6.80E-04	0.025	5.93E-03	0.22	2.76E-03	0.16	1.02E-01	7.63E-02
Sr-90	0.01	1.24E-03	0.087	0.011	6.97E-06	8.61E-07	7.87E-03	9.71E-04
Total	**1,213.8**	**37,673.2**	**10,582.0**	**32,8431.0**	**1,124.8**	**41,186.6**	**974.14**	**35,698.78**

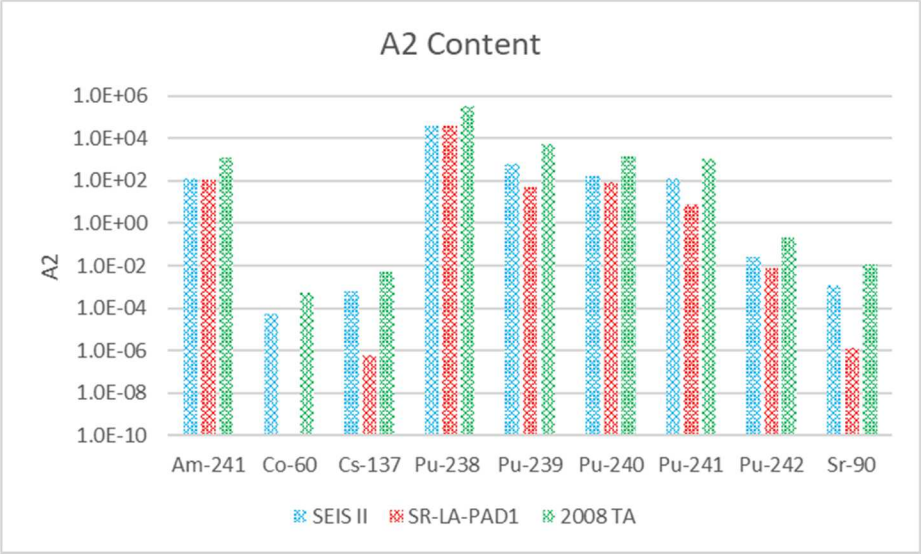

Figure 6-6. A_2 Content Radionuclide Composition Comparison.

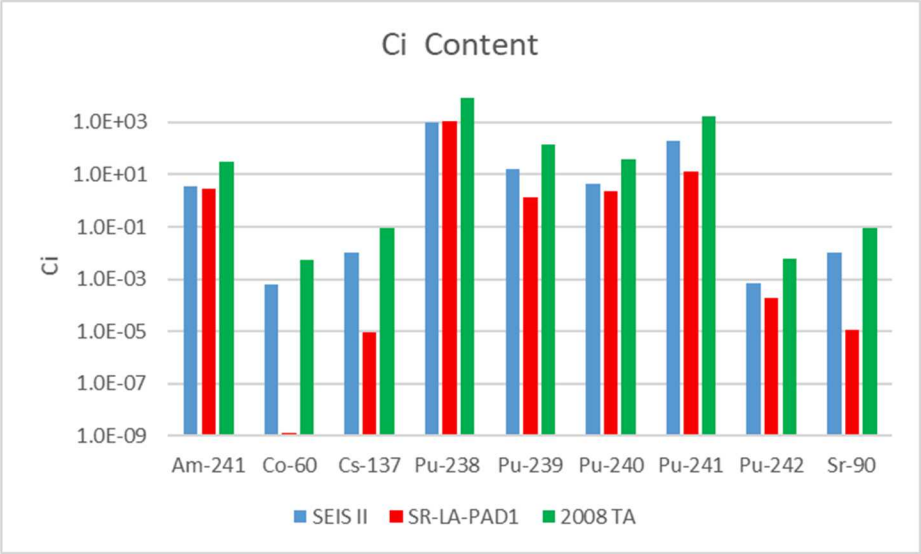

Figure 6-7. Ci Content Radionuclide Composition Comparison.

6.1.2.1 SWB

According to the inventory, 91 WIPP-bound waste streams with associated radionuclide activity reported in the database are either stored or projected to be generated in SWBs. The SWBs are either directly loaded with waste or are loaded with the waste in 55-gal drums. The major radionuclides for these waste streams were identified as described in Step 7. The contribution of the major radionuclides to the total Ci and A_2 content are shown in Figures 6-8 and 6-9 for the direct load SWB and SWB loaded with 55-gal drums. The combined major radionuclide contribution to the total A_2 is 99.7 percent (average A_2) and 99.7-99.8 percent (maximum A_2). The combined major radionuclide contribution to the total Ci is 52.3-70.4 percent (average Ci content) and 92.0 percent (maximum Ci content). In the case of the average Ci content the remaining contribution to the total Ci content is primarily from tritium which has a very small contribution to the total A_2 value.

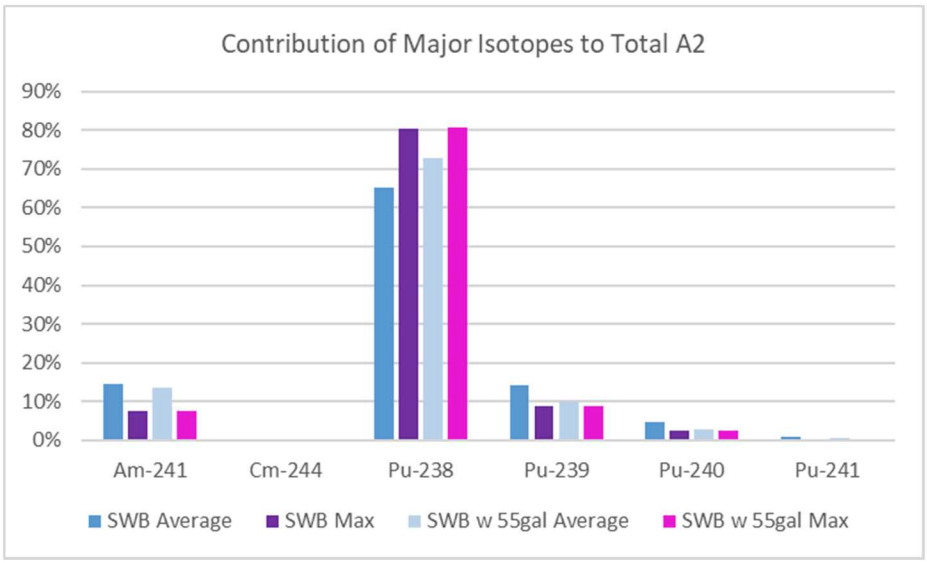

Figure 6-8. A_2 Contributions of the Major Radionuclides in Waste Streams Associated with SWBs.

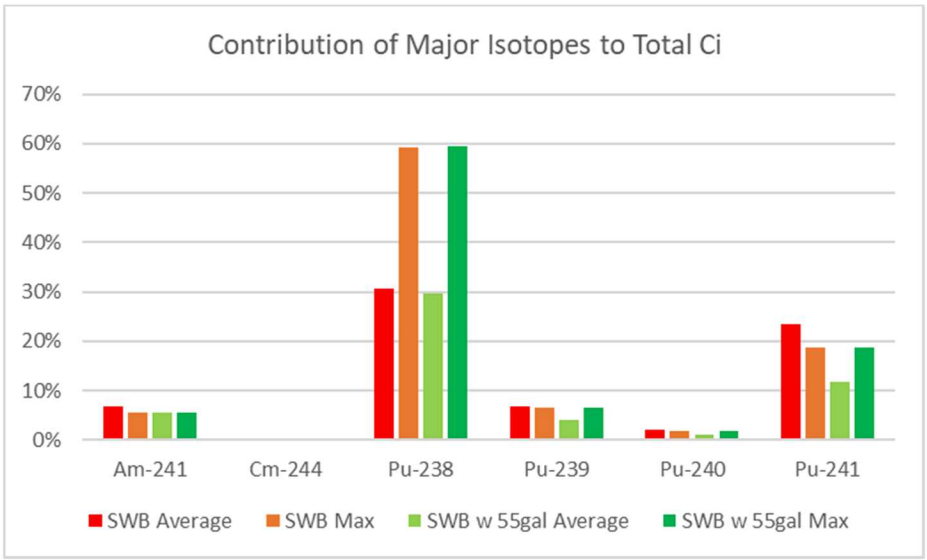

Figure 6-9. Ci Contributions of the Major Radionuclides in Waste Streams Associated with SWBs.

Figures 6-10 and 6-11 show the cumulative frequency distributions for A_2 and Ci of these waste streams assuming that two SWBs will be placed in a TRUPACT-II. The volume of waste used to calculate A_2 and Ci per directly loaded SWB was 1.88 m^3. The volume of waste used to calculate A_2 and Ci per SWB with 55-gal drums was 0.84 m^3. The fraction of the total waste stream going into a SWB was calculated as the total number of the SWB (direct load or with 55-gal drums) designated for this waste stream times the SWB volume (direct load or with 55-gal drums) divided by the total waste volume of the waste stream.

Also shown in Figures 6-10 and 6-11 are the total A_2 and Ci values from SEIS-II, waste stream SR-LA-PAD1, and waste stream SR-MD-PAD1. The SR-MD-PAD1 waste stream corresponds to 98.9 percentile (A_2) and 97.8 percentile Ci. The SEIS-II values, if placed on the measured (projected) frequency curves correspond to 99.1 percentile in A_2 and 99.2 percentile in Ci. The SR-LA-PAD1 A_2 value if placed on the measured (projected) frequency curve correspond to 99.5 percentile in A_2. The SR-LA-PAD1 Ci value if

placed on the measured (projected) frequency curve correspond to 98.6 percentile in Ci. The A2 (328,431) and Ci (10,582) values used in 2008 TA are greater than the maximum measured (projected) A_2 and Ci content and are not plotted in Figures 6-10 and 6-11.

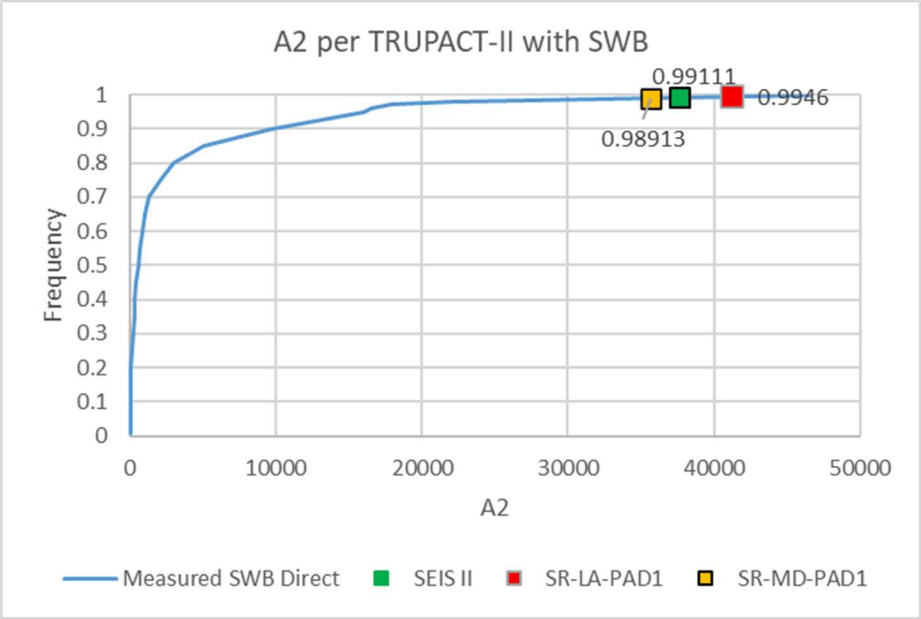

Figure 6-10. Estimated Total A_2 Content per TRUPACT-II with Two SWBs.

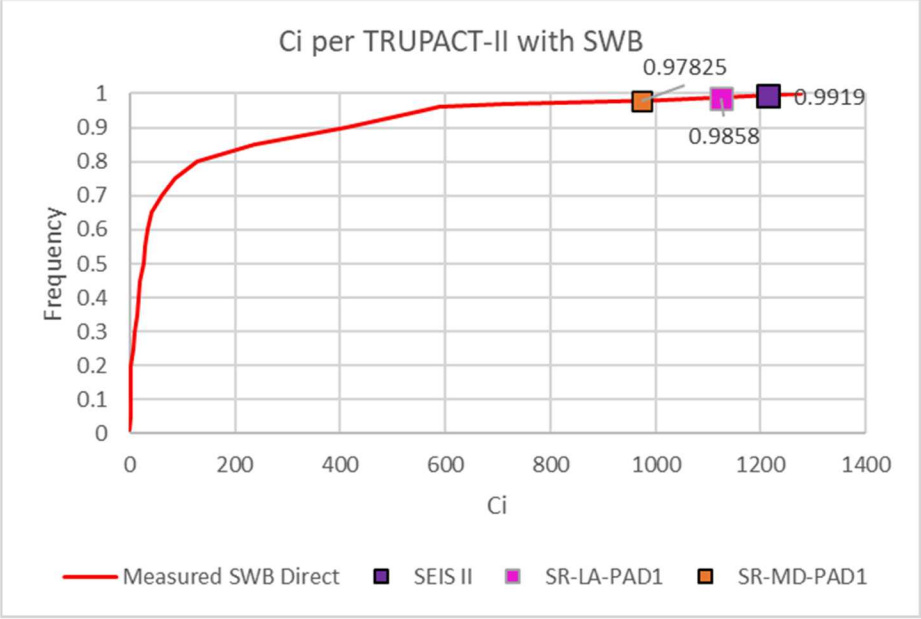

Figure 6-11. Estimated Total Ci Content per TRUPACT-II with Two SWBs.

Table 6-2 and Figures 6-12 and 6-13 compare the radionuclide composition of a TRUPACT-II with SR-LA-PAD1 in 55-gal drums and a TRUPACT-II with SR-MD-PAD1 in SWBs. The radionuclide compositions are very similar with slightly higher A_2 and Ci content in SR-LA-PAD1.

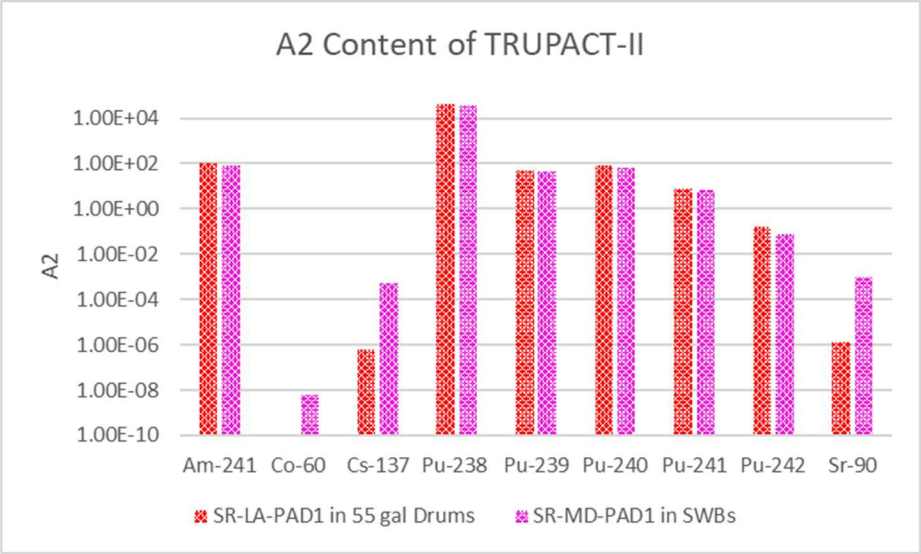

Figure 6-12. A_2 Content of TRUPACT-II with 55-gal Drums (SR-LA-PAD1) and TRUPACT-II with SWBs (SR-MD-PAD1).

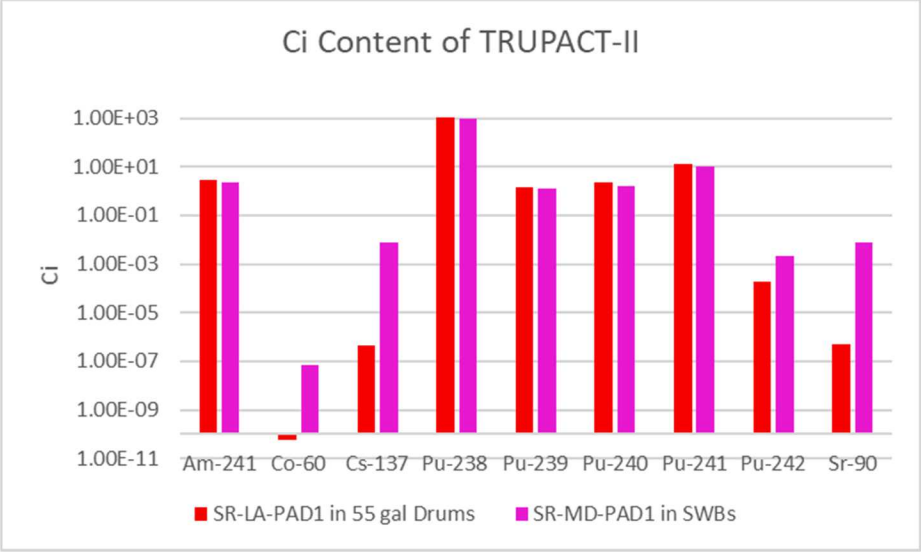

Figure 6-13. Ci Content of TRUPACT-II with 55-gal Drums (SR-LA-PAD1) and TRUPACT-II with SWBs (SR-MD-PAD1).

6.1.2.2 SLB2

According to the inventory, 15 WIPP-bound waste streams with associated radionuclide activity reported in the database are either stored or projected to be generated in SLB2s. The major radionuclides for these waste streams were identified as described in Step 7. The contribution of the major radionuclides to the total A_2 and Ci content are shown in Figures 6-14 and 6-15. The combined major radionuclides contribution to the total A_2 is 99.9 percent for both, average A_2 and maximum A_2. The combined major radionuclides contribution to the total Ci is 99.8 percent for both, average Ci content and maximum Ci content.

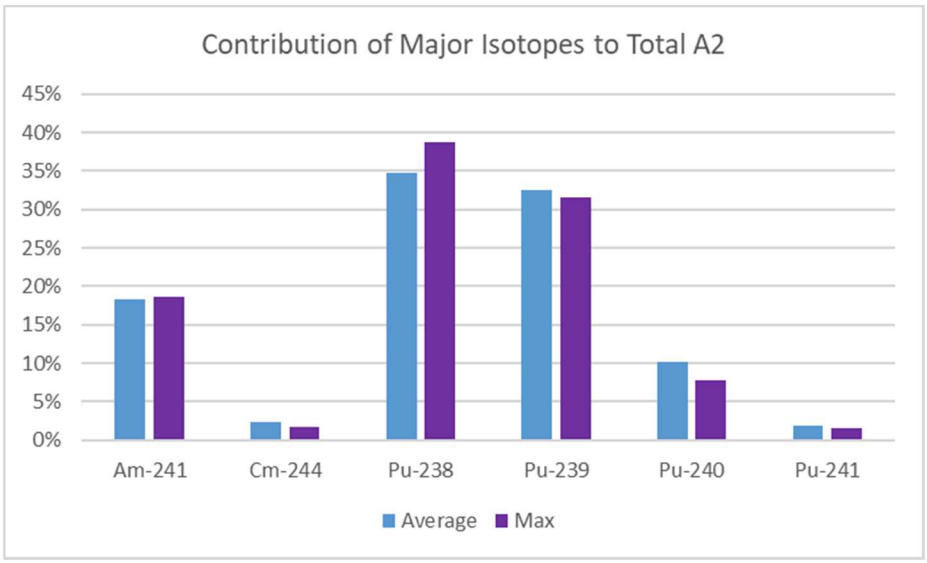

Figure 6-14. Contributions of the Major Radionuclides in Waste Streams Associated with SLB2.

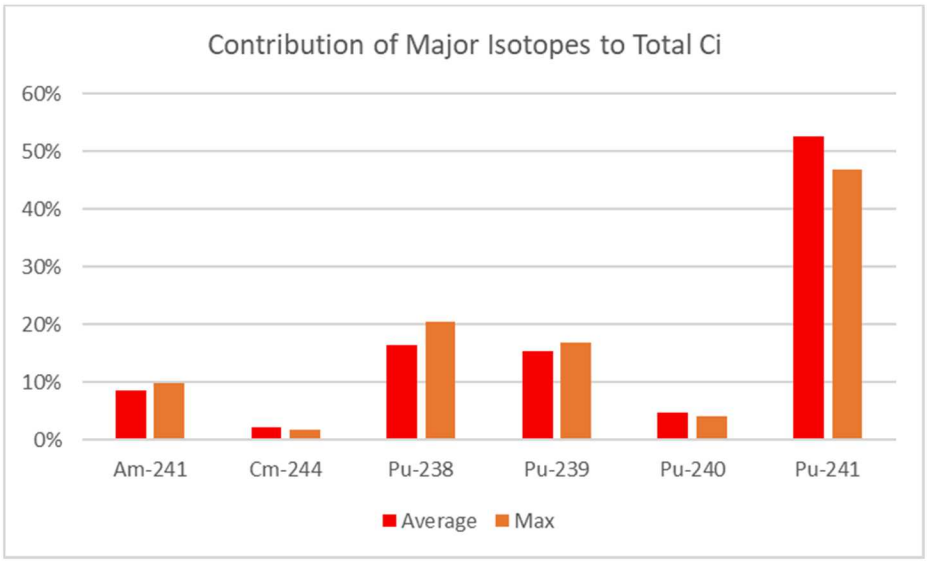

Figure 6-15. Ci Contributions of the Major Radionuclides in Waste Streams Associated with SLB2.

Figures 6-16 and 6-17 show the cumulative frequency distributions for A_2 and Ci of these waste streams for one SLB2 placed in a TRUPACT-III. The volume of waste used to calculate A_2 and Ci per SLB2 was 7.39 m^3. The fraction of the total waste stream going into a SLB2 was calculated as the total number of the SLB2 designated for this waste stream times the SLB2 volume divided by the total waste volume of the waste stream.

The waste stream SR-MD-PAD1 can be stored in both, SWB and SLB2. It has the maximum Ci and A_2 content out of the waste streams designated to SLB2s.

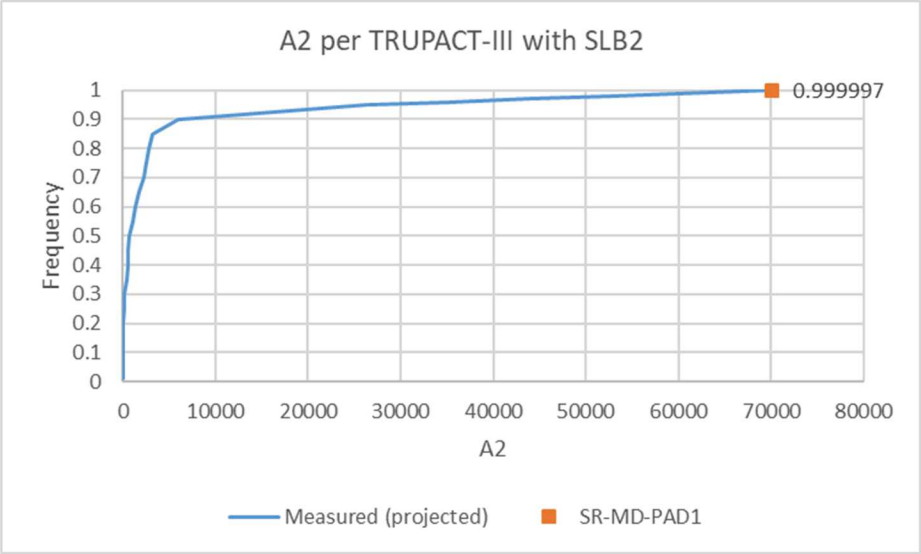

Figure 6-16. Estimated Total A_2 Content per TRUPACT-III with SLB2.

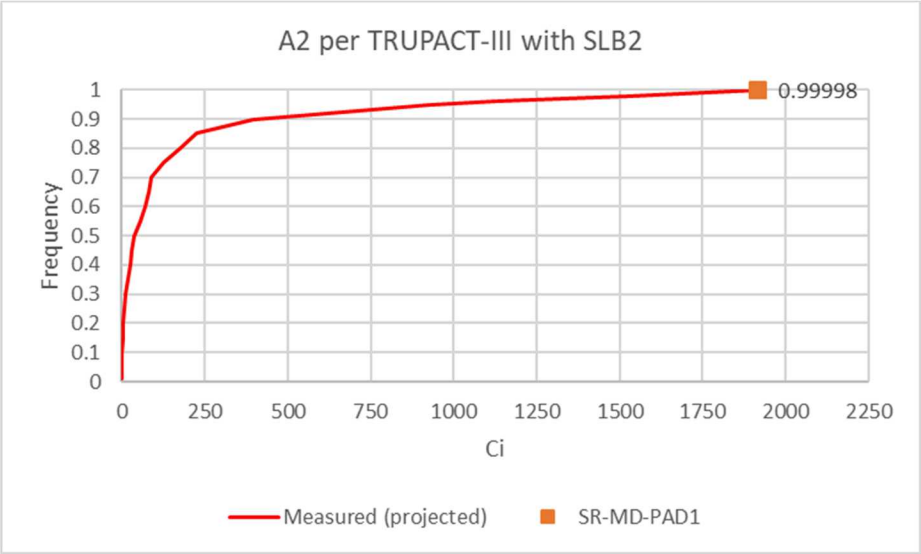

Figure 6-17. Estimated Total Ci Content per TRUPACT-III with SLB2.

6.1.2.3 POCs

According to the inventory, 32 WIPP-bound waste streams with associated radionuclide activity reported in the database are either stored or projected to be generated and packaged into either 12" or 6" POCs. The major radionuclides for these waste streams were identified as described in Step 7. The contribution of the major radionuclides to the total Ci and A_2 content are shown in Figures 6-18 and 6-19. The combined major radionuclides contribution to the total A_2 is 98.6-99.5 percent (average A_2) and 98.5-99.7 percent (maximum A_2). The combined major radionuclides contribution to the total Ci is 54.0-95.2 percent (average Ci content) and 92.0-95.0 percent (maximum Ci content). In the case of the average Ci content the remaining contribution to the total Ci content is primarily from tritium which has very small contribution to the total A_2 value.

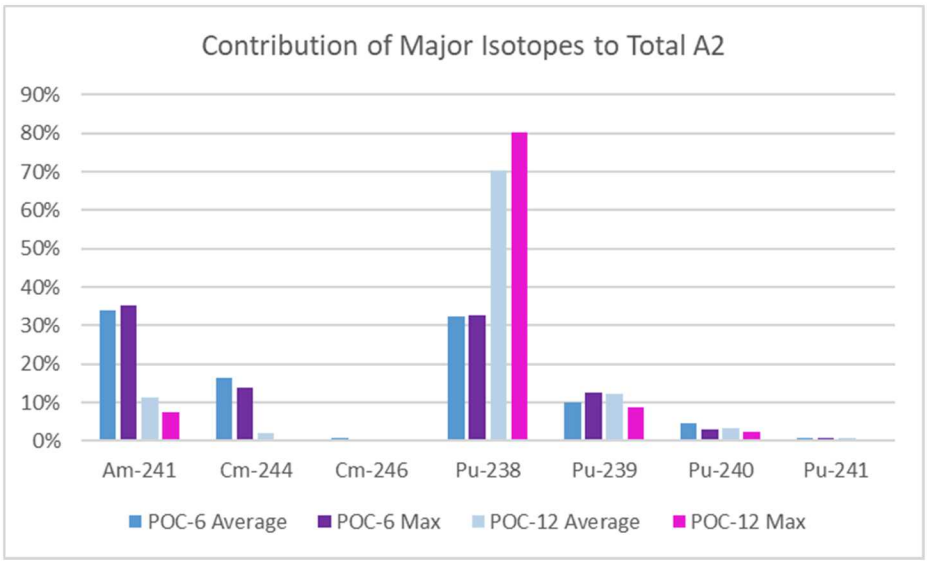

Figure 6-18. Contributions of the Major Radionuclides in Waste Streams Associated with POCs.

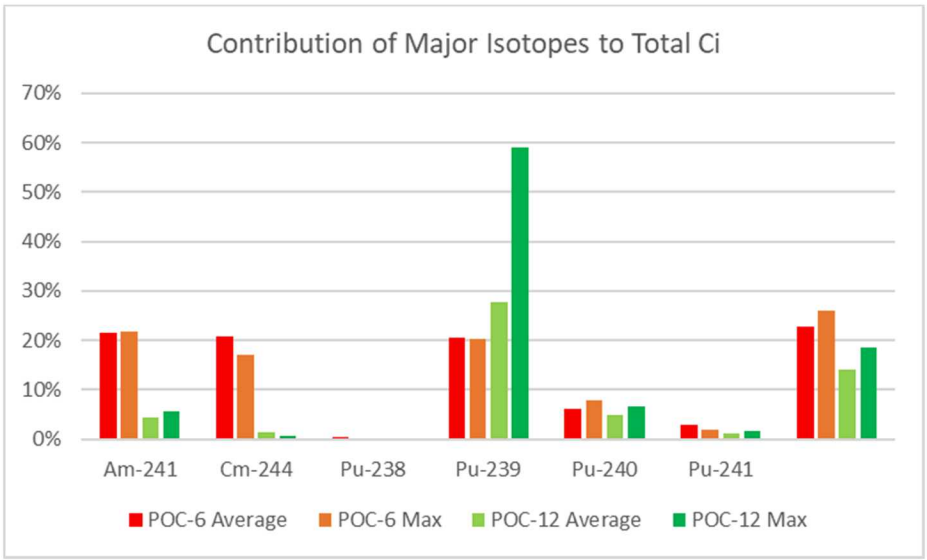

Figure 6-19. Ci Contributions of the Major Radionuclides in Waste Streams Associated with POCs.

Figures 6-20 and 6-21 show the cumulative frequency distributions for A_2 and Ci of these waste streams assuming that 14 POCs will be placed in a TRUPACT-II. The volume of waste used to calculate A_2 and Ci per 6" POC was 0.012 m^3. The volume of waste used to calculate A_2 and Ci per 12" POC was 0.0488 m^3. The fraction of the total waste stream going into a POC was calculated as the total number of the POC (6" or 12") designated for this waste stream times the POC volume (6" or 12") divided by the total waste volume of the waste stream. The OR-OXIDE-CH-HET waste stream designated to POCs corresponds to 97.2 percentile ($_{A2}$) and has maximum Ci value.

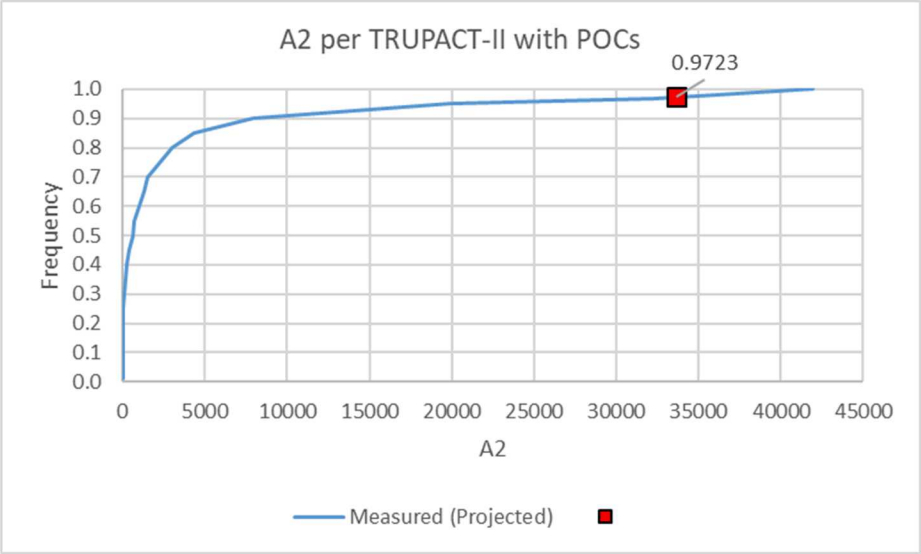

Figure 6-20. Estimated Total A_2 Content per TRUPACT-II with POCs.

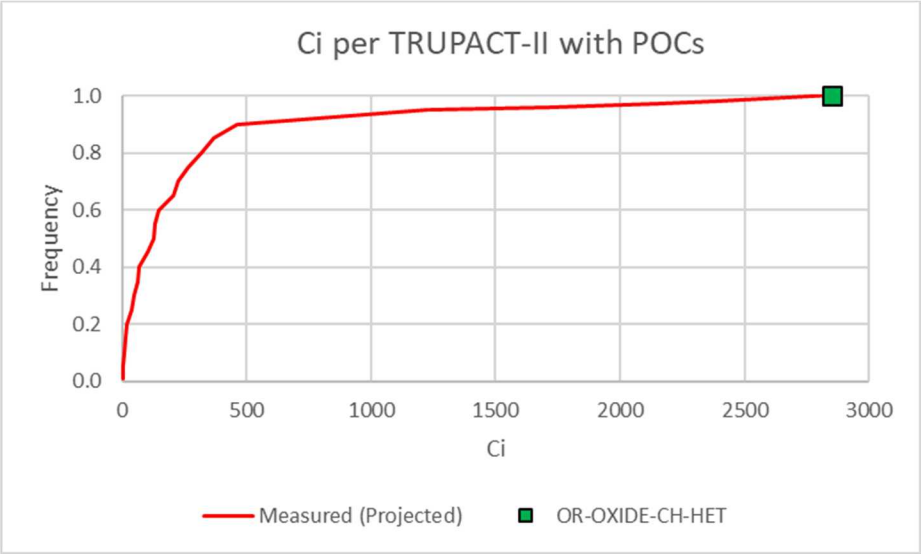

Figure 6-21. Estimated Total Ci Content per TRUPACT-II with POCs.

Figures 6-22 and 6-23 compare the radionuclide composition of a TRUPACT-II with SR-LA-PAD1 in 55-gal drums and a TRUPACT-II with OR-OXIDE-CH-HET in POCs. The waste stream OR-OXIDE-CH-HET contains more Am-241, Pu-239, Pu-240, and Pu-241 than the waste stream SR-LA-PAD1.

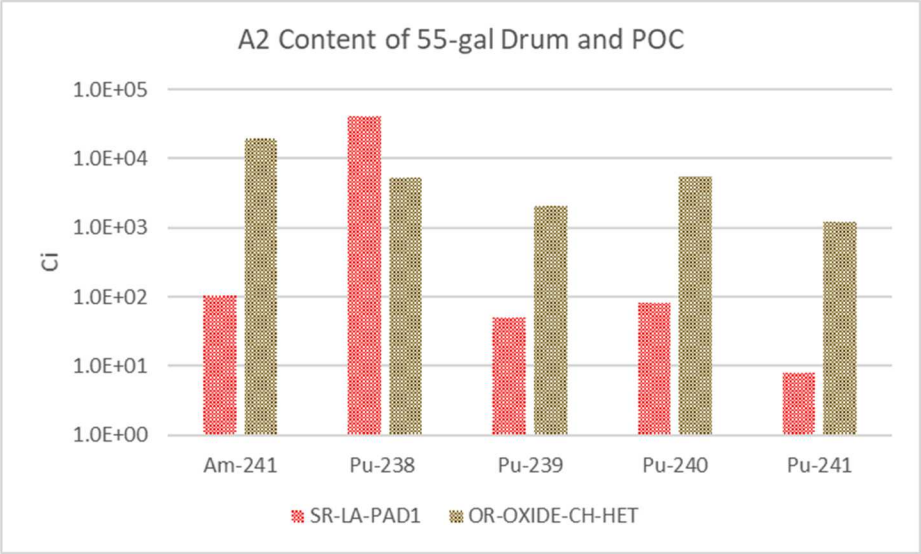

Figure 6-22. A_2 Content of TRUPACT-II with 55-gal Drums (SR-LA-PAD1) and TRUPACT-II with POCs (OR-OXIDE-CH-HET).

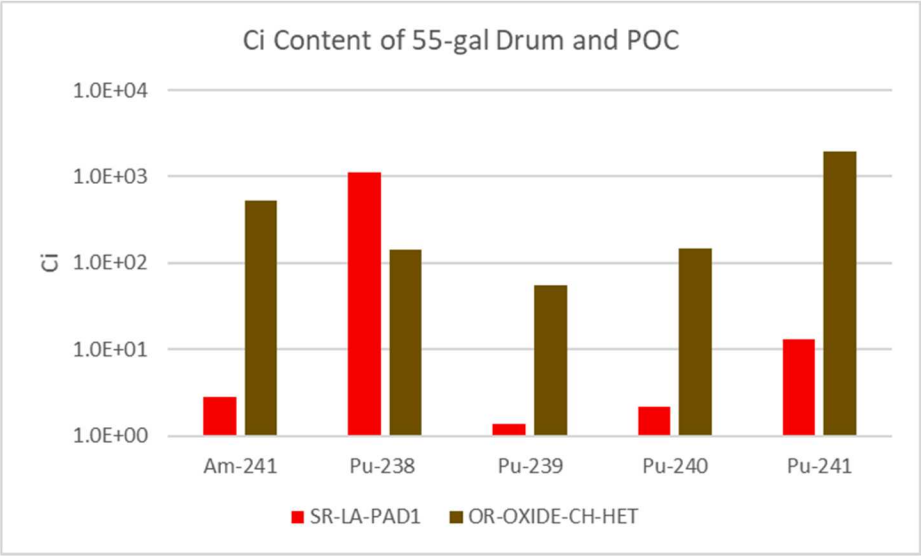

Figure 6-23. Ci Content of TRUPACT-II with 55-gal Drums (SR-LA-PAD1) and TRUPACT-II with POCs (OR-OXIDE-CH-HET)

6.1.2.4 CCOs

Six MT and 42.2 MT of surplus Pu waste streams are projected to be generated in CCOs. The contributions of the major radionuclides to the total A_2 and Ci content of 6 MT surplus Pu waste stream (SR-KAC-PuOx) are shown in Figures 6-24 and 6-25. The waste stream SR-KAC-PuOx is included in the database query. The combined major radionuclides contributions to the total A_2 and to the total Ci are 99.9995 percent and 99.998 percent respectively.

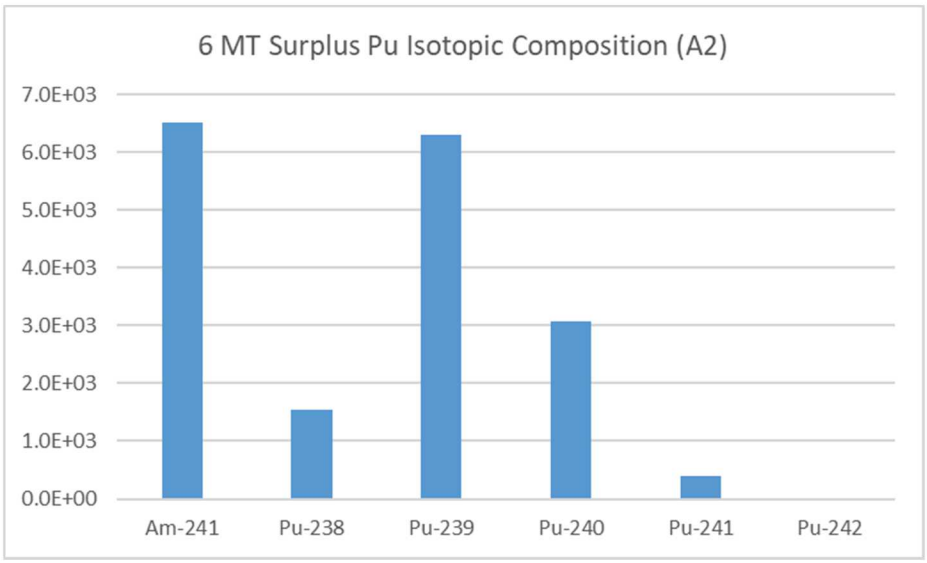

Figure 6-24. A_2 Contributions of the Major Radionuclides in 6 MT Surplus Pu Waste Stream.

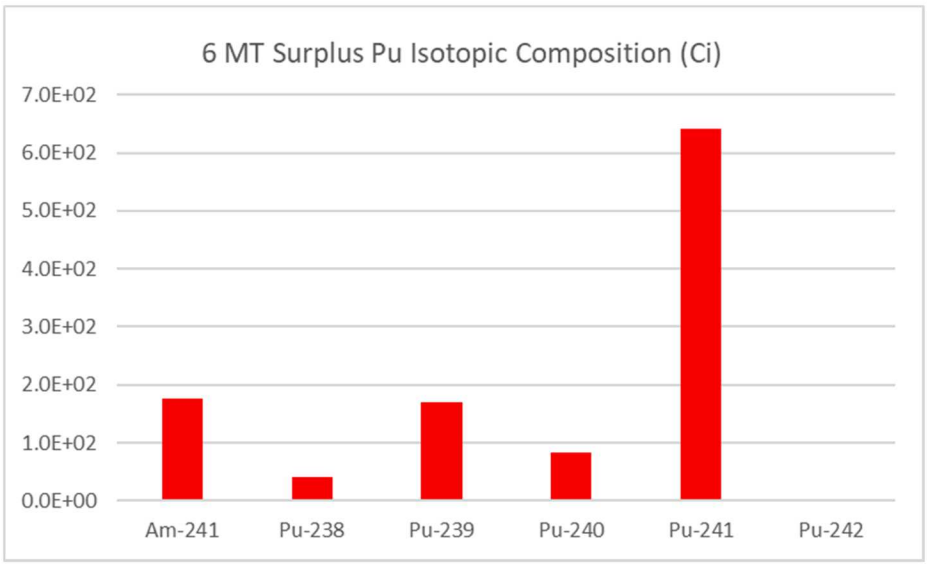

Figure 6-25. Ci Contributions of the Major Radionuclides in 6 MT Surplus Pu Waste Stream.

The total A_2 and Ci content of TRUPACT-II with CCOs loaded with 6 MT surplus Pu waste stream are 17,804 and 1,111 respectively.

The radionuclide content of 42.2 MT of surplus Pu is designated "Official Use Only" (OUO) and cannot be disclosed in this report. The major radionuclides are the same as in the 6 MT surplus Pu waste stream, but there is a larger contribution of Pu-239 to both, A_2 and Ci contents and a smaller contribution of the other radionuclides compared to the 6 MT of surplus Pu waste stream. The total A_2 and Ci content of TRUPACT-II loaded with the 42.2 MT surplus Pu waste stream are lower compared to the 6 MT of surplus Pu waste stream. Consequently, a TRUPACT-II with 6 MT of surplus Pu waste stream in CCOs is bounding with regard to both, its A_2 and Ci contents.

6.1.2.5 Bounding CH-TRU Waste Radionuclide Source Term for the 2020 TA Accident Analysis

The analysis of the CH waste streams demonstrated that five radionuclides (Am-241, Pu-238, Pu-239, Pu-240, and Pu-241) contribute more than 99 percent to the container A_2 and more than 90 percent to the container Ci content. The A_2 and Ci contents of these radionuclides in a TRUPACT-II is compared in Figures 6-26 and 6-27 for the following cases: fourteen 55-gal drums, two SWBs, fourteen POCs, and fourteen CCOs (6 MT surplus Pu waste stream). A TRUPACT-II with 55-gal drums has larger Pu-238 Ci and A_2 content and smaller content of the other radionuclides compared to POCs and CCOs. The Ci and A_2 contents of a TRUPACT-II with 55-gal drums and SWBs are very similar.

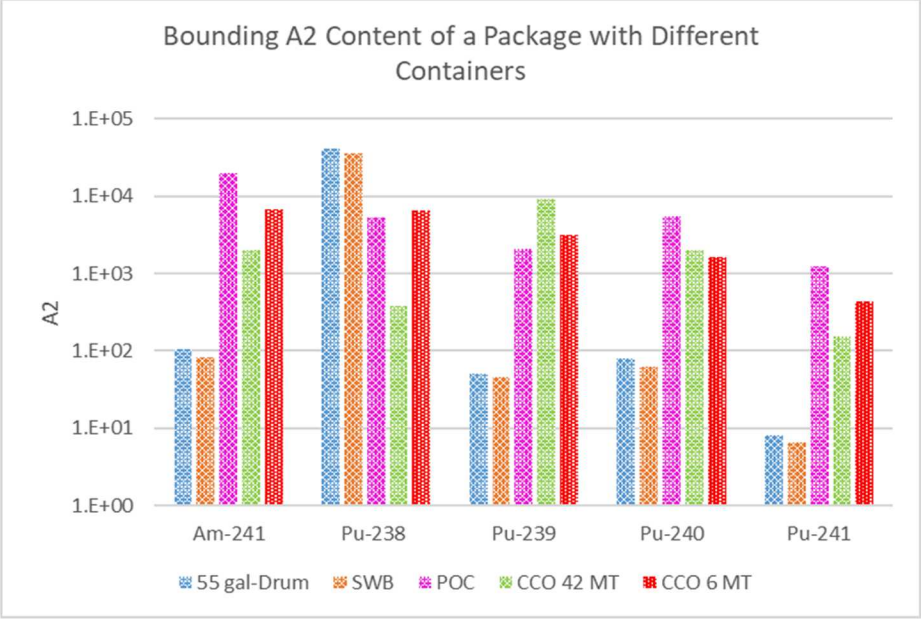

Figure 6-26. Comparison of A_2 Content of TRUPACT-II with Different Containers.

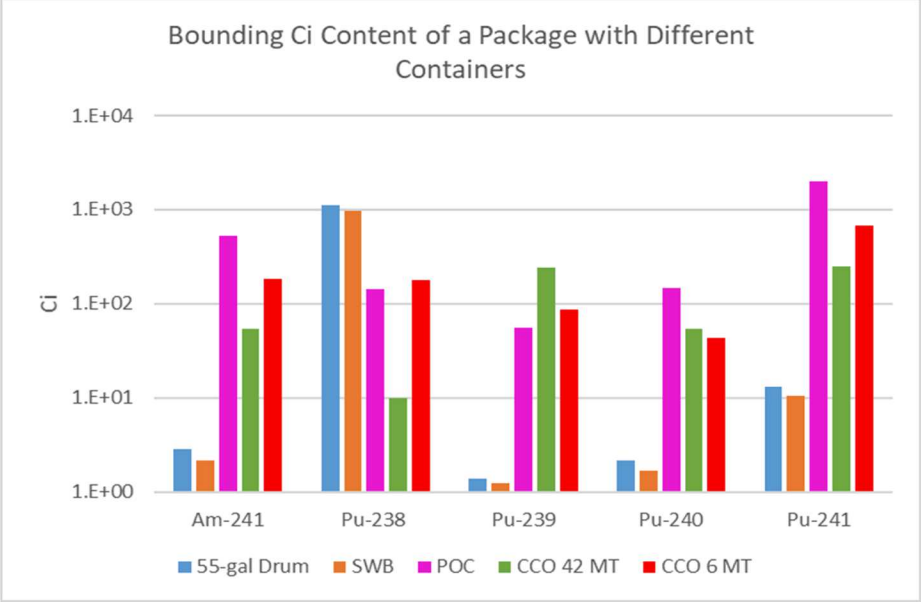

Figure 6-27. Comparison of Ci Content of TRUPACT-II with Different Containers.

Figure 6-28 compares the total A_2 and Ci contents of a TRUPACT-II for the four cases shown in Figures 6-26 and 6-27 and the total A_2 and Ci contents used in SEIS-II and the 2008 TA. A TRUPACT-II with 14 55-gal drums has the highest A_2 content, except the 2008 TA value. The total Ci contents of a TRUPACT-II with either 14 55-gal drums, or 2 SWBs, or 14 CCO (6 MT of surplus Pu) are very similar and close to the SEIS-II value. The 2008 TA total Ci value is significantly higher. A TRUPACT-II with 14 CCOs (42MT) has higher total Ci content than the other cases.

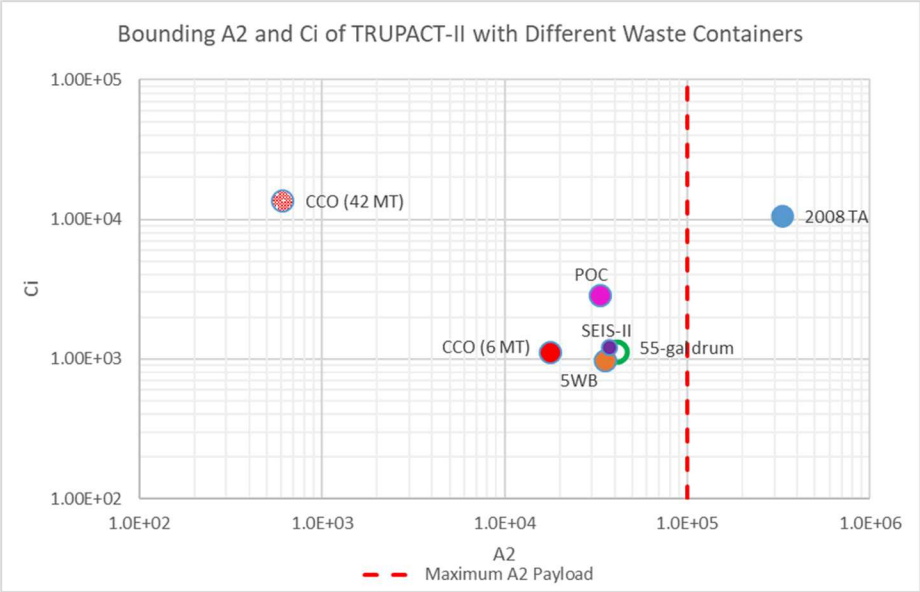

Note: Maximum A_2 payload from CH-TRAMPAC, Section 3.3.14.

Figure 6-28. Comparison of Total A_2 and Ci Contents of TRUPACT-II with Different Containers.

As it was previously discussed, the higher the total A_2 content, the greater are the radiological consequences in the case of an accident. Consequently, a TRUPACT-II with 14 55-gal drums represents the bounding case for the transportation accident scenarios. In addition, an accident in which a TRUPACT-II with 55-gal drums is breached will have highest release because the drums will be completely destroyed. The release from CCOs or POCs will be significantly smaller because of the additional containment.

Consequently, the CH-TRU waste bounding radiological composition is based on the waste stream SR-LA-PAD1 as the CH-TRU waste radiological source term. The contributions of Co-60, Cs-137, Sr-90, and Pu-242 to the total Ci and A_2 contents of this waste stream are negligible (Table 6-2) and these radionuclides can be excluded from the analysis. Note that the shipments of TRUPACT-IIs with either 55-gal drums or SWBs will constitute 70 percent of all the shipments.

6.1.3 RH-TRU Waste

There are 75 WIPP-bound RH-TRU waste streams with associated radionuclide activity reported in the database (Van Soest, G.D., 2019). The radionuclide composition of the RH TRU waste is reported for each waste stream in terms of Ci of each of 220 radionuclides. Note that only 157 radionuclides out of 220 have A_2 values. Waste stream information includes stored and projected container types and estimated numbers of stored and projected containers. The RH-TRU waste streams are shipped either in shielded containers (SCA) in HalfPACT packages (75 percent of RH-TRU waste shipments) or in RH-TRU 72-B packages (25 percent of RH TRU waste shipments). The approach used to define the bounding RH-TRU waste source term was the same as the one used to define the bounding CH-TRU waste source term.

6.1.3.1 RH-TRU 72-B

According to the inventory, 47 WIPP-bound waste streams with associated radionuclide activity reported in the database are either stored or projected to be generated and packed in RH canisters that will be shipped in the RH-TRU 72-B. Ninety one percent of the RH-TRU 72-B will be loaded with a RH canister containing three 55-gal drums and four percent containing NS15 or NS30 containers. The remaining 5 percent will be with directly loaded RH canisters. This analysis considers the inventory of an RH canister with three 55-gal drums. Even though the bounding inventory is developed for a RH-TRU 72-B shipment, it is not used in the accident analysis. As described in Section 6.5, it can be assumed that the RH-TRU 72-B cask does not breach in the extra regulatory accidents.

The major radionuclides for the waste streams that will be loaded in a RH canister with three 55-gal drums were identified as described in Step 7 in Section 6.2.1. The contribution of the major radionuclides to the total A_2 and Ci content are shown in Figures 6-29 and 6-30. The combined major radionuclides contribution to the total A_2 is 97.2 percent (average A_2) and 98.0 percent (maximum A_2). The combined major radionuclides contribution to the total Ci is 72.4 percent (average Ci content) and 71.4 percent (maximum Ci content). In both cases the remaining contribution to the total Ci content is primarily from Ba-137m. Note that Ba-137 contribution is included in A_2 value for Cs-137.

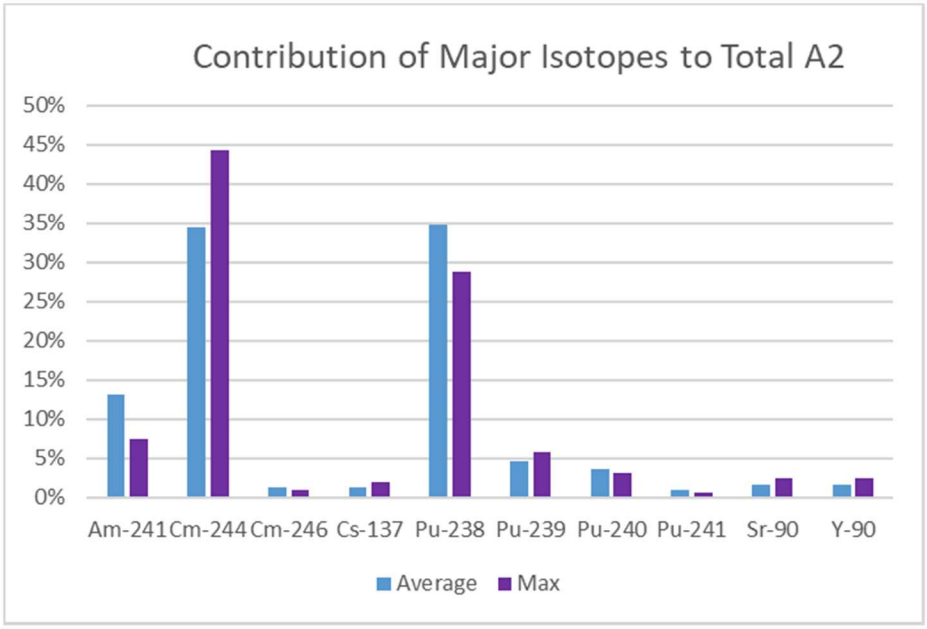

Figure 6-29. A_2 Contributions of the Major Radionuclides in Waste Streams Associated with RH-TRU 72-B.

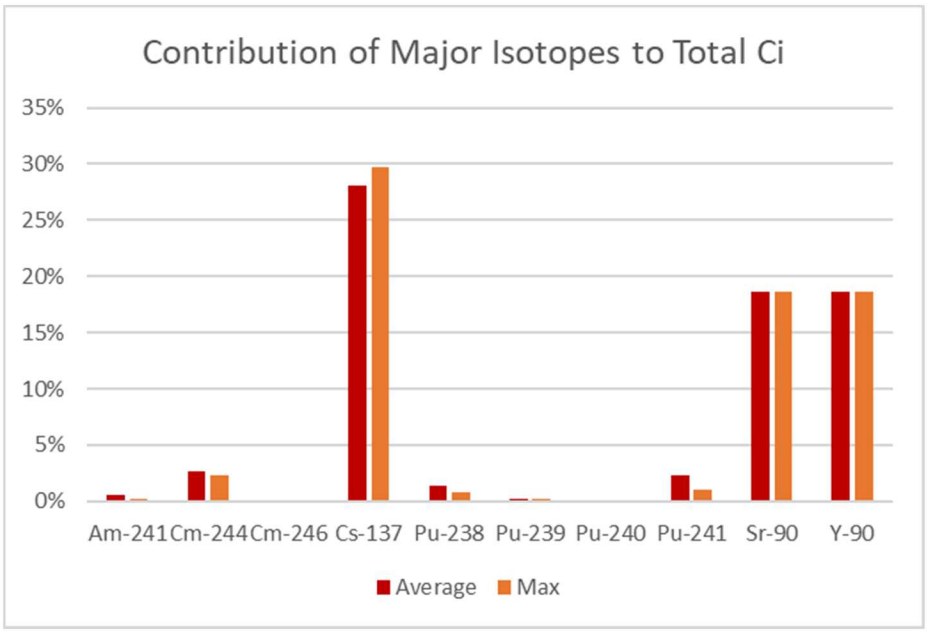

Figure 6-30. Ci Contributions of the Major Radionuclides in Waste Streams Associated with RH-TRU 72-B.

Figures 6-31 and 6-32 show the cumulative frequency distributions for A_2 and Ci of the waste streams in a RH-TRU 72-B with three 55-gal drums in an RH canister. Also shown in Figures 6-31 and 6-32 are the total A_2 and Ci values assumed for the RH-TRU 72-B in SEIS-II and waste stream SR-RH-235F.01. The SR-RH-235F.01 waste stream corresponds to 97.7 percentile (A_2) and maximum Ci value. The SEIS-II values, if placed on the measured (projected) frequency curves correspond to 98.7 percentile in Ci. The SEIS-II A_2 value exceeds the maximum measured (projected) A_2 value and is not plotted in Figure 6-31. The TA 2008 total A_2 and Ci values are greater than the maximum measured (projected) values and are not plotted in Figures 6-31 and 6-32. Table 6-3 summarizes the SEIS-II, 2008 TA, and this TA RH-TRU 72-B waste composition. Note that Pu-242, U-233, U-235, and U-238 are present in SR-RH-235F.01 in very small amounts and their contributions to the total Ci and A_2 are negligible.

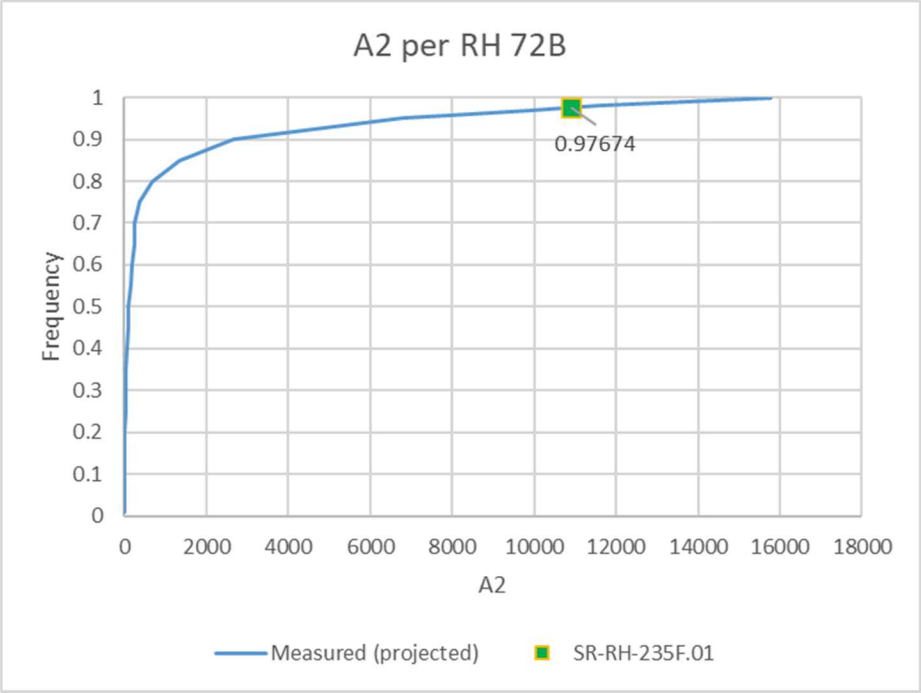

Figure 6-31. Estimated Total A_2 Content per RH-TRU 72-B with Three 55-gal Drums in RH Canister.

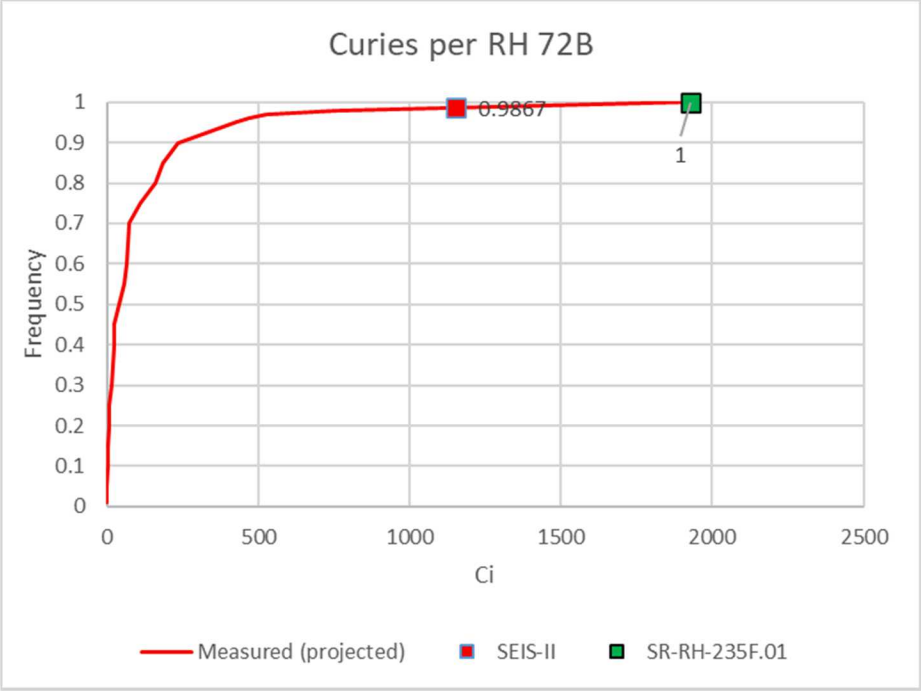

Figure 6-32. Estimated Total Ci Content per RH-TRU 72-B with Three 55-gal Drums in RH Canister.

Table 6-3. RH-TRU 72-B Waste Radionuclide Composition Comparison.

Radionuclide	SEIS II		2008 TA		SR-RH-235F.01	
	Ci	A_2	Ci	A_2	Ci	A_2
Am-241	12	444.4	64.6	2,392.6	85.80	3,177.74
Co-60	2.5	0.23	13.4	1.2		
Cs-137	49	3.06	263.6	16.5		
Pu-238	1,000	37,037	5,379.6	199.24	178.83	6,623.50
Pu-239	20	740.7	107.6	3,985.2	1.50	55.47
Pu-240	10	370.4	53.8	1,992.6	0.40	14.66
Pu-241	10	6.25	53.8	33.6	1,662.96	1,039.35
Pu-242					1.44E-04	5.33E-03
Sr-90	49	6.05	263.6	32.5		
U-233	0.03	5	0.161	26.8	9.20E-07	1.53E-04
U-235	0.0011		0.6E-3		1.77E-08	0
U-238	7.1E-5		3.8E-4		2.69E-13	0
Total	**1,153**	**38,613**	**6,200**	**20,7,725**	**1,929.48**	**10,910.72**

6.1.3.2 RH in Shielded Containers

According to the inventory, 31 WIPP-bound waste streams with associated radionuclide activity reported in the database are either stored or projected to be generated in SCAs. A HalfPACT with SCAs is referred to as a HalfPACT with SCA or as a HalfPACT (SCA). The major radionuclides for these waste streams were identified as described in Step 7 in Section 6.1.1. The contribution of the major radionuclides to the total Ci and A_2 content are shown in Figures 6-33 and 6-34. The combined major radionuclides contribution to the total A_2 is 95.3 percent (average A_2) and 99.4 percent (maximum A_2). The combined major radionuclides contribution to the total Ci is 96.8 percent (average Ci content) and 99.0 percent (maximum Ci content).

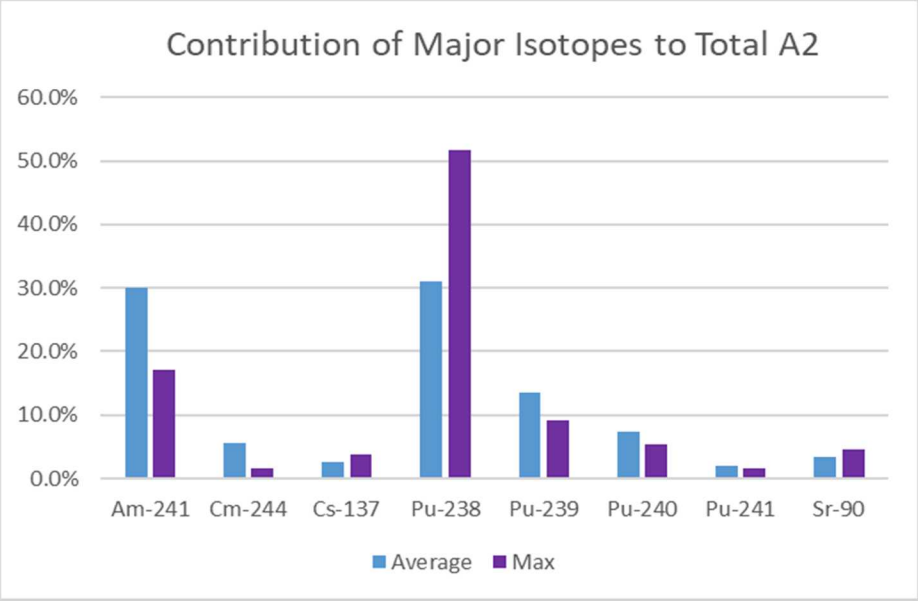

Figure 6-33. A_2 Contributions of the Major Radionuclides in Waste Streams Associated with Shielded Containers.

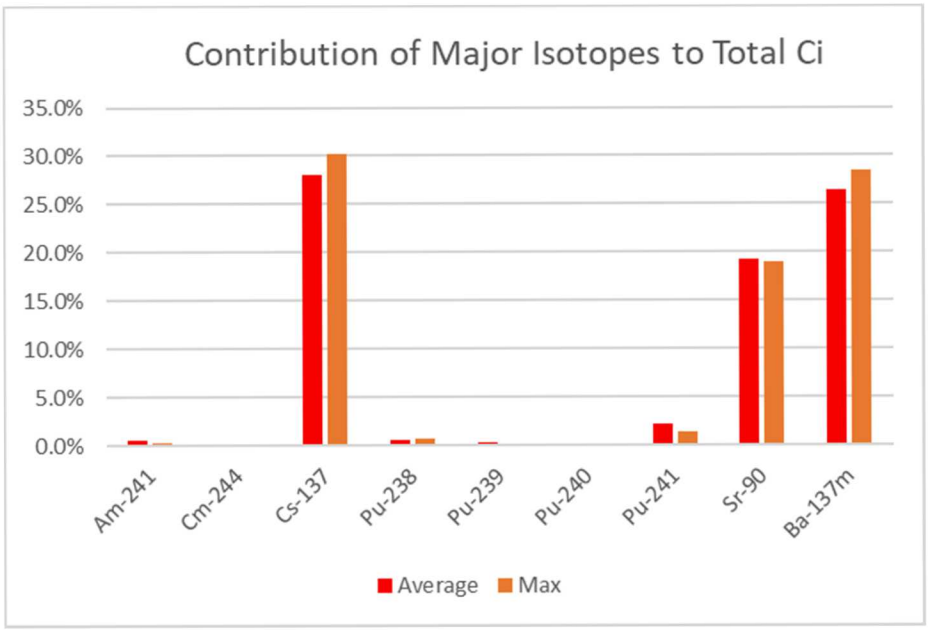

Figure 6-34. Ci Contributions of the Major Radionuclides in Waste Streams Associated with SCAs.

Figures 6-35 and 6-36 compare cumulative frequency distributions of total A_2 and Ci contents of the RH-TRU 72-B with an RH canister containing three 55-gal drums and a HalfPACT with 3 SCAs. The cumulative frequency distributions are similar in shape, but the median A_2 and Ci contents of a HalfPACT with SCAs are about 5 times lower.

Note that the number of SCAs used in calculation of total Ci and A_2 per SCA for each waste stream designated for SCAs was obtained from the Attachment D of WIPP Nuclear Waste Partnership, 2020. In this attachment the number of SCAs was determined considering 4 additional SCA designs. The database query (Van Soest, G.D., 2019) provides the container count based on the currently approved SCA design with ~1" of lead shielding in a 30-gallon drum.

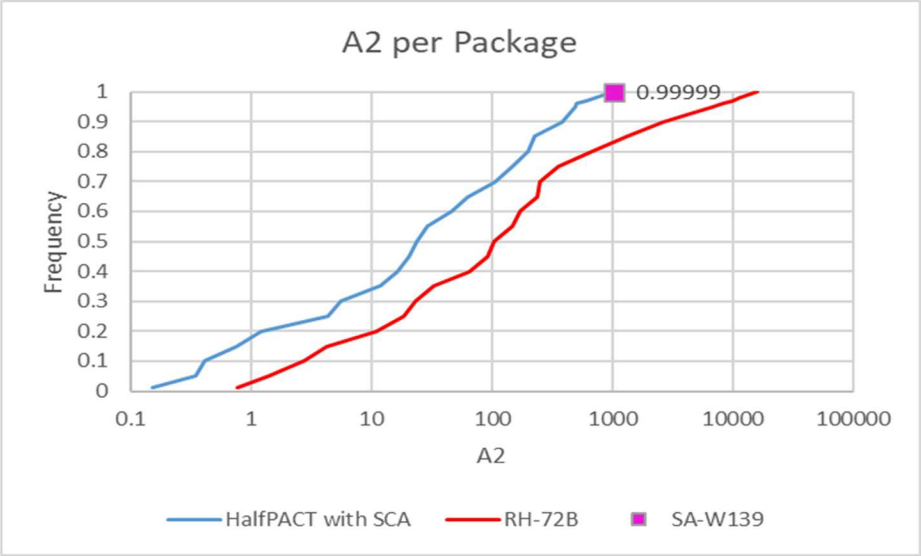

Figure 6-35. Comparison of Total A_2 Content of RH-TRU 72-B with RH Canister Containing Three 55-gal Drums and a HalfPACT with Three SCAs.

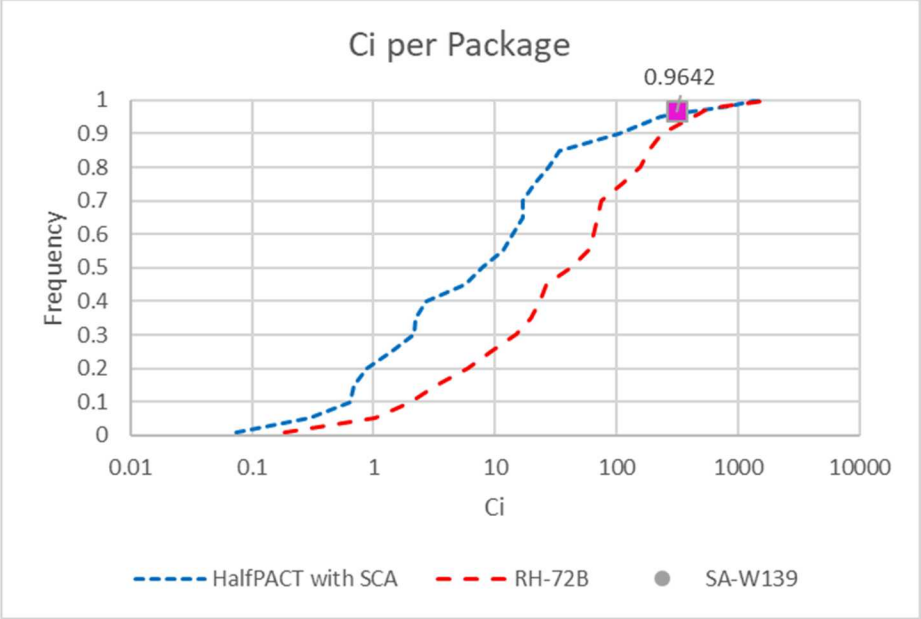

Figure 6-36. Comparison of Total Ci Content of RH-TRU 72-B with RH Canister Containing Three 55-gal Drums and a HalfPACT with Three SCAs.

Also shown in Figure 6-35 and 6-36 are the total A_2 and Ci values for the waste stream SA-W139. The SA-W139 waste stream corresponds to maximum A_2 and 96.4th percentile Ci. The radionuclide composition is provided in Table 6-4.

Table 6-4. Radionuclide Composition of Waste Stream SA-W139 per HalfPACT with SCA.

Radionuclide	Ci	A_2
Am-241	7.53	278.89
Cs-137	68.16	4.26
Pu-238	3.33	123.43
Pu-239	9.40	348.07
Pu-240	5.99	222.04
Pu-241	55.71	34.82
Sr-90	50.50	6.23
Y-90	50.52	6.24
Total	**251.15**	**1,023.97**

Figures 6-37 and 6-38 compare contributions of the major radionuclides to the total A_2 and Ci of RH waste streams designated for RH canisters containing three 55-gal drums and waste streams designated for SCAs. The contributions of Am-241, Pu-238, Pu-239, and Pu-240 to the total A_2 are larger in the SCAs waste streams than in RH canisters with three 55-gal drums waste streams. The contributions of Cm-244, Cs-137, Sr-90, and Y-90 to the total A_2 are smaller in the SCAs waste stream than in RH canisters with three 55-gal drums waste streams. The contributions to the total Ci are very similar. In both cases they are from Cs-137, Sr-90, and Y-90.

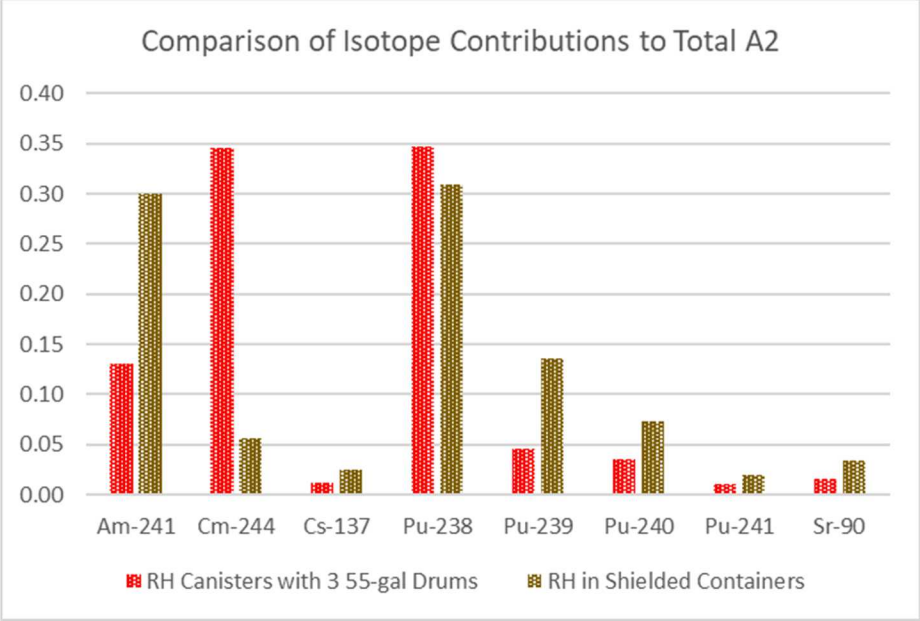

Figure 6-37. Radionuclide Composition Comparison of RH Canisters with Three 55-gal Drums and RH in SCAs Waste Streams.

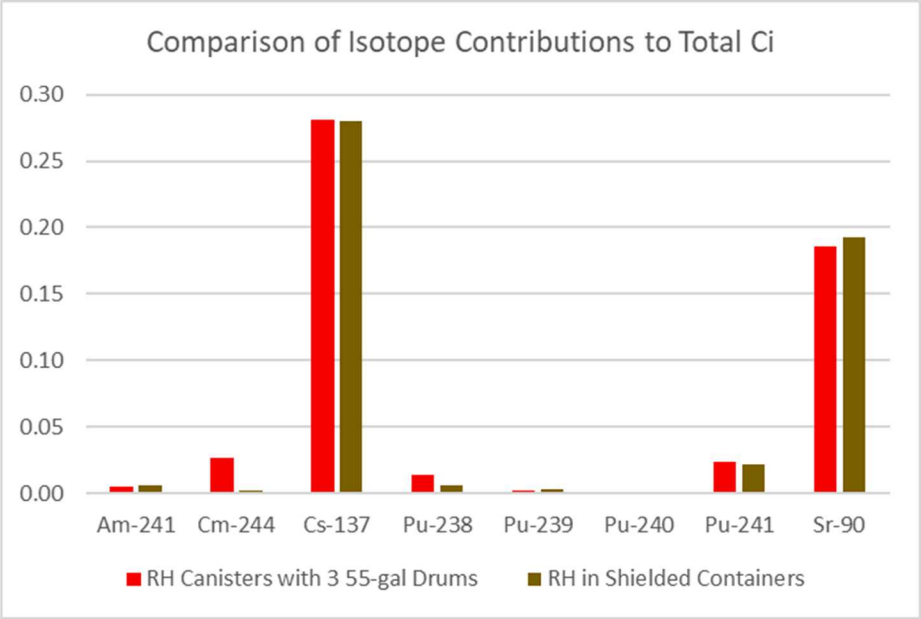

Figure 6-38. Ci Radionuclide Composition Comparison of RH Canisters with Three 55-gal Drums and RH in SCAs Waste Streams.

6.1.3.3 Bounding RH-TRU Waste Radiological Source Term for 2020 TA Accident Analysis

The analysis of the RH-TRU waste streams (RH-TRU 72-B and SCAs) demonstrated that nine radionuclides (Am-241, Cm-244, Cs-137, Pu-238, Pu-239, Pu-240, Pu-241, Sr-90, and Y-90) contribute more than 99 percent to the package total A_2 and more than 80 percent to the package total Ci content. However, the total A_2 and total Ci contents are about 20 times higher for RH-TRU 72-B compared to HalfPACT with SCAs.

The RH-TRU 72-B will behave differently in an accident than the HalfPACT. Consequently, the bounding source term for the RH-TRU 72-B is based on the waste stream SR-RH-235F.01 (Table 6-3). The bounding source term for the HalfPACT with SCAs is summarized in Table 6-4.

6.1.4 Bounding Radiological Source Terms for CH-TRU and RH-TRU Waste

Table 6-5 summarizes the bounding source terms for CH-TRU and RH-TRU waste. The CH TRU source term applies to CH-TRU waste (drums, SWBs, and SLB2) in TRUPACT-II and TRUPACT-III. Two bounding source terms are proposed for RH-TRU waste – one for the RH-TRU 72-B and another for the HalfPACT with RH-TRU waste in SCAs. The bounding composition for the RH-TRU 72-B was developed (Section 6.1.3.1) but was not used in the accident analysis as discussed in Section 6.5.

Table 6-5. Bounding Source Terms for CH-TRU and RH-TRU Waste.

Radionuclide	CH-TRU Waste		RH-TRU Waste			
			RH-TRU 72-B		HalfPACT (SCA)	
	Ci	A_2	Ci	A_2	Ci	A_2
Am-241	2.85	105.49	85.80	3,177.73	7.53	278.89
Cm-244			0.06	1.15		
Cs-137					68.16	4.26
Pu-238	1,105.41	40,941.28	178.83	6,623.67	3.33	123.43
Pu-239	1.38	50.95	1.50	55.47	9.4	348.07
Pu-240	2.18	80.56	0.40	14.67	5.99	222.04
Pu-241	12.98	8.11	1,662.97	1,039.33	55.71	34.82
Sr-90					50.5	6.23
Y-90					50.52	6.24
Total	**1,124.8**	**41,186.4**	**1,929.6**	**10,912.0**	**251.1**	**1,024.0**

6.2 TRUPACT-II IMPACT MODELING

6.2.1 Introduction

As part of the TA, seven structural finite element analyses of the TRUPACT-II package were conducted. The analyses are listed in Table 6-6. Three of the analyses were conducted to validate the finite element model and are compared to the hypothetical accident conditions (HAC) test results. The remaining four analyses were conducted at extra-regulatory velocities to determine the integrity of the package. These analyses focused on maintaining the integrity of the internal containment vessel (ICV), using the American Society of Mechanical Engineers (ASME) strain-based failure criteria (ASME 2019).

The three analyses simulating the free drop test show good agreement with the deformation observed in the posttest examinations. The 60-mph top and side impact analysis show that at this extra-regulatory velocity, the ICV maintains containment. Based on the application of the ASME stain-based criteria, the 60-mph center-of-gravity-over-corner (CGOC) impact analysis indicated that a rupture may occur in the ICV flange. As a result, an additional 45-mph CGOC analysis was performed. At this velocity and orientation, the ICV remained leak tight.

Table 6-6. List of TRUPACT-II Impact Analyses

	Orientation	Velocity
1	CGOC	30-mph
2	Top	30-mph
3	Side	30-mph
4	CGOC	45-mph
5	CGOC	60-mph
6	TOP	60-mph
7	Side	60-mph

6.2.2 TRUPACT-II Model

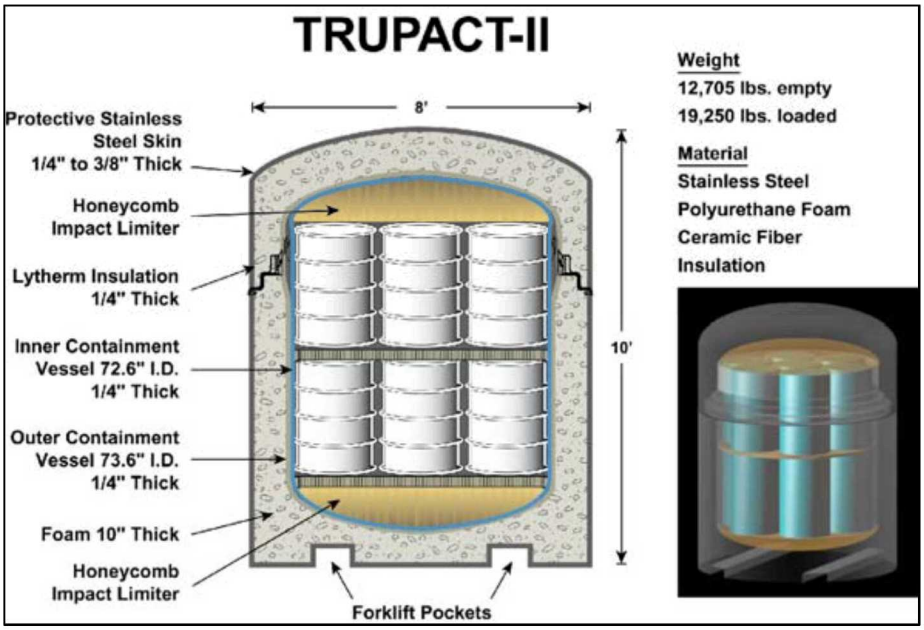

Figure 6-39. TRUPACT-II Transuranic Waste Transportation Container.

The TRUPACT-II packaging shown in Figure 6-39 is comprised of an outer confinement assembly (OCA) and an inner ICV that provides the primary containment boundary. The ICV and the OCA each have an upper and lower section joined together by a locking ring. Two aluminum honeycomb spacer assemblies are used within the ICV, one inside each ICV torispherical head. The OCA consists of an inner stainless-steel shell, a polyurethane layer, and an outer stainless steel shell. The inner stainless-steel shell of the OCA forms the outer confinement vessel (OCV). Inside the ICV, the payload will be within 55-gallon drums, 85-gallon drums, 100-gallon drums, SWBs, or TDOPs.

The impact analysis was conducted using Sandia's explicit dynamic finite element code Presto-SIERRA (SIERRA Solid Mechanics Team, 2019). The finite element model used in the analysis is shown in Figure 6-40. The model is a half-symmetry model. It contains the ICV, OCV, OCA, and a homogenized payload. The model contains 2,780,089 elements.

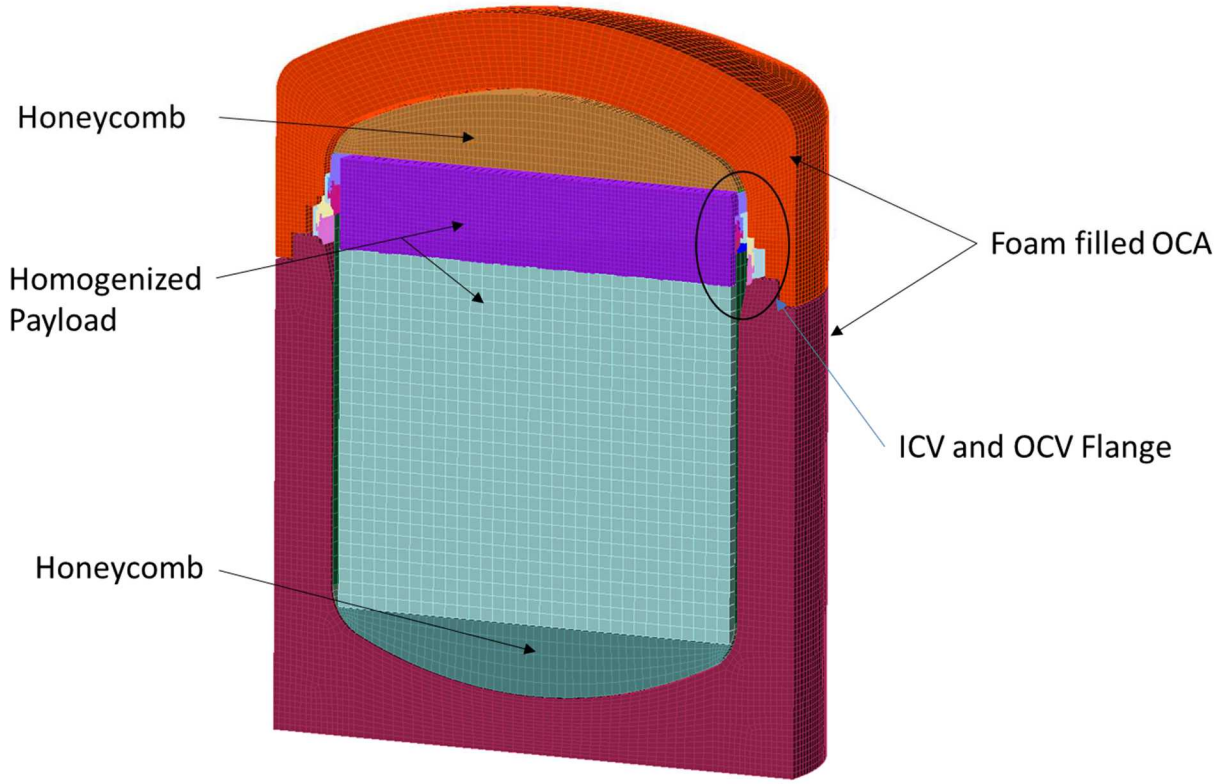

Figure 6-40. TRUPACT-II Finite Element Model.

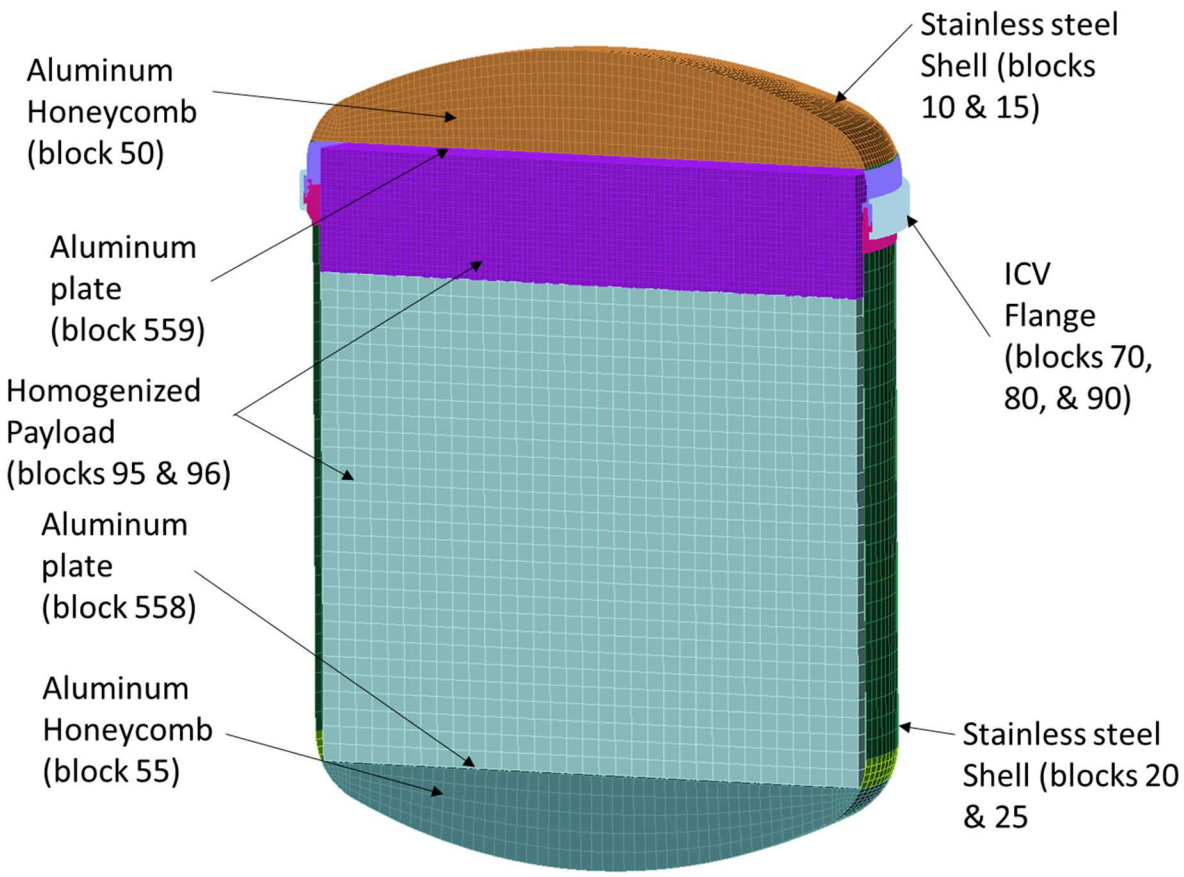

Figure 6-41. Inner Containment Vessel (ICV).

An isolated model of the ICV is shown in Figure 6-41. It consists of a stainless-steel shell, stainless-steel flanges and lock ring, aluminum honeycomb impact limiters, and a homogenized payload. The ICV upper and lower head, the upper and lower aluminum plates, and the ICV cylindrical wall are modeled using shell elements. The aluminum honeycomb, payload, and the locking flange are modeled using eight node hexahedral (hex) elements.

Figure 6-42 shows a magnified view of the ICV flange. The flanges and lock ring are modeled using hex elements. Five elements are used through the flange thickness to properly capture bending through the section. The coarser mesh of shell elements of blocks 10 and 20 are attached to the higher fidelity solid element mesh using shell solid constraint equations. This allows the deformations in the flange region to be accurately modeled while minimizing the size of the mesh.

The payload is modeled as a homogenous cylinder using solid hex elements. The density of the mesh is increased where the upper portion of the content contacts the flange and upper head to allow more deformation of the simulated payload material. The lower section, which primarily provides mass and momentum is modeled with a coarser mesh. The two section are joined with tied contact.

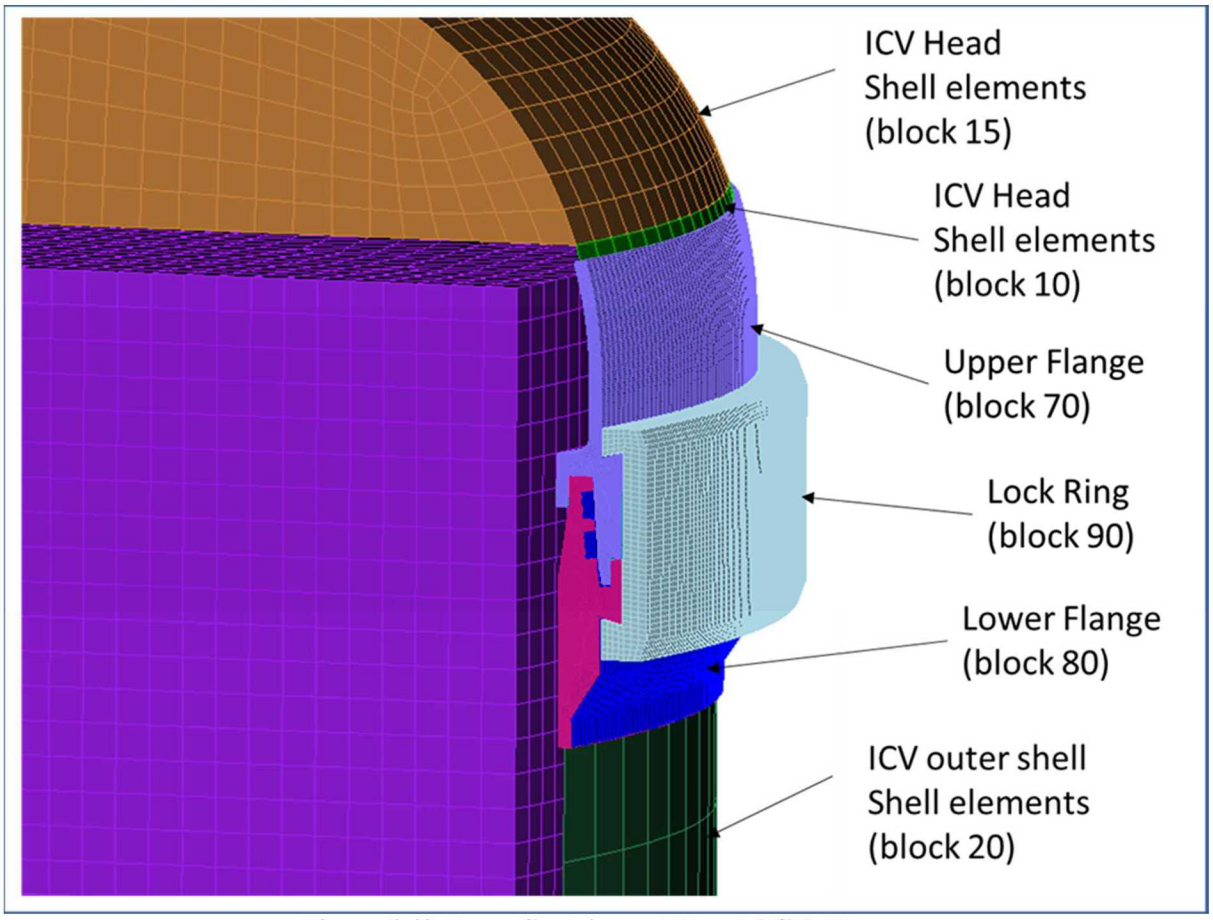

Figure 6-42. Inner Containment Vessel (ICV) Flange.

An isolated view of the OCA is shown in Figure 6-43. This figure shows the polyurethane foam, the OCV flange, and the outer OCA shells. A clearer illustration of the OCA shells is shown in Figure 6-44. This figure removes the polyurethane foam and reveals the inner shells and flange which form the OCV along with the outer shells and the shells forming the bottom and top of the upper and lower sections where they are joined in the flange region.

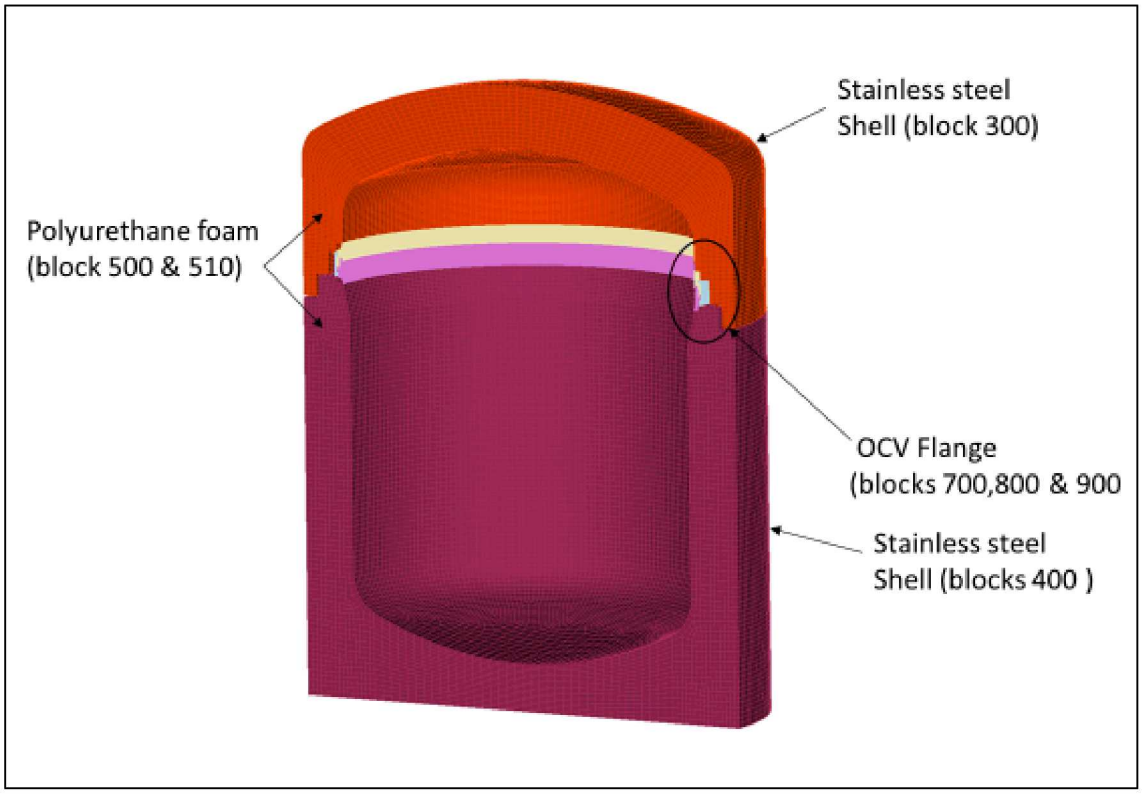

Figure 6-43. Isolated OCA Model.

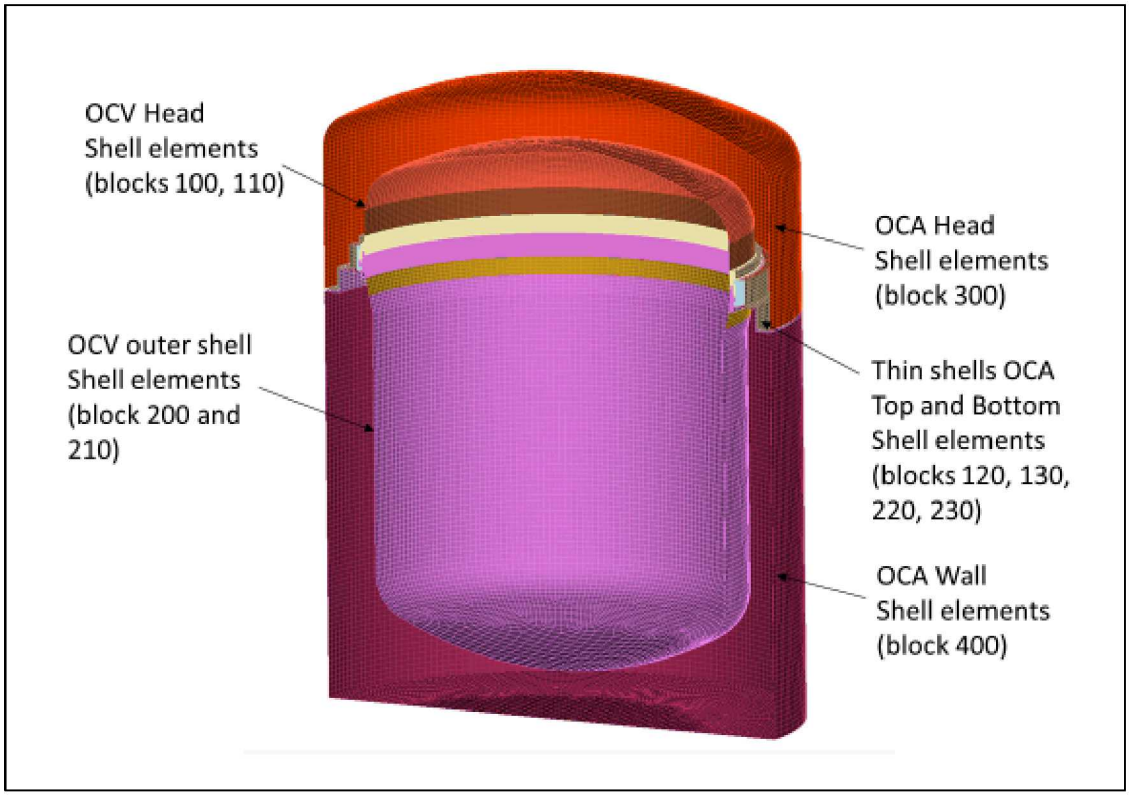

Figure 6-44. Shells of OCA (Foam Removed).

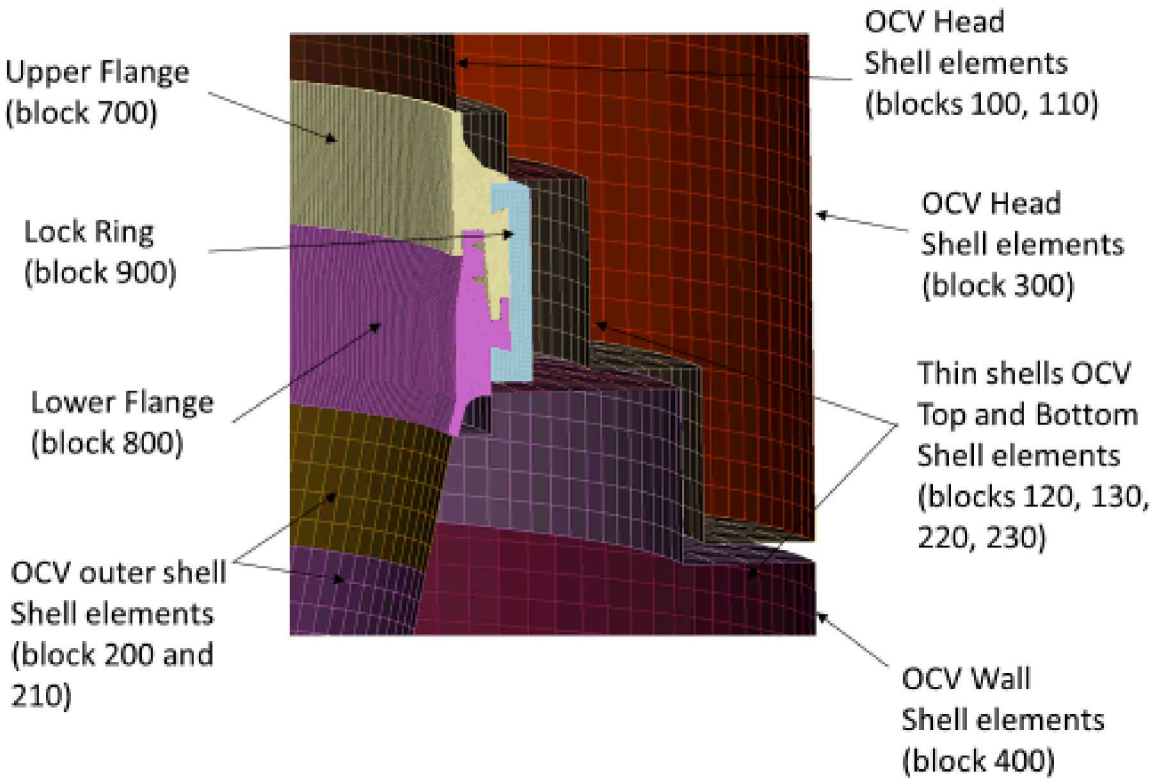

Figure 6-45. Flange Region of the OCA (Foam Removed).

Figure 6-45 is a magnified view of the OCV flange region. This figure clearly shows the flange and the shell between the upper head and the lower section of the package. Each figure provides the block number corresponding to the various components. The material and element type for each of the blocks are provided in Appendix B (Table B-1).

6.2.3 Model Conservatisms

There are two significant conservatisms in the finite element model. The first concerns the polyurethane foam material between the OCA and the OCV shell. This material is very compliant and is subject to large deformation during impact. As a result, the highly distorted elements can cause instabilities in the model and must be removed. The removal of these highly distorted elements during the analysis reduces the energy absorbing capability of the material and can result in higher impact velocity of the package components. This can result in higher loads and stresses. The second conservatism is related to the use of the ASME strain-based failure criterion. This criterion is based on the stress state and plastic strain in a component. However, by design, the criterion does not differentiate between tensile and compressive stresses. The former leads to the creation of voids in ductile material which lead to the formation of cracks, while the latter does not. This results in an over prediction of part failure under conditions where it may not occur. These two conditions increase the conservatism of the model.

6.2.4 Material Models

6.2.4.1 SA-240 Stainless-Steel

The ICV, OCV, and OCA shell and flange components are manufactured using 304 stainless-steel. Figure 6-46 shows the room temperature true stress-strain curve used in the model. The finite element model uses the multilinear Elastic-plastic hardening model. The multilinear elastic-plastic model is a generalization of the standard rate independent plasticity model. However, rather than having a specific functional form, the multilinear hardening model allows the user to input a piecewise linear function for the hardening curve.

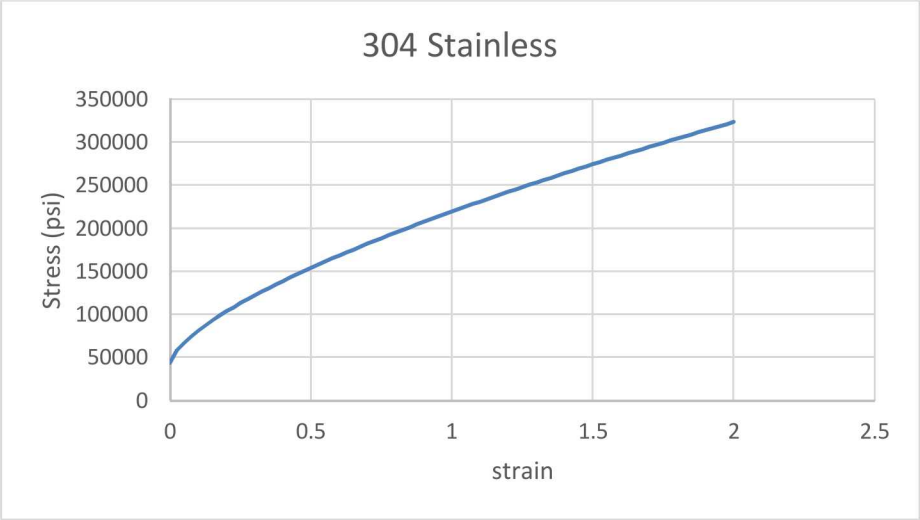

Figure 6-46. Engineering Stress-Strain Curve for 304 Stainless-Steel at Room Temperature.

Evaluation of the stainless-steel material is based on the stress triaxiality (η) which is calculated as:

$$\eta = -\frac{p}{\sigma_e} \tag{6-1}$$

where p is the pressure and σ_e is the effective stress. The pressure is given by:

$$p = -\frac{1}{3}\mathrm{tr}(\sigma) \tag{6-2}$$

and the effective stress by:

$$\sigma_e = \sqrt{3J_2} \tag{6-3}$$

where J_2 is the second stress invariant and is calculated from the stress σ as:

$$J_2 = \frac{1}{2}[\mathrm{tr}(\sigma^2)] - \frac{1}{3}\mathrm{tr}(\sigma)^2 \tag{6-4}$$

The failure criterion uses the strain-based acceptance criteria specified in ASME Nonmandatory Appendix FF. This is calculated at each time step in the analysis and the maximum value is tracked for each element for comparison to the allowable criteria:

$$[TF\epsilon^p]_{max} \leq \epsilon_{uniform} + 0.25\left(\epsilon_{fracture} - \epsilon_{uniform}\right) \tag{6-5}$$

Where $TF = 3 * \eta$, $\epsilon_{uniform}$ is the true strain just prior to the onset of necking in a uniaxial tensile specimen, and $\epsilon_{fracture}$ is the true strain at fracture in a uniaxial tension specimen. The eight-node, uniform-gradient hexahedron with a single integration point is used to model the solid elements of the stainless-steel flanges. The Four-node, quadrilateral shell with five integration points through the thickness

is used to model the shell components. The $[TF\ \epsilon^p\ ]_{max}$ values are calculated at the center of each hex element and at the two outer (1st and 5th) integration points in the shell elements.

Figure 6-47 presents engineering stress-strain data for 304L stainless-steel, which begins to neck at an engineering strain of 0.6. Using Equation 6-5 and the data from Ref[4] which is tabulated in Appendix B.1.1, the maximum values of $[TF\epsilon^p]_{max}$ for the base and weld material at -20°F and 70°F are presented in Table 6-7.

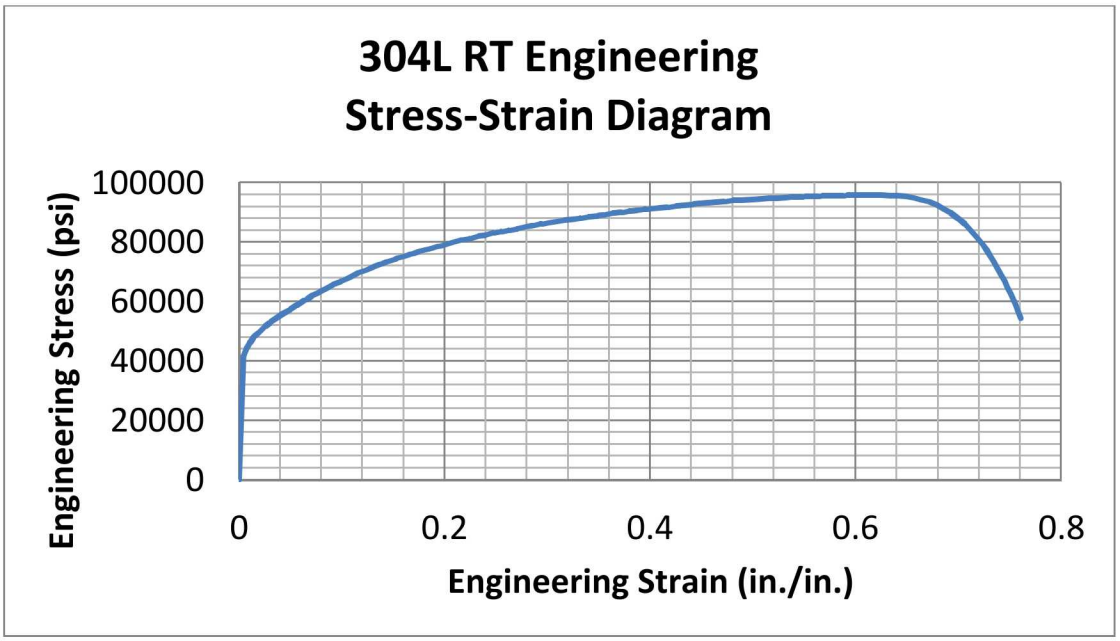

Figure 6-47. 304L RT Engineering Stress-Strain Diagram.

Table 6-7. Maximum Allowable Values of $[TF\epsilon^p]_{max}$

Temperature (F)	Material	TF_EQ_max
-20	base	0.691
-20	weld	0.684
70	base	0.815
70	weld	0.664

6.2.4.2 Foam Material Model

The layer between the OCA outer shell and the OCA inner shell (OCV) is filled with 8.25 lb/ft^3 polyurethane foam. This material acts as the impact limiter material for the package. It is modeled using the Low-Density Foam model (Neilson, M.K., Morgan, M.S. and Krieg, R.D., 1987). This model was based on decomposition of the foam response into two parts: (1) response of the polymer skeleton, and (2) response of the air inside the cells, which is completely volumetric. The parameters for this model were developed through testing and are based on the volume fraction of the material and the Young's modulus. The following equation taken from Neilson, M.K. et al. (1987) were used to derive the model parameters.

$$A = 3440\ \phi^{1.676}$$
$$B = 2780\ \phi^{1.645}$$
$$C = 2.11\ -\ 31.1\ \phi$$
$$E\ = 454000\ \phi^{2.20}$$

Based on these equations and the material properties taken from the SAR (TRUPACT-II Safety Analysis Report, 2013) the foam material modeling parameters are presented in Table 6-8.

Table 6-8. Low-Density Foam Model Parameters.

Parameter	Value
E	6,810 psi
ϕ	0.148
A	139.93
B	119.998
C	-2.4928

The foam material is very compliant and the high velocity impacts of the extra-regulatory analyses can generate large distortions in the foam elements. These highly distorted element can cause problems with the numerical stability of the model. Therefore, several criteria are applied to remove these distorted elements from the mesh. The following death criteria are checked during the run:

1. Death on inversion
2. Value of nodal_jacobian_ratio <= 0.0
3. Value of solid_angle <= 0.0
4. Value of timestep < 2.5E-08

The death criteria can remove a large number of elements from narrow regions of the impacted foam. This can result in less energy being absorbed by the foam and or a poor redistribution of the impacting load. This can cause higher, more localized loads to be transmitted to the ICV shell.

6.2.4.3 Honeycomb Material

Two aluminum honeycomb spacer assemblies are used within the ICV, one inside each ICV torispherical head. The honeycomb has a density of 3.6 lb/ft^3. It is modeled using the orthotropic crush model. This is an empirically based model designed to model energy absorbing material. Three response regimes are assumed in the model: (1) orthotropic elastic, (2) crush, and (3) complete compaction.

In the elastic regime, the model exhibits the response of an elastic, orthotropic material with all Poisson's ratio equal to zero. After full compaction, the response is taken to be that of an isotropic, perfectly plastic material and the response between these two stages is tailored to smoothly transition between the two extremes. Crushing, incorporating both nonlinear elastic and plastic-like behaviors, begins as soon as volumetric contraction is noted (J = det(Fij) < 1). An internal state variable, Jc, is introduced to track the crushed state of the material and is defined as the minimum J over the entire deformation history. In the crush phase a plastic-like response governed by a crush curve is observed.

The values for the material parameters are given in Tables 6-9, 6-10, and 6-11 for the three regimes in the model. These values have been scaled from modeling data for 32 lb/ft^3 honeycomb material (Hinnerichs et al. 2006). Note that while the model allows for orthotropic properties, for this analysis the material was assumed to be isotropic.

Table 6-9. Orthotropic Elastic Properties (Regime 1).

Parameter	Psi
EX	5×10^4
EY	5×10^4
EZ	5×10^4
GXY	2.5×10^4
GYZ	2.5×10^4
GZX	2.5×10^4

Table 6-10. Crush Function (Regime 2).

Crush (Jc)	Stress Psi
0	200
0.05	300
0.1	325
0.4	325
0.5	425
0.6	528
0.7	528
0.85	20 000
0.9	20 000

Table 6-11. Post Lock-up Properties (Regime 3).

Parameter	Value
Young's Modulus	4×10^6 psi
Poisson's Ratio	0.3
Yield Stress	40 x 103

6.2.4.4 Concrete Material

The payload is modeled as one solid cylinder. The material is modeled as an Elastic-Plastic low density, low strength, concrete material. The density was calculated to get the mass of the volume equal to the maximum weight of the payload assembly. The material properties were chosen to provide a soft dense material for impact to represent partially filled drums. The material properties used in the analysis are presented in Table 6-12.

Table 6-12. Material Properties of TDOP.

Parameter	Values
Density	5.95e-5 ($lb\text{-}s^2/in^{4)}$
Young's Modulus	2e5 psi
Poisson's Ratio	0.21
Yield Stress	300 psi
Beta	1
Hardening Modulus	2e5 psi

6.2.4.5 Aluminum Plate Material

The aluminum plates on the inner surface of the honeycomb spacer assemblies are modeled using an Elastic-Plastic Power-Law Hardening Model. This is a hypoelastic, rate independent plasticity model with power law hardening. Material parameters for 6061_T6 aluminum are given in Table 6-13.

Table 6-13. Elastic- Plastic Power-Law Material Properties for 6061-T6 Aluminum.

Parameter	Values
Density	2.59 x 10 $^{-4}$ (lb-s^2/in^4)
Young's Modulus	10 x 10^6 psi
Poisson's Ratio	0.35
Yield Stress	42 000 psi
Hardening Const - A	47 550 psi
Hardening Exponent	0.48
Luders Strain	0

6.2.4.6 Boundary/Initial Conditions

The TRUPACT-II model has half-symmetry on the X-Y plane as shown in Figure 6-48. The model is orientated such that the velocity for the different impact orientation is always in the Y-direction. The velocities for the seven analysis are given in Table 6-6. The target is modeled as a flat steel plate with fixed displacements in the x-y-z directions. A Coulomb friction model is used at the contact between the OCA outer shell and the target surface for the 30-mph impacts. A friction coefficient of 0.3 is used in these analyses. All other contact surfaces are frictionless.

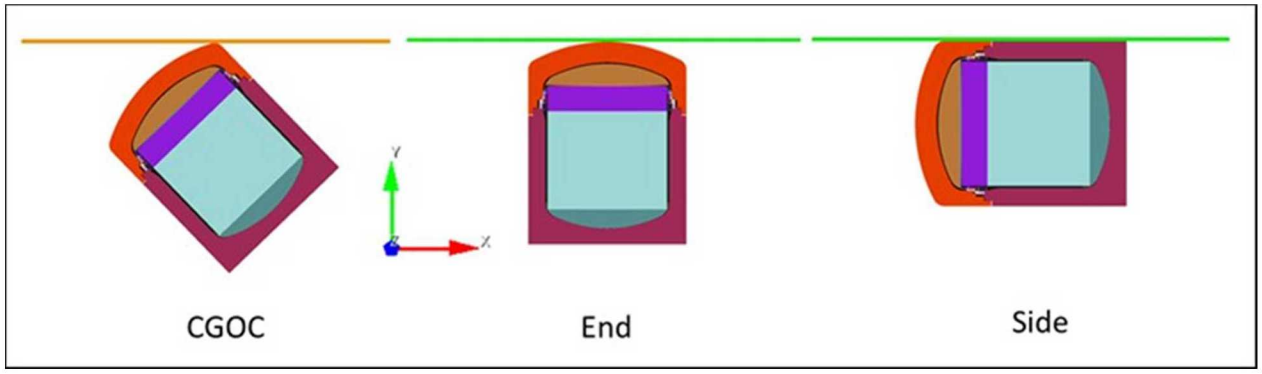

Figure 6-48. Analysis Impact Orientations.

6.2.5 30-mph Model and Test Comparison

To validate the finite element model, three analyses were conducted of the three free drop certification tests. The model results were compared to the test results documented in the TRUPACT-II SAR[3]. Table 6-14 lists the post-test deformations of the test articles taken from Table 2.10.2-1 of the SAR for the three HAC tests. Table 6-15 provides the deformed dimension taken from the three finite element analyses.

Table 6-14. TRUPACT-II SAR Test Results (TRUPACT-II Safety Analysis Report, 2013)

Test No.	Test Description	Test Unit Angle	CTU Temperature	Observation and Results
2	HAC, 30-foot side drop onto OCV vent port	0º (side)	Ambient	37" wide flat at top (OCA lid) × 35" wide flat at bottom (OCA body) × ~3-5/8" deep
3	HAC, 30-foot CG onto OCA lid knuckle near OCA lid lift pocket	-47º (CGOC)	Ambient	30" wide × 53" long flat at top (OCA lid) × ~3¾" deep
4	HAC, 30-foot top drop	-90º (End)	Ambient	53" diameter flat at top (OCA lid) × ~3¾" deep

Table 6-15. TRUPACT-II HAC Analysis Results

Test No.	Analysis	CTU Temperature	Crush Dimensions
2	30-mph Side Impact	Ambient	36.9" wide flat at top (OCA lid) × ~3.75" deep
3	30-mph CGOC impact	Ambient	31.4" wide × 63.7" long flat at top (OCA lid) × ~10" deep
4	30-mph Top Impact	Ambient	64" diameter flat at top (OCA lid) × ~5.3" deep

Photos taken from the SAR along with deformed figures of the model are shown in Figures 6-49 – 6-54. For the side impact orientation, the analysis shows very good agreement with the test deformation and measurements. The width and depth of the impact region match the test article very closely.

Figure 6-49. TRUPACT-II Test Unit Side Impact HAC Drop Test.

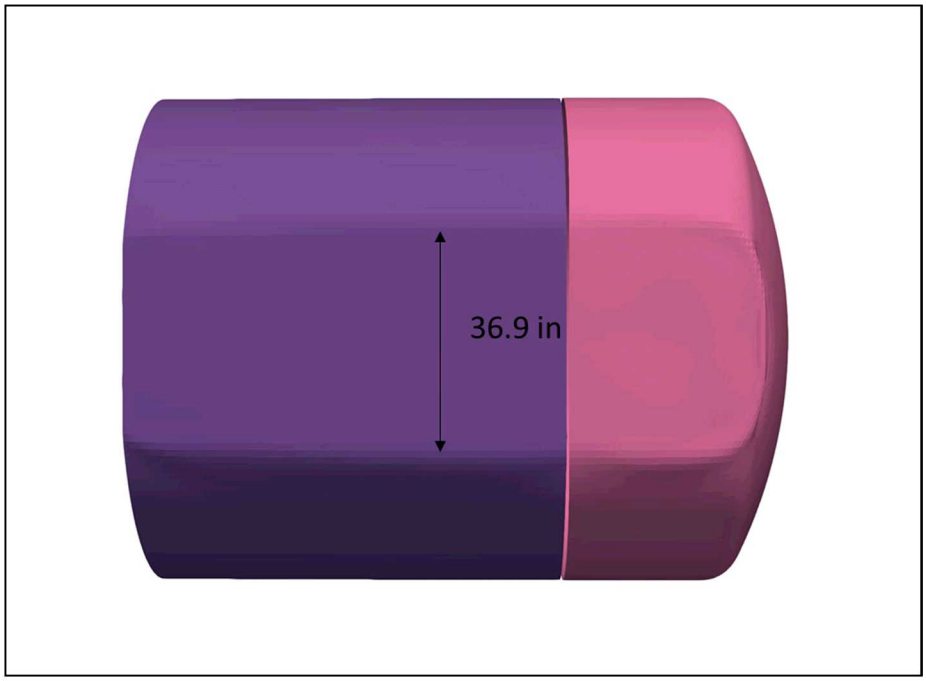

Figure 6-50. TRUPACT-II Side Impact Model Deformation.

For the end impact orientation, the model has a larger impact diameter that the impact diameter reported in the test (64.9 inches versus 53 inches). The depth of the impact region in the model is also larger than the depth recorded during the test (5.3 inches versus 3.74 inches). This indicated that the model foam material is slightly softer than the foam material in the test units.

Figure 6-51. TRUPACT-II Test Unit Top Impact HAC Drop Test.

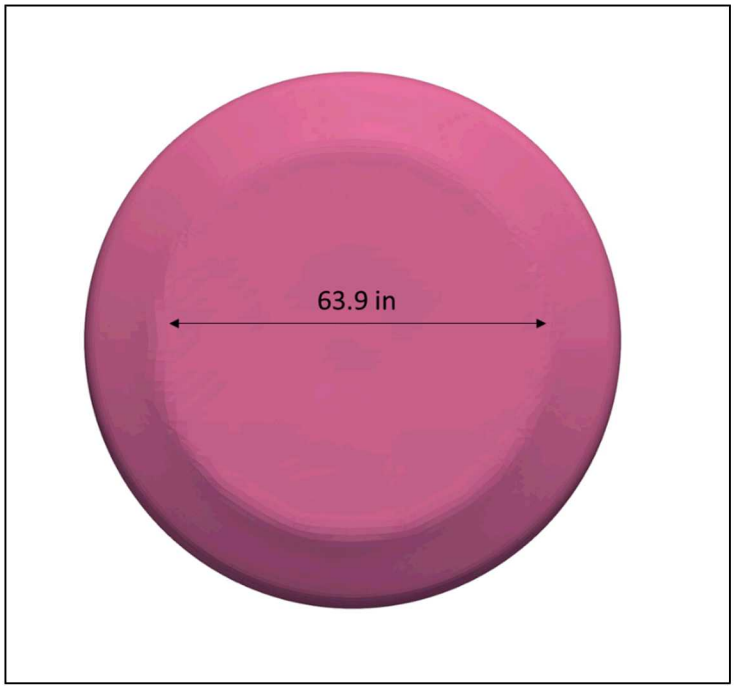

Figure 6-52. TRUPACT-II Top Impact Model Deformation.

Figure 6-53. TRUPACT-II Test Unit CGOC Impact HAC Drop Test.

The deformation of the model in the CGOC orientation is larger than the deformation of the test unit. The minor diameter of the ellipse is slightly larger (31 inches versus 30 inches) than the test unit. The major diameter is larger by about 10 inches (63.7 inches versus 53 inches). There is significant difference between the crush depth of the model and the crush measured in the test. The depth of crush in the model is almost 10 inches while the reported depth in the SAR is 3.75 inches. Figure 6-55 shows line and depth of crush based on the minor diameter of the ellipse. These lines were drawn by hand in the Paraview post processing code [6] to give an estimate of the crush depth and the minor diameter. Based on this approximation, the

minimum crush depth should be closer to 8 inches for a crush region with a minor diameter of 30 inches. This larger depth would reduce the difference between crush depth of the model and the test; resulting in better approximation and a model that is only slightly softer than the test unit.

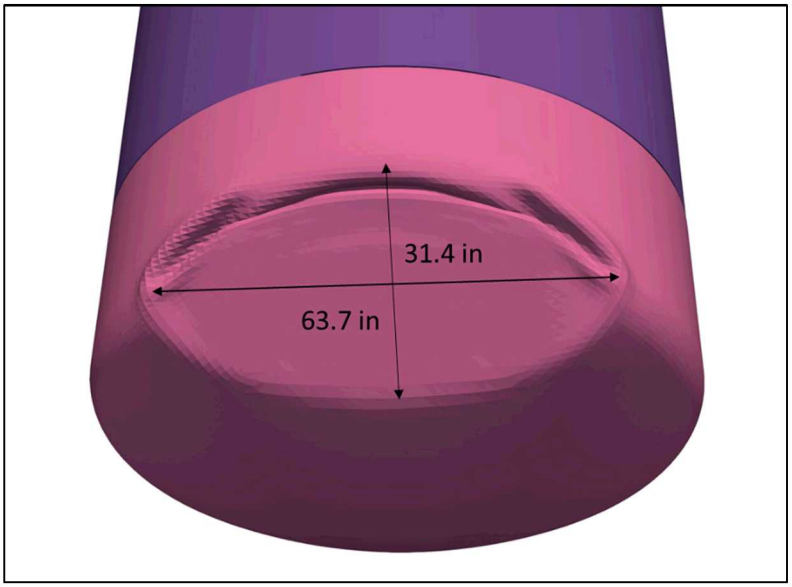

Figure 6-54. TRUPACT-II CGOC Impact Model Deformation.

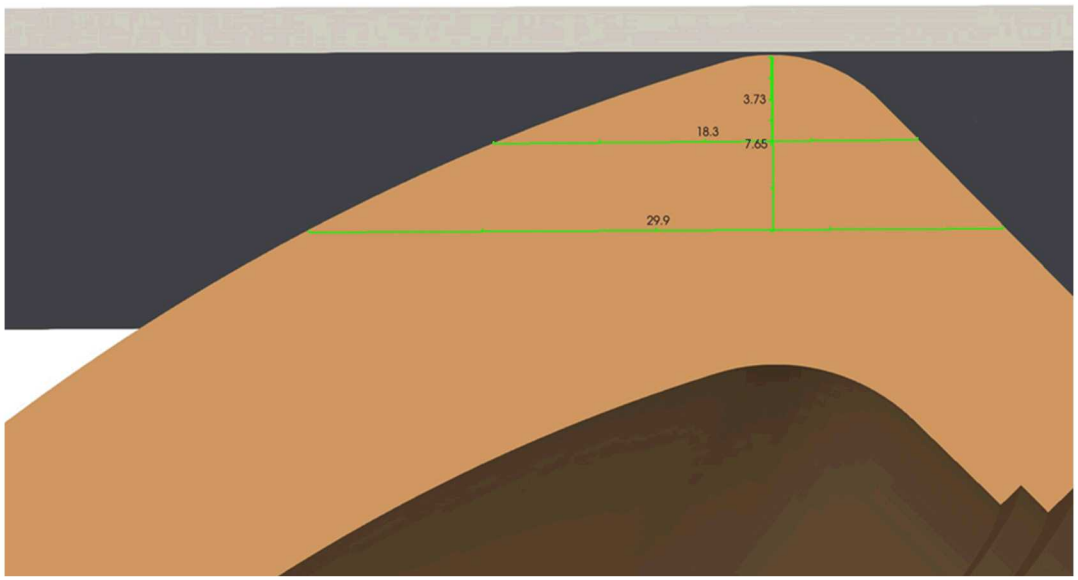

Figure 6-55. CGOC Length versus Crush Depth for the CGOC Impact.

6.2.6 Extra-Regulatory Impacts

Four impact analyses were performed to determine the TRUPACT-II response to extra-regulatory impacts. Three analyses were performed in the top, side, and CGOC orientation at an impact velocity of 60-mph. The structural integrity of the ICV was used to determine whether the package remained leak tight or to

estimate the size of the potential leak path. The limits developed for the ASME strain-based criteria were used as a failure criterion for the potential rupture of the ICV.

Due to the severe distortion in the polyurethane foam impact limiter material, several death criteria were employed to allow foam elements to be eliminated from the analyses in order to prevent the code from crashing. These are discussed in the material section above. As a result of the element removal, the ability of the foam material to absorb energy is reduced. This reduction in energy absorption along with the use of the ASME stain-based criteria which does not discriminate between compressive strain and tensile strains results in an analysis that overestimates the damage. A fourth analysis of the TRUPACT-II package in the CGOC orientation at a velocity of 45-mph was performed because using this model and these conservative assumptions results in possible rupture and the generation of a leak path in the ICV in the 60-mph CGOC analysis.

6.2.7 Top Impact 60-mph

The overall model deformation for the 60-mph top impact is shown in Figure 6-56 and a magnified view of the impact region is shown in Figure 6-57. There is significant compression of the polyurethane foam and outer OCA shell. The kinetic energy and impact force on the target for the half symmetry model are shown in Figures 6-58 and 6-59. Note that the initial kinetic energy is four times that of the 30-mph impact.

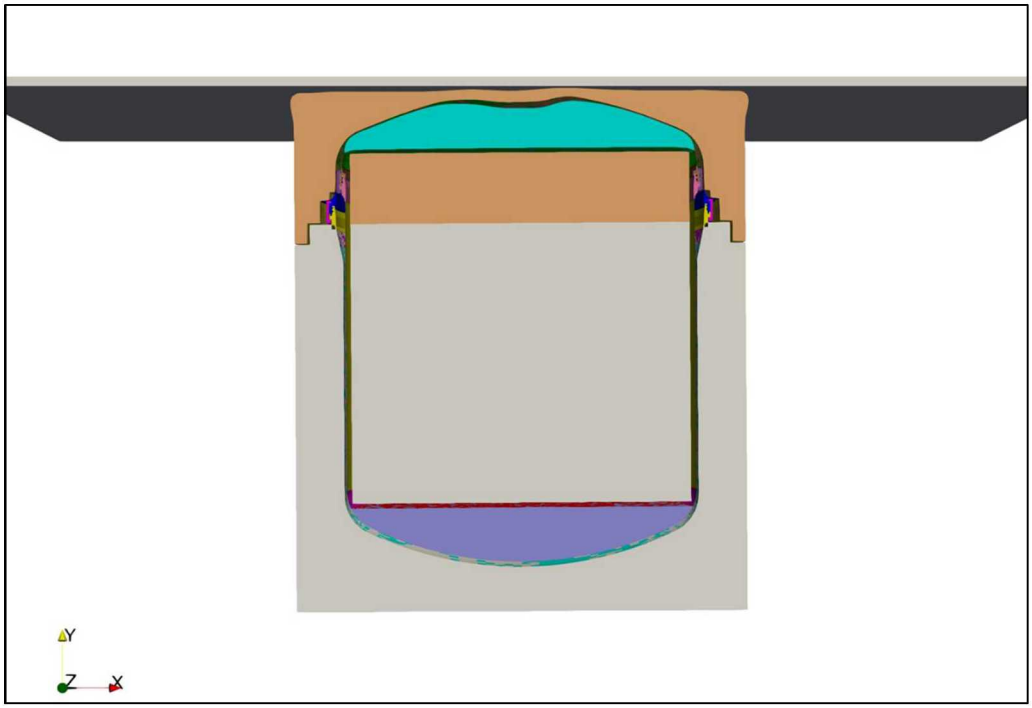

Figure 6-56. Deformation for 60-mph Top Impact Orientation.

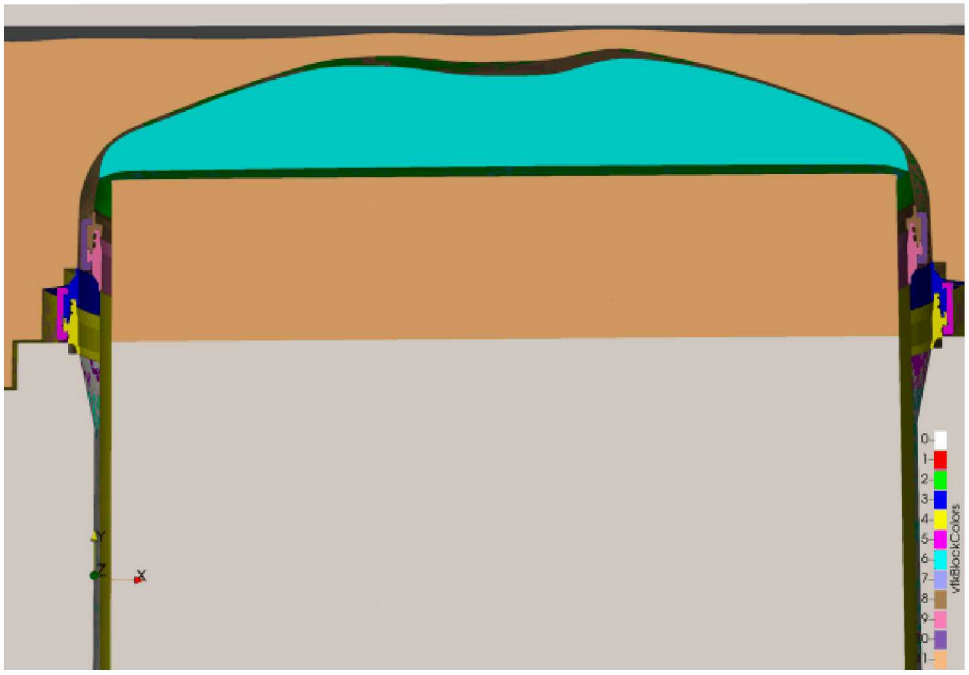

Figure 6-57. Magnified View of 60-mph Top Impact.

The impact and rebound takes approximately 0.027 sec with some residual kinetic energy remaining in the rebounding package. A peak reaction force of 1.84 x 10^6 lbf is reached at 0.019 sec.

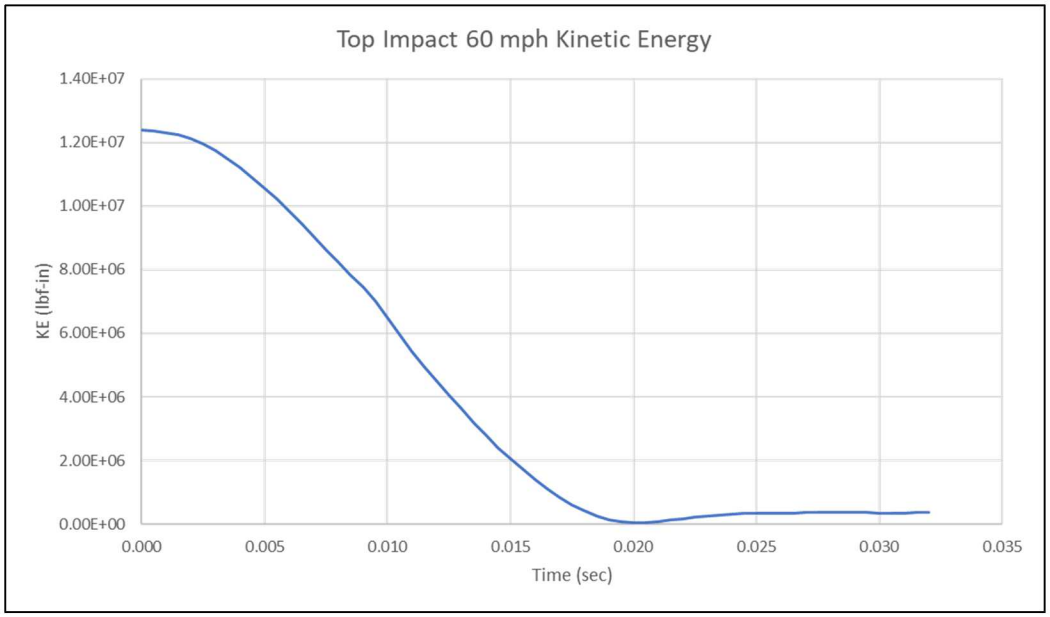

Figure 6-58. Kinetic Energy versus Time 60-mph Top Impact.

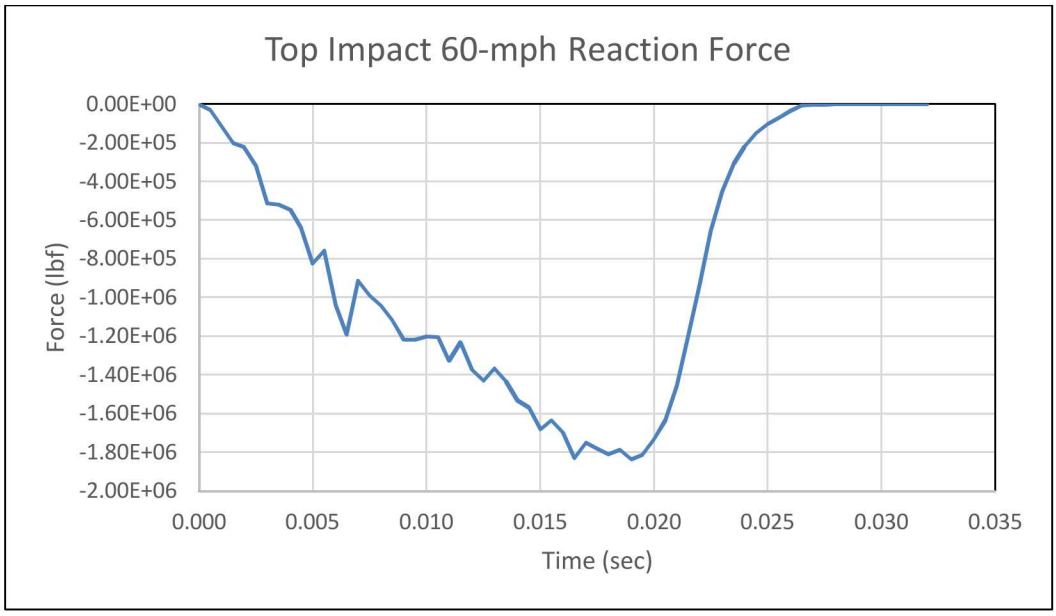

Figure 6-59. Reaction Force for 60-mph Top Impact Orientation.

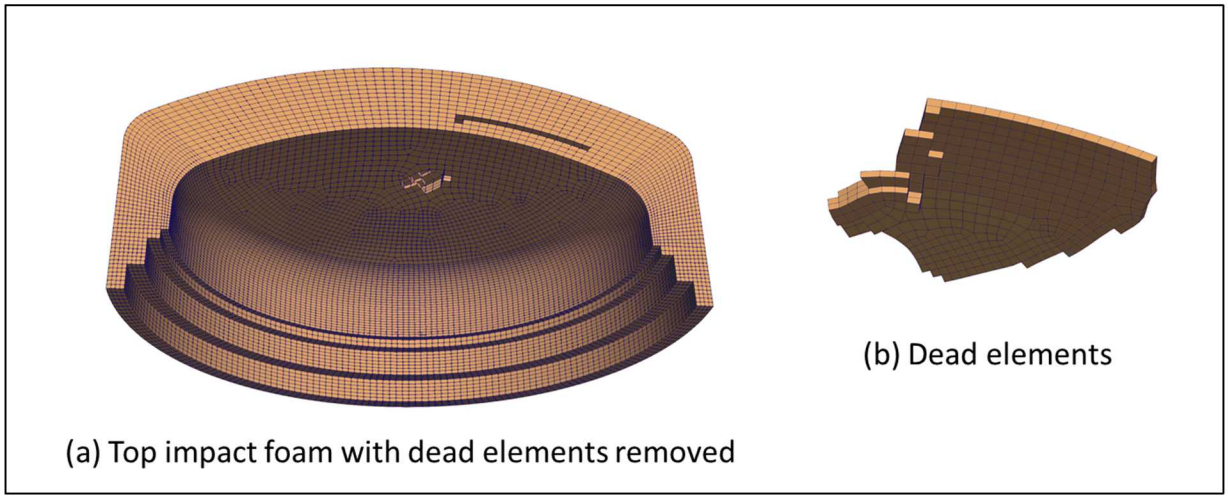

Figure 6-60. Upper Foam with Killed Elements Removed (a) Elements that Were Killed during the Analysis (b).

During impact, foam elements in the upper head are killed and removed from the analysis. Figure 6-60(a) shows the elements removed during the impact. The foam is shown in the undeformed configuration to clearly show the missing elements. Figure 6-60(b) shows the undeformed group of elements that were removed. A total of 412 elements were killed and removed during the analysis.

Figure 6-61 presents the $[TF\epsilon^p]_{max}$ values calculated for the flange elements and the highest shell integration point values. Figure 6-62 presents the corresponding equivalent plastic strain (EQPS) values. The peak shell integration point $[TF\epsilon^p]_{max}$ value is 0.16, which is a factor of four less than the allowable previously calculated. The peak value of $[TF\epsilon^p]_{max}$ for the hex elements in the upper flange is 0.45. As indicated in the figure, this high range is limited to a single patch of elements near the symmetry plane that attached the shell elements of the upper dome to the solid elements of the upper flange using a shell-to-

solid constraint. This is believed to be a numerical artifact. Figure 6-63 shows the same section of the flange with one layer thick by one-inch long section of elements removed. The highest value of $[TF\epsilon^p]_{max}$ in the remaining solid section of the flange is 0.025. Therefore, the ICV easily survives the 60-mph top impact.

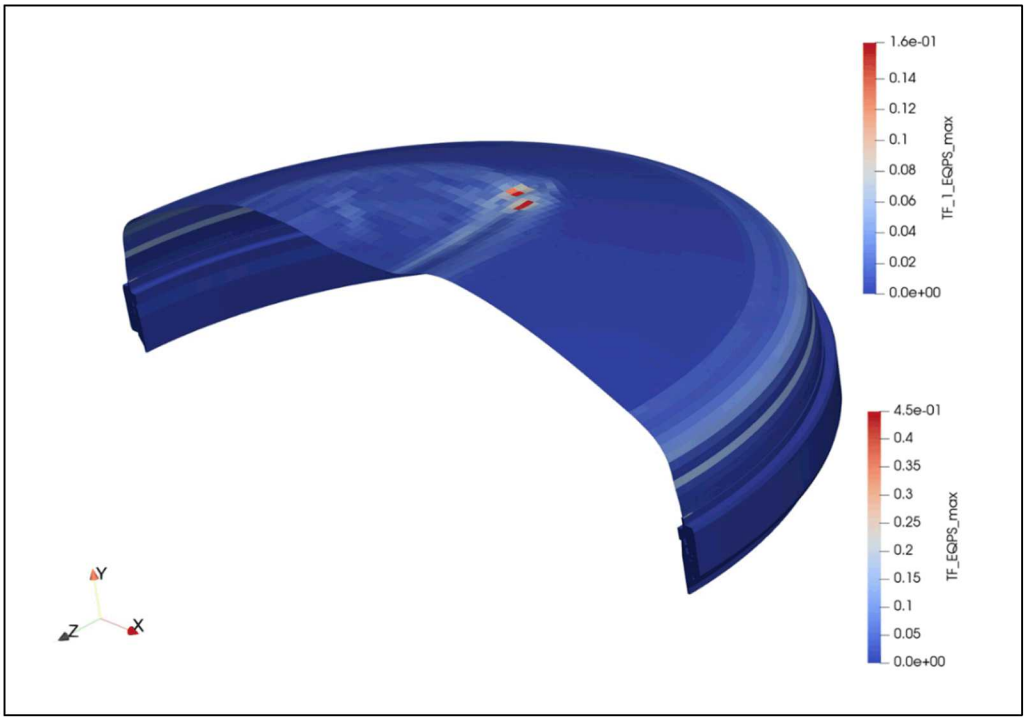

Figure 6-61. $[TF\epsilon^p]_{max}$ Values for the ICV Flange and Upper Shell Components for a 60-mph Top Impact.

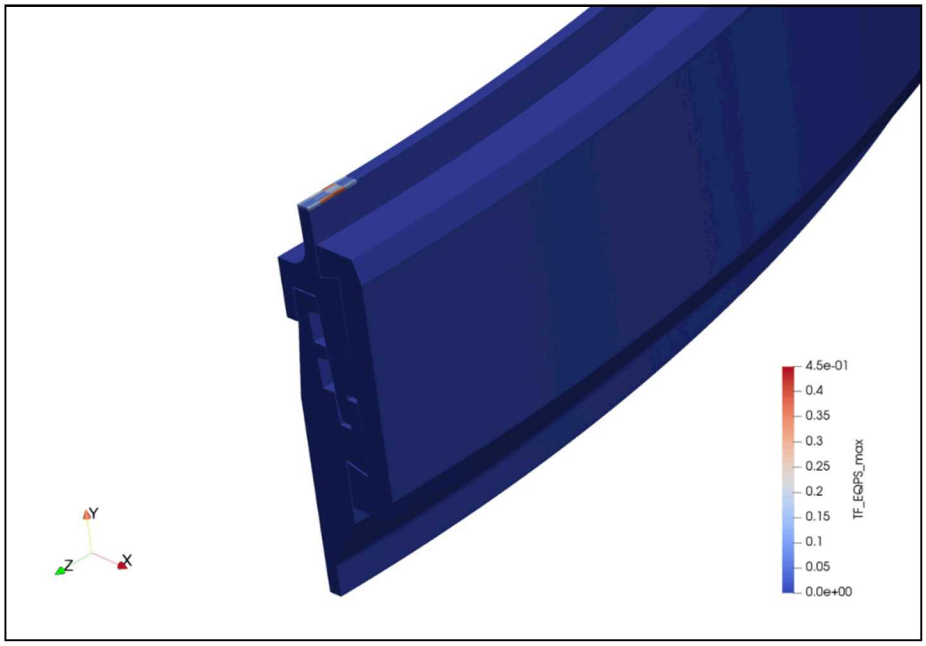

Figure 6-62. Magnified View Showing the High $[TF\epsilon^p]_{max}$ Region of the ICV Flange.

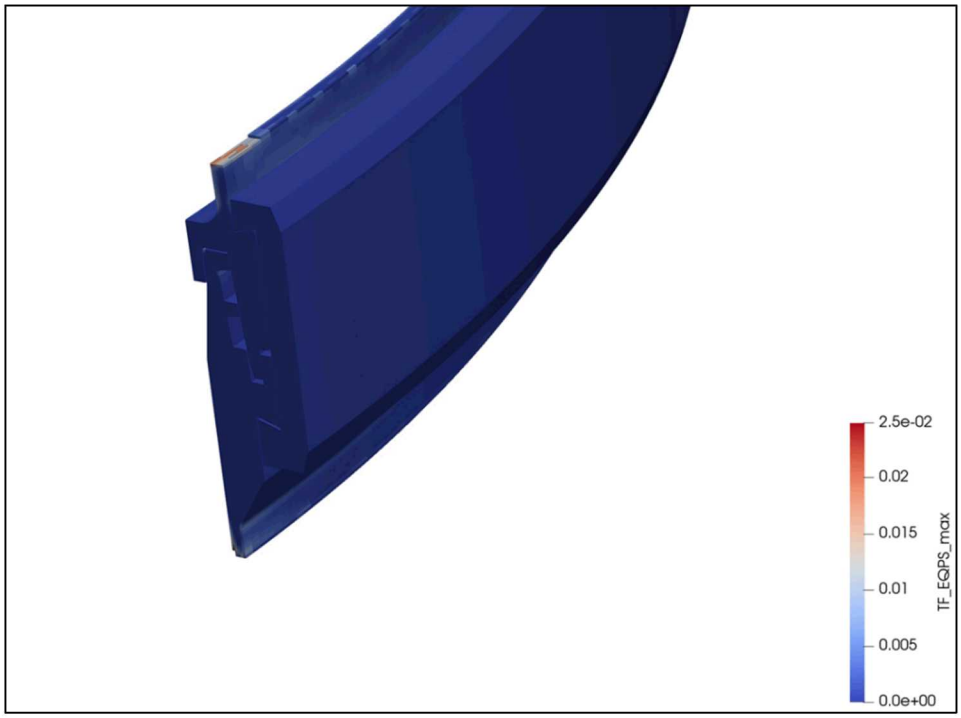

Figure 6-63. The High $[TF\epsilon^p]_{max}$ Region of the ICV Flange with Single Row Removed.

6.2.8 Side Impact 60-mph

The overall model deformation for the 60-mph side impact is shown in Figure 6-64 and a magnified view of the impact region is shown in Figure 6-65. There is significant compression of the polyurethane foam and outer OCA shell. There is also contact between the OCV and ICV flanges.

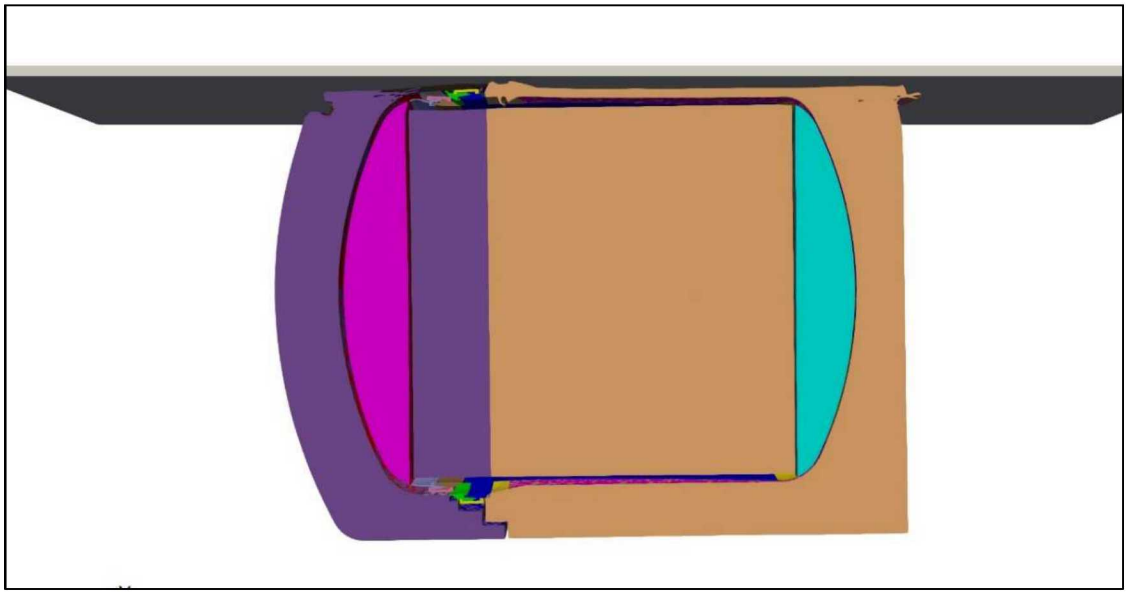

Figure 6-64. Deformation for 60-mph Side Impact Orientation.

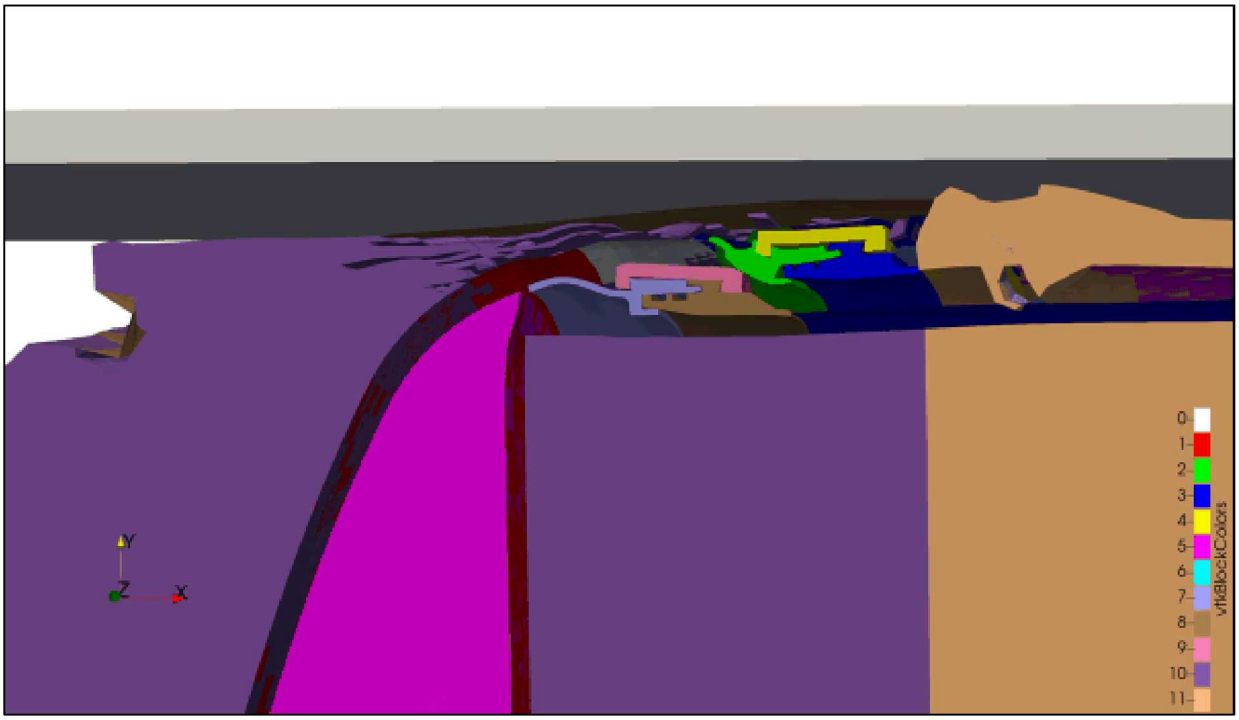

Figure 6-65. Magnified Flange Region for 60-mph Side Impact.

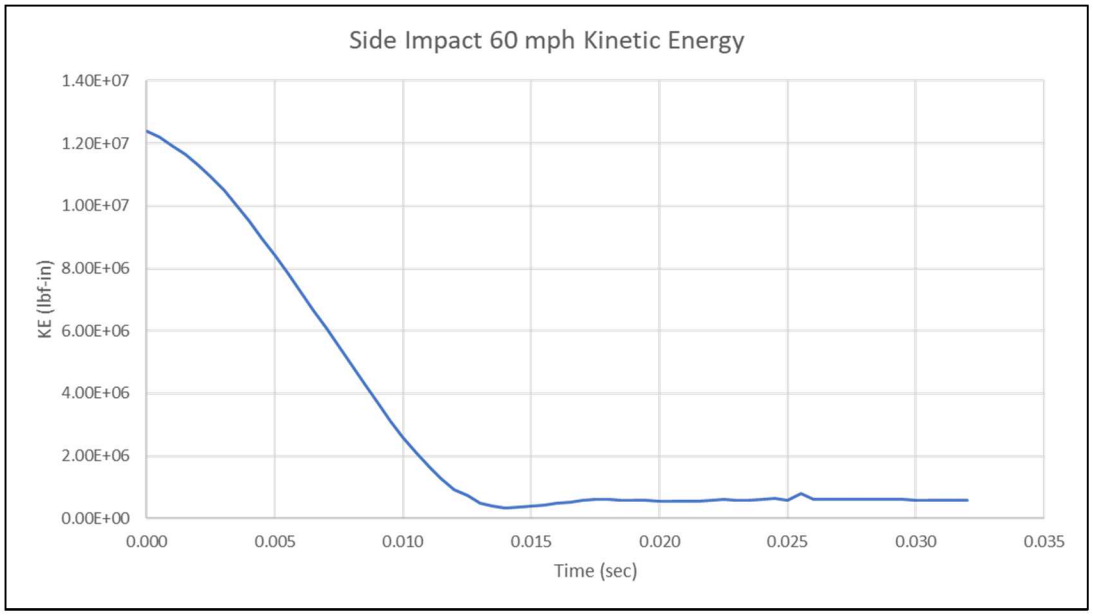

Figure 6-66. Kinetic Energy versus Time 60-mph Side Impact.

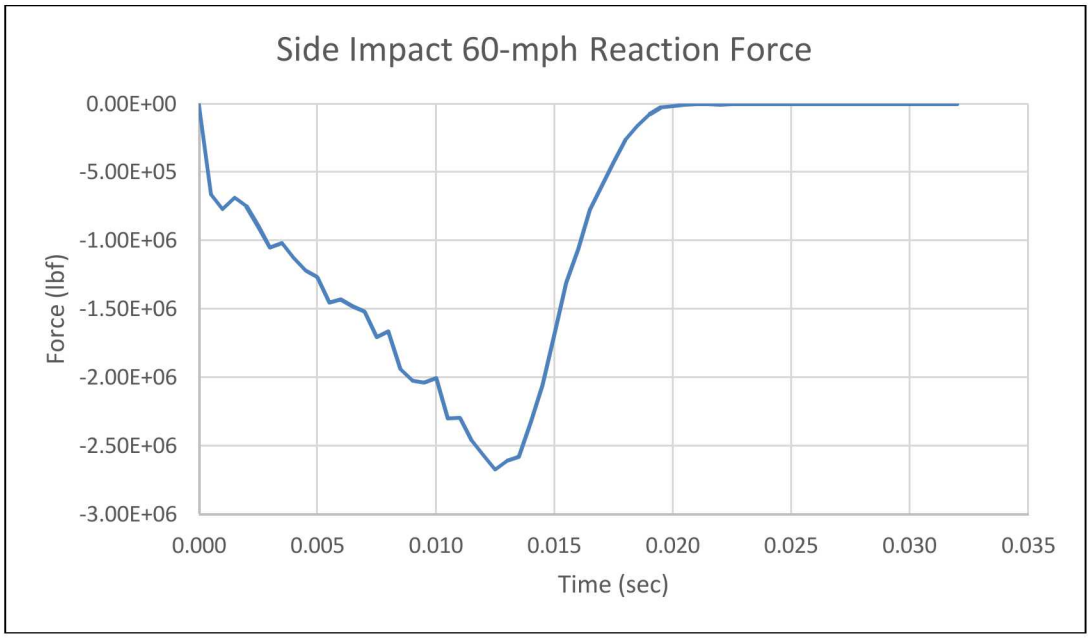

Figure 6-67. Reaction Force for 60-mph Side Impact Orientation.

The kinetic energy and impact force on the target for the half symmetry model are shown in Figures 6-66 and 6-67. The side impact is a short and more severe impact. The impact and rebound takes approximately 0.022 sec with some residual kinetic energy remaining in the rebounding package. A peak reaction force of 2.6×10^6 lbf is reached at 0.0125 sec.

Similar to the top impact analysis, foam elements are killed and removed from the analysis. Figure 6-68(a) shows the elements removed during the impact. The foam is shown in an undeformed configuration to clearly show the missing elements. Figure 6-68(b) shows the undeformed group of elements that were removed. A total of 5,728 foam elements were removed during the analysis.

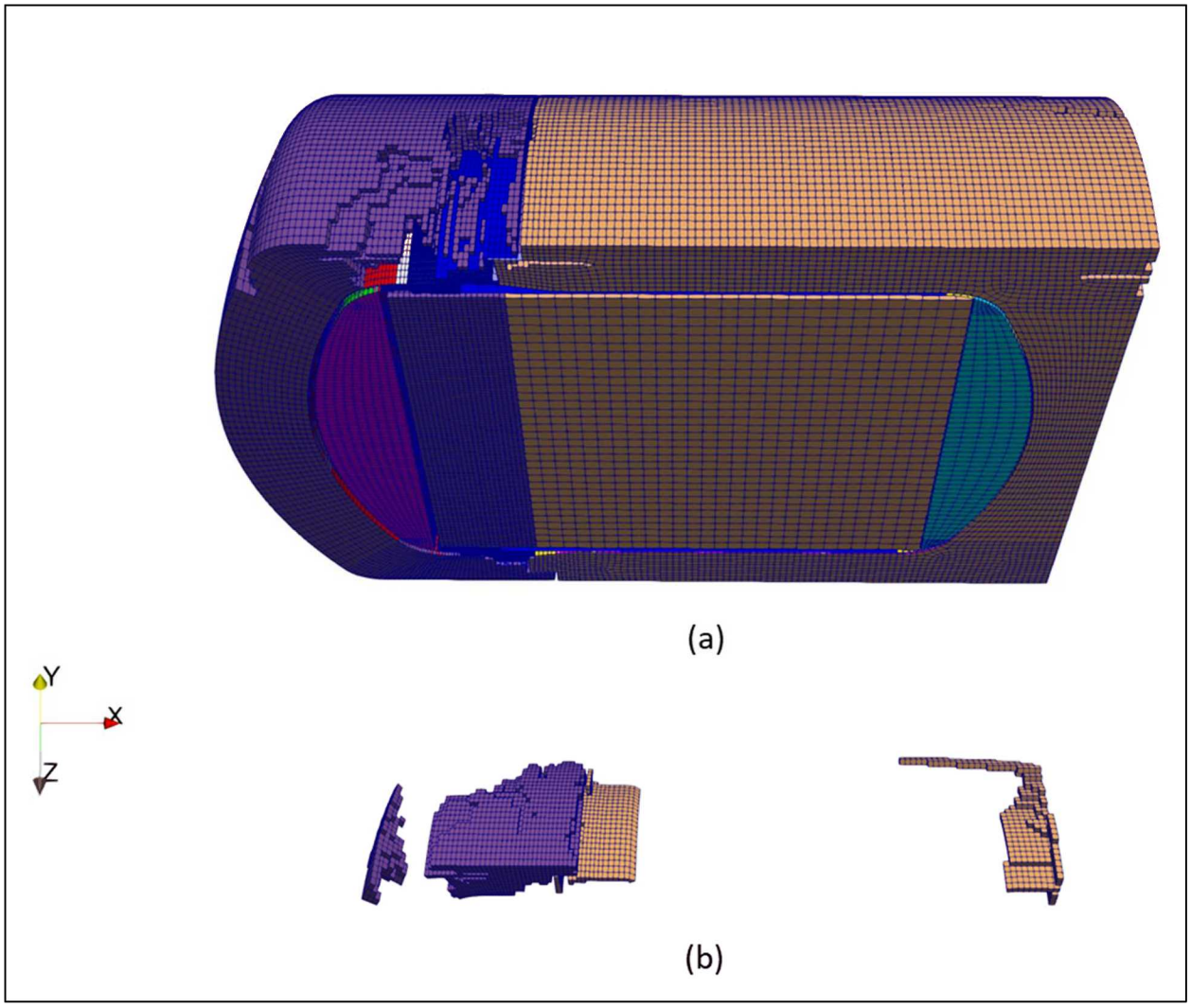

Figure 6-68. Model Showing Elements Removed during the Analysis (a) Elements that Were Removed (b).

Figure 6-69 presents the $[TF\epsilon^p]_{max}$ values calculated for the flange elements and the highest shell integration point values. The peak shell integration point $[TF\epsilon^p]_{max}$ value is 0.13, which is a factor of four less than the allowable previously calculated. The peak value of $[TF\epsilon^p]_{max}$ for the hex elements in the upper flange is shown in Figure 6-70 and has a peak value of 1.0. As in the previous analysis, this high range is limited to a single patch of elements at the symmetry plane that attach the shell elements of the upper dome to the solid elements of the flange using the shell-to-solid constraint. Again, this is believed to be a numerical artifact.

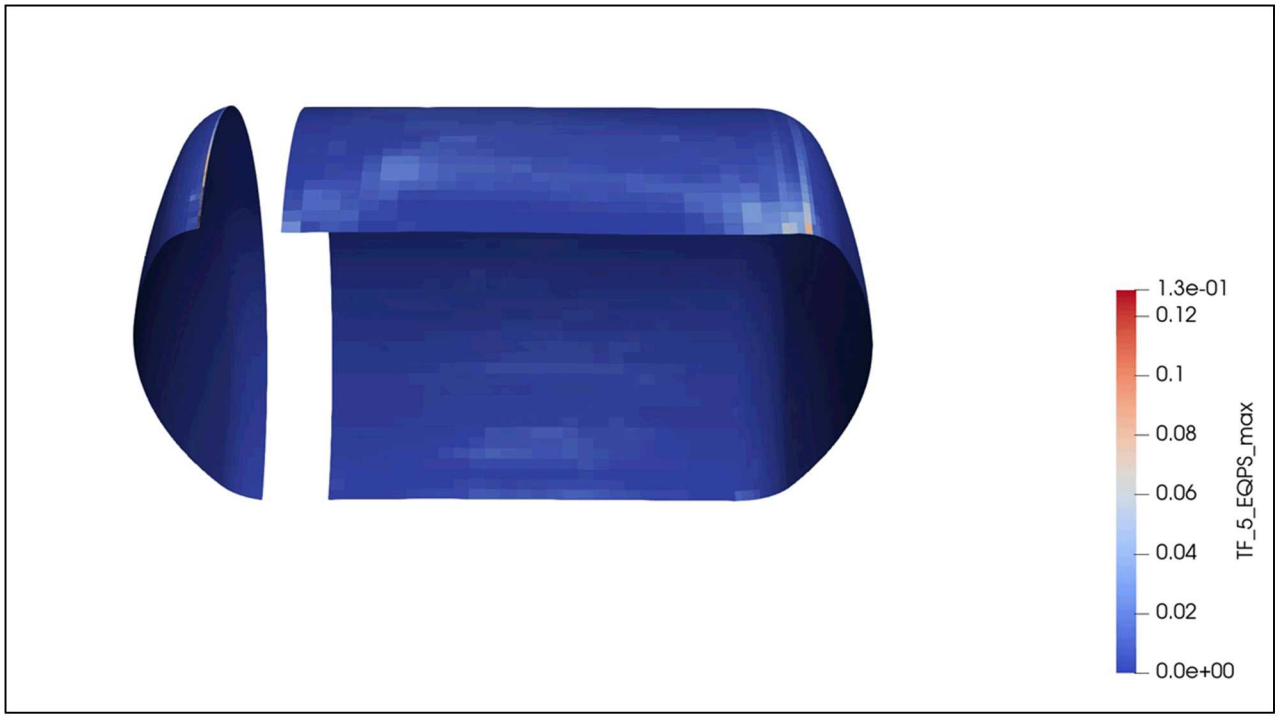

Figure 6-69. Maximum TF_5_EQPS in the ICV Shell.

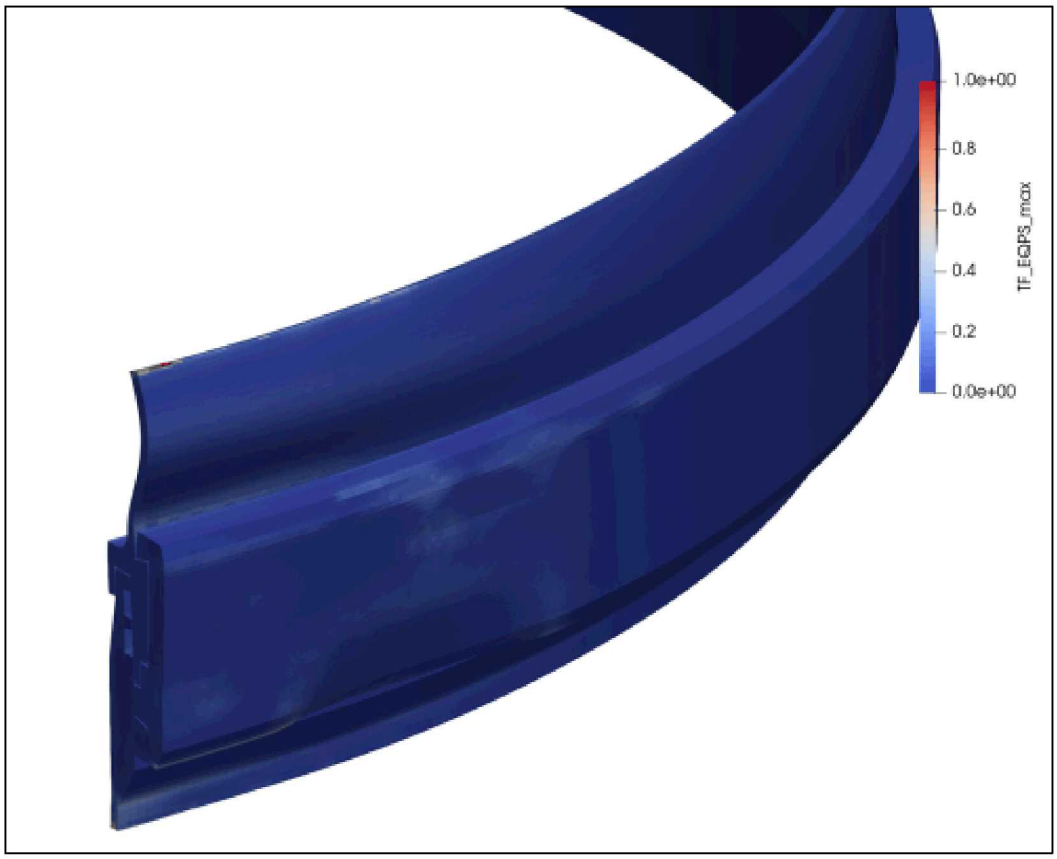

Figure 6-70. Maximum TF_EQPS in the ICV Flange.

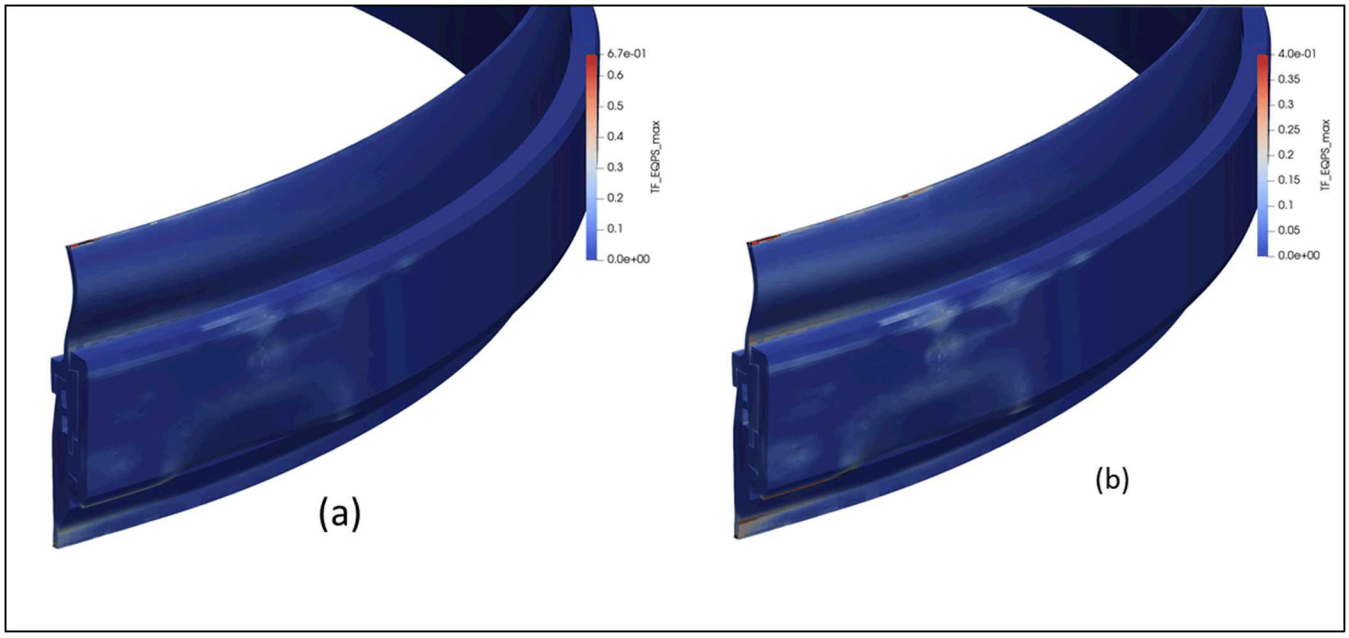

Figure 6-71. Maximum TF_EQPS in the ICV Flange (a) scaled to 0.67, (b) scaled to 0.4.

Figure 6-71(a) and (b) show a rescaling of the flange in Figure 6-70. In Figure 6-71(a) $[TF\epsilon^p]_{max}$ is rescaled to the peak value of 0.67, which is the maximum material allowable. In Figure 6-71(b) $[TF\epsilon^p]_{max}$ is rescaled to the peak value of 0.40, which indicates a higher region in the lower flange which is bending due to impact with the OCV flange. These lower values in the shell and body of the flange indicate that the ICV easily survives the 60-mph side impact.

6.2.9 CGOC Impact 60-mph

The overall model deformation for the 60mph CGOC impact is shown in Figure 6-72 and a magnified view of the impact region is shown in Figure 6-73. There is significant compression of the polyurethane foam and outer OCA shell. There are a large number of foam elements killed and removed in this analysis. This causes direct contact between the target and the three shell layers of the model (OCA, OCV, and ICV). This leads to severe bending in the ICV lid and flange.

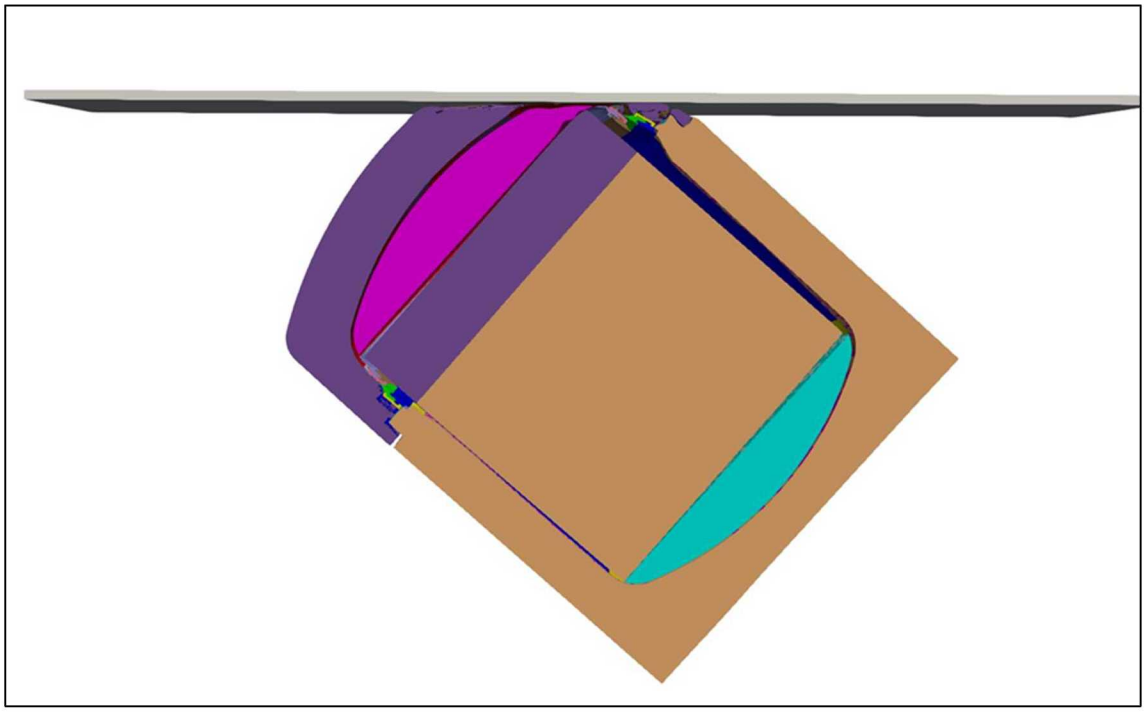

Figure 6-72. Deformation for 60-mph CGOC Impact Orientation.

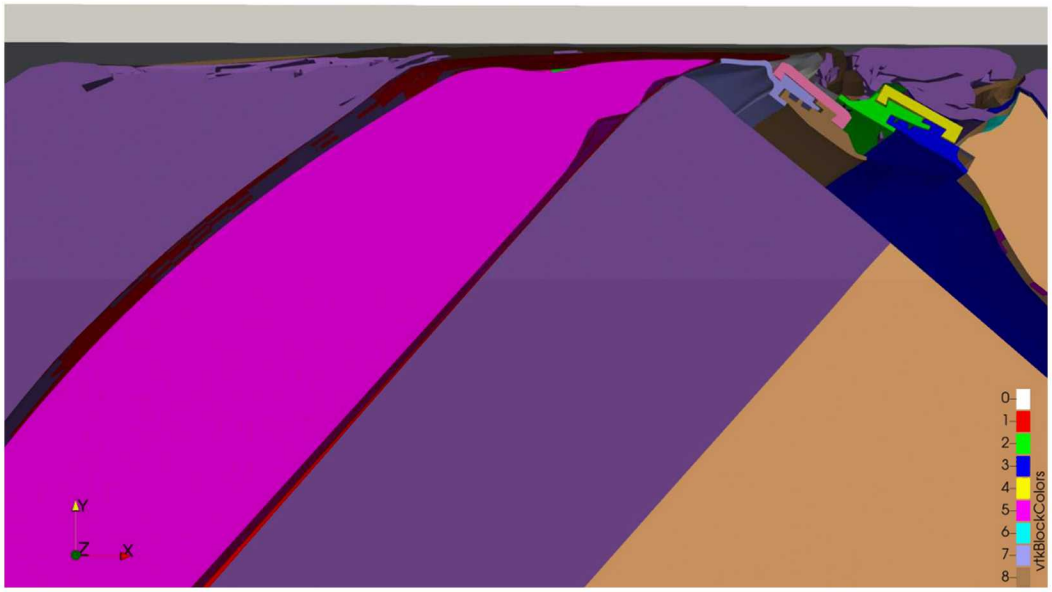

Figure 6-73. Magnified Flange Region for 60-mph CGOC Impact.

The kinetic energy and impact force on the target for the half symmetry model are shown in Figures 6-74 and 6-75. The impact and rebound takes approximately 0.032 sec with some residual kinetic energy remaining in the rebounding package. A peak reaction force of 3.44×10^6 lbf is reached at 0.020 sec.

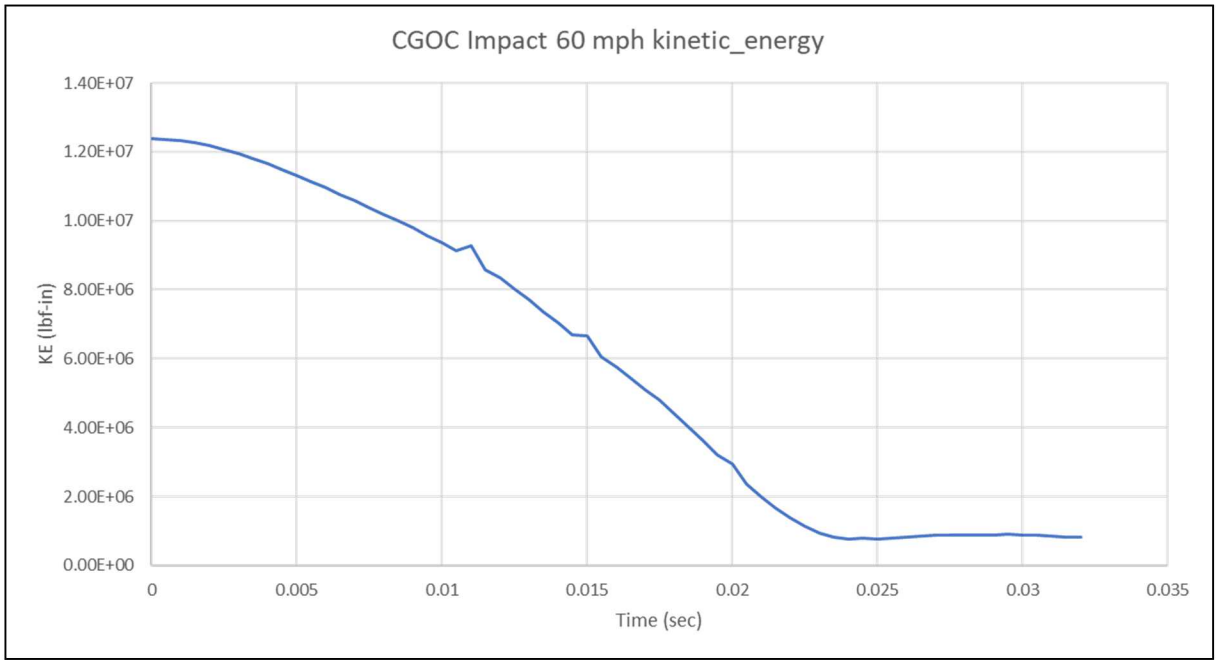

Figure 6-74. Kinetic Energy versus Time 60-mph CGOC Impact.

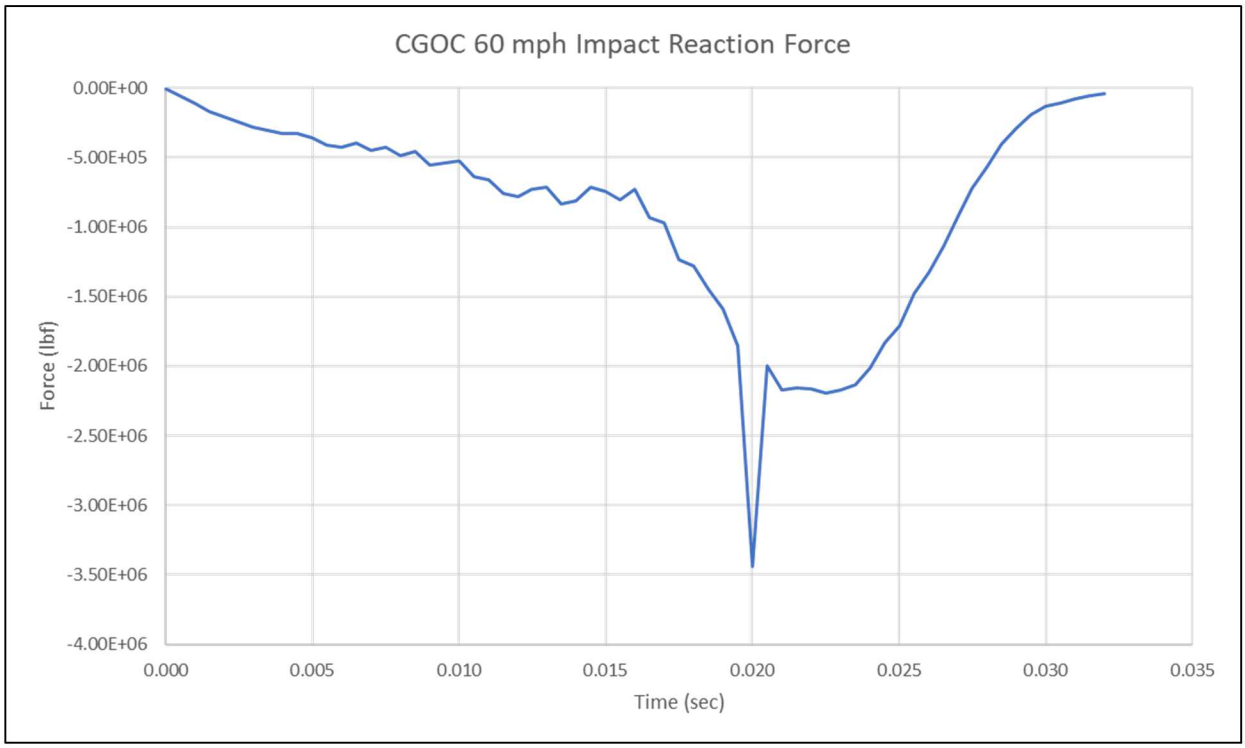

Figure 6-75. Reaction Force versus Time for the 60-mph CGOC Impact.

As in the two previous analyses, foam elements in the upper head are killed and removed during the analysis. This removal is more severe in this orientation, over 15,000 foam elements are removed during the analysis. Figure 6-76 shows the impact region at 0.020 seconds into the analysis. At this time the package has

approximately the same amount of kinetic energy as the 30-mph impact. However, due to the removal of a large number of foam elements, the ICV shell, ICV flange and the OCV shell impact directly into the target. This results in the flattening of these components as shown in the figure and also the spike in the reaction force shown in Figure 6-75. Figures 6-77 and 6-78 show the impact region at the final times step. In Figure 6-78 the elements are shown with zero displacement.

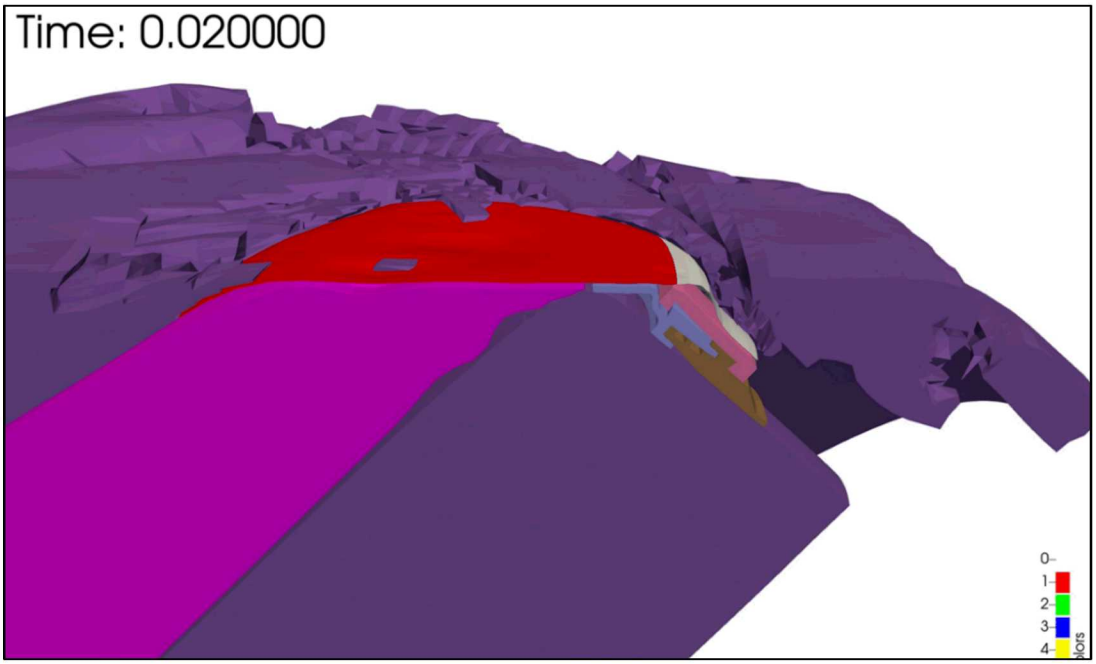

Figure 6-76. Impact Region with Outer Shell Removed to Show Missing Foam Elements at Time 0.020 sec.

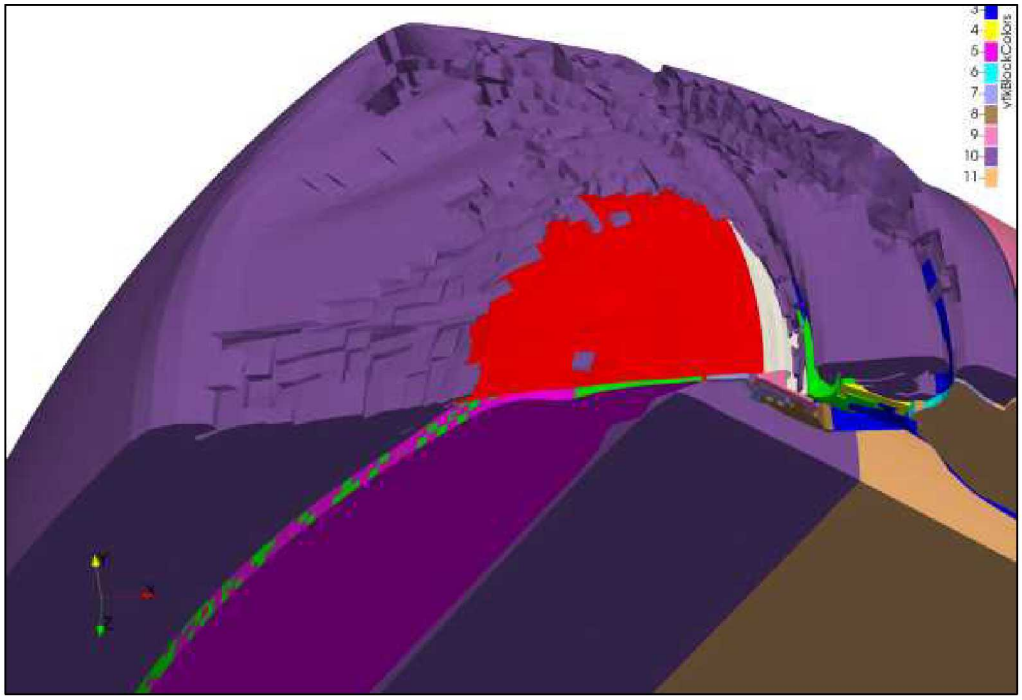

Figure 6-77. Impact Region with Outer Shell Removed at Final Time.

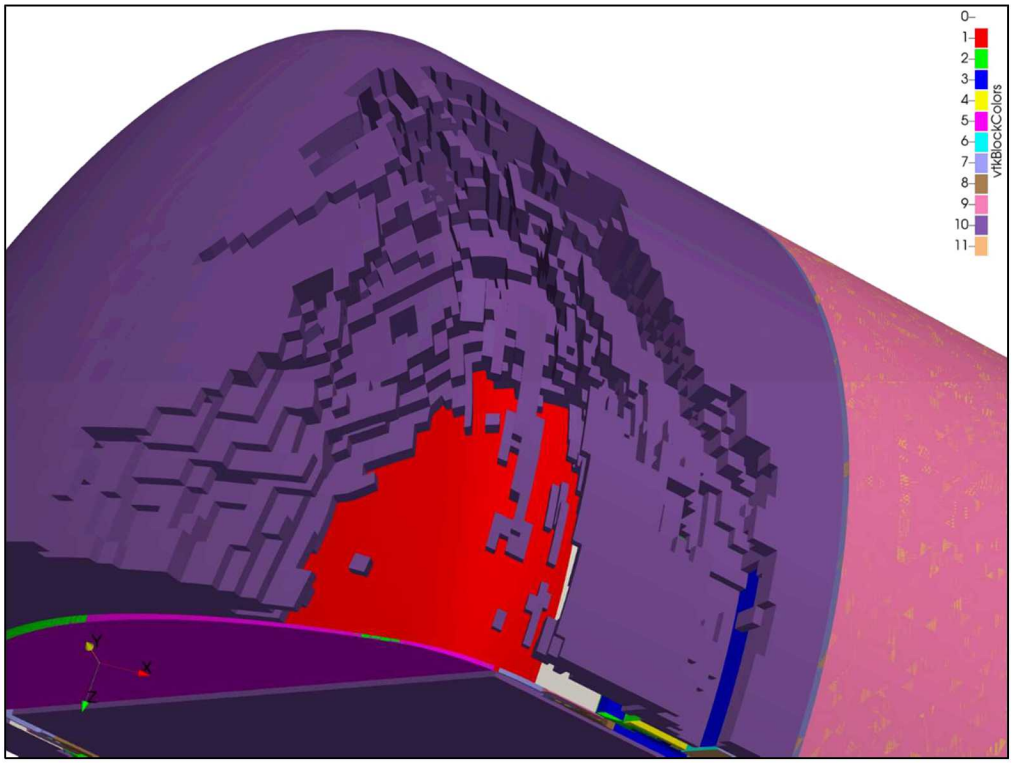

Figure 6-78. Impact Region Shown with Removed Elements at Time 0.032 sec and No Element Displacement.

Figure 6-79 presents the $[TF\epsilon^p]_{max}$ values calculated for the flange elements and the highest shell integration point values with the color map scaled to 0.67. The high stress region at the connection between the shell elements and the hex flange elements is visible. The upper head shell elements have acceptable values.

Figure 6-80 and 6-81 show the $[TF\epsilon^p]_{max}$ values in the upper flange. In addition to high values in the shell-solid interface region, there are high values in segments of the flange where there is severe bending. In these regions the $[TF\epsilon^p]_{max}$ meet or exceed the ASME limits previously calculated. Therefore, the ICV may fracture and does not remain leak tight.

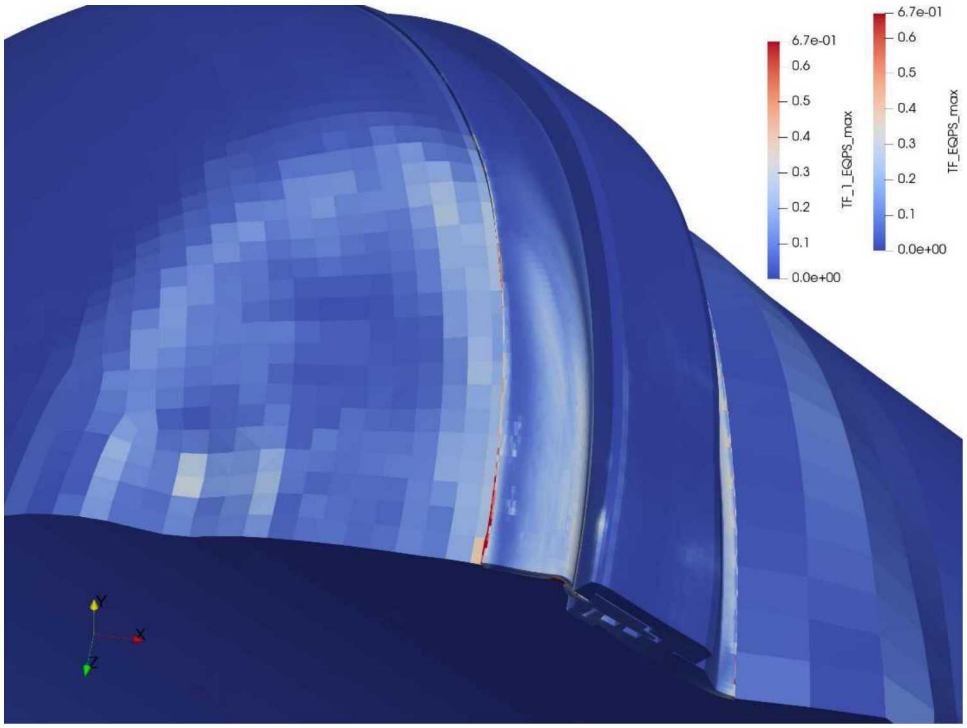

Figure 6-79. Maximum TF_1_EQPS in the ICV Shell and TF_EQPS in the Flange Both Scaled to 0.67.

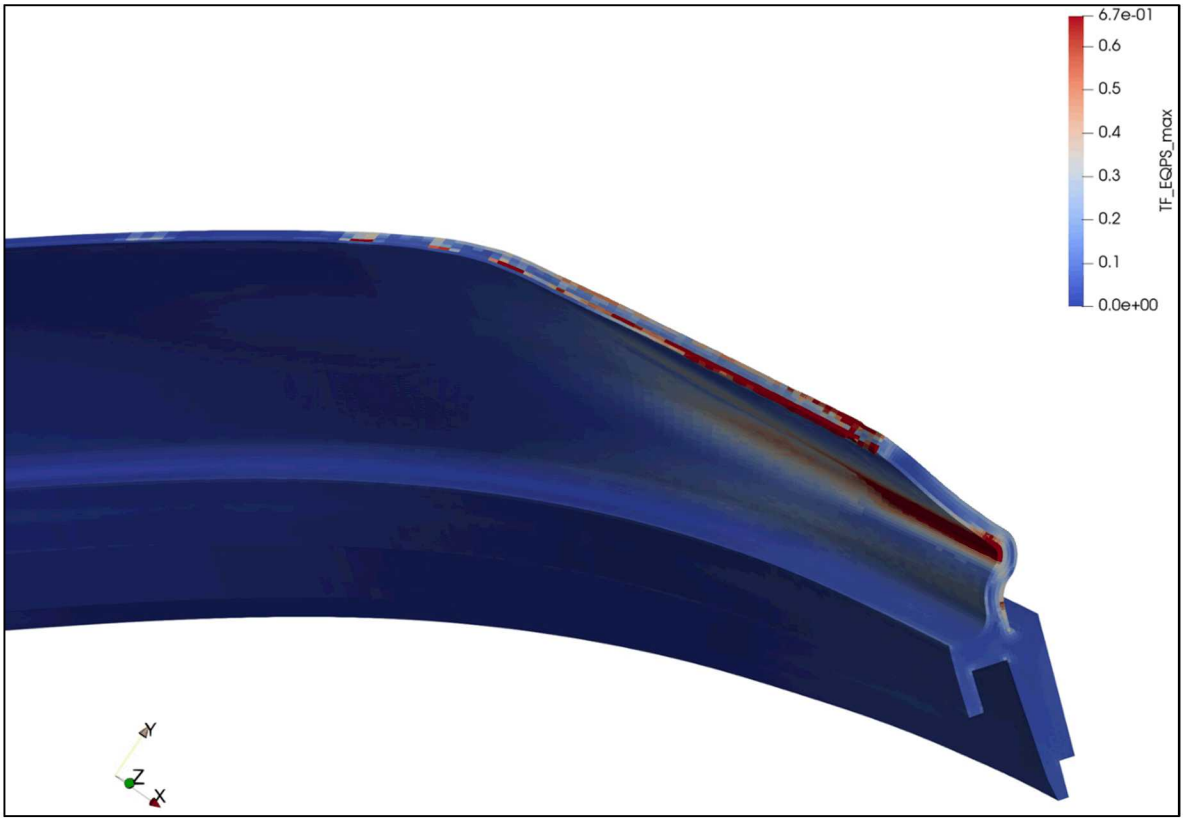

Figure 6-80. Maximum TF_EQPS in the ICV Flange, Inside View.

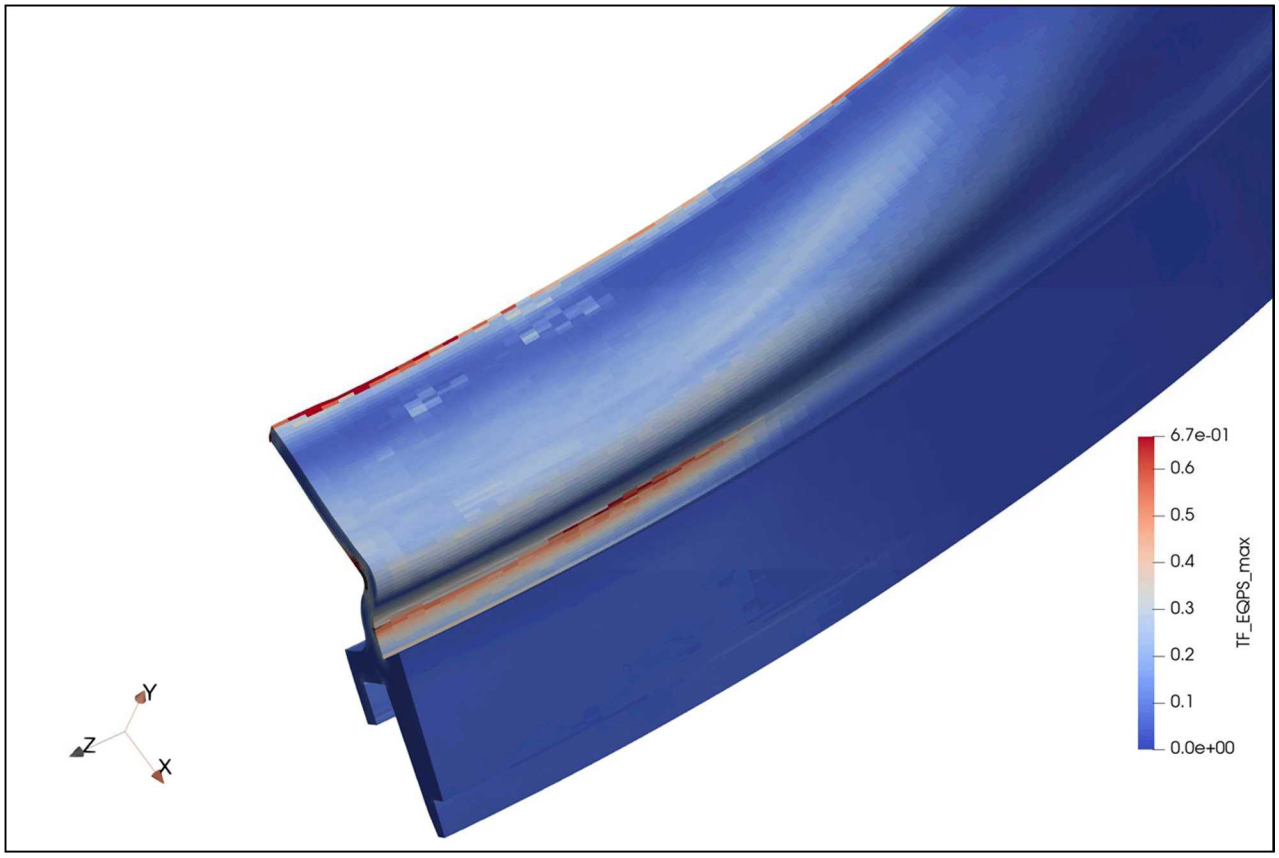

Figure 6-81. Maximum TF_EQPS in the ICV Flange, Outside View.

6.2.10 CGOC Impact 45-mph

As a result of the high strain regions calculated in the 60-mph CGOC analysis, an anaysis was conducted in the CGOC orientation at a velocity of 45-mph. The overall model deformation for the 45-mph CGOC impact is shown in Figure 6-82 and a magnified view of the impact region is shown in Figure 6-83. There is significant compression of the polyurethane foam and outer OCA shell. There are also a large number of foam elements killed and removed in this analysis, with over 7,600 killed and removed. However, due to the lower amount of energy and the fact that contact between the shell and target occur much later in the analysis the stresses and bending in the ICV is significantly less than in the 60-mph analysis.

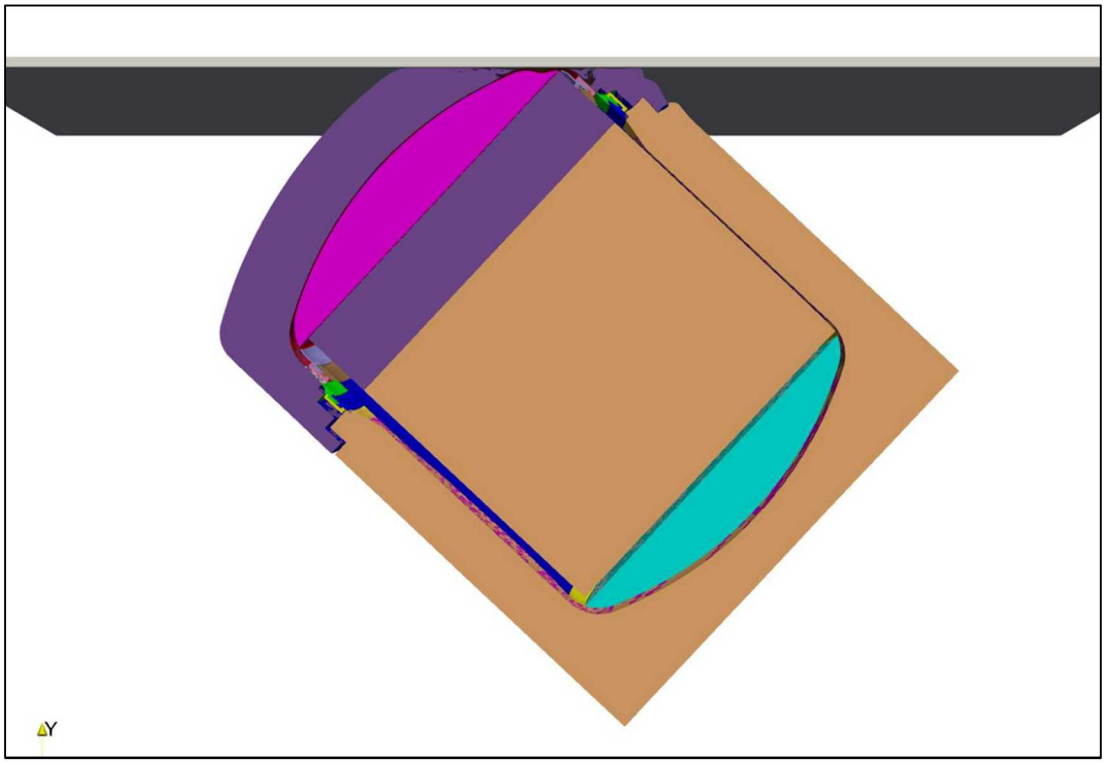

Figure 6-82. Deformation for 45-mph CGOC Impact Orientation.

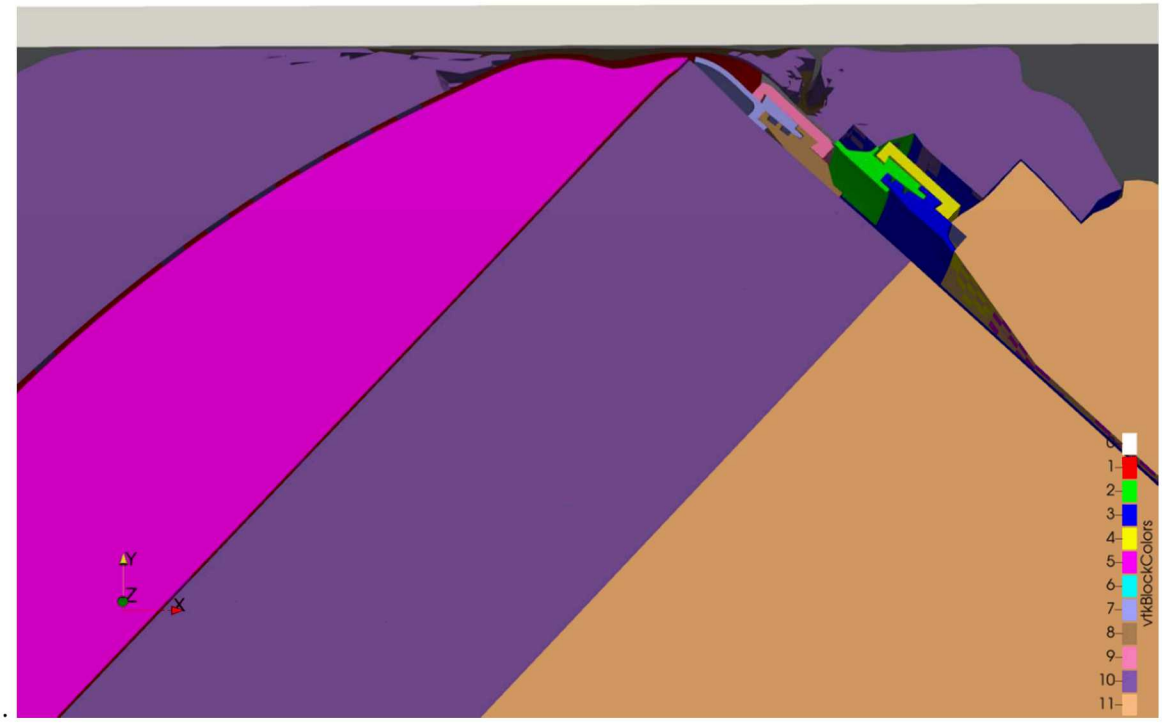

Figure 6-83. Magnified Flange Region for 45-mph CGOC Impact

The kinetic energy and impact force on the target for the half symmetry model are shown in Figures 6-84 and 6-85. For this velocity and orientation, the impact takes the full 0.032 sec of the analysis run time. The lower velocity and the fact that this orientation is the most compliant in addition to elements being eliminated during the impact causes the impact to take longer and the force to peak for a longer time. A peak reaction force of 8.35 x 10^5 lbf is reached at 0.0195 sec. Figure 6-86 illustrates that the analysis has completed; the momentum in the impact direction at the end of the analysis has decreased by over 99 percent .

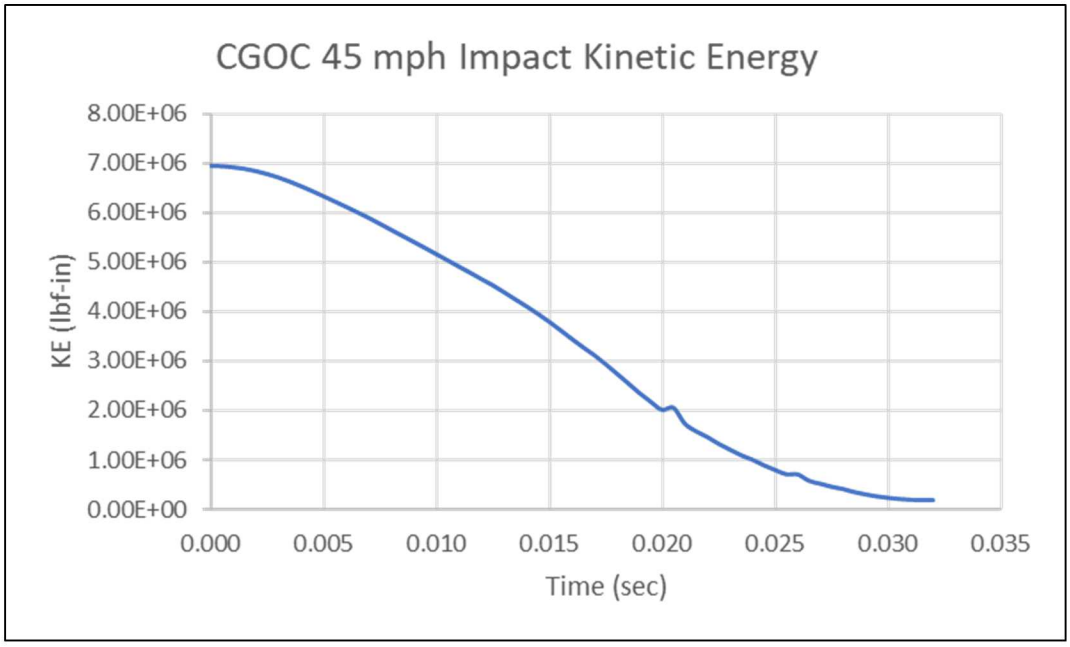

Figure 6-84. Kinetic Energy versus Time 45-mph CGOC Impact.

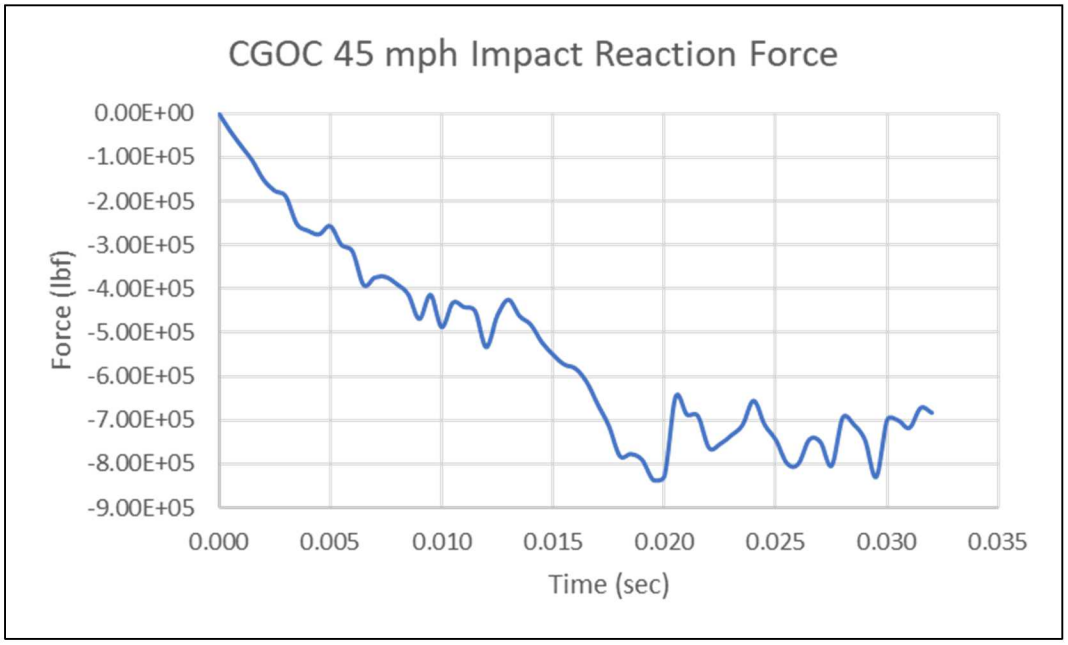

Figure 6-85. Reaction Force versus Time 45-mph CGOC Impact.

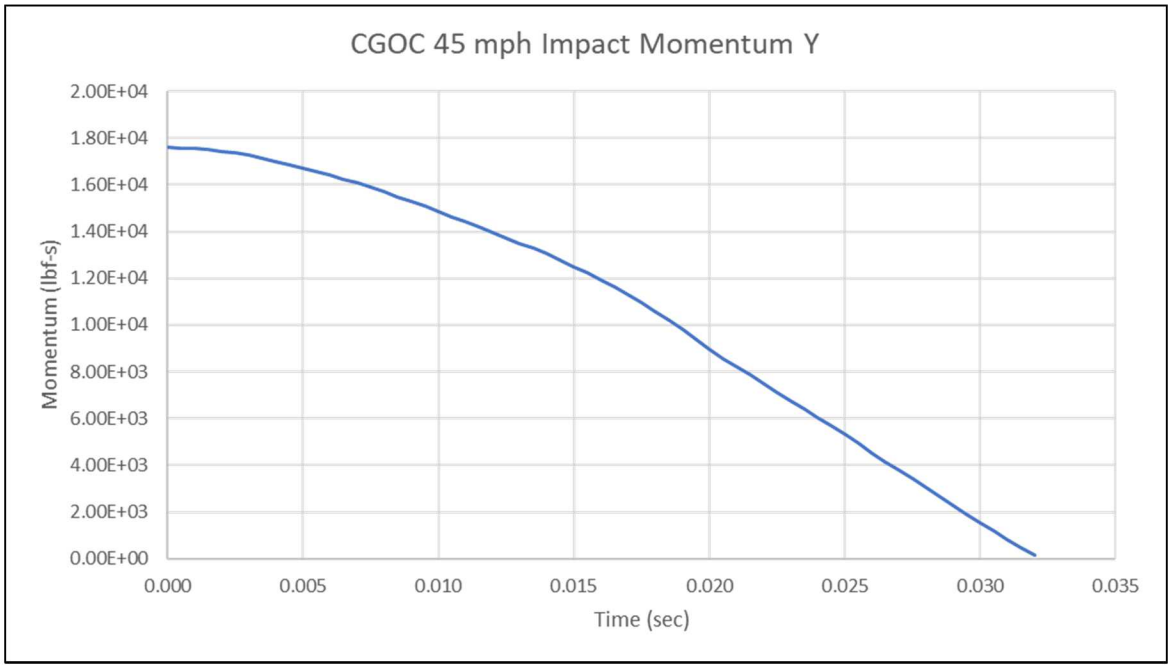

Figure 6-86. Momentum in the Y-Direction versus Time 45-mph CGOC Impact.

Figures 6-87 and 6-88 show the impact region at the final time step with the outer shell removed. As discussed, about 7,606 elements have been killed and removed. Bare contact does occur between the shells and the target, but this near the end of the analysis. Figure 6-88 shows the missing elements with no displacement applied to the mesh.

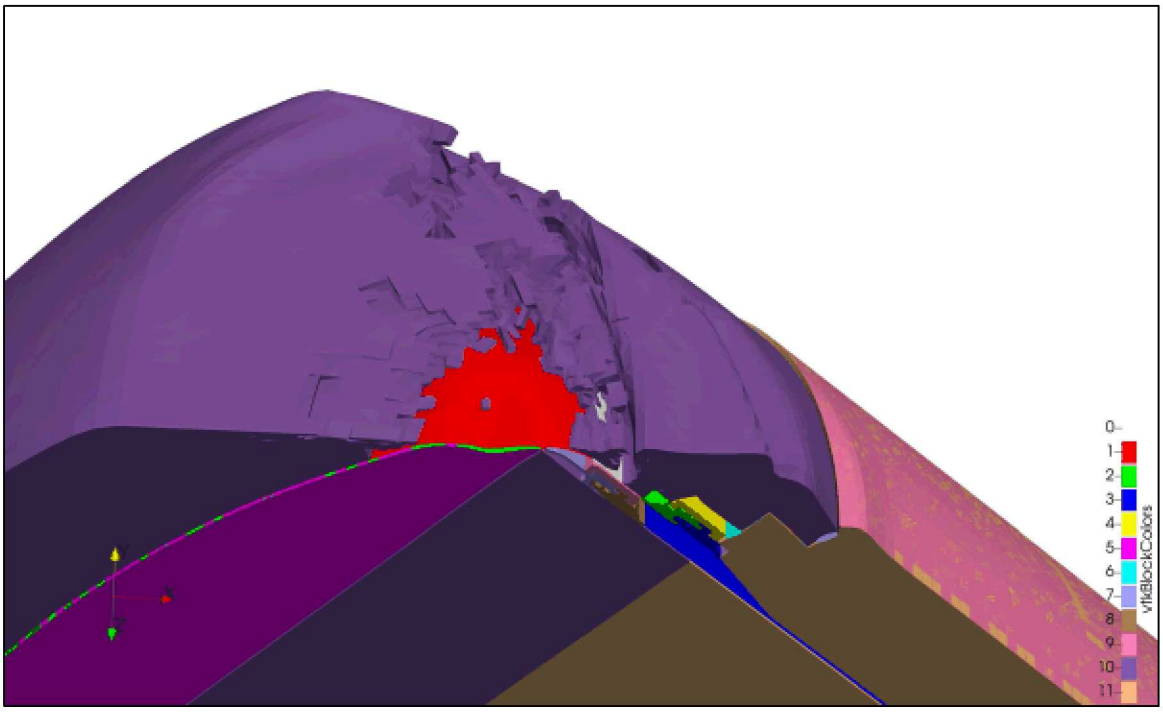

Figure 6-87. Impact Region with Outer Shell Remove at Final Time.

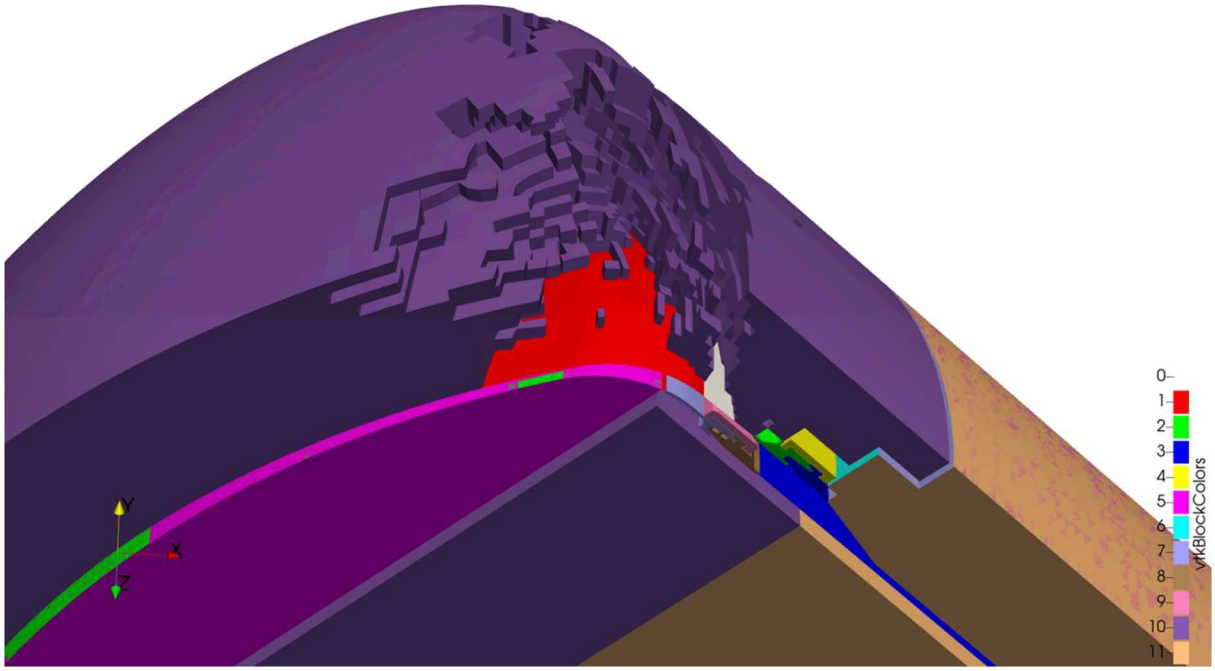

Figure 6-88. Impact Region Shown with Removed Elements at Time 0.032 sec and No Element Displacement.

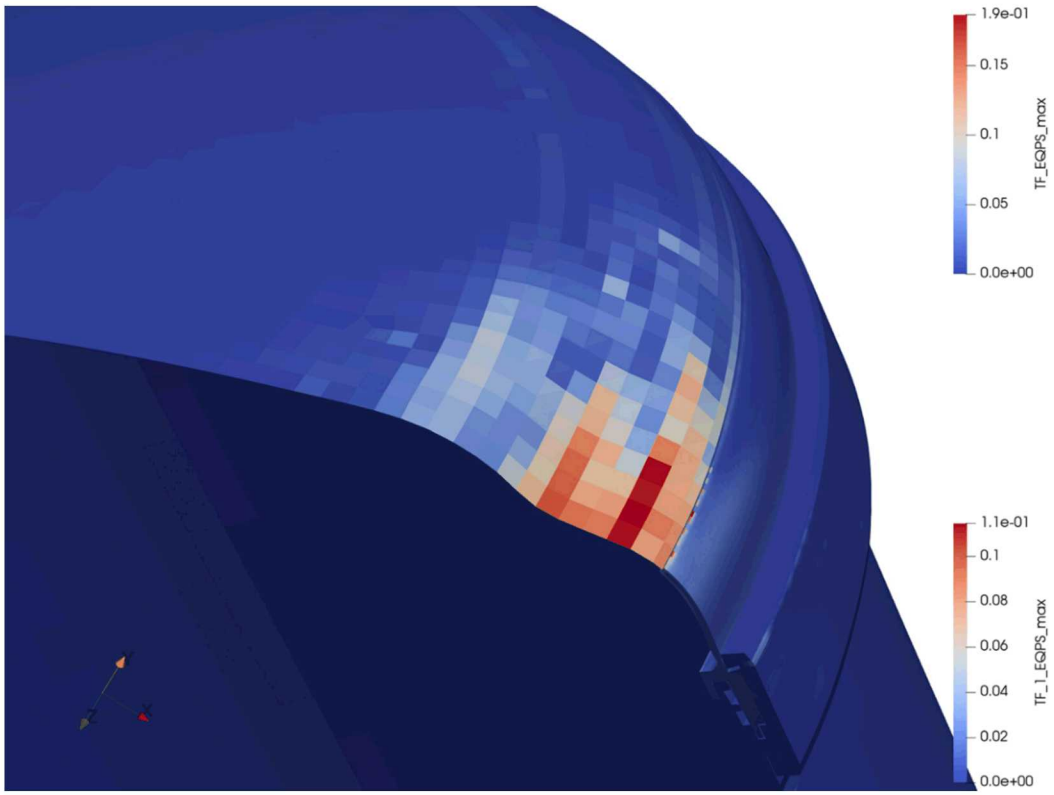

Figure 6-89. TF_EQPS in the Shell Head and Flange Region.

Figure 6-89 presents the $[TF\epsilon^p]_{max}$ values calculated for the ICV flange elements and the highest shell integration point values of the upper head with the color map at the full range for these components. The high stress region at the connection between the shell elements and the hex flange elements is visible. Both the upper head shell elements and the flange region have low values.

The equivalent plastic strain in the upper head and flange region are shown in Figure 6-90. The largest plastic strains range from 5-8 percent .

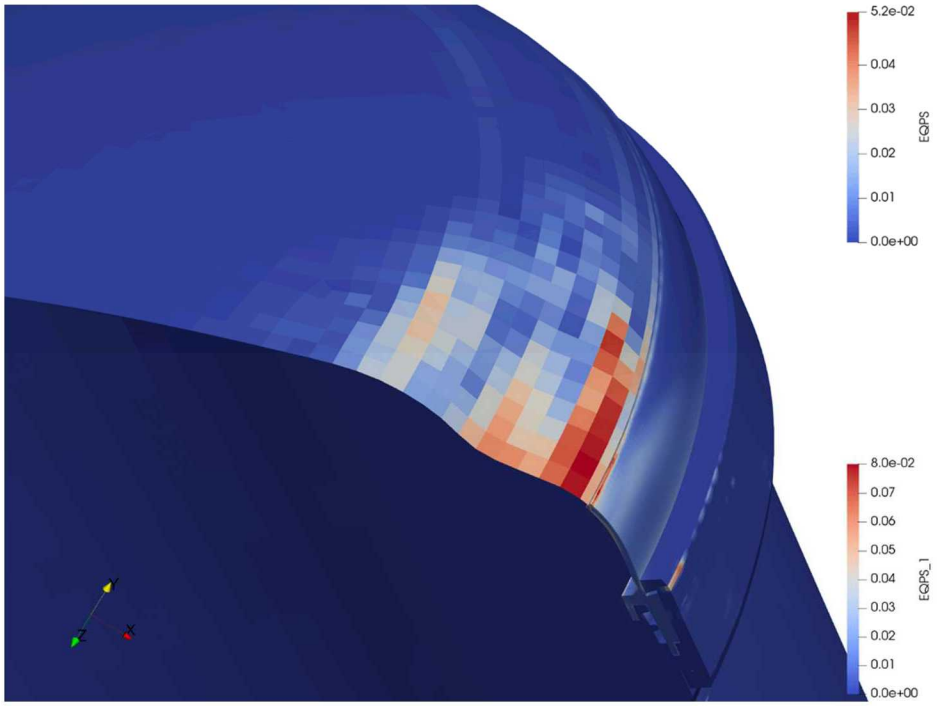

Figure 6-90. EQPS in the Shell Head and Flange Region.

Figure 6-91 shows the distribution of $[TF\epsilon^p]_{max}$ in the upper flange. This clearly shows that the peak values are in the elements that attach the shell elements of the upper dome to the solid elements of the flange using the shell-to-solid constraint. While these values are low, the level throughout the body of the flange are 1/6 or less then $[TF\epsilon^p]_{max}$ limiting value. Therefore, the ICV remains leak tight.

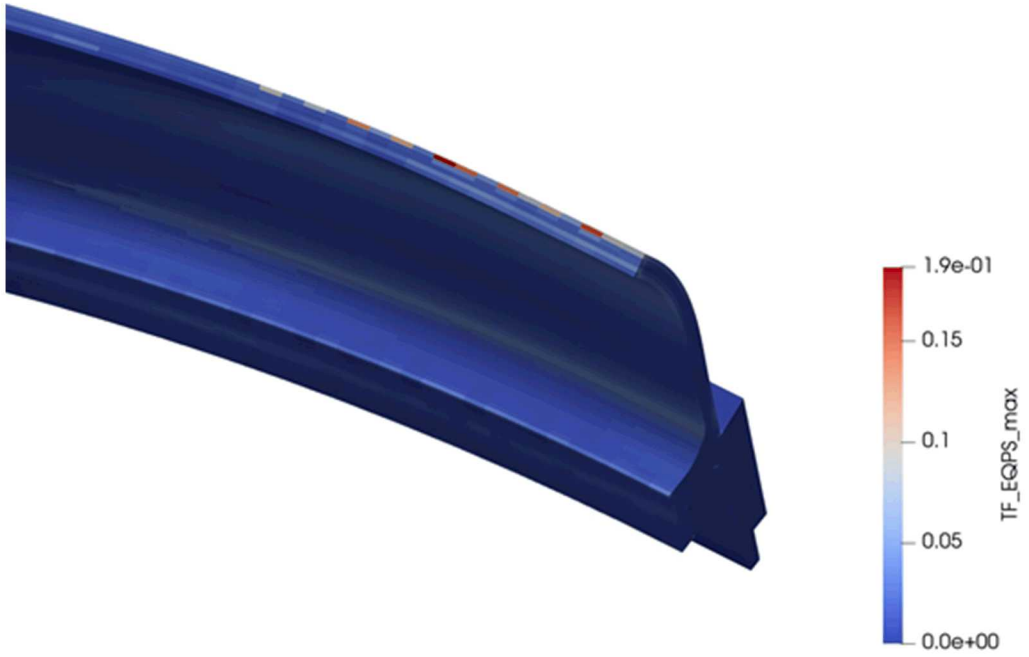

Figure 6-91. TF_EQPS in the Upper Flange.

6.2.11 Structural Analysis Summary

Seven structural analyses were conducted of the TRUPACT-II package as part of this TA. The first three were to calibrate the model by comparing the model results to the certification free drop tests. These analyses showed good agreement with the deformation produced during the tests. Four additional analyses were performed to determine the package response to higher impact velocities. These analyses focused on maintaining the integrity of the ICV, using the ASME strain-based failure criteria. Three analyses were performed at an impact velocity of 60-mph in the top, side, and CGOC orientations. The top and side analyses show that the ICV would remain leak tight. In the CGOC orientation, the ASME strain-based criteria showed that a break in the ICV flange may occur. An additional analysis was conducted in the CGOC orientation at a velocity of 45-mph. At this velocity the ICV remained leak tight.

6.3 Impacts with Yielding Targets

The analyses in the previous section all assume that the impact surface is rigid, and all the initial kinetic energy of the TRUPACT-II is absorbed by the package. Real accidents involve impacts with surfaces that are yielding, and the initial kinetic energy is absorbed somewhat by the target. The amount of energy that is absorbed by the target reduces the damage to the TRUPACT-II. The distribution of absorbed energy between the package and the target will depend on the relative strength and stiffness of the two bodies.

In order for an impact on a yielding target to produce as much damage to the cask as the impact on the unyielding target, the contact force between the package and the yielding target has to be as large as the peak contact force between the package and the unyielding target. For the contact force to be of this magnitude, the target must be strong enough to exert this magnitude of force. Impacts with low mass, non-fixed objects, such as automobiles, signposts, telephone poles, etc. cannot produce a force this large;

consequently, none of these impacts is as severe as the regulatory impact, no matter how large the impact velocity. Impacts with objects of large mass, such as trucks and trains, and with fixed surfaces or objects (soil, asphalt, concrete, rock) have the potential to be as severe as the regulatory impact if the impact velocity is sufficiently large.

The general method used to compare impacts with yielding targets to the regulatory impact onto an unyielding target is to calculate the amount of energy absorbed by the target, add this energy to the initial kinetic energy of the package, and compute an equivalent velocity for the package that gives this sum as its kinetic energy. A basic assumption of this method is that the damage to the package as a result of an impact onto a yielding target is in the same mode as the damage due to impact onto the unyielding target. This is generally the case for relatively flat targets or targets for which the impact interface between the package and the target remains essentially planar.

6.3.1 Impacts with Soil Targets

High-speed impacts of radioactive material packages on soils have been studied at Sandia by Gonzales (1987), Bonzon (1977), and Waddoups (1975). In the work by Gonzales a 20-in diameter steel test article weighing 5'200 pounds was impacted onto native desert soil at impact speeds of 30, 45, and 60-mph in an end-on orientation. These impacts led to penetration distances of 19, 25, and 36 inches, respectively. The tests by Bonzon involved an impact of an LLD-1 plutonium package (2R containment vessel in an outer container) weighing 76 lbs at 460-mph in a side-on orientation, three impacts of a 10-gallon 6M (2R containment vessel in a 15-inch diameter by 18-inch high drum weighing 55 pounds) (286 mph in a side-on orientation, 267 mph in a corner orientation, and 518-mph in a slapdown orientation), and an impact of a FL-10 package (steel pipe containment vessel in a 110-gal. drum weighing 500 pounds) at 317-mph in a side-on orientation. The tests by Waddoups involved an impact of a B of E 83 cask weighing 6,720 pounds at 246-mph and an OD-1 cask weighing 16,300 pounds at 230-mph. The results of these tests have been used to develop a force-deflection relationship for soil targets being penetrated by a package (Ammerman 1992). Using this method for the TRUPACT-II corner impact results in the soil force deflection curve shown in Figure 6-92. Hard Soil Target Force-Deflection Curve for a Corner Impact of the TRUPACT-II.

The soil impacted in the tests was hard desert soil typical of the region around Albuquerque, NM. To adjust this curve for softer soils, the force was scaled by the number of blows required to produce a one-foot penetration by a cone penetrometer. For hard soils this number is 30, for stiff soils it is 12, for medium soils it is 6, and for soft soils it is 3.

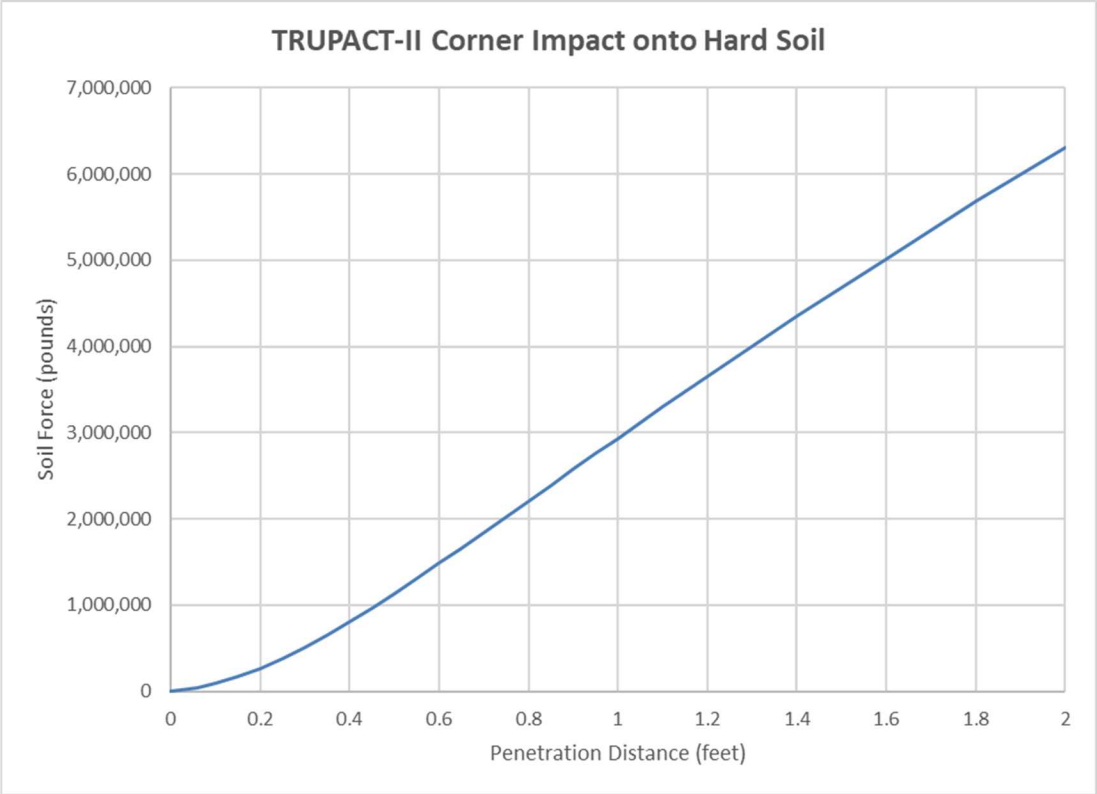

Figure 6-92. Hard Soil Target Force-Deflection Curve for a Corner Impact of the TRUPACT-II.

The absorbed energy for a given penetration depth is equal to the integral of the force-deflection curve up to that penetration depth. For the 60-mph corner impact of the TRUPACT-II onto a rigid target, Figure 6-75 shows the peak contact force is about 3,000,000 pounds (because of the additional force absorbed after this peak is reached, it is possible that a 50-mph impact could also reach this same peak force). For an impact onto hard soil, this level of force is reached when there is slightly over 1 foot of penetration. The amount of energy absorbed by the soil for this penetration can be determined by numerical integration of the force deflection curve up to this penetration depth. This yields an absorbed energy of 1,240,000 foot-pounds. The energy absorbed by the TRUPACT-II up to the point of reaching 3,000,000 pounds of contact force is 1,610,000 foot-pounds. The total energy absorbed by the impact is then the sum of that absorbed by the target and that absorbed by the TRUPACT-II, or 2,850,000 foot-pounds. An impact velocity of 67-mph is required to have this amount of kinetic energy.

Similar calculations performed for the softer soils lead to the results given in

Table 6-16. Impact Velocity onto Soil Required to Produce Equivalent Damage as a 50-mph Impact onto a Rigid Target.

6. From these results, it can be seen that for any impact onto soil, the TRUPACT-II impact velocity would need to be greater than 67-mph. Since WIPP trucks have mechanical governors on them that limit their travel speed to 65-mph, no soil impact will cause the TRUPACT-II to release any radioactive material.

Table 6-16. Impact Velocity onto Soil Required to Produce Equivalent Damage as a 50-mph Impact onto a Rigid Target.

Soil Type	Number of Blows	Soil Energy (foot-pounds)	Equivalent Velocity (mph)
Hard	30	1,240,000	67
Stiff	12	3,470,000	89
Medium	6	7,620,000	120
Soft	3	17,600,000	173

6.3.2 Impacts with Concrete Targets

The severity of an impact on a concrete target depends on the thickness of the concrete, the size and stiffness of the package, and the impact velocity. A limited amount of data for package impacts faster than 30-mph on concrete targets is available (Gonzales 1987). Concrete targets resist penetration in two ways. First is by the shear stiffness of the concrete itself. After the concrete slab fails in shear, further penetration is resisted by the stiffness of the sub-grade material beneath the slab. For the TRUPACT-II, the peak contact force is sufficient to generate a shear failure in the slab, and total penetration of 9-12 inches, depending on the concrete thickness. Table 6-17. gives the energy absorbed by slabs of 6-in, 9-in, 12-in, and 18-in thickness and equivalent velocity for TRUPACT-II corner impacts with peak contact force of 3,000,000 pounds. From these results, it can be seen that for any impact onto concrete, the TRUPACT-II impact velocity is generally less than accident velocity. Since WIPP trucks have mechanical governors on them that limit their travel speed to 65-mph, and impact velocity is always less than accident velocity, no concrete target impact will cause the TRUPACT-II to release any radioactive material.

Table 6-17. Impact Velocity onto Concrete Required to Produce Equivalent Damage as a 50-mph Impact onto a Rigid Target.

Concrete Thickness (inches)	Target Energy (foot-pounds)	Equivalent Velocity (mph)
6	1,230,000	66
9	1,140,000	65
12	1,050,000	64
18	995,000	64

6.3.3 Impacts with Rock Targets

There is a range of stiffness for exposed rock faces. In much of the country, the exposed rock is weathered sedimentary rock. This type of rock (soft rock) is only slightly stiffer than hard soil. To determine impact velocities, that produce the same amount of damage as the regulatory impact on an unyielding target, for this type of rock, the forces obtained for hard soil impacts were doubled. This is equivalent to 60 blows on a cone penetrometer rating system used for soils.

In some areas of the country there are exposed rock surfaces that are nearly unyielding, i.e. sufficiently stiff to approximate an unyielding target for a TRUPACT-II package. Table 6-18. gives the target energy absorbed and equivalent impact velocities for impacts onto rock surfaces.

Table 6-18. Impact Velocity onto Rock Required to Produce Equivalent Damage as a 50-mph Impact onto a Rigid Target.

Rock Type	Number of Blows	Target Energy (foot-pounds)	Equivalent Velocity (mph)
Hard	∞	0	50
Soft	60	703,000	60

6.3.4 Impacts with Trucks and Trains

Tests at Sandia involving head-on impacts of trucks into a 600-ton concrete target have shown that the peak contact force is about 1,500,000 pounds (Young 1995). This force is much smaller than the 3,000,000-pound force required to cause failure of the TRUPACT-II.

During the 1970s, Sandia performed a test with a locomotive impacting a spent fuel cask on a flat-bed trailer at a speed of 81-mph. The cask and locomotive positions were determined at each frame of the high-speed film. The cask position information was used to generate an acceleration time history. Multiplication of these accelerations by the mass of the cask gives a force time history. The difference in position between the cask and the locomotive was used to determine the amount of locomotive crush. Figure 6-93 shows the resulting force-deflection curve for the locomotive derived from the data. The maximum force was about 1,800,000 pounds, which is less than the 3,000,000-pound force required to cause failure of the TRUPACT-II.

Since the peak force generated by either a truck or train impacting a TRUPACT-II is less than the force required to cause a release of radioactive material, neither of these types of accidents will result in a release.

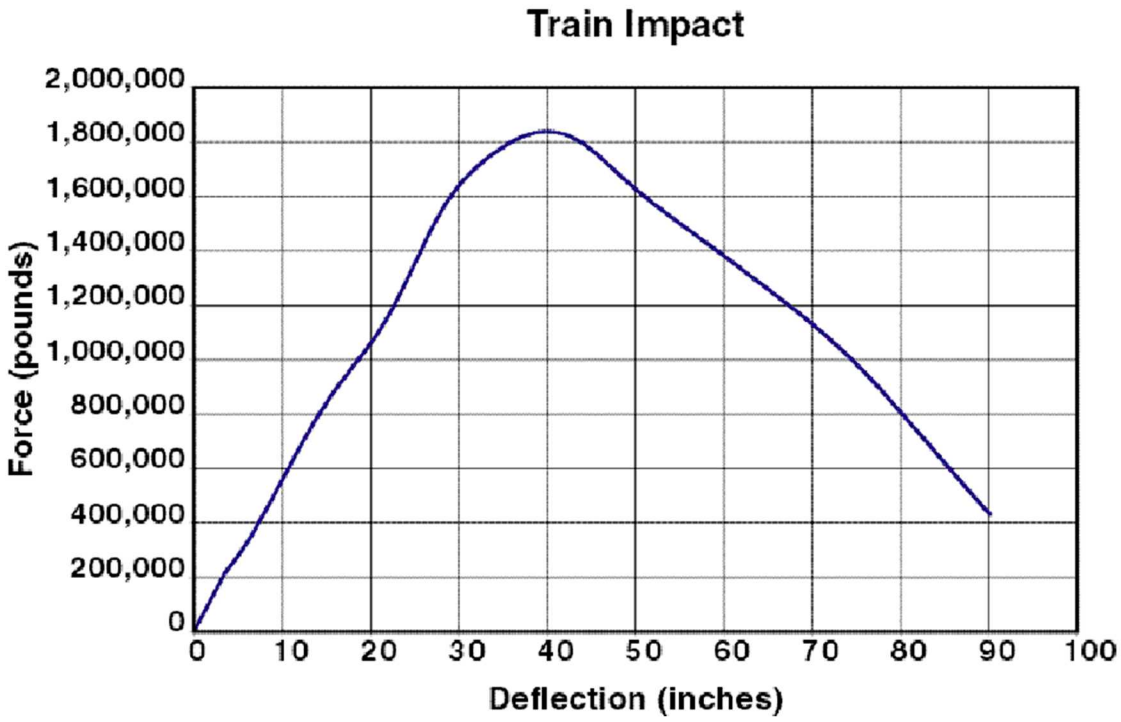

Figure 6-93. Force-Deflection Curve Generated from a Locomotive Impacting a Truck at 81-mph Carrying a Spent Fuel Cask.

6.4 Transportation Accidents with Fires

The thermal analyses were performed using a 2D-axisymmetric model in the ANSYS/Mechanical finite element code (ANSYS 2019). Figure 6-94 shows the model. The steel components were modeled as stainless-steel using the default material properties from ANSYS/Mechanical and the foam was modeled using the Suffield and Fort (2019) model. The original purpose of this thermal model was to monitor the maximum temperature rise of the contents, so the gap between the ICV and the OCV was neglected and these two shells were modeled as a single shell with the combined thickness which reduces the resistance to heat transfer from the fire to the inside of the package. The thicker flange region also was not explicitly modeled, but instead a material with average thermal properties of the wall at this section was included to represent the flanges.

The analysis was performed with an initial 38°C temperature of all components. The waste was assumed to generate 13W of decay heat. Prior to the HAC analyses, a thermal boundary condition of 193.5 W/m^2 on the vertical surfaces of the package and 580.5 W/m^2 on the domed top of the package from solar insolation were applied for 12 hours.

The maximum fire duration for a large engulfing fire during truck transport is reported in NUREG-2125 (NRC, 2014) as 1 hour. The fire analysis was conducted by assuming a radiation boundary condition of 850°C (slightly higher than the 800°C regulatory boundary condition to account for additional heat that could be imparted to the package from natural convection) completely surrounding the TRUPACT-II. At the end of the 1-hour fire the temperature distribution within the TRUPACT-II is shown in Figure 6-95. For parts of the package inboard of the outer shell the temperature continues to rise even after the end of the fire. Figure 6-96 shows the temperature distribution 7 hours after the end of the fire. The portion of the containment vessel most likely to be damaged by a fire is the O-ring seals. The thermal analysis is very conservative in the way that it models the heat transfer to this region, but even so, the maximum temperature

reached is only 177°C. The temperature history for the O-ring region is shown in Figure 6-97. The first 12 hours of this plot are the period of solar insolation. The 1-hour fire is assumed to start at t=12 hours and end at t=13 hours.

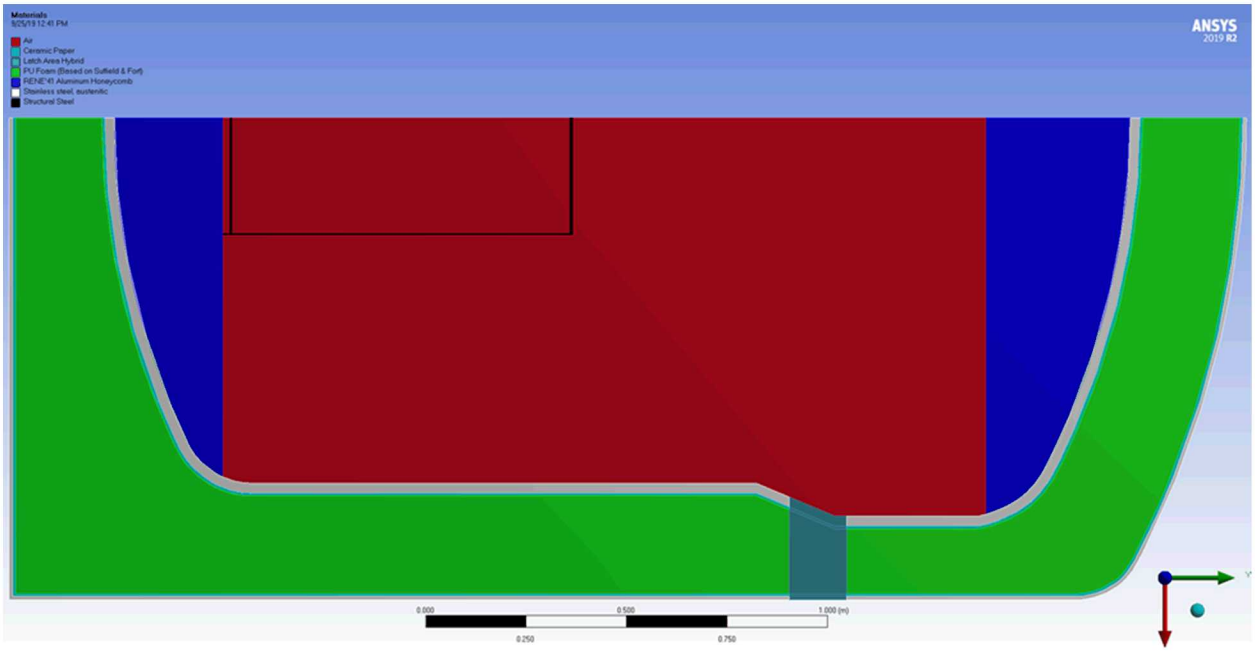

Figure 6-94. 2D Axisymmetric Thermal Model of the TRUPACT-II.

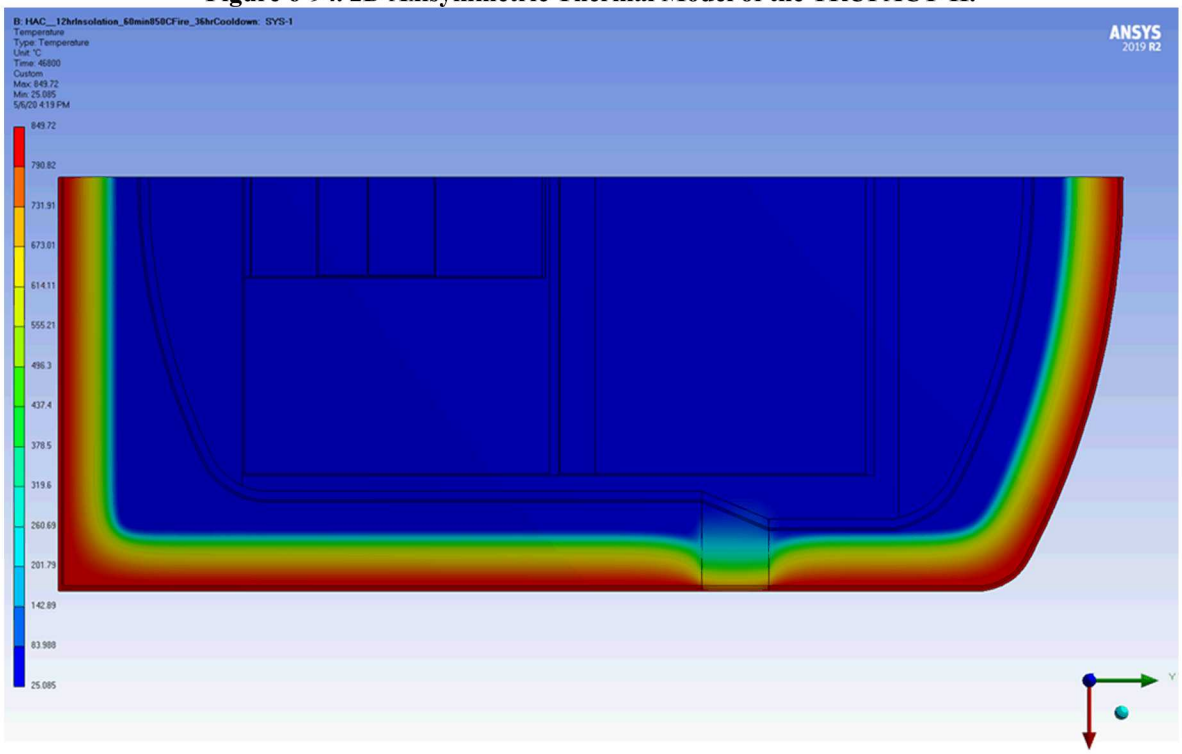

Figure 6-95. Temperature Distribution in the TRUPACT-II at the End of the 1-Hour Fire.

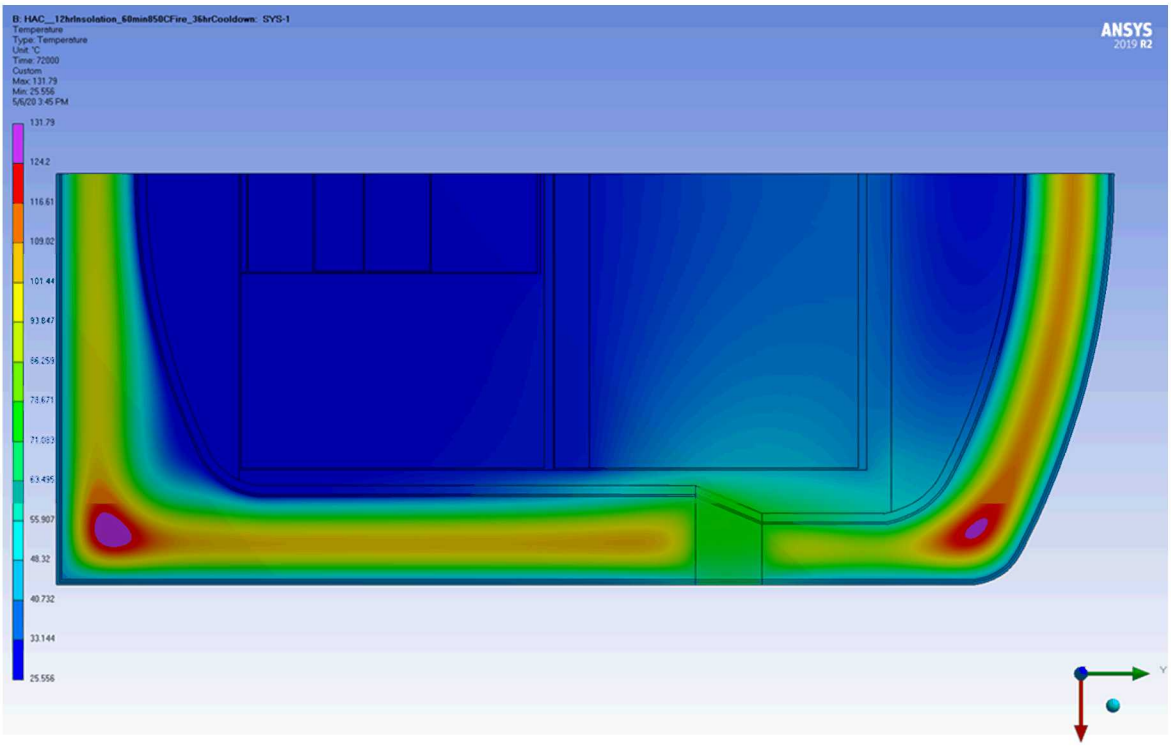

Figure 6-96. Temperature Distribution in the TRUPACT-II 7 Hours after the End of the 1-Hour Fire.

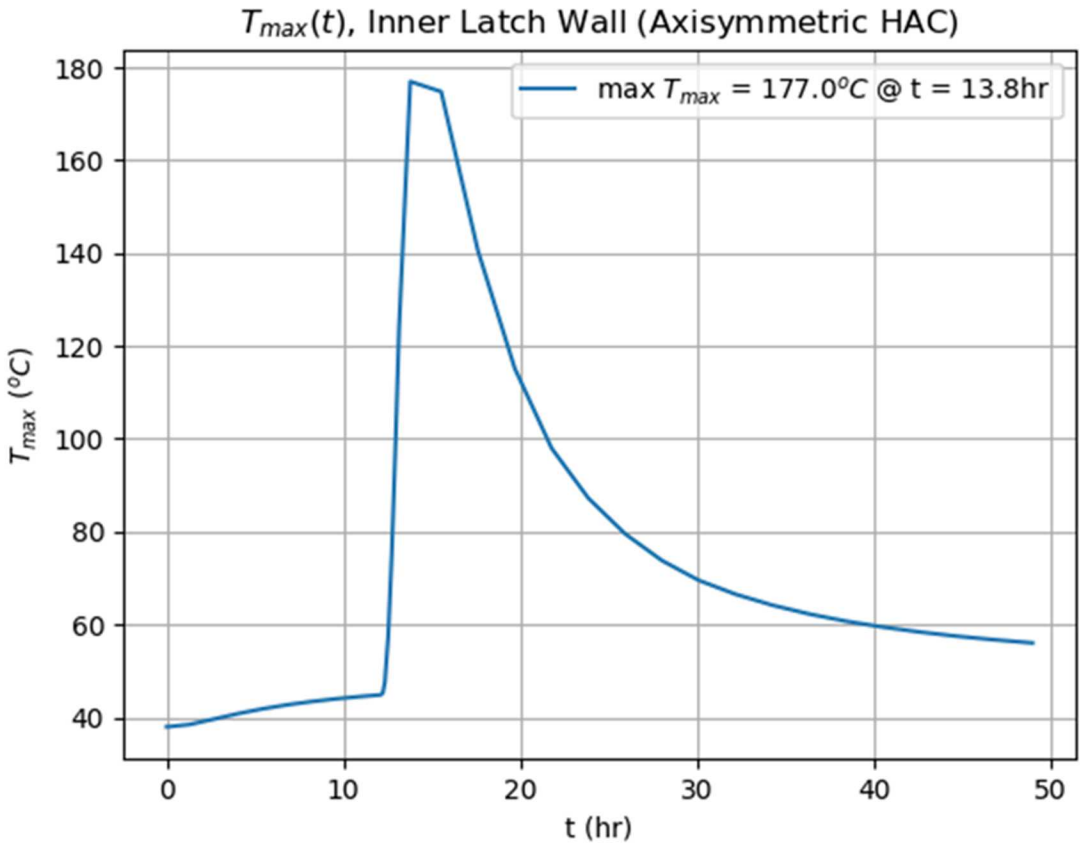

Figure 6-97. Temperature History in the O-Ring Region.

Section 3.3 of the TRUPACT-II SAR states "The butyl rubber O-ring seals have an allowable short-term temperature limit of 360 ºF (up to 8 hours). The allowable long-term temperature range of -40 ºF to 225 ºF is conservatively bounded by data in Figure 2-25 of Parker O-ring Handbook Table 3.1-1 for butyl rubber and by Rainier Rubber Company material data for butyl rubber compound R0405-70." The analysis shows an 8-hour temperature of about 104ºC, which is 219ºF and a peak temperature of 177ºC. which is 350ºF. Even the peak temperature of this conservative analysis is below the 8-hour duration temperature limit, and the temperature of the O-rings exceed the continuous use temperature for less than 8 hours. From this analysis it can be concluded that there is no risk of the TRUPACT-II losing containment due to a fire accident.

6.5 Severity Fractions and Release Fractions

The severity fractions estimated for CH-TRU waste in TRUPACT-II packages and for RH-TRU waste in HalfPACT packages were based on the event tree presented in Mills et al. (2006). Modeling of the TRUPACT-II (Sections 6.2) showed that an impact equivalent to the impact resulting from the shipping container traveling at 60-mph onto an unyielding surface would be required to rupture the inner containment vessel of the shipping containers. In addition, the impact would have to occur on the corner of the shipping container at an angle steep enough to cause failure. The event tree branches considered in developing the severity fractions were those associated with hard rock or columns. These event tree branches are denoted indices 5, 10, and 15 in Figure 6-94 (Mills et al. 2006).

The analysis of severity fractions also included the probability of an accident occurring at a speed of greater than 60-mph. These probabilities were taken from Sprung et al. (2000) and were given for different impact surfaces, speed distributions, and impact orientations. Severity fractions were estimated using the equation:

$$\text{Total Severity Fraction} = \sum_{i=1-3} \sum_{j=1-3} \text{P[Event Tree Branch]}_i \times \text{P[Velocity Bin]}_j \times \times \text{P[Corner Impact]} \times \text{P[Failure Angle]} \quad (6\text{-}6)$$

Total Severity Fraction	=	Total severity fraction summed over all event tree branches and velocity bins
$\text{P[Event Tree Branch]}_i$	=	Probability of event tree branch i. Three event tree branches were evaluated, corresponding to indices 5, 10, and 15 in Figure 6-94.
P[Velocity]_j	=	Probability of velocity bin j. Three velocity bins were evaluated, 60-90-mph, 90-120-mph, and > 120-mph
P[Corner Impact]	=	Probability of a corner impact (0.722)
P[Failure Angle]	=	Probability of an angle steep enough to cause inner containment vessel failure (0.377)

This analysis does not take credit for the WIPP tractor being governed to a maximum speed limit of 65-mph (DOE 2016).

The RH-TRU 72-B package (Docket No. 71-9212) is also used to transport RH-TRU waste. The RH-TRU 72-B consists of a cylindrical stainless steel and lead cask body, a separate inner stainless vessel, and foam-filled impact limiters at the end of the cask body (DOE 2015).

The cask body (outer cask) consists of a 1.5-inch thick stainless-steel outer shell, and a 1-inch thick stainless steel inner shell, with 1.875 inches of lead shielding between the two shells. The cask bottom is 5-inch thick stainless-steel plate. The cask is closed by a 6-inch thick stainless-steel lid (DOE 2015).

The separate inner vessel consists of a 0.375-inch thick stainless-steel shell and a 1.5-inch thick stainless-steel bottom plate. The inner vessel is closed by a 6.5-inch thick stainless-steel lid. The cask and inner vessel lids are leak testable (DOE 2015).

The outer cask, which has been designed, manufactured, and maintained to provide a containment function, establishes the primary containment boundary. The inner vessel, which has also been designed, manufactured and maintained to provide a containment function, provides a secondary containment boundary (DOE 2015).

The RH-TRU 72-B package is similar in construction to the rail transportation casks evaluated in NUREG-2125 (NRC 2014). The analyses in NUREG-2125 showed that there would be no release from transportation casks with inner canisters under the most severe accidents analyzed. Therefore, severity fractions and release fractions were not estimated for transportation accidents involving the RH-TRU 72-B package containing RH-TRU waste.

Table 6-16 contains the calculated severity fractions. The total severity fraction was estimated to be 1.9985×10^{-6} (see Table 1). The probability of an accident without a release was estimated to be 0.999998. The release fractions estimated for CH-TRU waste in TRUPACT-II packages were based on the CH-TRU being contained in 55-gallon drums. Three cases were evaluated:

- A maximum waste payload drum (196.8 kg waste/drum, waste density of 1.183 g/cm^3)

- An average waste payload drum (73.6 kg waste/drum, waste density of 0.442 g/cm^3)
- A 20 kg of waste payload drum (waste density of 0.120 g/cm^3)

A 20 kg of waste payload drum was calculated by dividing the total weight of the bounding CH waste stream SR-LA-PAD1 (Section 6.1) by the number of 55-gal drums (22) in which this waste stream is stored. The total waste mass (432.7 kg) was calculated by multiplying the total final form volume (4.6 m^3) by the sum of the mass densities for the waste material (not including packaging material) provided in Appendix A (p. 333) of the Annual Transuranic Waste Inventory Report-2019 (DOE 2019). Each TRUPACT-II contains 14 55-gallon drums, the volume of a 55-gallon drum was 208 L, each drum was assumed to be 80 percent full, and the drums were assumed to be damaged in an accident.

The release fractions estimated for RH-TRU waste in HalfPACTs were based on the RH-TRU waste being contained in shielded containers. Three cases were evaluated:

- A maximum payload shielded container (204.1 kg waste/shielded container, waste density of 2.247 g/cm^3)
- An average payload shielded container (30.1 kg waste/shielded container, waste density of 0.331 g/cm^3)
- An 8.84 kg of waste payload shielded container (waste density of 0.0917 g/cm^3).

An 8.84 kg of waste payload drum was calculated by dividing the total weight of the bounding RH waste stream SA-W139 (Section 6.1) by the number of shielded containers (6) in which this waste stream is projected to be stored. The total waste mass (53 kg) was calculated by multiplying the total final form volume (0.7 m^3) by the sum of the mass densities for the waste material (not including packaging material) provided in Appendix A (p. 319) of the Annual Transuranic Waste Inventory Report-2019 (DOE 2019).

Each HalfPACT contains three shielded containers and a shielded container contains a 30-gallon (113.6 L) drum into which waste is placed. Each drum was assumed to be 80 percent full, and the shielded containers and drums were assumed to be damaged in an accident.

The waste was considered to be a brittle solid material and the respirable release fraction was estimated using the equation (Sprung et al. 2000, Section 7.3.3; DOE 1994):

$$\text{Respirable Release Fraction} = 0.5 \times A \times \rho \times v_{impact}^2 \times \left(1 - \frac{OP}{OP + AP}\right) \qquad (6\text{-}7)$$

A	=	2×10^{-11} cm^3-s^2/g-cm^2
ρ	=	Waste density (g/cm^3)
v_{impact}	=	Impact velocity (cm/s)
OP	=	Operating Pressure (50 psig)
AP	=	Atmospheric Pressure (14.7 psia)

Three impact velocities were evaluated, 60-mph, 90-mph, and 120-mph. The operating pressure of the TRUPACT-II and HalfPACT was 50 psig (DOE 2013a, 2013b). The total respirable release fraction was estimated using the equation:

$$\text{Total Respirable Release Fraction} = \sum_{i=1-3} \sum_{j=1-3} \frac{\text{Severity Fraction}_{i,j} \times \text{Respirable Release Fraction}_{i,j}}{\text{Total Severity Fraction}}$$

(6-8)

The subscript “i” in the equation above denotes the event tree branches with indices 5, 10, and 15 in Figure 6-94. The subscript “j” in the equation above denotes the three velocity bins (60-90-mph, 90-120-mph, and > 120-mph).

Tables 6-19 - 6-25 contain the total respirable release fractions for CH-TRU in TRUPACT-II packages and RH-TRU in HalfPACT packages. Table 6-26 summarizes the total respirable release fractions.

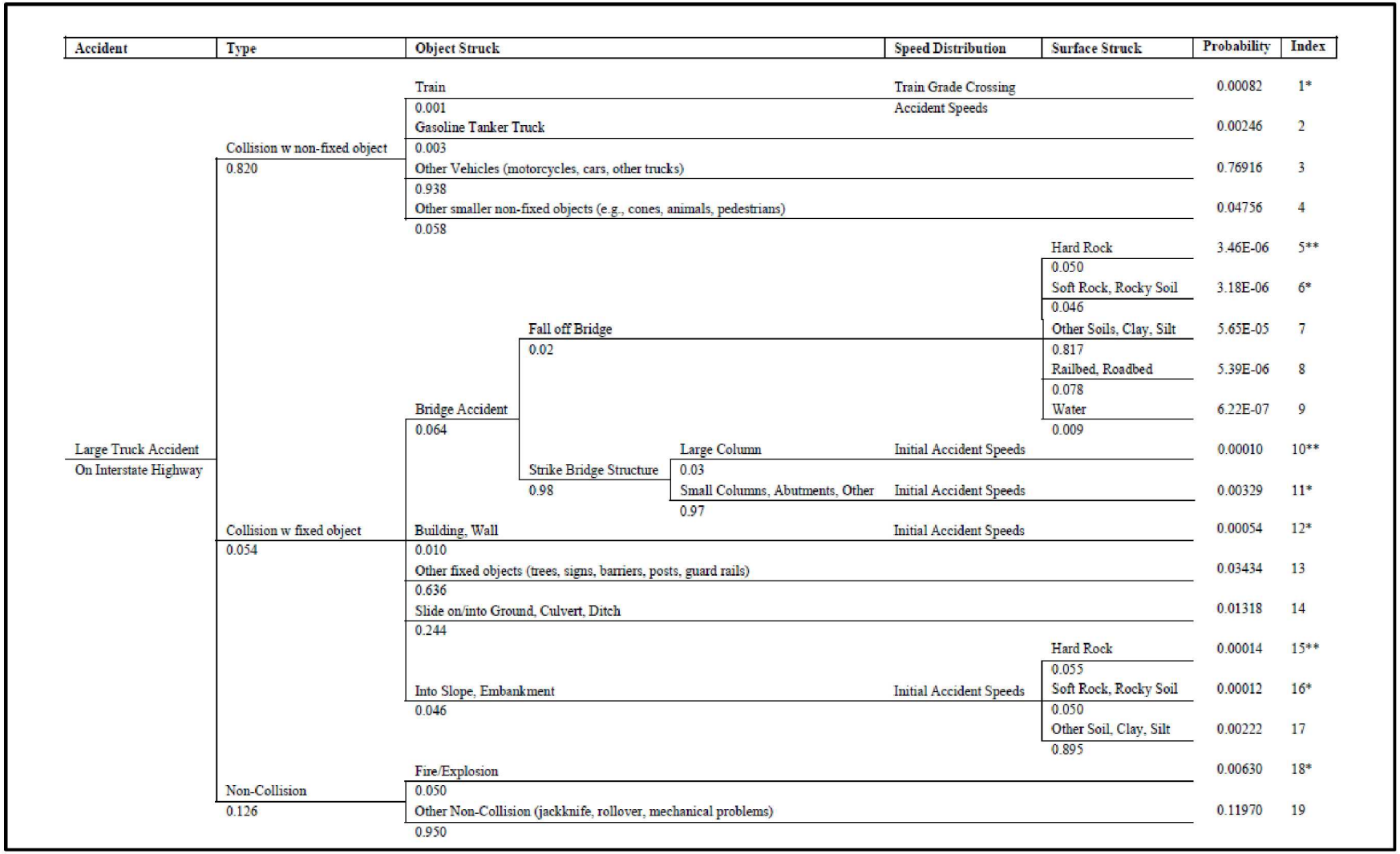

Accident	Type	Object Struck	Speed Distribution	Surface Struck	Probability	Index
Large Truck Accident On Interstate Highway	Collision w non-fixed object 0.820	Train 0.001	Train Grade Crossing Accident Speeds		0.00082	1*
		Gasoline Tanker Truck 0.003			0.00246	2
		Other Vehicles (motorcycles, cars, other trucks) 0.938			0.76916	3
		Other smaller non-fixed objects (e.g., cones, animals, pedestrians) 0.058			0.04756	4
		Bridge Accident 0.064		Hard Rock 0.050	3.46E-06	5**
				Soft Rock, Rocky Soil 0.046	3.18E-06	6*
				Other Soils, Clay, Silt 0.817	5.65E-05	7
				Railbed, Roadbed 0.078	5.39E-06	8
				Water 0.009	6.22E-07	9
		Fall off Bridge 0.02				
		Strike Bridge Structure 0.98	Large Column 0.03	Initial Accident Speeds	0.00010	10**
			Small Columns, Abutments, Other 0.97	Initial Accident Speeds	0.00329	11*
	Collision w fixed object 0.054	Building, Wall 0.010	Initial Accident Speeds		0.00054	12*
		Other fixed objects (trees, signs, barriers, posts, guard rails) 0.636			0.03434	13
		Slide on/into Ground, Culvert, Ditch 0.244			0.01318	14
		Into Slope, Embankment 0.046	Initial Accident Speeds	Hard Rock 0.055	0.00014	15**
				Soft Rock, Rocky Soil 0.050	0.00012	16*
				Other Soil, Clay, Silt 0.895	0.00222	17
		Fire/Explosion 0.050			0.00630	18*
	Non-Collision 0.126	Other Non-Collision (jackknife, rollover, mechanical problems) 0.950			0.11970	19

Figure 6-98. Truck Accident Event Tree Structure (Mills et al. 2006).

Table 6-19. Severity Fractions.

Index and Scenario	Event Tree Probability	Speed Distribution	Impact Surface	Probability 60-90-mph Velocity Bin	Probability 90-120-mph Velocity Bin	Probability > 120-mph Velocity Bin	Probability 60-90-mph Velocity Bin (with corner impact and failure angle)	Probability 90-120-mph Velocity Bin (with corner impact and failure angle)	Probability > 120-mph Velocity Bin (with corner impact and failure angle)	Severity Fraction 60-90-mph Velocity Bin	Severity Fraction 90-120-mph Velocity Bin	Severity Fraction > 120-mph Velocity Bin
5 (Fall Off Bridge)	3.460E-06	V2 (Bridge)	Hard Rock	0.000E+00	0.000E+00	0.000E+00	0.000E+00	0.000E+00	0.000E+00	0.000E+00	0.000E+00	0.000E+00
10 (Large Column)	1.000E-04	V1 (Level)	Column (Hard Rock)	1.948E-02	4.325E-04	7.500E-06	5.301E-03	1.177E-04	2.041E-06	5.301E-07	1.177E-08	2.041E-10
15 (Embankment)	1.400E-04	V3 (Slope)	Hard Rock	3.723E-02	9.814E-04	8.571E-06	1.013E-02	2.671E-04	2.333E-06	1.419E-06	3.740E-08	3.266E-10
Total	2.435E-4									1.949E-06	4.917E-08	5.308E-10
Total Severity Fraction= 1.9985E-06 Notes Event tree probabilities were taken from Mills et al. (2006). Velocity bin probabilities were taken from Sprung et al. (2000), Appendix D.5.												

Table 6-20. TRUPACT-II with Maximum Payload Drum.

Index and Scenario	Severity Fraction 60-90-mph Velocity Bin	Severity Fraction 90-120-mph Velocity Bin	Severity Fraction > 120-mph Velocity Bin	Respirable Release Fraction 60-90-mph Velocity Bin	Respirable Release Fraction 90-120-mph Velocity Bin	Respirable Release Fraction > 120-mph Velocity Bin	Severity Fraction Weighted Respirable Release Fraction 60-90-mph Velocity Bin	Severity Fraction Weighted Respirable Release Fraction 90-120-mph Velocity Bin	Severity Fraction Weighted Respirable Release Fraction > 120-mph Velocity Bin
5 (Fall Off Bridge)	0.000E+00	0.000E+00	0.000E+00	6.576E-05	1.480E-04	2.631E-04	0.000E+00	0.000E+00	0.000E+00
10 (Large Column)	5.301E-07	1.177E-08	2.041E-10	6.576E-05	1.480E-04	2.631E-04	1.744E-05	8.716E-07	2.687E-08
15 (Embankment)	1.419E-06	3.740E-08	3.266E-10	6.576E-05	1.480E-04	2.631E-04	4.669E-05	2.769E-06	4.299E-08
Total	1.949E-06	4.917E-08	5.308E-10				6.413E-05	3.641E-06	6.986E-08
Total Respirable Release Fraction= 6.7840E-05									

Table 6-21. TRUPACT-II with Average Payload Drum.

Index and Scenario	Severity Fraction 60-90-mph Velocity Bin	Severity Fraction 90-120-mph Velocity Bin	Severity Fraction > 120-mph Velocity Bin	Respirable Release Fraction 60-90-mph Velocity Bin	Respirable Release Fraction 90-120-mph Velocity Bin	Respirable Release Fraction > 120-mph Velocity Bin	Severity Fraction Weighted Respirable Release Fraction 60-90-mph Velocity Bin	Severity Fraction Weighted Respirable Release Fraction 90-120-mph Velocity Bin	Severity Fraction Weighted Respirable Release Fraction > 120-mph Velocity Bin
5 (Fall Off Bridge)	0.000E+00	0.000E+00	0.000E+00	2.458E-05	5.530E-05	9.831E-05	0.000E+00	0.000E+00	0.000E+00
10 (Large Column)	5.301E-07	1.177E-08	2.041E-10	2.458E-05	5.530E-05	9.831E-05	6.519E-06	3.257E-07	1.004E-08
15 (Embankment)	1.419E-06	3.740E-08	3.266E-10	2.458E-05	5.530E-05	9.831E-05	1.745E-05	1.035E-06	1.607E-08
Total	1.949E-06	4.917E-08	5.308E-10				2.397E-05	1.361E-06	2.611E-08
Total Respirable Release Fraction= 2.5353E-05									

Table 6-22. TRUPACT-II with 20 kg Payload Drum.

Index and Scenario	Severity Fraction 60-90-mph Velocity Bin	Severity Fraction 90-120-mph Velocity Bin	Severity Fraction > 120-mph Velocity Bin	Respirable Release Fraction 60-90-mph Velocity Bin	Respirable Release Fraction 90-120-mph Velocity Bin	Respirable Release Fraction > 120-mph Velocity Bin	Severity Fraction Weighted Respirable Release Fraction 60-90-mph Velocity Bin	Severity Fraction Weighted Respirable Release Fraction 90-120-mph Velocity Bin	Severity Fraction Weighted Respirable Release Fraction > 120-mph Velocity Bin
5 (Fall Off Bridge)	0.000E+00	0.000E+00	0.000E+00	6.682E-06	1.504E-05	2.673E-05	0.000E+00	0.000E+00	0.000E+00
10 (Large Column)	5.301E-07	1.177E-08	2.041E-10	6.682E-06	1.504E-05	2.673E-05	1.772E-06	8.857E-08	2.730E-09
15 (Embankment)	1.419E-06	3.740E-08	3.266E-10	6.682E-06	1.504E-05	2.673E-05	4.744E-06	2.814E-07	4.369E-09
Total	1.949E-06	4.917E-08	5.308E-10				6.516E-06	3.699E-07	7.099E-09
Total Respirable Release Fraction= 6.8933E-06									

Table 6-23. HalfPACT with Maximum Payload Shielded Container.

Index and Scenario	Severity Fraction 60-90-mph Velocity Bin	Severity Fraction 90-120-mph Velocity Bin	Severity Fraction > 120-mph Velocity Bin	Respirable Release Fraction 60-90-mph Velocity Bin	Respirable Release Fraction 90-120-mph Velocity Bin	Respirable Release Fraction > 120-mph Velocity Bin	Severity Fraction Weighted Respirable Release Fraction 60-90-mph Velocity Bin	Severity Fraction Weighted Respirable Release Fraction 90-120-mph Velocity Bin	Severity Fraction Weighted Respirable Release Fraction > 120-mph Velocity Bin
5 (Fall Off Bridge)	0.000E+00	0.000E+00	0.000E+00	1.249E-04	2.811E-04	4.997E-04	0.000E+00	0.000E+00	0.000E+00
10 (Large Column)	5.301E-07	1.177E-08	2.041E-10	1.249E-04	2.811E-04	4.997E-04	3.313E-05	1.656E-06	5.104E-08
15 (Embankment)	1.419E-06	3.740E-08	3.266E-10	1.249E-04	2.811E-04	4.997E-04	8.868E-05	5.260E-06	8.166E-08
Total	1.949E-06	4.917E-08	5.308E-10				1.218E-04	6.915E-06	1.327E-07
Total Respirable Release Fraction= 1.2886E-04									

Table 6-24. HalfPACT with Average Payload Shielded Container.

Index and Scenario	Severity Fraction 60-90-mph Velocity Bin	Severity Fraction 90-120-mph Velocity Bin	Severity Fraction > 120-mph Velocity Bin	Respirable Release Fraction 60-90-mph Velocity Bin	Respirable Release Fraction 90-120-mph Velocity Bin	Respirable Release Fraction > 120-mph Velocity Bin	Severity Fraction Weighted Respirable Release Fraction 60-90-mph Velocity Bin	Severity Fraction Weighted Respirable Release Fraction 90-120-mph Velocity Bin	Severity Fraction Weighted Respirable Release Fraction > 120-mph Velocity Bin
5 (Fall Off Bridge)	0.000E+00	0.000E+00	0.000E+00	1.839E-05	4.139E-05	7.358E-05	0.000E+00	0.000E+00	0.000E+00
10 (Large Column)	5.301E-07	1.177E-08	2.041E-10	1.839E-05	4.139E-05	7.358E-05	4.879E-06	2.438E-07	7.516E-09
15 (Embankment)	1.419E-06	3.740E-08	3.266E-10	1.839E-05	4.139E-05	7.358E-05	1.306E-05	7.745E-07	1.202E-08
Total	1.949E-06	4.917E-08	5.308E-10				1.794E-05	1.018E-06	1.954E-08
Total Respirable Release Fraction= 1.8974E-05									

Table 6-25. HalfPACT with 8.84 kg Payload Shielded Container.

Index and Scenario	Severity Fraction 60-90-mph Velocity Bin	Severity Fraction 90-120-mph Velocity Bin	Severity Fraction > 120-mph Velocity Bin	Respirable Release Fraction 60-90-mph Velocity Bin	Respirable Release Fraction 90-120-mph Velocity Bin	Respirable Release Fraction > 120-mph Velocity Bin	Severity Fraction Weighted Respirable Release Fraction 60-90-mph Velocity Bin	Severity Fraction Weighted Respirable Release Fraction 90-120-mph Velocity Bin	Severity Fraction Weighted Respirable Release Fraction > 120-mph Velocity Bin
5 (Fall Off Bridge)	0.000E+00	0.000E+00	0.000E+00	5.410E-06	1.217E-05	2.164E-05	0.000E+00	0.000E+00	0.000E+00
10 (Large Column)	5.301E-07	1.177E-08	2.041E-10	5.410E-06	1.217E-05	2.164E-05	1.435E-06	7.170E-08	2.210E-09
15 (Embankment)	1.419E-06	3.740E-08	3.266E-10	5.410E-06	1.217E-05	2.164E-05	3.840E-06	2.278E-07	3.537E-09
Total	1.949E-06	4.917E-08	5.308E-10				5.275E-06	2.995E-07	5.747E-09
Total Respirable Release Fraction= 5.5806E-06									

Table 6-26. Summary of Total Respirable Release Fractions for CH-TRU and RH-TRU Waste.

Waste Type	Case	Total Severity Fraction	Total Respirable Release Fraction
CH-TRU	TRUPACT-II with Maximum Payload Drum	1.9985E-06	6.7840E-05
CH-TRU	TRUPACT-II with Average Payload Drum	1.9985E-06	2.5353E-05
CH-TRU	TRUPACT-II with 20 kg Payload Drum	1.9985E-06	6.8933E-06
RH-TRU	HalfPACT with Maximum Payload Shielded Container	1.9985E-06	1.2886E-04
RH-TRU	HalfPACT with Average Payload Shielded Container	1.9985E-06	1.8974E-05
RH-TRU	HalfPACT with 8.33 kg Payload Shielded Container	1.9985E-06	5.5806E-06

Figure 6-99 compares the respirable release fractions for severity categories 2-6 (categories with non-zero releases) assumed in the 2008 TA for TRUPACT-II to the corresponding release rate in Table 6-26. The respirable release fraction is about 2 orders of magnitude higher in this TA.

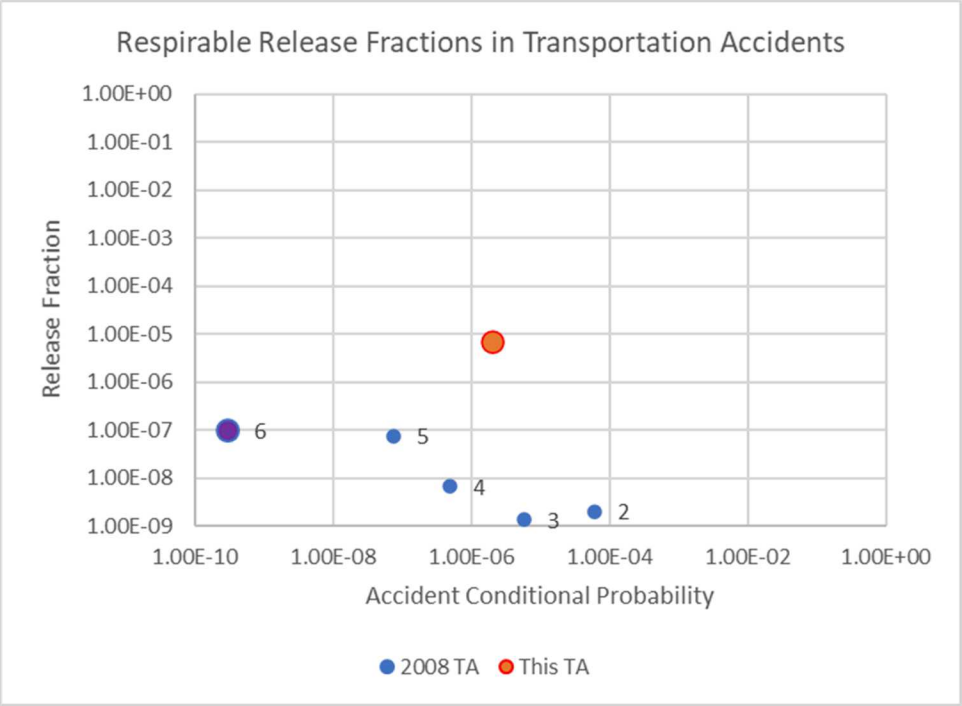

Note: The labels 2-6 are the severity categories for which the release fractions were assumed in the 2008 TA.

Figure 6-99. Comparison of the Respirable Release Fractions in the 2008 TA and this TA Truck Accident.

7. RADIOLOGICAL IMPACTS FROM TRANSPORTATION ACCIDENTS

The transportation accident analysis considers an accident in which radioactive materials are released and an accident in which there is no release of radioactive materials. The unit risk factors used to calculate the consequences of these accidents are described in Section 7.1. Sections 7.2.1 and 7.2.2 provide the results of analyses of accidents with a release of radioactive materials. Section 7.2.3 provides the results of the analysis of an accident without a release of radioactive materials.

As was explained in Section 6, the release of the radioactive materials (if any) may only occur in the case of an extra-regulatory accident, a very low probability event. This is because the extra-regulatory accident scenarios extend beyond the HAC defined for regulatory accidents in 10 CFR Part 71. Consideration of low probability extra-regulatory accidents (probability-based analysis) are included per Department of Energy (DOE) National Environmental Policy Act (NEPA) accident analysis guidance (DOE, 2002).

7.1 Unit Risk Factors for Transportation Accident Analysis

7.1.1 Transportation Accidents with Release of Radioactive Materials

Two scenarios of transportation accidents with release of radioactive materials were considered. In both cases, the conditional probability of an accident resulting in release of radioactive materials is 1.9985×10^{-6}. The conditional probability of an accident without release of radioactive materials is then 0.999998. Only one severity category was specified in this TA based on the results of TRUPACT-II extra regulatory accident analysis (Section 6.2) as described in Section 6.5. This is different from the 2008 TA that assumed five severity categories with non-zero release. The conditional probability of an accident without release of radioactive materials was 0.99993. The 2008 TA assumptions were based on data for impacts of spent nuclear fuel casks that are very different from TRUPACT-II. No other data were available at that time.

The first scenario applies to an accident involving the shipment of one HalfPACT and two TRUPACT-IIs. It is assumed that one TRUPACT-II is damaged to the extent that the radioactive materials are released. The respirable release fraction in this accident is 6.8933×10^{-6} (Section 6.5). The bounding inventory for this accident is provided in Table 6-5 under CH-TRU waste. It is assumed that an accident with TRUPACT-III is bounded by an accident with TRUPACT-II.

The second scenario applies to an accident with three HalfPACTs with SCAs. The respirable release fraction in this accident is 5.2586×10^{-6} (Section 6.5). The bounding inventory for this accident is provided in Table 6-5 under RH-TRU waste. As described in Section 6.5, there is 0 probability of an accident with release of radioactive materials in the case of a RH-TRU 72-B shipment.

The unit risk factors for transportation accidents with release of radioactive materials were calculated using RADTRAN 6.02 assuming:

- CH-TRU inventory defined in Table 6-5
- RH-TRU inventory defined in Table 6-5
- Accident rate equal to 1 accident/km
- One severity category with non-zero release
- Conditional probability of the accident with release equal to 1
- Respirable fractions of 6.8933×10^{-6} (CH inventory) and 5.5806×10^{-6} (RH inventory) (Section 6.5)
- Link distance equal to 1 km
- Population density equal to 1 person per km^2 (0.39 persons/mi^2)

The following RADTRAN parameters were defined as in the 2008 TA:

- Evacuation time of 24 hours (population exposure to emitted materials).
- Class F meteorological conditions stability
- Building dose factor equal to 0.05
- Fraction of urban areas with buildings equal to 0.5
- Fraction of urban areas with sidewalks 0.48
- Ratio of sidewalk pedestrian density equal to 6
- Deposition velocity equal to 0.01 m/s
- Wind speed equal to 0.5 m/s

Note that Class F corresponds to very stable meteorological conditions. This limits dispersion of the radioactive material plume and results in higher radiation doses.

The unit risk factors are summarized in Table 7-1. As was described in Section 2.2.2, the radiological impacts in the rural and suburban areas are calculated in RADTRAN 6.02 using the same pathway-specific equation. The population dose in an urban area includes a factor that takes into account the population inside buildings and the population outside (pedestrians). As a result, the unit risk factors are the same for the rural and suburban links and different for the urban links.

Table 7-1. Unit Risk Factors for Transportation Accident with Release of Radioactive Materials.

Shipment	Unit Risk Factors (km^2)					
	Link	Inhaled	Resuspended	Cloudshine	Groundshine	Total
TRUPACT-II	Urban	1.32E-01	1.10E-03	6.07E-11	4.68E-09	1.33E-01
	Suburban and Rural	4.54E-02	3.79E-04	2.09E-11	1.61E-09	4.58E-02
HalfPACT (SCA)	Urban	2.70E-03	2.25E-05	1.19E-08	1.43E-07	2.72E-03
	Suburban and Rural	9.28E-04	7.76E-06	4.09E-09	4.93E-08	9.36E-04

The total unit risk factors in Table 7-1 are used to calculate collective population dose risks (Section 7.2.1) and collective population doses (Section 7.2.2). As evident from Figures 7-1 and 7-2, the total dose is primarily due to inhalation in both accident scenarios. The contribution to inhalation to the total dose is 99.2 percent.

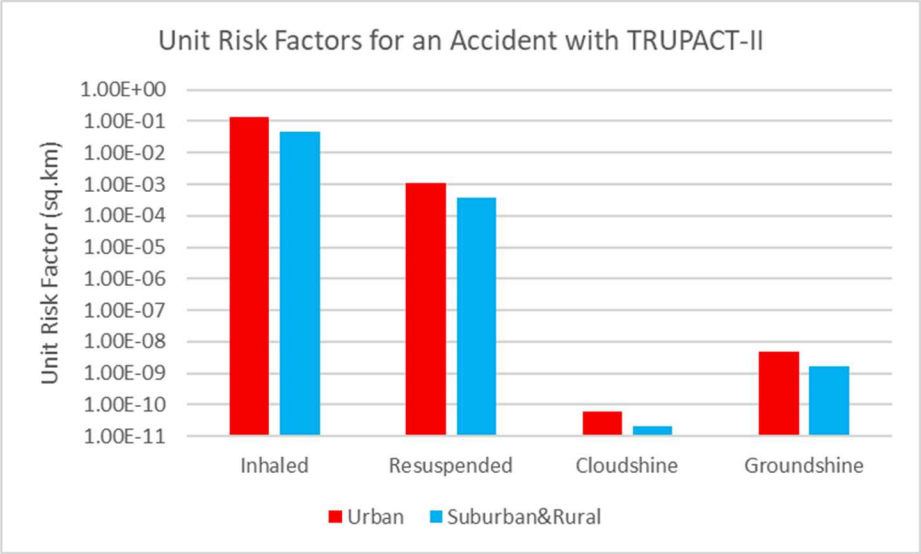

Figure 7-1. Unit Risk Factors for an Accident with TRUPACT-II.

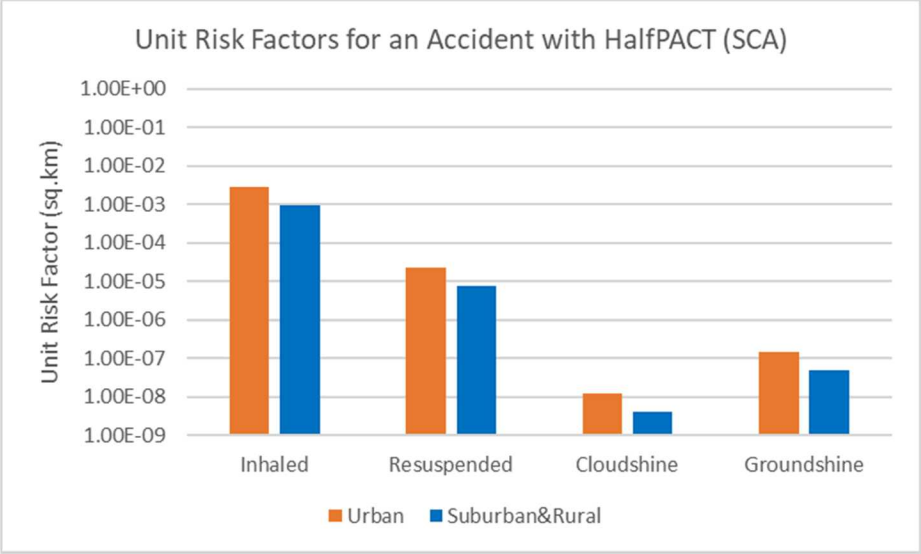

Figure 7-2. Unit Risk Factors for an Accident with HalfPACT.

7.1.2 Transportation Accidents without Release of Radioactive Materials

This scenario assumes that a truck involved in an accident in which no radioactive materials were released stays at or near the place of the accident for many hours. The nearby population and an individual who happened to be in the vicinity are exposed to the external radiation from the package(s) on the truck. The individual is considered to be a maximum exposed individual (MEI).

The unit risk factors were calculated using RADTRAN 6.02 for the different shipment types defined in Table 4-2 assuming:

- Dose rate at 1 m (TI) equal to 1 mrem/hr
- Shielding factor equal to 1 (no shielding)

- Population density equal to 1 person per km^2 (0.39 persons/mi^2)
- Exposure time equal to 1 hr

Table 7-2 provides the unit risk factors for the population and the MEI for this accident without release scenario.

Table 7-2. Unit Risk Factors for Transportation Accident without Release of Radioactive Materials.

Receptor	Notation	Unit Risk Factors (km^2)		
		Shipment ID (from Table 4-2)		
		1	2	3
Population (30-800 m from the source)	$URF_{nracc,p}$	3.17E-07	2.64E-07	1.68E-07
MEI (30 m from the source)	$URF_{MEI\_nr,p}$	1.70E-05	1.42E-05	9.03E-06

7.2 Transportation Accident Analysis

7.2.1 Transportation Accidents with Release of Radioactive Materials

As described in Section 2.2.2, the radiological impacts from the transportation accidents with release of radioactive materials are calculated for rural, suburban, and urban segment for each state crossed by the transportation route and for each route. Credit is not taken for the fact that an accident will occur at only one place. This is the same approach as in the 2008 TA.

The radiological impacts are reported as total population collective dose risks calculated with Eq. 2-14 and 2-15 using the accident unit risk factors (Table 7-1) multiplied by the accident conditional probability. The state-specific accident rates used in these calculations are described in Section 3.4. The population density along the routes is for 2018 (Section 3.2).

The collective dose risks per shipment of CH-TRU waste (first accident scenario) are summarized in Table 7-3. The collective dose risks for all CH shipments are summarized in Table 7-4.

Table 7-3. Collective Dose Risks per Shipment of CH-TRU Waste.

Route	Collective Dose Risk (person-rem)											
ANL	IL	IA	NE	WY	CO	NM						
Rural	1.30E-10	2.85E-10	2.04E-10	1.07E-11	2.85E-10	2.04E-10						
Suburban	1.13E-09	9.55E-10	6.50E-10	9.68E-11	3.96E-09	2.42E-10						
Urban	8.35E-11	2.87E-10	1.10E-09	1.20E-10	1.55E-08	0.00E+00						
Hanford	WA	OR	ID	UT	WY	CO	NM					
Rural	1.16E-11	1.56E-10	1.94E-10	9.22E-11	1.68E-10	2.85E-10	2.04E-10					
Suburban	4.82E-10	3.13E-10	9.61E-10	6.22E-10	3.11E-10	3.96E-09	2.42E-10					
Urban	1.33E-11	2.83E-11	4.43E-10	3.10E-11	1.93E-12	1.55E-08	0.00E+00					
INL	ID	UT	WY	CO	NM							
Rural	7.92E-11	8.98E-11	1.68E-10	2.85E-10	2.04E-10							
Suburban	3.40E-10	6.29E-10	3.11E-10	3.96E-09	2.42E-10							
Urban	1.93E-10	3.10E-11	1.93E-12	1.55E-08	0.00E+00							
Knolls	NY	PA	MD	WV	VA	TN	GA	AL	MS	LA	TX	NM
Rural	2.26E-10	3.41E-10	1.36E-12	8.33E-12	4.41E-10	1.96E-10	2.82E-11	3.09E-10	1.02E-10	1.33E-10	5.43E-10	1.24E-11
Suburban	3.09E-09	3.90E-09	8.69E-10	3.60E-10	3.13E-09	1.91E-09	9.15E-11	1.56E-09	8.64E-10	9.37E-10	3.39E-09	1.33E-10
Urban	1.83E-09	3.59E-10	0.00E+00	1.14E-11	1.77E-09	2.07E-09	0.00E+00	6.56E-10	2.56E-10	3.07E-10	3.45E-09	7.00E-11
LANL	NM											
Rural	2.43E-10											
Suburban	4.30E-10											
Urban	0.00E+00											
ORNL	TN	GA	AL	MS	LA	TX	NM					
Rural	6.32E-11	2.82E-11	3.09E-10	1.02E-10	1.33E-10	5.43E-10	1.24E-11					
Suburban	1.03E-09	9.15E-11	1.56E-09	8.64E-10	9.37E-10	3.39E-09	1.33E-10					
Urban	4.02E-10	0.00E+00	6.56E-10	2.56E-10	3.07E-10	3.45E-09	7.00E-11					
SNL	NM											
Rural	1.18E-10											
Suburban	3.93E-10											
Urban	7.32E-10											

Route	Collective Dose Risk (person-rem)											
SRS	SC	GA	AL	MS	LA	TX	NM					
Rural	2.49E-11	1.62E-10	2.22E-10	1.02E-10	1.33E-10	5.43E-10	1.24E-11					
Suburban	1.34E-10	3.59E-09	1.83E-09	8.64E-10	9.37E-10	3.39E-09	1.33E-10					
Urban	0.00E+00	1.14E-09	6.56E-10	2.56E-10	3.07E-10	3.45E-09	7.00E-11					
LLNL	CA	NV	UT	ID								
Rural	1.82E-10	3.50E-10	9.61E-11	7.92E-11								
Suburban	3.87E-09	1.02E-09	1.26E-09	3.40E-10								
Urban	1.78E-08	5.57E-09	3.09E-09	1.93E-10								
NNSS	NV	UT	ID									
Rural	1.34E-10	9.61E-11	7.92E-11									
Suburban	2.89E-10	1.26E-09	3.40E-10									
Urban	0.00E+00	3.09E-09	1.93E-10									
NRD	NY	PA	WV	OH	IN	IL	IA	NE	WY	UT	ID	
Rural	1.34E-10	4.01E-10	9.14E-12	2.33E-10	1.83E-10	2.25E-10	2.85E-10	2.04E-10	1.82E-10	8.98E-11	7.92E-11	
Suburban	6.12E-10	3.26E-09	2.84E-10	3.00E-09	1.95E-09	1.13E-09	9.55E-10	6.50E-10	4.48E-10	6.29E-10	3.40E-10	
Urban	7.90E-10	1.11E-09	0.00E+00	2.24E-09	5.92E-09	2.85E-10	2.87E-10	1.10E-09	1.13E-10	3.10E-11	1.93E-10	

Table 7-4. Collective Dose Risks for All Shipment of CH TRU Waste.

Route	Collective Dose Risk (person-rem)											
ANL	IL	IA	NE	WY	CO	NM						
Rural	3.64E-09	7.98E-09	5.70E-09	3.00E-10	7.98E-09	5.72E-09						
Suburban	3.18E-08	2.67E-08	1.82E-08	2.71E-09	1.11E-07	6.79E-09						
Urban	2.34E-09	8.04E-09	3.09E-08	3.36E-09	4.34E-07	0.00E+00						
Hanford	WA	OR	ID	UT	WY	CO	NM					
Rural	7.18E-08	9.67E-07	1.20E-06	5.70E-07	1.04E-06	1.76E-06	1.26E-06					
Suburban	2.98E-06	1.93E-06	5.94E-06	3.85E-06	1.92E-061.84E-06	2.45E-05	1.50E-06					
Urban	8.22E-08	1.75E-07	2.74E-06	1.92E-07	1.20E-08	9.58E-05	0.00E+00					
INL	ID	UT	WY	CO	NM							
Rural	2.61E-07	2.97E-07	5.55E-07	9.41E-07	6.75E-07							
Suburban	1.12E-06	2.08E-06	1.03E-06	1.31E-05	8.01E-07							
Urban	6.38E-07	1.02E-07	6.39E-09	5.12E-05	0.00E+00							
Knolls	NY	PA	MD	WV	VA	TN	GA	AL	MS	LA	TX	NM
Rural	7.00E-09	1.06E-08	4.22E-11	2.58E-10	1.37E-08	6.06E-09	8.73E-10	9.58E-09	3.15E-09	4.11E-09	1.68E-08	3.86E-10
Suburban	9.57E-08	1.21E-07	2.69E-08	1.12E-08	9.70E-08	5.93E-08	2.84E-09	4.82E-08	2.68E-08	2.90E-08	1.05E-07	4.13E-09
Urban	5.68E-08	1.11E-08	0.00E+00	3.52E-10	5.48E-08	6.43E-08	0.00E+00	2.03E-08	7.94E-09	9.52E-09	1.07E-07	2.17E-09
LANL	NM											
Rural	1.35E-06											
Suburban	2.39E-06											
Urban	0.00E+00											
ORNL	TN	GA	AL	MS	LA	TX	NM					
Rural	1.89E-07	8.44E-08	9.26E-07	3.04E-07	3.97E-07	1.63E-06	3.73E-08					
Suburban	3.09E-06	2.74E-07	4.66E-06	2.59E-06	2.81E-06	1.02E-05	3.99E-07					
Urban	1.21E-06	0.00E+00	1.97E-06	7.67E-07	9.20E-07	1.03E-05	2.10E-07					
SNL	NM											
Rural	9.47E-10											
Suburban	3.14E-09											

Route	Collective Dose Risk (person-rem)											
Urban	5.86E-09											
SRS	SC	GA	AL	MS	LA	TX	NM					
Rural	1.09E-07	7.11E-07	9.76E-07	4.46E-07	5.82E-07	2.38E-06	5.46E-08					
Suburban	5.90E-07	1.58E-05	8.03E-06	3.79E-06	4.11E-06	1.49E-05	5.84E-07					
Urban	0.00E+00	5.01E-06	2.88E-06	1.12E-06	1.35E-06	1.51E-05	3.07E-07					
LLNL	CA	NV	UT	ID								
Rural	4.53E-08	8.71E-08	2.39E-08	1.97E-08								
Suburban	9.63E-07	2.53E-07	3.15E-07	8.46E-08								
Urban	4.43E-06	1.39E-06	7.69E-07	4.81E-08								
NNSS	NV	UT	ID									
Rural	4.54E-09	3.27E-09	2.69E-09									
Suburban	9.82E-09	4.30E-08	1.15E-08									
Urban	0.00E+00	1.05E-07	6.56E-09									
NRD	NY	PA	WV	OH	IN	IL	IA	NE	WY	UT	ID	
Rural	1.34E-10	4.01E-10	9.14E-12	2.33E-10	1.83E-10	2.25E-10	2.85E-10	2.04E-10	1.82E-10	8.98E-11	7.92E-11	
Suburban	6.12E-10	3.26E-09	2.84E-10	3.00E-09	1.95E-09	1.13E-09	9.55E-10	6.50E-10	4.48E-10	6.29E-10	3.40E-10	
Urban	7.90E-10	1.11E-09	0.00E+00	2.24E-09	5.92E-09	2.85E-10	2.87E-10	1.10E-09	1.13E-10	3.10E-11	1.93E-10	

Figures 7-3 to 7-5 show route specific per CH shipment collective dose risks for rural, suburban, and urban links. The collective dose risks are a function of the link distance, accident rates in the states crossed by the route, and the population density along the link.

The higher collective dose risks for the rural links are associated with the rural links in Colorado (ANL, Hanford, and INL), Texas (Knolls, ORNL, and SRS), Nevada (LLNL and NNSS), and Pennsylvania (NRD). The higher collective dose risks for the suburban links are associated with the suburban links in Colorado (ANL, Hanford, and INL), Pennsylvania (Knolls and NRD), Texas (ORNL), Georgia (SRS), California (LLNL), and Utah (NNSS). The higher collective dose risks for the urban links are associated with the urban links in Colorado (ANL, Hanford, and INL), Texas (Knolls, ORNL, and SRS), California (LLNL), Utah (NNSS), and Indiana (NRD).

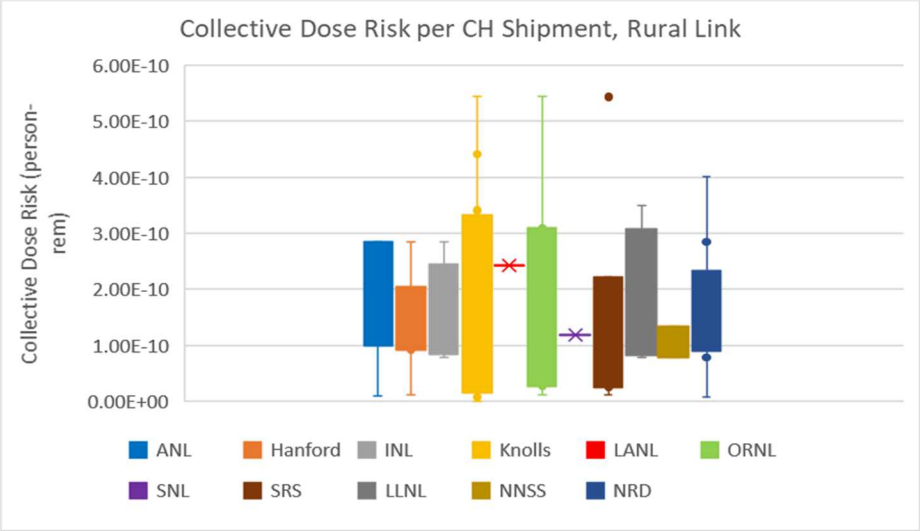

Figure 7-3. Collective Dose Risks per CH Shipment for Rural Links.

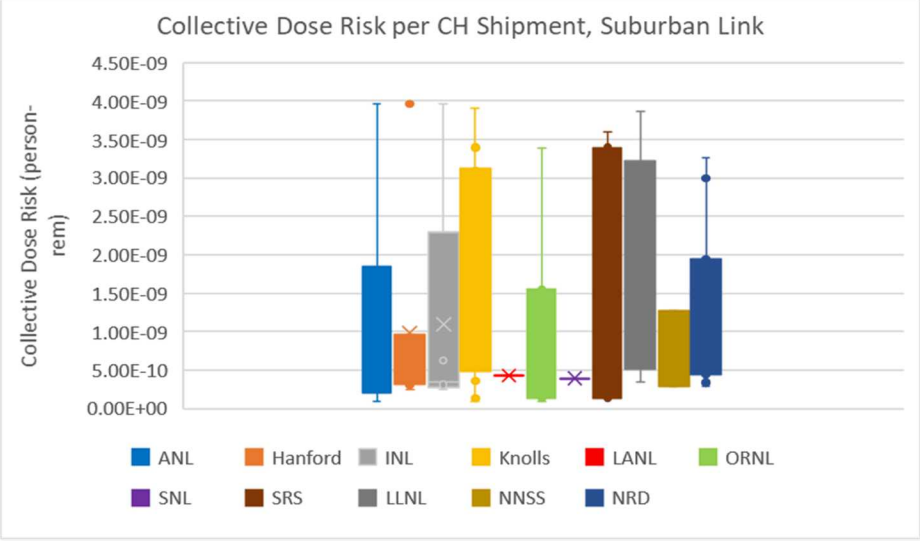

Figure 7-4. Collective Dose Risks per CH Shipment for Suburban Links.

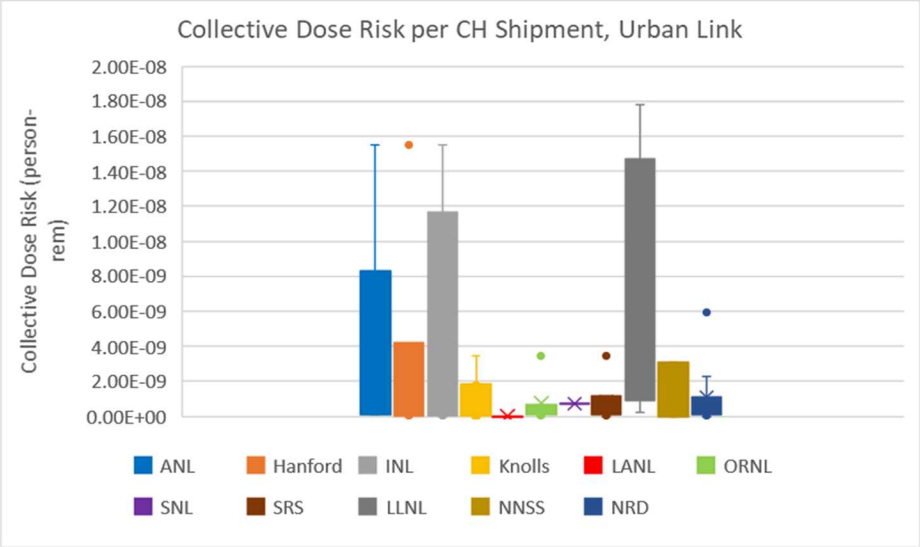

Figure 7-5. Collective Dose Risks per CH Shipment for Urban Links.

Figure 7-6 compares the collective dose risks per CH shipment calculated for rural, suburban, and urban links for all transportation routes. The collective dose risks are about one order of magnitude lower for the rural links than for the suburban links. The interquartile ranges (25th to 75th percentile) are very similar for the suburban and urban links. However, the maximum dose risk is significantly higher for the urban links than for the suburban links. The two highest values are related to the urban links in Colorado and California.

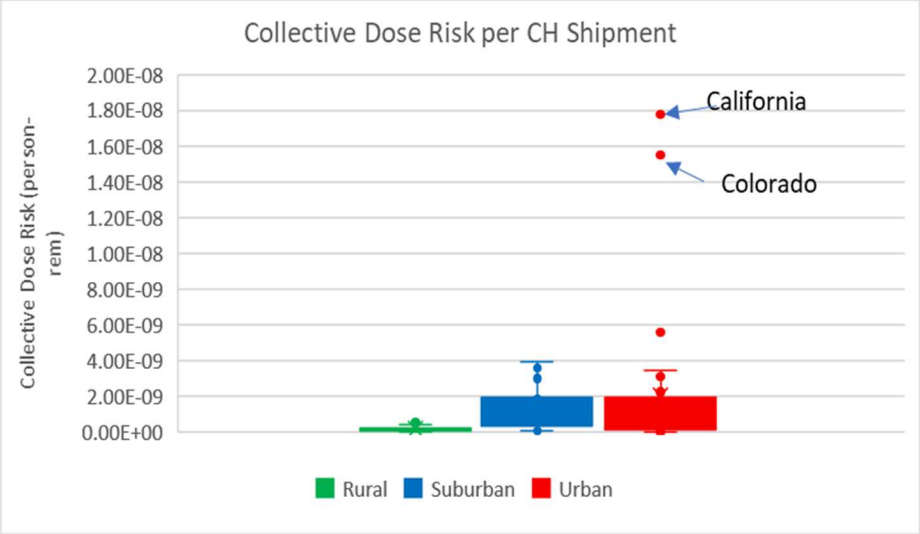

Figure 7-6. Comparison of the Collective Dose Risks per CH Shipment on Rural, Suburban, and Urban Links.

Figures 7-7 to 7-9 show route specific collective dose risks for all CH shipment for rural, suburban, and urban links. The collective dose risks are dominated by the number of CH shipments along the route. The dose risks are higher for Hanford, INL, ORNL, and SRS routes.

The Hanford route has a higher collective dose risk quartile range than the other routes for the rural links. The SRS route has the highest maximum collective dose risk value. The SRS route has a higher collective

dose risk quartile range than the other routes for the suburban links. The Hanford route has the highest maximum collective dose risk value. The INL route has a higher collective dose risk quartile range than the other routes for the urban links.

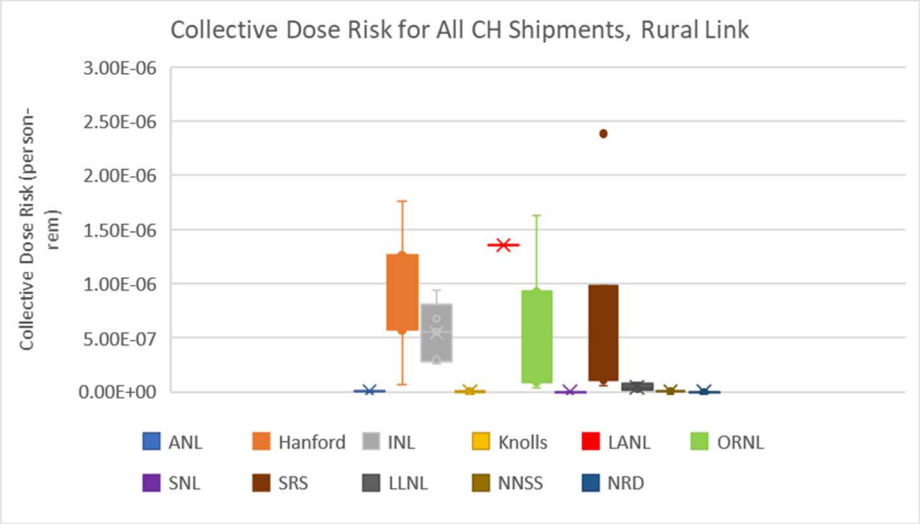

Figure 7-7. Collective Dose Risks for All CH Shipment for Rural Links.

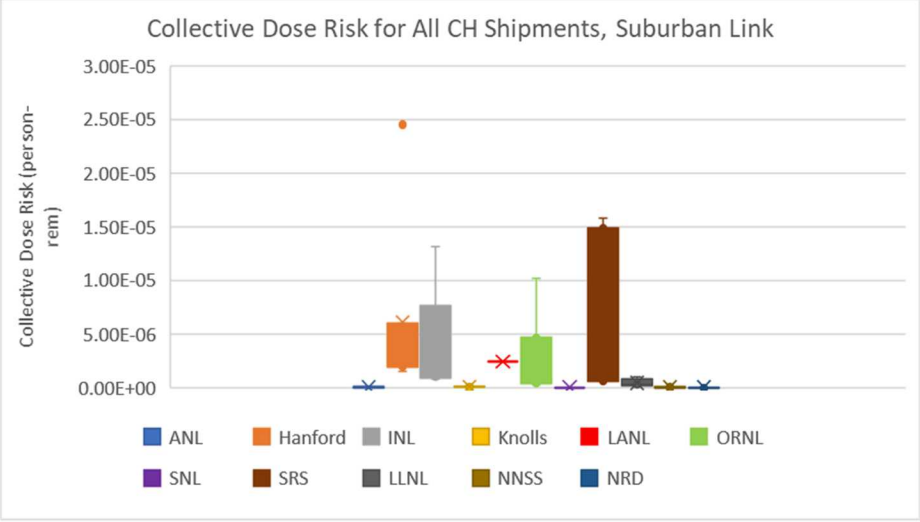

Figure 7-8. Collective Dose Risks for All CH Shipment for Suburban Links.

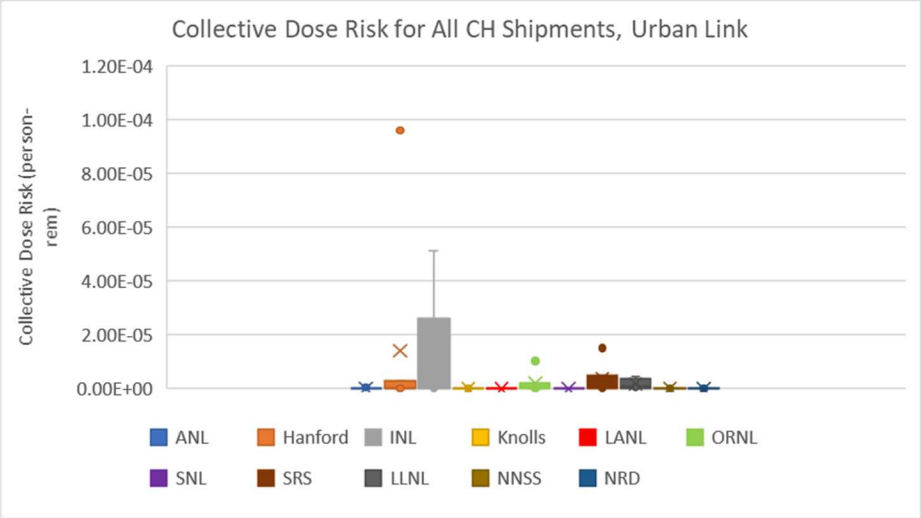

Figure 7-9. Collective Dose Risks for All CH Shipment for Urban Links.

Figures 7-10 to 7-12 compare the collective dose risks calculated in this TA and in the 2008 TA for rural, suburban, and urban links. The collective dose risks are higher, and their ranges are larger in the 2008 TA on all (rural, suburban, and urban) links compared to this TA. This is primarily related to the higher (~ one order of magnitude) curie and A_2 content (Section 6.1) and higher accident rates (Section 5). As was discussed in Section 6.5, the accident conditional probability and associated respirable fraction are higher in this TA than in the 2008 TA as well as the population density along the transportation routes.

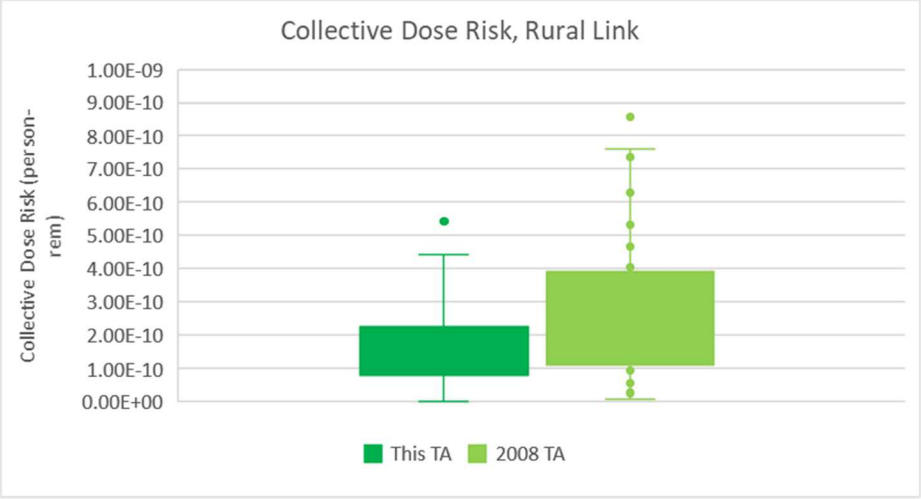

Figure 7-10. Collective Dose Risks for Rural Links in this TA and 2008 TA.

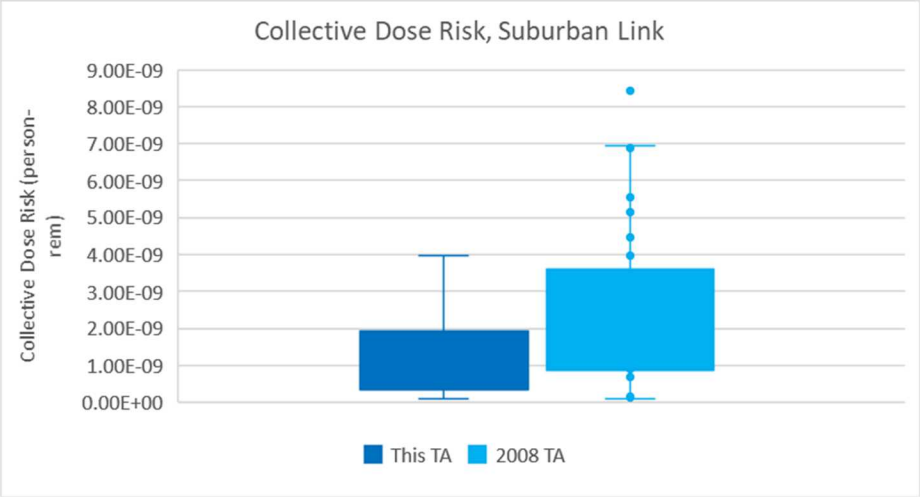

Figure 7-11. Collective Dose Risk on Suburban Link in this TA and 2008 TA.

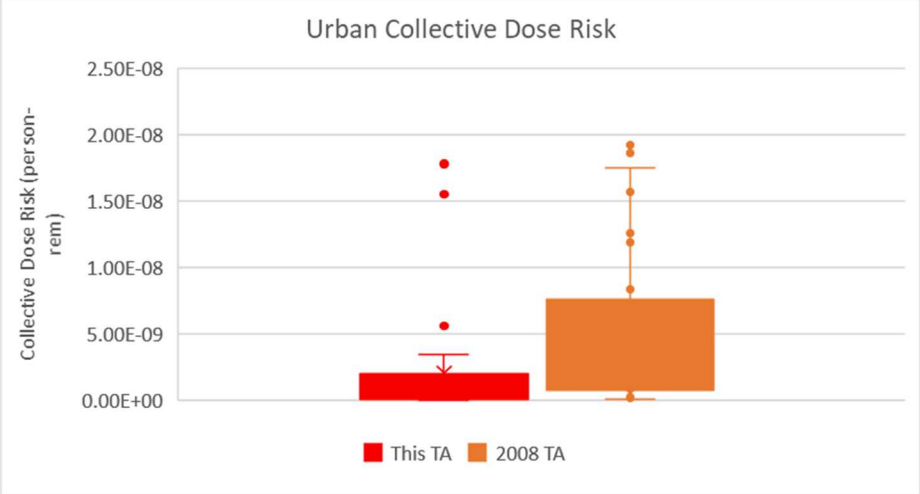

Figure 7-12. Collective Dose Risk on Suburban Link in this TA and 2008 TA.

The collective dose risks per shipment of RH-TRU Waste (second accident scenario) are summarized in Table 7-5. The collective dose risks for all RH shipments are summarized in Table 7-6.

Table 7-5. Collective Dose Risks per Shipment of HalfPACT (SCA).

Route	**Collective Dose Risk (person-rem)**						
ANL	IL	IA	NE	WY	CO	NM	
Rural	2.66E-12	5.82E-12	4.16E-12	2.19E-13	5.82E-12	4.18E-12	
Suburban	2.32E-11	1.95E-11	1.33E-11	1.98E-12	8.10E-11	4.96E-12	
Urban	1.71E-12	5.87E-12	2.25E-11	2.45E-12	3.17E-10	0.00E+00	
Hanford	WA	OR	ID	UT	WY	CO	NM
Rural	2.37E-13	3.20E-12	3.96E-12	1.88E-12	3.44E-12	5.82E-12	4.18E-12
Suburban	9.85E-12	6.39E-12	1.96E-11	1.27E-11	6.36E-12	8.10E-11	4.96E-12
Urban	2.72E-13	5.78E-13	9.04E-12	6.33E-13	3.95E-14	3.17E-10	0.00E+00

Route	Collective Dose Risk (person-rem)						
SNL	NM						
Rural	2.42E-12						
Suburban	8.03E-12						
Urban	1.50E-11						
SRS	SC	GA	AL	MS	LA	TX	NM
Rural	5.09E-13	3.31E-12	4.55E-12	2.08E-12	2.71E-12	1.11E-11	2.54E-13
Suburban	2.75E-12	7.35E-11	3.74E-11	1.77E-11	1.91E-11	6.94E-11	2.72E-12
Urban	0.00E+00	2.33E-11	1.34E-11	5.23E-12	6.28E-12	7.05E-11	1.43E-12

Table 7-6. Collective Dose Risks for All Shipments of HalfPACT (SCA).

Route	Collective Dose Risk (person-rem)						
ANL	IL	IA	NE	WY	CO	NM	
Rural	2.10E-10	4.60E-10	3.29E-10	1.73E-11	4.60E-10	3.30E-10	
Suburban	1.83E-09	1.54E-09	1.05E-09	1.56E-10	6.40E-09	3.92E-10	
Urban	1.35E-10	4.63E-10	1.78E-09	1.93E-10	2.50E-08	0.00E+00	
Hanford	WA	OR	ID	UT	WY	CO	NM
Rural	3.96E-10	5.34E-09	6.61E-09	3.14E-09	5.74E-09	9.72E-09	6.97E-09
Suburban	1.64E-08	1.07E-08	3.28E-08	2.12E-08	1.06E-08	1.35E-07	8.27E-09
Urban	4.54E-10	9.65E-10	1.51E-08	1.06E-09	6.60E-11	5.28E-07	0.00E+00
SNL	NM						
Rural	2.42E-11						
Suburban	8.03E-11						
Urban	1.50E-10						
SRS	SC	GA	AL	MS	LA	TX	NM
Rural	4.58E-12	2.98E-11	4.09E-11	1.87E-11	2.44E-11	9.99E-11	2.29E-12
Suburban	2.47E-11	6.61E-10	3.37E-10	1.59E-10	1.72E-10	6.24E-10	2.45E-11
Urban	0.00E+00	2.10E-10	1.21E-10	4.71E-11	5.65E-11	6.35E-10	1.29E-11

Figures 7-13 to 7-15 show route specific per RH shipment collective dose risks for rural, suburban, and urban links. Note that there are only four transportation routes with the shipments of 3xHalfPACTs (SCA). The collective dose risks are a function of the link distance, accident rates in the states crossed by the route, and the population density along the link.

The higher collective dose risks for the rural links are associated with the rural links in Colorado (ANL and Hanford) and Texas (SRS). The higher collective dose risks for the suburban links are associated with the suburban links in Colorado (ANL and Hanford) and Georgia (SRS). The higher collective dose risks for the urban links are associated with the urban links in Colorado (ANL and Hanford) and Texas (SRS).

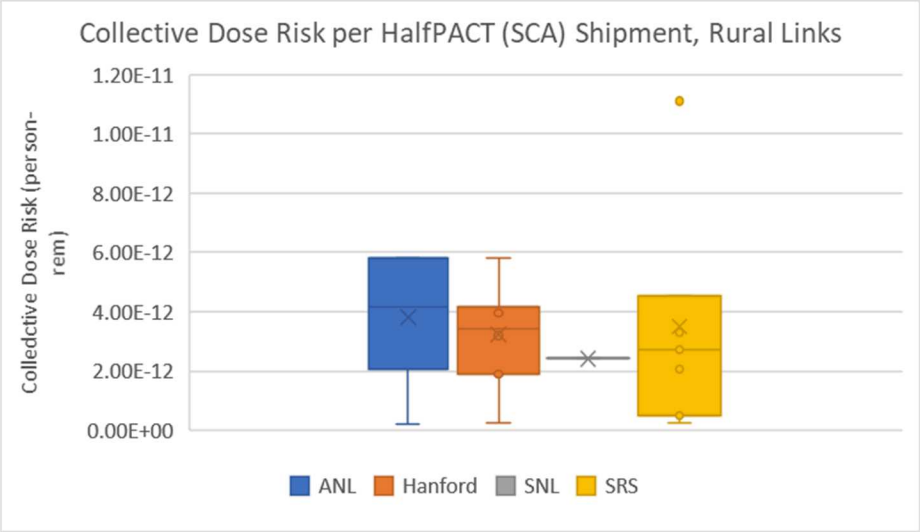

Figure 7-13. Collective Dose Risk per HalfPACT (SCA) Shipment for Rural Link.

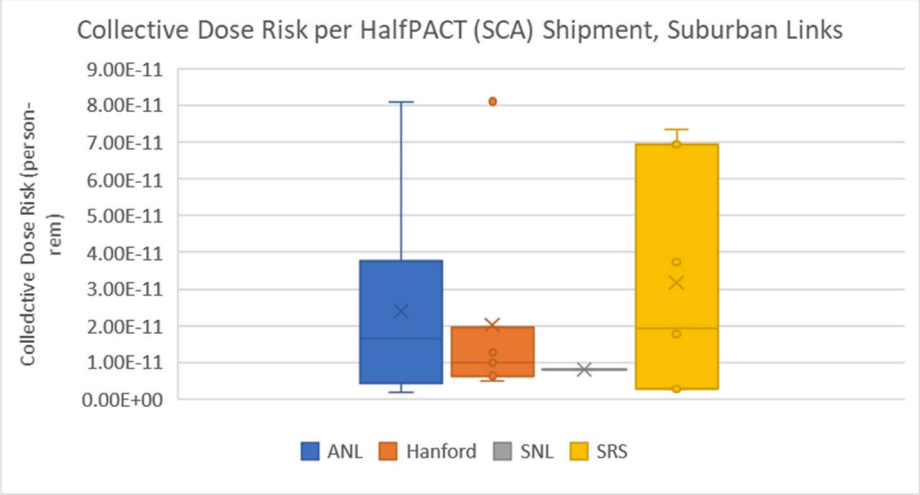

Figure 7-14. Collective Dose Risk per HalfPACT (SCA) Shipment for Suburban Link.

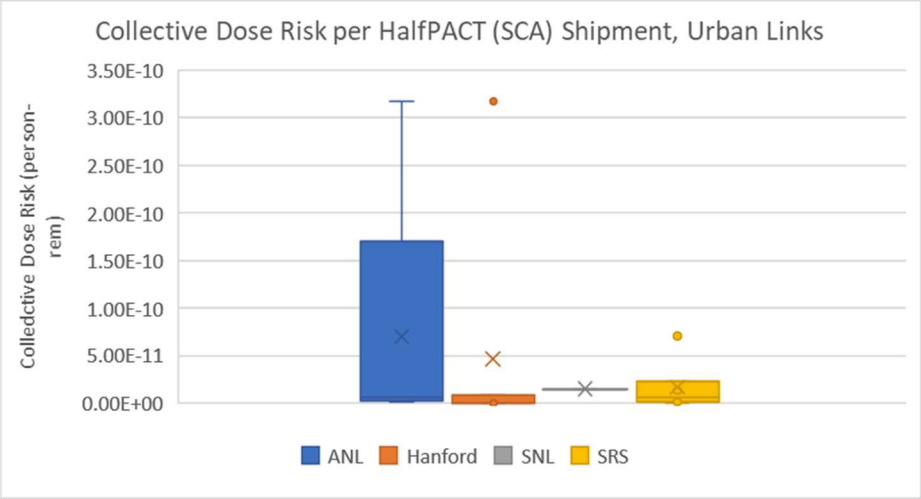

Figure 7-15. Collective Dose Risk per HalfPACT (SCA) Shipment for Urban Link.

Figure 7-16 compares the collective dose risks per RH shipment calculated for rural, suburban, and urban links for all transportation routes. The collective dose risks are the lowest for the rural links than for the suburban and urban links. The collective dose risk interquartile range is higher for the suburban links compared to the urban links. However, the maximum dose risk value is associated with the urban link in Colorado.

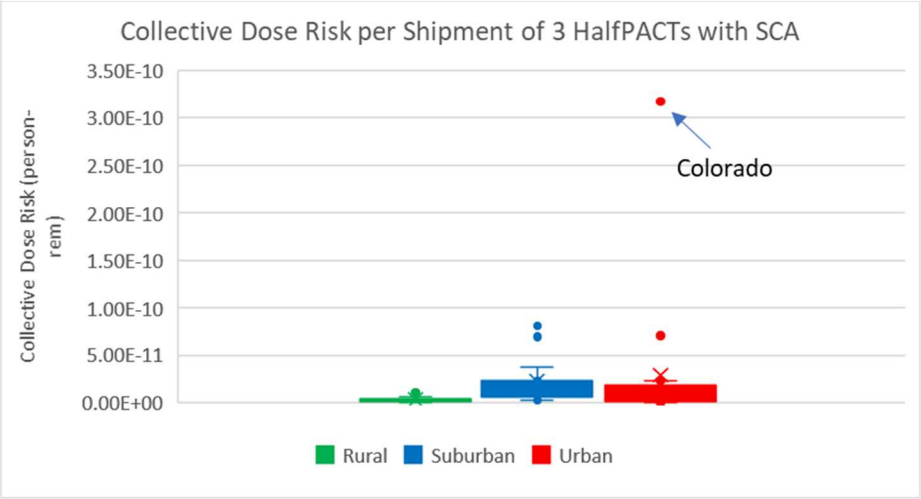

Figure 7-16. Comparison of the Collective Dose Risks per HalfPACT (SCA) Shipment on Rural, Suburban, and Urban Links.

Figures 7-17 to 7-19 show route specific collective dose risks for all RH shipment for rural, suburban, and urban links. The collective dose risks are dominated by the number of RH shipments along the route. The dose risks are highest for the Hanford route on rural, suburban, and urban links.

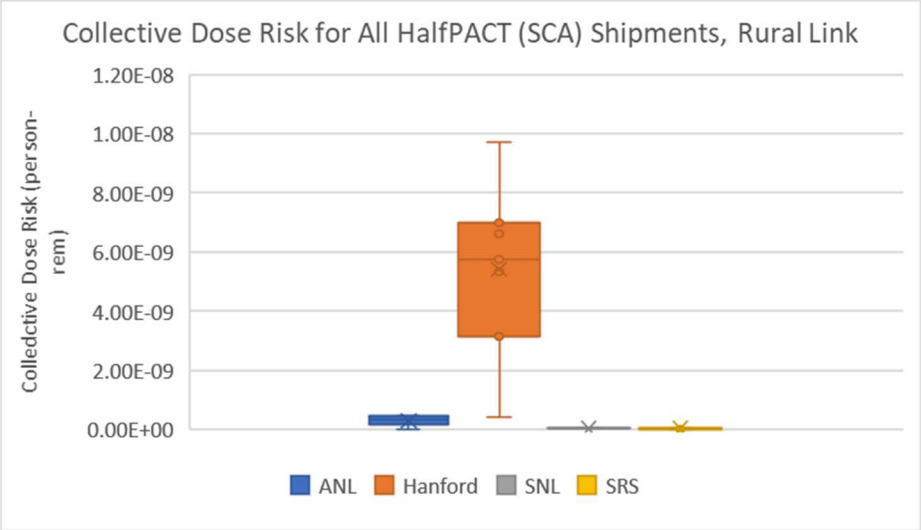

Figure 7-17. Collective Dose Risks for All HalfPACT (SCA) Shipments for Rural Links.

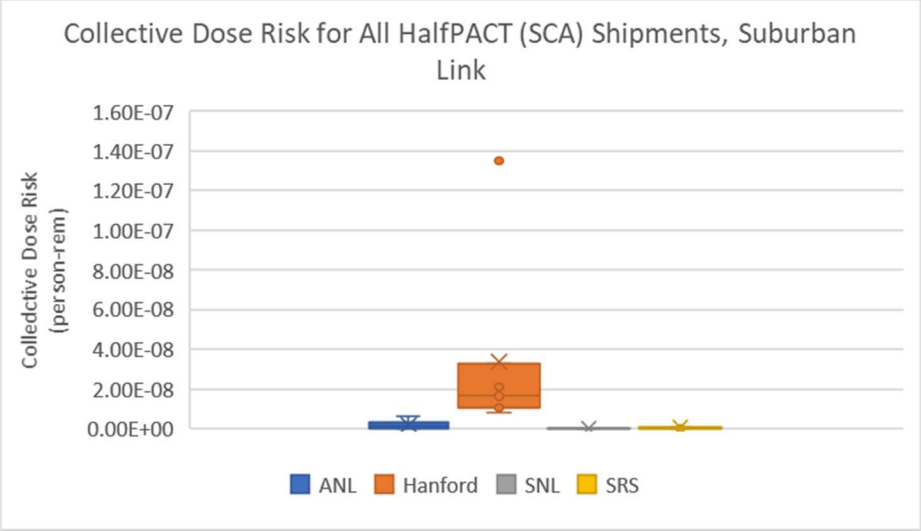

Figure 7-18. Collective Dose Risks for All HalfPACT (SCA) Shipments for Suburban Links.

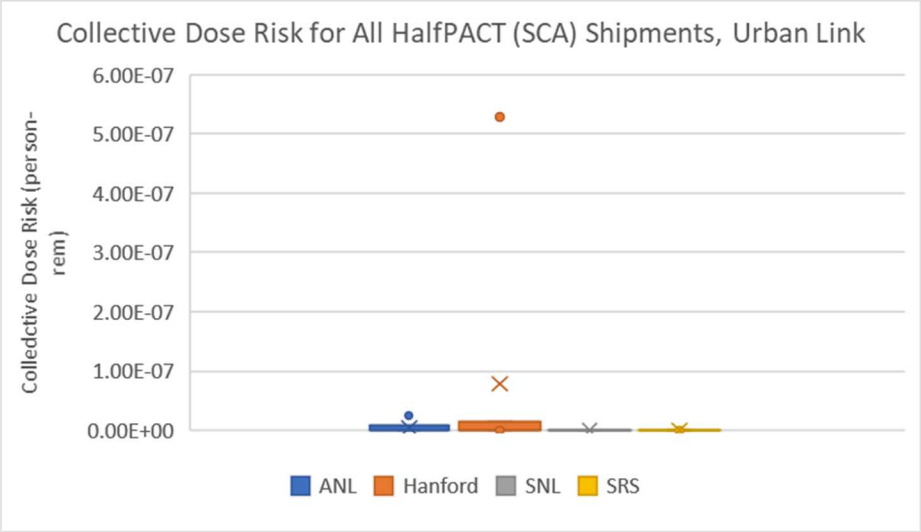

Figure 7-19. Collective Dose Risks for All HalfPACT (SCA) Shipments for Urban Links.

The comparison with the 2008 TA is not provided because the 2008 TA considered an accident with the RH-TRU 72-B. As was previously explained in Section 6.5, the probability of an accident with release of radioactive material from the RH-TRU 72-B is considered to be 0 in this TA. The RH-TRU 72-B package is similar in construction to the rail transportation casks evaluated in NUREG-2125 (NRC 2014). The analyses in NUREG-2125 showed that there would be no release from transportation casks with inner canisters under the most severe accidents analyzed.

Figure 7-20 compares average collective dose risk per CH and RH shipment. The collective dose risk per RH shipment is more than one order of magnitude lower. This is primarily due to the assumed bounding HalfPACT (SCA) inventory that has lower curie and A_2 (A_2 content is about one order of magnitude lower) content. Also, the respirable release fraction is slightly lower in an accident with the RH shipment.

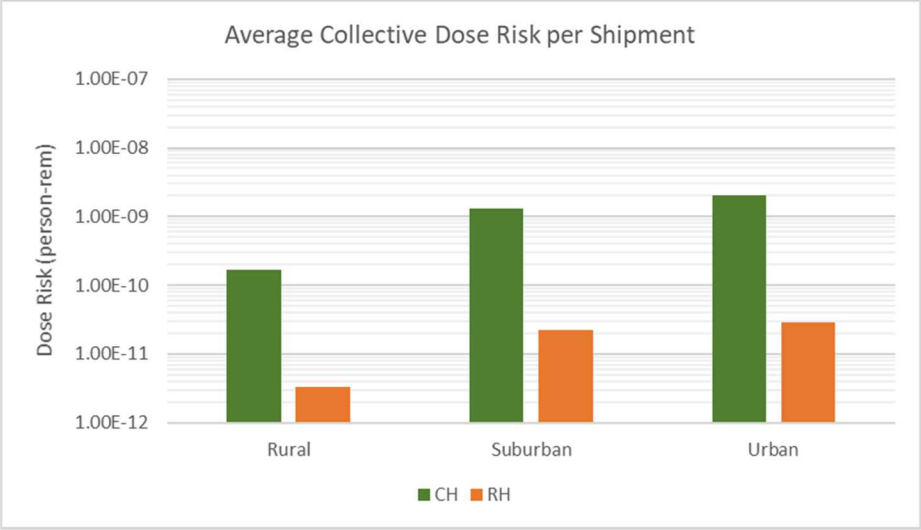

Figure 7-20. Average Collective Dose per CH and RH Shipment.

The differences between the different links can be expressed using link factor F_L [accidents-person/km^2] defined as:

$$F_L = D_L \cdot P_L \cdot p_{acc} \cdot l \qquad (7\text{-}1)$$

where D_L is the link distance (km), P_L is the population density (people/km^2), p_{acc} is the accident rate (accidents/km), and l is 1 for rural and suburban link and 2.9 for the urban link. The coefficient l was derived from the unit risk factors values (Table 7-1). The urban unit risk factor is 2.9 greater than the rural and suburban unit risk factor for both accident scenarios.

The link factors were calculated for each link and for each route. Figure 7-21 compares the maximum link factors for each route calculated with 2018 and 2040 population densities. The maximum link factor corresponds to the link with the maximum per shipment collective dose risk. The highest link factors are associated with ANL, Hanford, and INL routes (urban link in Colorado) and LLNL route (urban link in California). The maximum link factors for the other routes are significantly smaller. All maximum link factors are related to the urban links, except the suburban link in Georgia. Using the 2040 population density results in 13 – 37 percent increase in the maximum link factors.

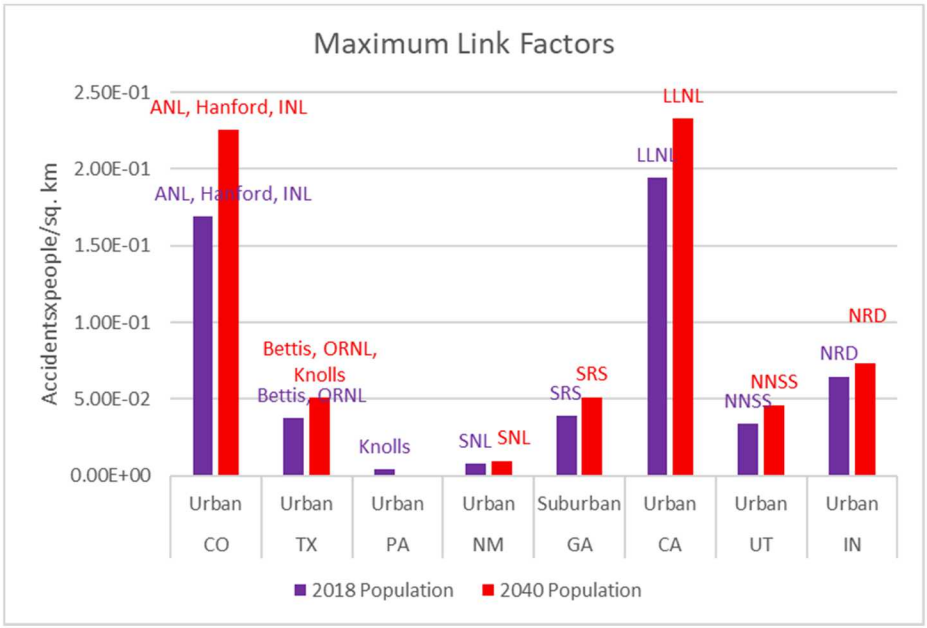

Figure 7-21. Maximum Link Factors for 2018 and 2040 Population.

Two major parameters affect the dose risk calculations. The first parameter is the respirable release fraction. The respirable release fractions used in the above calculations was based on the actual waste mass of the bounding waste streams. The maximum respirable fractions based on the maximum weight are 6.784E-05 (CH) and 1.2886E-04 (RH) (Section 6.5).

The second parameter is the population density along the transportation routes. The population density used in the above calculations was for 2018.

Higher respirable fractions and the higher population density in 2040 will result in higher per CH and RH shipment collective dose risks. To quantify these impacts, the calculations were performed using maximum respirable fractions and 2040 population density.

Figures 7-22 and 7-23 compare the results of these calculations with the results of the base case calculations in terms of the average collective dose risks for rural, suburban, and urban links. The collective dose risks per CH shipment increase by factor of 12. The collective dose risks per RH shipment increase by factor of 31. The main increase is due to the increase in the respirable release fraction by a factor of 9.8 (CH) and 24 (RH).

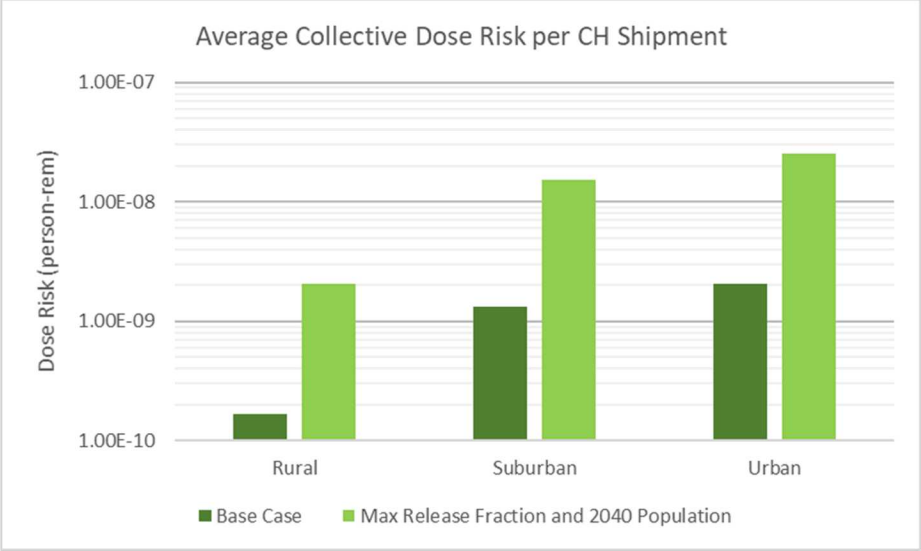

Figure 7-22. Comparison of the Average Collective Dose Risks per CH Shipment.

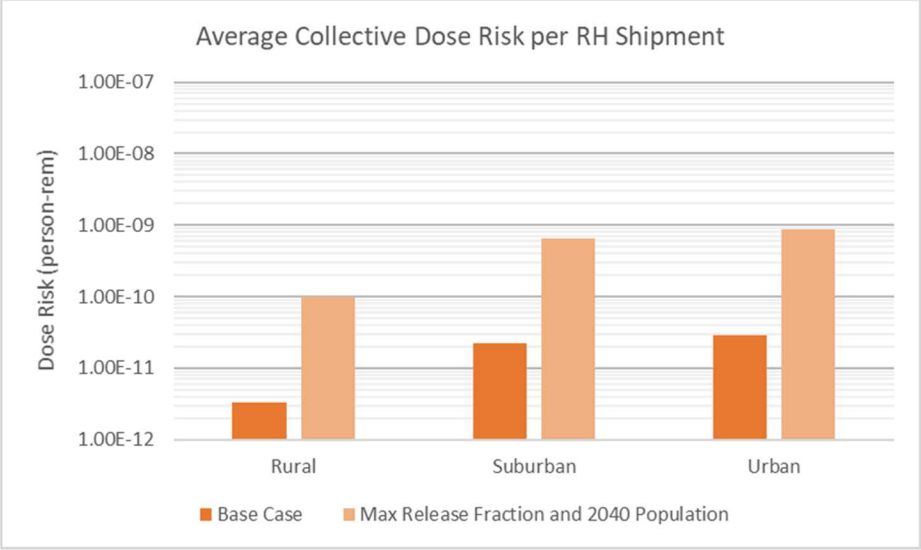

Figure 7-23. Comparison of the Average Collective Dose Risks per RH Shipment.

7.2.2 Severe Transportation Accident

The severe transportation accident analysis considers a severe accident with TRUPACT-II and a severe accident with HalfPACT (SCA). The bounding inventories and respirable fractions associated with these severe accidents as well as the RADTRAN 6.02 parameters are the same as the ones described in Section 7.1.1.

The consequences of the severe accidents are reported in terms of doses, not dose risks as was done in Section 7.2.1. The probability of these accidents was not taken into the account. This is the same approach as in the 2008 TA.

The same as in the 2008 TA, the severe accidents were assumed to occur under conditions which maximize the radiological impacts - urban area and stable meteorological conditions.

In the 2008 TA, a severe accident was postulated to occur in a non-specific large metropolitan area. The assumed population density was 2,750 persons per km^2 (Table 36 in the 2008 TA and RADTRAN input files), the largest population density of any U.S metropolitan area in 2005 based on the data from U.S. Census Bureau (2006). Note that in the beginning of Section 3.3.4.1 of the 2008 TA, the population density is shown as 2,570 persons/km^2. This is considered to be a typographical error.

In the 2010 Census, the largest metropolitan area was Los Angeles–Long Beach–Santa Ana (CA) with a population density 2,702.5 persons/km^2.

In this TA, the urban population density is defined based on the actual route data. The link with the second highest link factor (2018 population) and highest link factor (2040 population) is the urban Colorado link (Figure 7-21). Three transportation routes include this link – ANL, Hanford, and INL.

Figure 7-24 shows the population and the population density of the cities in Colorado crossed by the transportation route from the 2010 Census. The city of Denver (including Aurora and Lakewood) has the largest population and population density. Note that Colorado is also one of the fastest growing states (Section 3.2). It was assumed that the Denver metropolitan area represents an adequate proxy of a large urban metropolitan area.

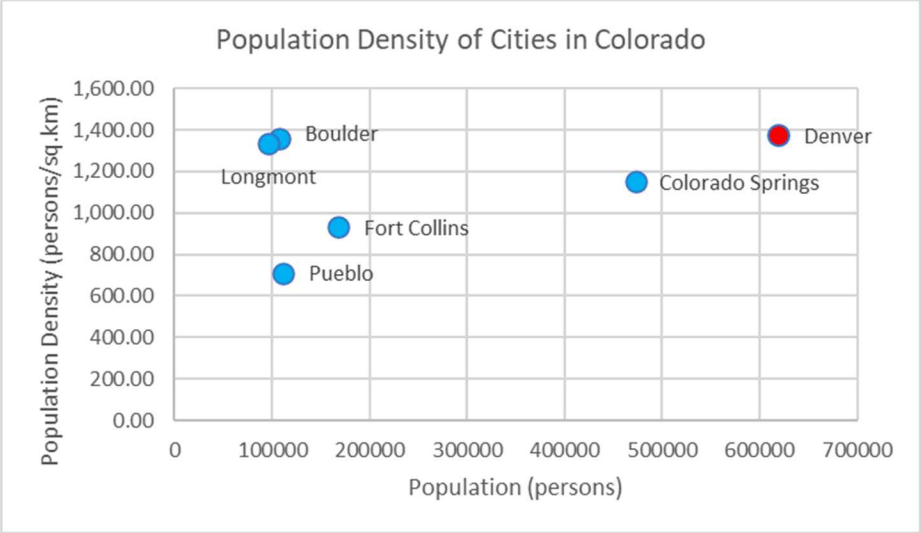

Figure 7-24. Population and Population Density of the Cities in Colorado Crossed by the Transportation Routes.

Figure 7-25 shows Denver population density from 2009 to 2018 and projected population density in 2030 assuming the same trend continues. The data are from: https://www.opendatanetwork.com. The highest metropolitan population density from the 2010 Census and from the 2008 TA are shown in this figure for comparison.

The data for Dallas are shown in Figure 7-25 because it is large metropolitan area, it is crossed by four transportation routes (Bettis, Knolls, ORNL, and SRS), and Texas is one of the fastest growing states. Dallas had two times the population of Denver (2010 Census), but lower population density. The projected population density is lower as well.

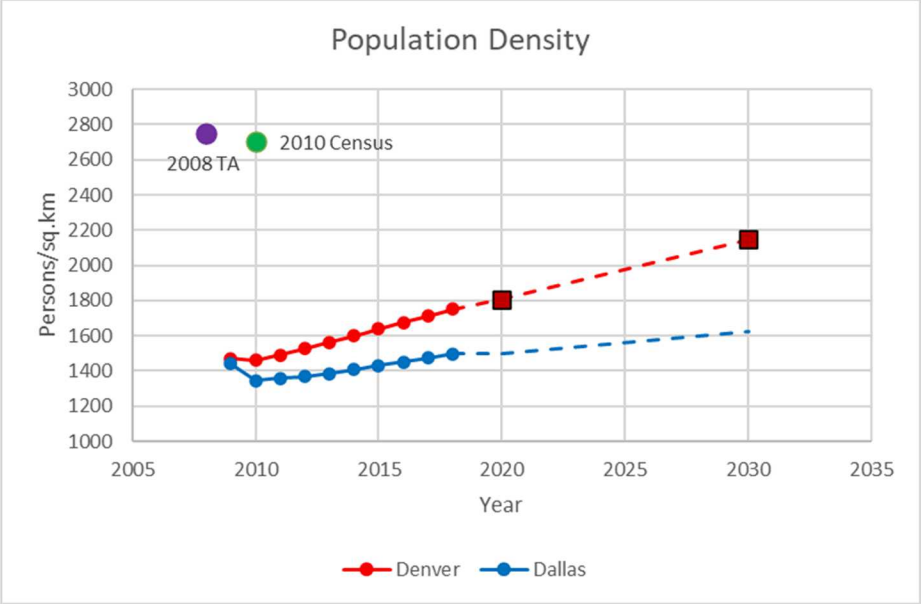

Figure 7-25. Population Density Projection for Denver and Dallas.

Figures 7-26 and 7-27 show the cities (population of 50,000 persons or more) in Colorado and Texas crossed by the WIPP transportation routes. The red markers show the cities with the census designated borders located up to 3 mi from the routes. The blue markers show the nearby cities with the census designated borders located farther than 3 mi from the routes.

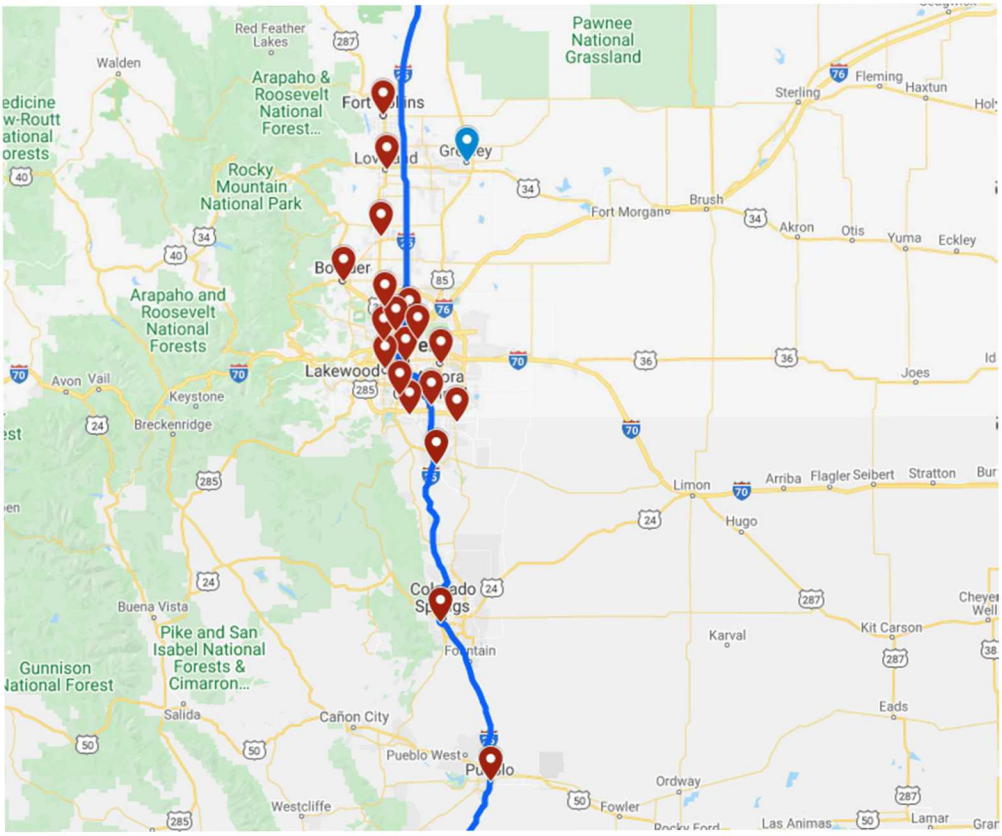

Figure 7-26. Cities in Colorado Crossed by the WIPP Transportation Routes.

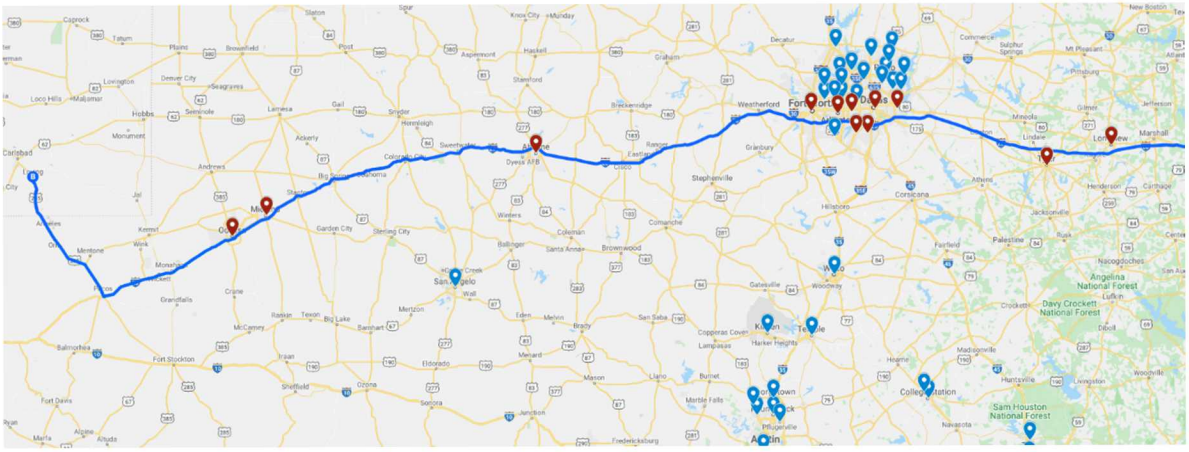

Figure 7-27. Cities in Texas Crossed by the WIPP Transportation Routes.

The population density specified for a large urban area and used in the population dose calculations was 1,808 persons/km^2 (2020) and 2,147 persons/km^2 (2030). The population doses were calculated using the urban unit risk factors in Table 7-1. The maximum exposed individual (MEI) doses are from the corresponding RADTRAN 6.02 output files. The MEI doses are independent of the population density.

Table 7-7. Consequences of Severe Accident in an Urban Area.

Receptor	Dose		LCF Risk	
	TRUPACT-II	HalfPACT (SCA)	TRUPACT-II	HalfPACT (SCA)
	2020 Population			
Population Dose (person-rem)	240.5	4.91	0.14	2.95E-03
MEI dose (rem)	5.91	0.121	3.55E-03	7.26E-05
	2030 Population			
Total Dose, person-rem	285.55	5.83	1.71E-01	3.5E-03
MEI dose, rem	5.91	0.121	3.55E-03	7.26E-05
	2008 TA			
	TRUPACT-II	RH-TRU 72-B	TRUPACT-II	RH-TRU 72-B
Total Dose, person-rem	2.89	92.8	1.73E-03	5.57E-02
MEI dose, rem	0.17	3.14	1.01E-04	1.88E-03

Also provided in Table 7-7 are the doses from the 2008 TA. Note that the 2008 TA assumed a severe accident with RH-TRU 72-B. In this TA the probability of such an accident is considered to be 0 as described in Section 6.5 and reiterated in Section 7.2.1.

The doses are higher in this TA mainly because of the higher respirable fraction. The particulate respirable fraction in the 2008 TA was 1.00E-07. The 2008 TA assumed that the respirable fraction was the same as in an accident with a SNF transportation cask. A SNF cask and its content (SNF assemblies) are very different from the TRUPACT-II and its content. Data for release fractions from a TRUPACT-II subjected to an extra-regulatory accident were not available in 2008. The respirable fraction calculated in this TA was 6.89E-06. It was calculated for the TRUPACT-II specific waste based on the results of modeling TRUPACT-II integrity in extra-regulatory accidents. The MEI doses in both severe accidents scenarios are smaller than the maximum annual occupational dose recommended in 10 CFR Part 835 (5 rem).

Figure 7-28 compares MEI doses versus distance from the source for a severe accident with TRUPACT-II and HalfPACT (SCA) and a severe accident with RH-TRU 72-B (2008 TA). In all the cases, the doses are very small at distances greater than 350 m from the source.

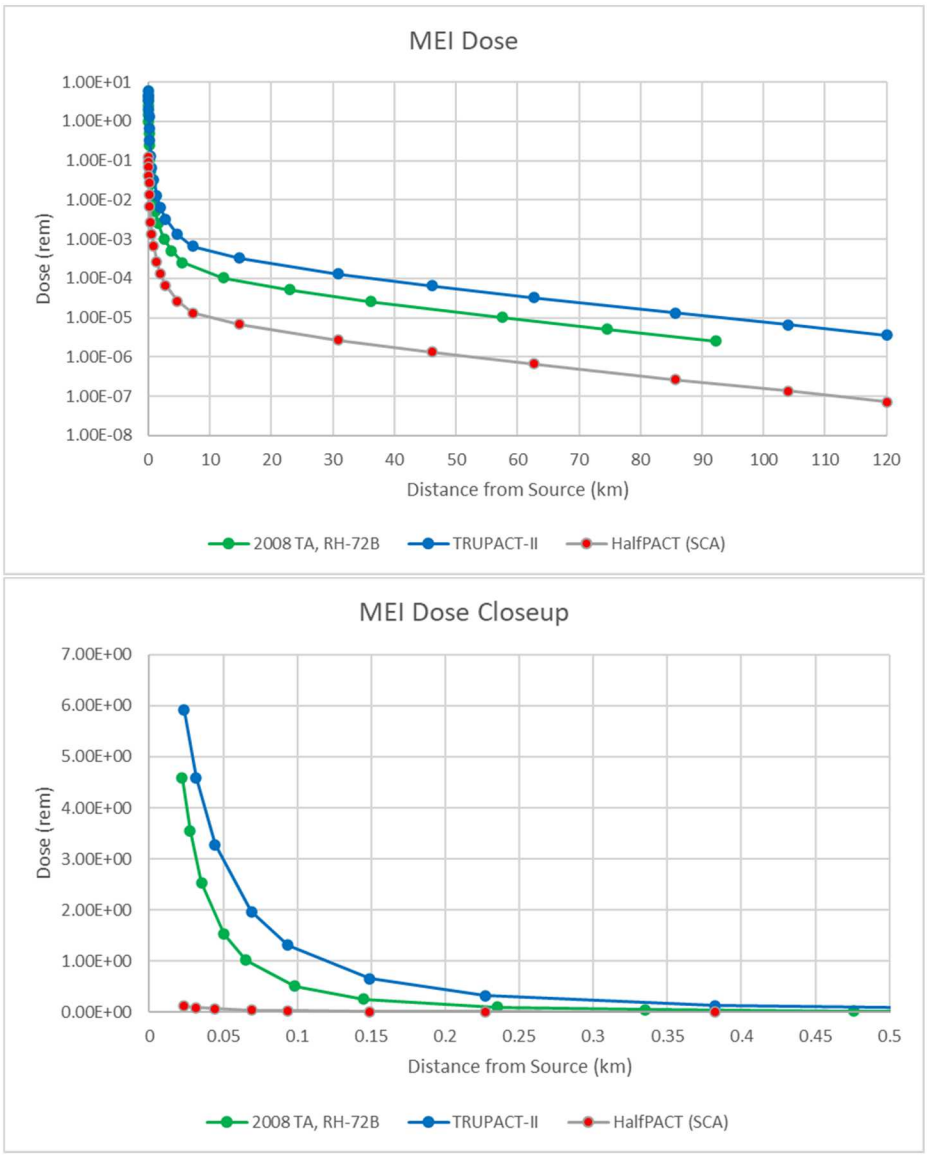

Figure 7-28. MEI Dose as a Function of Distance from the Source.

7.2.3 Transportation Accidents without Release of Radioactive Materials

The conditional probability of an accident that does not result in release of radioactive materials is 0.999998 (Section 6.5). It was assumed that if such an accident occurs, a truck with the radioactive cargo will sit at the place of the accident or in its vicinity for many hours and will be a source of external radiation. This is the same assumption as in the 2008 TA. The time required to clear the accident was assumed to be 10 hours, the same as in the 2008 TA.

The accident was assumed to happen in a large metropolitan area. The population density in this area was assumed to be the same as in the case of a severe accident (Section 7.2.2). Two cases were considered – one with 2020 and another with 2030 population density. The population was assumed to be at a distance from 30 to 800 m from the source and the MEI was assumed to be at a distance of 30 m from the source (same as in the 2008 TA). No credit was taken for shielding (shielding factor equal to 1). The doses to the

population and to the MEI were calculated using the unit risk factors defined in Table 7-2. Table 7-8 summarizes the results of these calculations. The doses calculated in the 2008 TA are provided in this table for comparison.

The population doses calculated in this TA for 1xHalfPACT&2xTRUPACT-II shipment are slightly lower than in the 2008 TA. The population doses calculated in this TA for 1xRH-TRU 72-B shipment are noticeably lower than in the 2008 TA. The lower population doses are due to the lower population density. Examining the 2008 TA RADTRAN input file revealed that the population distance from the source was from 1 to 15 m (not 30 to 800 m) and the population density was 9,950 persons/km^2. This resulted in the higher calculated doses.

Table 7-8. Population and MEI Doses for an Accident without Release.

Shipment Type	Population Dose (person-rem)			MEI Dose (rem)	
	Population Density		2008 TA	This TA	2008 TA
	2020	2030			
1xHalfPACT&2xTRUPACT-II	4.01E-03	4.76E-03	4.95E-03	1.19E-04	9.69E-05
3xHalfPACT (RH)	1.63E-02	1.94E-02		4.86E-04	
3xTRUPACT-II (CCO)	2.29E-02	2.72E-02		6.82E-04	
1xTRUPACT-III	2.39E-03	2.83E-03		7.12E-05	
1xRH-TRU 72-B	1.22E-02	1.44E-02	2.15E-02	3.61E-04	2.26E-04

Figure 7-29 shows the MEI doses for the different types of shipments as well as the 2008 TA MEI doses. The MEI doses are independent of the population density. The MEI dose from the shipment of 1xHalfPACT&2xTRUPACT are very similar in this TA and the 2008 TA. The MEI dose from RH-TRU 72-B shipment is somewhat higher in this TA because a higher TI index was assumed.

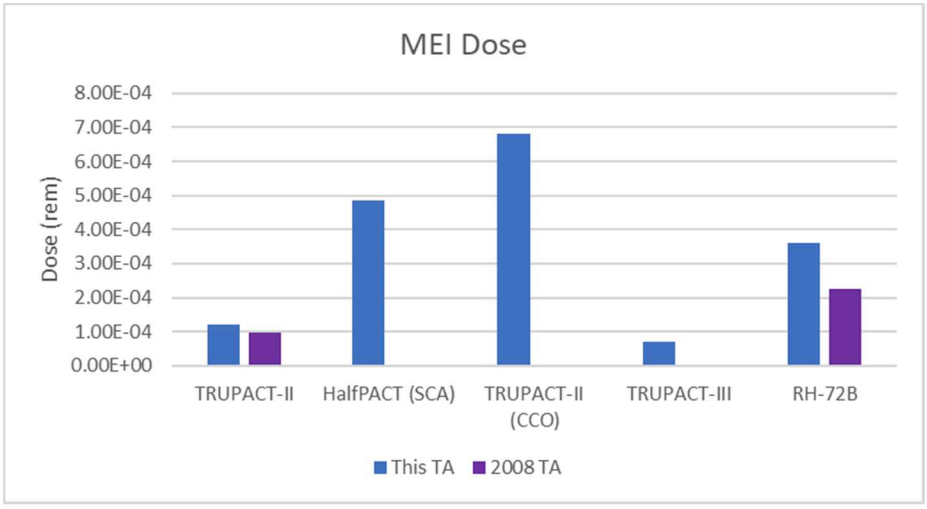

Figure 7-29. MEI Doses for An Accident without Release.

8. SUMMARY

The goal of this TA was to evaluate the impacts associated with the transportation of TRU waste from waste generator sites to the WIPP facility (direct routes) and from waste generator sites to INL (indirect routes). Twelve routes, including nine direct routes and three indirect routes, were considered in this TA.

This TA is an update to the 2008 TA (Weiner and Dunagan, 2009). The update uses more recent input data. In addition, accident scenario parameters were developed based on modeling that was not available in 2008. The TA results are presented in a format similar to the results in the 2008 TA. The results are also compared to the corresponding 2008 TA results and the differences are explained.

The following sections provide a summary of the input data, results, and findings.

8.1 Input Data

A large amount of data was collected and analyzed to develop the input parameters for the radiological and non-radiological impact evaluation.

Some transportation routes changed since 2008, some were terminated, and some did not exist at that time. The updated (or new) routes were generated using WebTragis and route specific data including the population density within 800 m (2,625 ft) of the highway were obtained (Section 3.1).

The population densities in WebTragis are based on the 2010 Census data. Data on state specific population increase since 2010 to 2018 (most recent available) were collected and used to adjust the population densities. In addition, estimated change in population multipliers were developed for 2030 and 2040 (Section 3.2). These data were used in the sensitivity analysis.

The most recent state specific traffic count data were collected and analyzed to obtain state specific averages of the number of vehicles per hour (Section 3.3).

The most recent data on the state specific number of accidents, injuries and fatalities and miles traveled for large trucks was collected. These data were used to derive state specific accident, injury, and fatality rates in the form of incidents per vehicle-km (Section 3.4). Note that in the 2008 TA the injuries were not considered, and the national fatality rate was used for all states.

The annual number of shipments by package type was estimated for each generator site in Attachments D and E of WIPP Nuclear Waste Partnership (2020). This information was used to define the number of shipments for each waste type and site for the duration of the transportation campaign (Section 3.5). This included the shipments of CCOs with surplus plutonium that were not considered in the 2008 TA.

The transportation index values (TIs) were derived from analysis of the actual data (measured TIs) of the WIPP shipments from the beginning of the transportation campaign through October 4, 2019. The 50^{th}, 75^{th}, and 95^{th} percentile TI values were developed for each shipment type (Section 3.6). The 95^{th} percentile TI values were used in the base case and the 50^{th}, 75^{th} percentile values were used in the sensitivity analysis. The TIs in the 2008 TA were based on modeling. The values for TRUPACT-II and RH-TRU 72-B in the 2008 TA correspond to the 80^{th} and 91.5^{th} percentiles of the measured data respectively.

The updated inventory as of December 31, 2018, which includes about 6MT of surplus, non-pit plutonium and about 42.2MT of surplus pit plutonium (included in the WIPP inventory so that potential impacts can be estimated) was analyzed to derive bounding radionuclide compositions for the different types of

packages) (Section 6.1). To develop a bounding source term, both the Ci and A_2 contents of all WIPP-bound CH and RH waste streams were analyzed. The selected bounding waste streams correspond to the 99^{th} percentile of the A_2 content and 90^{th} (CH) and 80^{th} (RH) percentile of the Ci content. It was concluded that a TRUPACT-II with 14 55-gal drums containing waste stream SR-LA-PAD1 represents the bounding case for a transportation accident with a CH shipment. A HalfPACT with 3 30-gal shielded containers containing waste stream SA-W139 represents the bounding case for a transportation accident with RH-TRU waste. A bounding waste stream was identified for the RH-TRU 72-B. However, it was concluded that in case of an accident with a RH-TRU 72-B shipment, the probability of release of radioactive materials is zero because no credible accident will cause this package to fail. Note that Ci and A2 contents of the bounding CH and RH wastes assumed in the 2008 TA are higher than the maximum Ci and A2 contents of the WIPP-bound waste streams. The 2008 TA also considered an accident with a shipment of RH-TRU 72-B.

The accident scenario parameters, such as the conditional probabilities of the accidents that result in breach of a package and release of a fraction of the package inventory were developed based on the modeling of extra regulatory accidents. The structural finite element model was developed to simulate the behavior of TRUPACT-II when it impacts an unyielding target at different velocities (Section 6.2). Three analyses (top, side, and upper corner impacts) were conducted at the regulatory velocity of 30-mph for model calibration and validation purposes. The results were compared to the HAC test results from the TRUPACT-II Safety Analysis Report (the certification free drop tests). The deformation obtained with the model is in a good agreement with the test results. Four analyses were conducted at extra-regulatory velocities – 45 and 60-mph. It was demonstrated that the inner containment vessel (ICV) has a potential to breach only in the case of a corner impact at a velocity of 60-mph where a large number of foam elements are removed from the analysis due to extreme distortion during the impact. Note that the ASME strain-based criteria used to define the failure is conservative and overestimates this potential. The modeling capabilities to perform such analysis within reasonable cost and schedule did not exist in 2008. Five accidents of different severities with release of radioactive materials were considered in the 2008 TA based on data from finite element analyses of spent nuclear fuel (SNF) casks from NUREG/CR-6672 (Sprung et al. 2000) which are structurally very different from TRUPACT-II.

The corner impact at 60-mph onto an unyielding target was compared to impacts into different yielding targets using an equivalent velocity approach. This analysis demonstrated that the only feasible real targets that could cause leakage of a TRUPACT-II are hard rock and large columns. An impact velocity greater than 60-mph is required to generate the equivalent amount of kinetic energy in the case of other yielding targets. The probability of an accident with release of radioactive materials was calculated based on the event tree in Mills et al. (2006) (Section 6.5). However only the corner accidents at 60-mph or greater involving hard rock and large columns were considered.

A thermal model of TRUPACT-II was developed to analyze an accident involving fire (Section 6.4). A radiation boundary condition assumed 850°C which is slightly higher than the 800°C regulatory boundary condition to account for additional heat that could be imparted to the package from natural convection. The modeling results demonstrated that even the peak temperature is below the 8-hour duration temperature limit, and the temperature of the O-rings exceed the continuous use temperature for less than 8 hours. From this analysis it can be concluded that there is no risk of the TRUPACT-II losing containment due to a fire accident. Note that the thermal modeling was not performed at the time of the 2008 TA and it was assumed that an accident with fire may result in a release of radioactive materials.

Respirable release fractions were calculated for an accident with a TRUPACT-II and a HalfPACT with shielded containers using the approach from Sprung et al. (2000) and DOE (1994) (Section 6.5). The waste was considered to be a brittle solid material. Three impact velocities were evaluated, 60-mph, 90-mph, and 120-mph. Note that the respirable release fractions derived in this TA are noticeably higher than in the 2008

TA. The 2008 TA release fractions are based on data for SNF assemblies from NUREG/CR-6672 (Sprung et al. 2000).

8.2 Results

The results include radiological impacts from incident-free transport, non-radiological impacts, and radiological impacts from transportation accidents. The results are conservative because they were obtained with conservative input parameters and conservative models. The actual impacts associated with the transportation of TRU waste will be lower than the impacts reported in this TA. The major conservative assumptions in the input parameters and models are summarized below.

- The 95th percentile values were used for the package TIs (dose rate at 1 m from the package). Thus, 95 percent of the packages will have TIs smaller than the TIs assumed in the base case. The collective and individual doses in incident-free transportation are directly proportional to the package TIs. Using 95th percentile values results in overestimating the radiological impacts in incident-free transport.

- The package inventories (radionuclide composition) considered in the accident analysis corresponded to the 99.5th (CH TRU) and 99.99th (RH-TRU) percentile A_2 (measure of radiological toxicity) and 99th (CH TRU) and 96.4 (RH TRU) percentile Curies. This means that the consequences of an accident with release of radioactive material will be smaller than calculated for 99.5 percent (CH TRU) and 99.99 percent (RH TRU) of the packages.

- The radiological impacts in the incident-free transport and in transportation accident with release of radioactive material were calculated for rural, suburban, and urban links for each state crossed by the transportation route. Only one rural, suburban, and urban segment within each state was assumed (multiple segments were combined into one) with the corresponding aggregated population. This approach results in overestimating the population density and thus, the radiological impacts.

- An accident with release of the radioactive material was assumed to occur under stable meteorological conditions (higher radionuclide activities within the plume due to smaller dispersion) which maximizes the radiological impacts.

- The conservative assumptions in the structural finite element impact model of TRUPACT-II used to simulate the extra-regulatory accidents lead to predicting higher loads and stresses. In addition, using the ASME strain-based failure criterion resulted in an over prediction of containment failure under conditions where it may not occur. Consequently, assuming a release of radioactive material from a TRUPACT-II in any extra-regulatory accident is conservative.

8.2.1 Radiological Impacts from Incident-Free Transport and an Accident without Release of Radioactive Materials

The radiological impacts from incident-free transport include radiation exposures to the general public (along the transportation route, sharing the road, and people at refueling stations and residents near refueling and other stops), transportation workers (crew while the truck is moving and during stops), refueling station employees, site and state border inspectors, and for a hypothetical person in a traffic jam next to the WIPP truck with cargo. The radiological impacts from a transportation accident without release of radioactive materials include exposure to the residents near the place of an accident and a maximum exposed individual

(MEI), a person that happened to be near the accident. An accident without release is treated as a long duration stop.

The results are reported in terms of collective doses (persons-rem) when multiple persons are exposed or doses (rem) when an individual is exposed. This is because the estimated probability of the incident-free transport is 99.91 percent. The incident-free transport collective/individual doses were calculated for each type of shipment for each transportation route and for all shipments along each transportation route, except the scenarios in which an individual is exposed only to a portion of all shipments. The accident without release collective/individual doses were calculated assuming that one accident occurs in a highly populated urban area. The results are presented in a similar format to the one in the 2008 TA.

The sensitivity analysis was performed to evaluate the impacts from population increase (from 2018 to 2030 and 2040), higher traffic count during rush hour, larger suburban and urban areas affected by rush hour traffic, different exposure duration during refueling stops and inspection, and different TI values (50^{th} and 75^{th} percentiles). In the bounding sensitivity case, the collective dose increased by 41 percent to residents along the route, by 109 percent to people sharing the route, and by 2 percent to the truck crew. If the 75^{th} percentile TI values are used, the collective doses decrease by 21-23 percent for CH shipments and by 73-86 percent for RH shipments.

Figure 8-1 shows the annual collective doses for each type of shipment. For incident-free transport these doses were calculated by dividing the total collective dose from all the shipments of each type along all the transportation routes by the duration of the transportation campaign. For an accident without release, these doses were calculated using the accident rate (~ 0.5 accident per year one way) from the non-radiological impact assessment. The maximum annual collective dose is 4 person-rem. This includes multiple persons the number of which is different in the different exposure scenarios. Note that the maximum annual individual occupational dose is limited to 5 rem (10 CFR Part 835).

The collective doses are higher for people sharing the route and these doses are more affected by the scenario parameters considered in the sensitivity analysis. The second highest are the collective doses to people at refueling stops. The collective dose contributions are smaller for people residing along the transportation routes and people residing near the stops. The collective doses calculated in this TA are slightly higher than in the 2008 TA. This is due to the difference in routes, increase in population density of the people residing along the routes, additional stops not considered in the 2008 TA, and differences in the state-specific vehicle densities. The differences are smaller than the differences due to the uncertainties in the input parameters. The collective doses calculated for an accident without release are significantly lower than the collective doses calculated for incident-free transport because this dose includes the small probability of an accident.

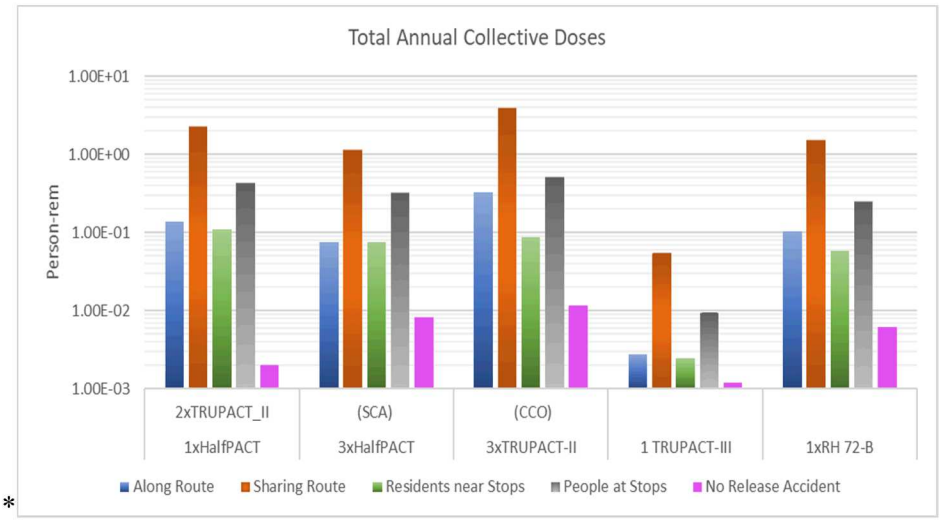

*

Figure 8-1. Total Annual Collective Dose for Different Types of Shipments.

Figure 8-2 shows the number of persons exposed in the base case and in the bounding sensitivity case scenarios. In calculating the number of persons residing along the transportation route and near stops it was assumed that each year during the campaign there will be a 10 percent change in the individual residents. In calculating the number of persons sharing the route it was assumed that 10 percent of the persons sharing the route with one shipment will share the route with other shipments. It was assumed that the persons at refueling stops are always different. The largest exposed population category is the persons sharing the route with the WIPP shipment. The increase in the number of exposed persons in the bounding sensitivity case is small (4 -24 percent) for all categories except for people at refueling stops (100 percent).

The average individual doses shown in Figure 8-3 were calculated by dividing the campaign total collective dose by the number of exposed persons in each exposure category. The average individual doses are shown for the base case and for the bounding sensitivity case scenarios. The doses are very small and reflect the number of exposed persons in the different exposure categories. The increase in the average individual dose in the bounding sensitivity case is small (less than 17 percent) for all categories except for people sharing the route (113 percent).

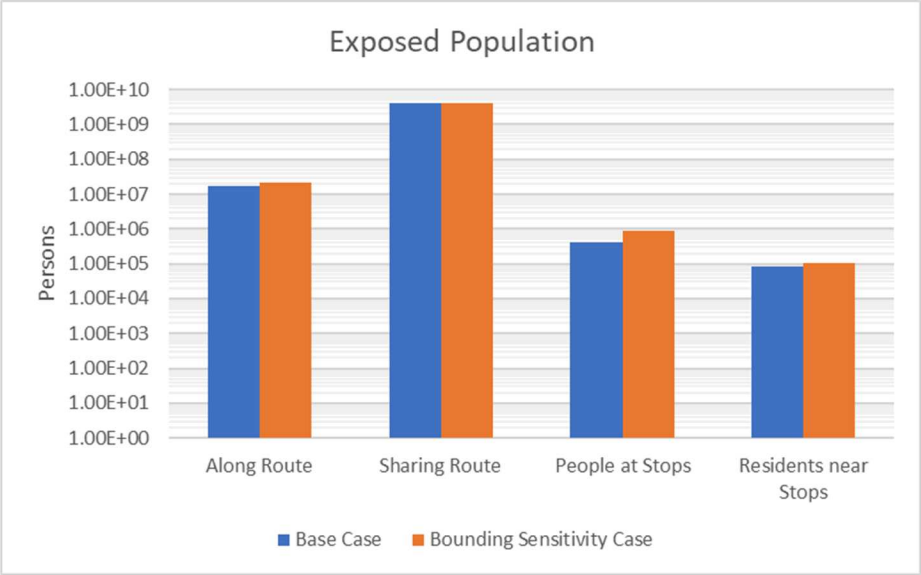

Figure 8-2. Number of Exposed People in Different Exposure Categories.

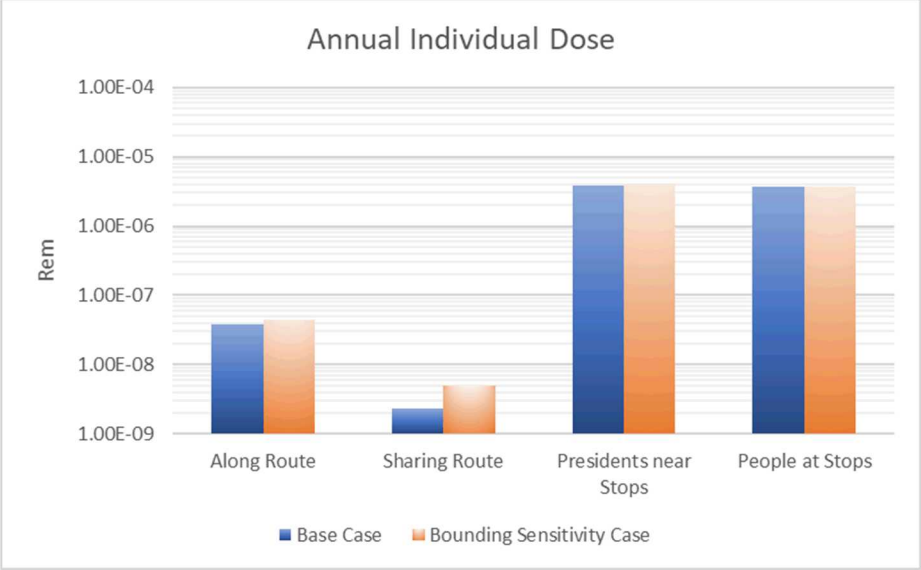

Figure 8-3. Average Individual Doses for the Different Exposure Categories.

Figure 8-4 shows the maximum annual individual doses for various receptors in the incident-free scenarios and a receptor (maximum exposed individual) in the accident without release of radioactive material scenario. The doses to an individual in a traffic jam and a MEI in the accident without release scenario are one-time exposures. Also shown in this figure are the maximum allowed occupational dose and the average annual individual background dose. The calculated annual individual doses are below the average annual individual background dose.

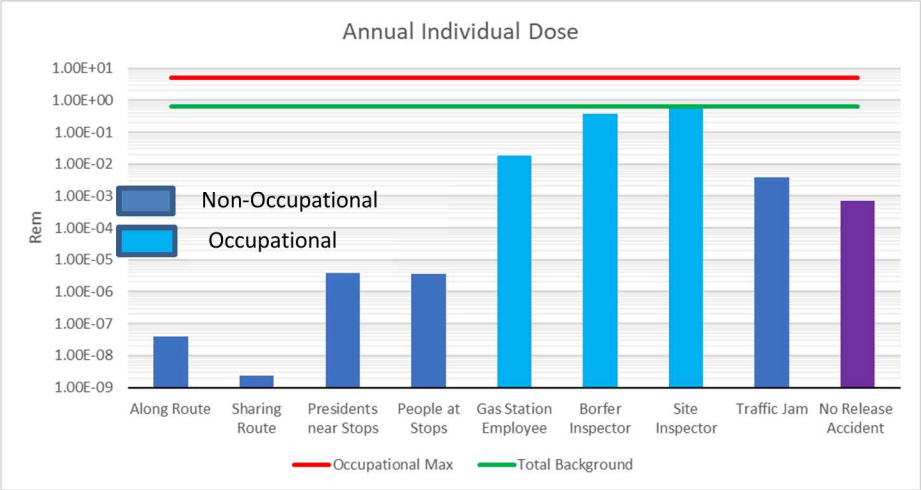

Note: Total annual background dose is the sum of the natural and man-made background doses (NCRP No. 160).

Figure 8-4 Annual Individual Doses for Incident-Free and Accident without Release Scenarios.

8.2.2 Non-Radiological Impacts

The non-radiological impacts per shipment and per campaign for each route were calculated using the same approach as in the 2008 TA. They are expressed in the form of an aggregate number of accidents, injuries, and fatalities likely to occur as a result of transporting the TRU waste packages round trip between generator sites and the WIPP facility and between generator sites and INL.

The total number of accidents per year calculated in this TA is 0.94, which is very close to the observed value of 1.17 accidents per year (21 accidents during 18 operational years of the WIPP transportation campaign). The number of accidents per year calculated in the 2008 TA was 10.44, which is due to much higher assumed accident rates.

The total number of injuries per year calculated in this TA is 0.35. The number of injuries per year were not considered in the 2008 TA.

The total number of fatalities per year calculated in this TA is 0.03. The expected number of fatalities expected to have occurred in the shipments to date calculated using the data in this TA is 0.47 meaning that no fatalities were estimated to occur. This is consistent with the actual data (no fatalities in the WIPP transportation accidents that have occurred). The annual number of fatalities in the 2008 TA was 0.04. The 2008 TA used the national fatalities per accident rate for all the states compared to the state-specific fatalities used in this TA.

In summary, the total non-radiological impacts estimated for the duration of the WIPP transportation campaign are small – 49 accidents, 18 injuries, and 1 fatality.

8.2.3 Radiological Impacts from Transportation Accidents with Release of Radioactive Materials

If an accident happens, the estimated probability of the accident resulting in release of radioactive materials is 1.9985×10^{-6} or 1 in 500,000. The conditional probability of an accident without release of radioactive materials is then 0.999998. Note that the conditional probability of an accident without release of radioactive materials was 0.99993 in the 2008 TA.

The estimated number of roundtrip accidents during the WIPP transportation campaign is 49 (25 one-way accidents). Consequently, the probability of an accident with release of radioactive materials is 5.00×10^{-5}. Because the probability of an accident with release is very small, the consequences are reported as dose risk (dose times the probability of the accident with release). However, the consequences of a severe accident are reported as doses.

Two scenarios for transportation accidents with release of radioactive materials were considered. The first scenario assumes an accident with the shipment of one HalfPACT and two TRUPACT-IIs. In this accident one TRUPACT-II is breached, fourteen 55-gal drums inside it are completely destroyed, and a fraction of the CH-TRU waste is released into the environment. The second scenario assumes an accident with three HalfPACTs with SCA. In this accident one HalfPACT is damaged, three 30-gal drums are completely destroyed, and a fraction of the RH-TRU waste is released into the environment.

The radiological impacts are calculated for rural, suburban, and urban segment for each state crossed by the transportation route and for each route. Credit is not taken for the fact that an accident will occur at only one place. This is the same approach as in the 2008 TA. The results are reported as the population dose risks and are presented in a similar format to that of the 2008 TA.

The population dose is the sum of the inhalation, cloudshine, resuspension, and groundshine doses. For both TRUPACT-II and HalfPACT accidents the main contribution to the total dose (99.2 percent) is from inhalation. Figures 8-5 and 8-6 show the route collective dose risks for rural, suburban, and urban links for all CH and all RH shipments respectively. The dose risks are plotted versus percentile to better show the range and the distribution in the dose risk values. In both scenarios the dose risks are very low. The dose risk in the accident with a RH shipment is more than 2 orders of magnitude lower than in an accident with a CH shipment, primarily because of the smaller number of RH shipments. The dose risks are higher in urban areas due to the higher population density and additional factors, such as pedestrians on city streets.

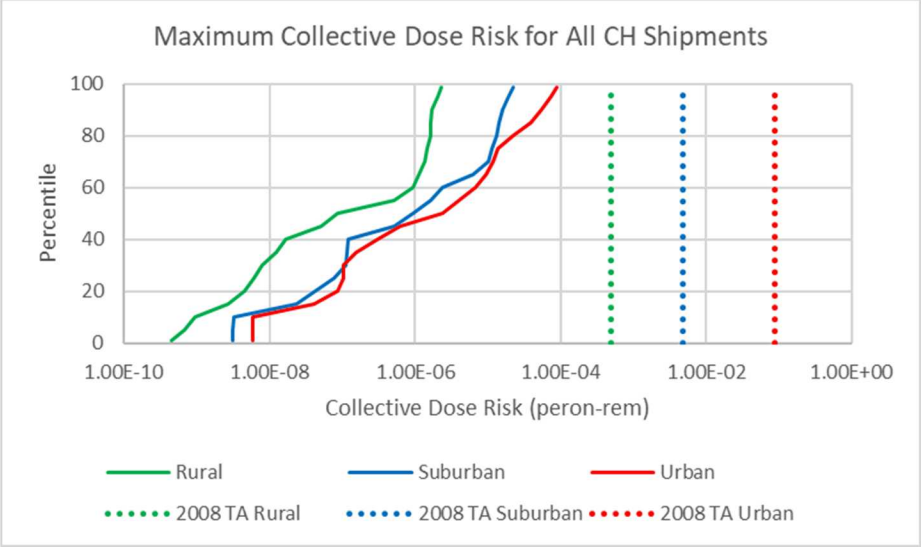

Figure 8-5. Transportation Route Maximum Collective Dose Risk Distribution for All CH Shipments.

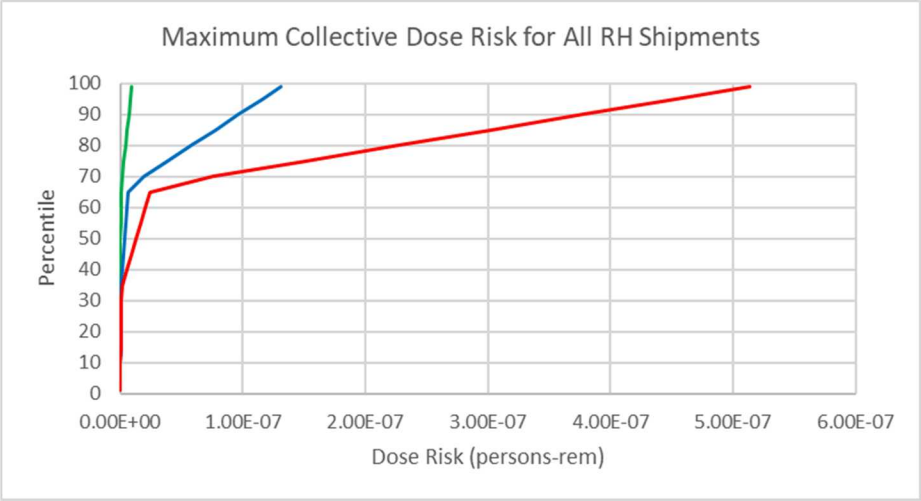

Figure 8-6. Transportation Route Maximum Collective Dose Risk Distribution for All RH Shipments.

The collective dose risks per CH shipment are higher and their ranges are larger in the 2008 TA on all (rural, suburban, and urban) links compared to this TA (Figure 8-3). This is primarily related to the higher (about one order of magnitude) Ci and A2 content and higher assumed accident rates. The collective dose risk per RH shipment was calculated in the 2008 TA for an accident with release for an RH-TRU 72-B. This TA assumes that the probability of this accident is zero as described in Section 6.5. The RH-TRU 72-B package is similar in construction to the rail transportation casks evaluated in NUREG-2125 (NRC 2014). The analyses in NUREG-2125 showed that there would be no release from transportation casks with inner canisters under the most severe accidents analyzed. The calculated dose risks per RH shipment for an accident with HalfPACT (SCA) calculated in this TA are significantly lower than the dose risks per RH shipment calculated for an accident with RH-TRU 72-B in the 2008 TA.

The severe transportation accident analysis considered a severe accident with TRUPACT-II and a severe accident with HalfPACT (SCA). The consequences of the severe accidents are reported in terms of doses. The probability of these accidents was not taken into the account.

As in the 2008 TA, the severe accidents were assumed to occur under conditions which maximize the radiological impacts - urban area and stable meteorological conditions. In this TA, the urban population density is defined based on actual route data. Based on the analysis of the urban links it was concluded that the Denver metropolitan area was an adequate proxy of a large urban metropolitan area. The population density was assumed to be 1,808 persons/km^2 in 2020 and 2,147 persons/km^2 in 2030. Note that in the 2008 TA, a severe accident was postulated to occur in a non-specific large metropolitan area. The assumed population density was 2,750 persons per km^2, the largest population density of any U.S metropolitan area in 2005.

Figures 8-7 and 8-8 show the collective population doses and MEI doses calculated in this TA and in the 2008 TA. The doses are higher in this TA mainly because of the higher respirable fraction.

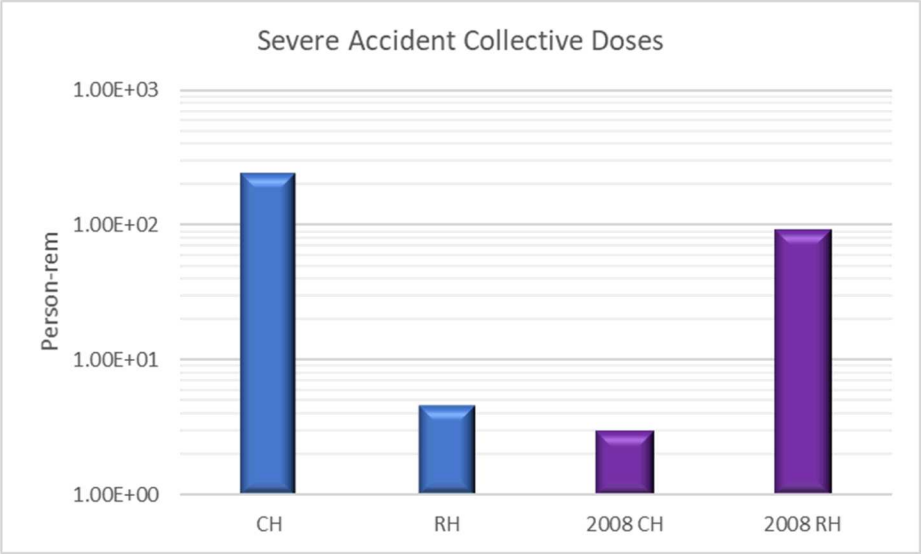

Figure 8-7. Collective Population Doses in Severe Accident with CH and RH Shipments.

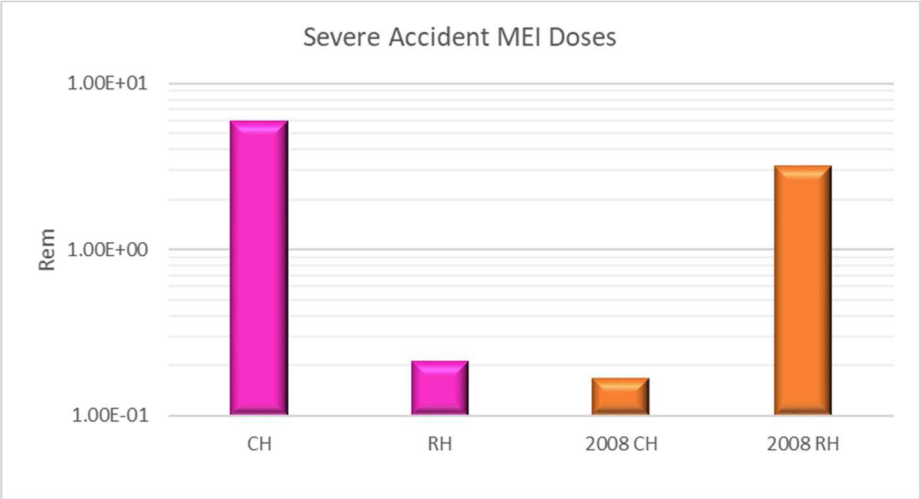

Figure 8-8. MEI Doses in Severe Accident with CH and RH Shipments.

8.3 Findings

This section presents the findings that are important for understanding what can affect the input parameters used in this analysis in the future.

The analysis of the state specific accident data showed that on average, the accident rates (accident/km) increased 2.1 times from 1999 until present while the fatalities rates increased 1.5 times and the number of fatalities per accident decreased by 25 percent. The higher accident rates are correlated with the population increase. The lower number of fatalities per accident is probably due to improvements in car safety since 1999. A similar trend can be assumed for the future.

The highest population doses for incident-free transport were calculated for people sharing the route with the truck transporting TRU waste. This dose is directly proportional to the traffic count and the number of

people per vehicle. This TA does not consider the correlation between the population increase and the traffic count (vehicles/hr). However, it is possible that the projected increase in population will result in an increase in the traffic count. This TA (as well as the 2008 TA) assumed 2 people per vehicle. This number can be different in the future if more people use carpools.

The population doses to people residing along the transportation routes and to people sharing the route are a function of the truck speed. The lower the speed, the higher the collective doses. This will mostly affect the suburbs. If the suburbs continue to grow (which is the current trend), larger areas will be affected by rush hour traffic and the rush hour speed might be lower.

The collective dose to the people at refueling stations is directly proportional to the number of people assumed to be at the station at the same time as the WIPP truck. This TA (as well as the 2008 TA) assumed seven people. It is important to understand how this number can change in the future. This also means that this exposure can be reduced by selecting a time when fewer people attend a refueling station.

This TA introduced a link factor. This factor is a convenient way to identify the links with the highest potential dose risks. The link factor (accidents-person/km^2) is calculated as a product of link distance (km), population density (people/km^2), accident rate (accident/km), and link ID (Eq. 7-1). The link ID is equal to 1 for rural and suburban links and is >1 for urban links (the actual value is scenario specific). The maximum link factor corresponds to the link with the maximum per shipment collective dose risk. The link factor can be used to identify the links with the highest dose risks under different population density and accident rate conditions.

The population dose and dose to a MEI in an accident with release is proportional to the evacuation time. An evacuation time of 24 hours was assumed in this TA (as well as the 2008 TA). In the future, it may become possible to reduce this time and the corresponding doses.

9. REFERENCES

10 CFR Part 71 Subpart E; *US Code of Federal Regulations*, Volume 10 (Energy), Part 71, Washington, DC 2008/

10 CFR PART 835—*Occupational Radiation Protection*.

49 CFR 392.9; *US Code of Federal Regulations*.

49 CFR 395; *US Code of Federal Regulations*.

Abkowitz, M. and North Wind Services, LLC, 2017. *START, Version 3.0 User Manual*, Prepared for Department of Energy Nuclear Fuels Storage and Transportation Planning Project, FCRD-NST-2014-000092, Rev. 5, June 2017.

AEC (U.S. Atomic Energy Commission), 1972. *Environmental Survey of Transportation of Radioactive Materials to and from Nuclear Power Plants*, WASH-1238, AEC, Washington, DC.

American Society of Mechanical Engineers (ASME), 2015. *Boiler and Pressure Vessel Code Nonmandatory* Appendix FF, 2015 Edition, New York, NY, U.S.A., July 1, 2015.

Ammerman, D. J., 1992. *A Method for Comparing Impacts with Real Targets to Impacts onto the IAEA Unyielding Target*, Proceedings of PATRAM 92, Yokohama, Japan. 1992.

Blandford, R. K., D. K. Morton, Snow, S.D. and T.E. Rahl, 2007. *Tensile Stress-Strain Results for 304L an 316L Stainless Steel Plate*, ASME Pressure Vessels and Piping Division Conference, San Antonio, TX, 2007.

Bonzon, L. L., 1977. *Final Report on Special Impact Tests of Plutonium Shipping Containers: Description of Test Results*, SAND76-0437, Sandia National Laboratories, Albuquerque, NM, 1977.

DOE (U.S. Department of Energy), 2019. *Annual Transuranic Waste Inventory Report-2019*, Revision 0 (December). Carlsbad Field Office, Carlsbad, NM. DOE/TRU-19-3425.

DOE (U.S. Department of Energy), 2017. *WIPP Transportation Safety Program Implementation Guide,* DOE Carlsbad Field Office, 2017.

DOE (U.S. Department of Energy), 2016. *TRU Waste Transportation Plan*. Revision 4. Report No. DOE/CBFO-98-3103, U.S. Department of Energy, Carlsbad Field Office, Carlsbad, New Mexico.

DOE (U.S. Department of Energy), 2015. *RH-TRU 72-B Shipping Package Safety Analysis Report*. Revision 7. USNRC Certificate of Compliance 71-9212, U.S. Department of Energy, Carlsbad Field Office, Carlsbad, New Mexico.

DOE (U.S. Department of Energy), 2013a. *TRUPACT-II Shipping Package Safety Analysis Report*. Revision 23. USNRC Certificate of Compliance 71-9218, U.S. Department of Energy, Carlsbad Field Office, Carlsbad, New Mexico.

DOE (U.S. Department of Energy), 2013b. *HalfPACT Shipping Package Safety Analysis Report*. Revision 6. USNRC Certificate of Compliance 71-9279, U.S. Department of Energy, Carlsbad Field Office, Carlsbad, New Mexico.

DOE (U.S. Department of Energy), 2009. *Contact-Handled Transuranic Waste Authorized Methods for Payload Control (CH-TRAMPAC)*, Rev. 3, U.S. Department of Energy, February 2009.

DOE (U.S. Department of Energy), 2008. *Transuranic Waste Baseline Inventory Report 2007, Revision 1,* U.S. Department of Energy, Carlsbad Field Office, Carlsbad, NM. DOE/TRU2008-3379.

DOE (U.S. Department of Energy), 2004. *DOE Standard Radiological Control*, DOE-STD-1098-99.
DOE (U.S. Department of Energy), 2002. *Recommendations for Analyzing Accidents under the National Environmental Policy Act*, DOE, Environment, Safety and Health Office of NEPA Policy and Compliance, 2002.

DOE (U.S. Department of Energy), 1994. *DOE Handbook, Airborne Release Fractions/Rates and Respirable Fractions for Nonreactor Nuclear Facilities*. Report No. DOE HDBK-3010-94. U.S. Department of Energy, Washington, D.C.

Dunagan, S. and Weiner, R., 2008. *Analysis Plan for Update to Disposal Phase Supplemental Environmental Impact Statement Transportation Analysis of the Waste Isolation Pilot Plant*, Sandia National Laboratories, Albuquerque, NM, 2008.

Gonzales, A., 1987.*Target Effects on Package Response: An Experimental and Analytical Evaluation*, SAND86-2275, Sandia National Laboratories, Albuquerque, NM,.1987.

Johnson, P.E. and Michelhaugh, R.D., 2000. *Transportation Routing Analysis Geographic Information System (WebTRAGIS) User's Manual*, ORNL/TM-2000/86, Oak Ridge, Tennessee: Oak Ridge National Laboratory.

Hinnerichs, T.D., Carne, T.G., Lu, W, Strasiunas, E.C., Neilson, M.K., Scherzinger, W., and Rogillio, B.R., 2006. *Characterization of Aluminum Honeycomb and Experimentation for Model Development and Validation.* Tech Rept. SAND2006-4455. Sandia National Laboratories.

Mills, G.S., J.L. Sprung, and Osborn, D.M., 2006. *Tractor/Trailer Accident Statistics*. Report No. SAND2006-7723. Sandia National Laboratories, Albuquerque, NM.

National Council on Radiation Protection and Measurements, 2009. *Ionizing radiation exposure of the population of the United States,* National Council on Radiation Protection and Measurements. NCRP No. 160, ISBN 978-0-929600-98-7, 2009.

Neilson, M.K., Morgan, M.S. and Krieg, R.D., 1987. *A Phenomenological Constitutive Model for Low density Polyurethane Foams*. Tech Rept. SAND86-2927. Sandia National Laboratories, 1987.

NRC (U.S. Nuclear Regulatory Commission). 2014. *Spent Fuel Transportation Risk Assessment*. Report No. NUREG-2125. U.S. Nuclear Regulatory Commission, Washington, D.C.

Peterson, S., 2018. *WebTRAGIS User Manual Final*, Oak Ridge National Laboratory, Oak Ridge, Tennessee, 2018.

Saricks, C.L. and Tompkins, M.M., 1999. *State-Level Accident Rates of Surface Freight Transportation: A Reexamination*, Center for Transportation Research, Argonne National Laboratory, ANL/ESD/TM-150, 1999.

SIERRA Solid Mechanics Team, 2019, *Sierra/SolidMechanics 4.52 Users Guide*. Tech Report SAND2019-2715. Sandia National Laboratories.

Sprung J.L., Ammerman, D.J., Breivik, N.L., Dukart, R.J., Kanipe, F.L., Koski, J.A., Mills, G.S., Neuhauser, K.S., Radloff, H.D., Weiner, R.F., and Yoshimura, H.R., 2000. *Reexamination of Spent Fuel Shipment Risk Estimates*. Report No. NUREG/CR-6672. Teo volumes, U.S. Nuclear Regulatory Commission, Washington, D.C.

Toothman, M., 2019. *Data Request 20191008_Chavez (OUO – Pre-decisional draft)*. October 9, 2019.

TRUPACT-II Safety Analysis Report, 2013, Revision 23.

Van Soest, G.D., 2019. *Comprehensive Inventory Database data version D.18.00*. August 26, 2019, and September 24, 2019.

Waddoups, I. G.,1975. *Air Drop Test of Shielded Radioactive Material Containers*, SAND75-0276, Sandia National Laboratories, Albuquerque, NM, 1975.

Waste Isolation Pilot Plant Land Withdrawal Act of 1992, Public Law 102-579, October 30, 1992.

Weiner, R.F., Hinojosa, D., Heames, T.J., Farnum, C.O., and Kalinina, E.A., 2013. *RADTRAN 6/RadCat 6 User Guide*, SAND2013-8095, Sandia National Laboratories, Albuquerque, NM.

Weiner, R.F., Neuhauser, K.S., Heames, T.J., O'Donnell, B.M., and Dennis, M.L., 2014. *RADTRAN 6 Technical Manual*, SAND2013-0780, Sandia National Laboratories, Albuquerque, NM.

Weiner, R.F. and Dunagan, S.., 2009. *Summary Report for Update to Disposal Phase Supplemental Environmental Impact Statement Transportation Analysis of the Waste Isolation Pilot Plant, WIPP*: 1.6.4:PM:QA L549453. Carlsbad, NM.

WIPP Nuclear Waste Partnership, 2020. *Data for the Transportation Risk Analysis, Additional Panels Project, NEPA Data Call*, Inter-Office Correspondence, RES:20:125, UFC:1100.00, January 15, 2020

Young, E. M., 1995. *SST-2/90 Scale Model Impact Tests Test Report*, Sandia National Laboratories, Albuquerque, NM (UCNI), 1995.

APPENDIX A. DETAILS OF THE INVENTORY ANALYSIS

This appendix provides the A2 values (Table A-1) used in Section 6.1 to develop bounding CH and RH inventories. The A2 values are from:
https://www.nrc.gov/reading-rm/doc-collections/cfr/part071/part071-appa.html

Table A-1. Radionuclide A_2 Values.

Radionuclide	A_2 (Ci)	Radionuclide	A_2 (Ci)	Radionuclide	A_2 (Ci)	Radionuclide	A_2 (Ci)
Ac-225	1.60E-01	Es-254	16	Pb-211	N/A	Sn-113	5.40E+01
Ac-227	2.40E-03	Eu-149	16	Pb-212	5.4	Sn-119m	8.10E+02
Ac-228	1.40E+01	Eu-152	2.70E+01	Pb-214	N/A	Sn-121	N/A
Ag-108	N/A	Eu-154	1.60E+01	Pd-107	Unlimited	Sn-121m	2.40E+01
Ag-108m	1.90E+01	Eu-155	8.10E+01	Pm-145	270	Sn-123	24
Ag-109m	N/A	Fe-55	1.10E+03	Pm-146	N/A	Sn-126	1.10E+01
Ag-110	N/A	Fe-59	1100	Pm-147	5.40E+01	Sr-85	5.40E+01
Ag-110m	1.10E+01	Fr-221	N/A	Pm-148	54	Sr-89	1.60E+01
Am-241	2.70E-02	Fr-223	N/A	Pm-148m	54	Sr-90	8.10E+00
Am-242	N/A	Gd-152	N/A	Po-210	5.40E-01	Ta-182	1.40E+01
Am-242m	2.70E-02	Gd-153	2.40E+02	Po-211	N/A	Tb-157	14
Am-243	2.70E-02	H-3	1.00E+03	Po-212	N/A	Tb-160	14
Am-245	N/A	Hf-175	1000	Po-213	N/A	Tc-97	14
Am-246	N/A	Hf-181	1000	Po-214	N/A	Tc-97m	14
Ar-37	1100	Ho-166m	1.40E+01	Po-215	N/A	Tc-98	14
Ar-39	540	I-125	14	Po-216	N/A	Tc-99	2.40E+01
Ar-42		I-129	unlimited	Po-218	N/A	Te-121	24
At-217	N/A	In-113m	5.40E+01	Pr-144	N/A	Te-121m	24
Ba-133	8.10E+01	In-114	54	Pr-144m	N/A	Te-123	N/A
Ba-137m	N/A	In-114m	54	Pu-236	8.10E-02	Te-123m	2.70E+01
Be-10	16	In-115	54	Pu-238	2.70E-02	Te-125m	2.40E+01
Bi-210	1.60E+01	In-115m	54	Pu-239	2.70E-02	Te-127	24
Bi-211	N/A	Ir-192	1.60E+01	Pu-240	2.70E-02	Te-127m	24
Bi-212	1.60E+01	Ir-194	16	Pu-241	1.60E+00	Th-227	1.40E-01
Bi-213	N/A	K-40	2.40E+01	Pu-242	2.70E-02	Th-228	2.70E-02
Bi-214	N/A	K-42	24	Pu-243	N/A	Th-229	1.40E-02
Bk-249	8.1	Kr-85	2.70E+02	Pu-244	2.70E-02	Th-230	2.70E-02
Bk-250	N/A	La-137	270	Pu-246	N/A	Th-231	5.40E-01
C-14	8.10E+01	Lu-177	270	Ra-223	1.90E-01	Th-232	Unlimited
Ca-45	2.70E+01	Lu-177m	270	Ra-224	5.40E-01	Th-234	8.10E+00
Cd-109	5.40E+01	Mn-54	2.70E+01	Ra-225	1.10E-01	Tl-206	N/A
Cd-113	N/A	Mo-93	27	Ra-226	8.10E-02	Tl-207	N/A
Cd-113m	1.40E+01	Na-22	1.40E+01	Ra-228	5.40E-01	Tl-208	N/A
Cd-115m	14	Nb-91	14	Rb-87	Unlimited	Tl-209	N/A

Radionuclide	A_2 (Ci)	Radionuclide	A_2 (Ci)	Radionuclide	A_2 (Ci)	Radionuclide	A_2 (Ci)
Ce-139	5.40E+01	Nb-92	14	Re-188	11	Tm-170	16
Ce-144	5.40E+00	Nb-93m	8.10E+02	Rh-102	14	Tm-171	1100
Cf-249	2.20E-02	Nb-94	1.90E+01	Rh-103m	1.10E+03	U-232	2.70E-02
Cf-250	5.40E-02	Nb-95	2.70E+01	Rh-106	N/A	U-233	6.00E-03
Cf-251	1.90E-02	Nb-95m	N/A	Rn-219	N/A	U-234	1.60E-01
Cf-252	8.10E-02	Nd-144	N/A	Rn-220	N/A	U-235	Unlimited
Cf-254	2.70E-02	Ni-59	Unlimited	Rn-222	1.10E-01	U-236	1.60E-01
Cl-36	1.60E+01	Ni-63	8.10E+02	Ru-103	5.40E+01	U-237	N/A
Cm-242	2.70E-01	Np-235	810	Ru-106	5.4	U-238	Unlimited
Cm-243	2.70E-02	Np-237	5.40E-02	S-35	8.10E+01	U-240	N/A
Cm-244	5.40E-02	Np-238	N/A	Sb-124	81	V-49	1100
Cm-245	2.40E-02	Np-239	1.10E+01	Sb-125	2.70E+01	W-181	810
Cm-246	2.40E-02	Np-240	N/A	Sb-126	1.10E+01	W-185	22
Cm-247	2.70E-02	Np-240m	N/A	Sb-126m	N/A	W-188	8.1
Cm-248	8.10E-03	Os-185	27	Sc-46	14	Xe-127	54
Cm-250	N/A	Os-194	8.1	Se-75	81	Y-89m	N/A
Co-58	2.70E+01	Pa-231	1.10E-02	Se-79	5.40E+01	Y-90	8.1
Co-60	1.10E+01	Pa-233	1.90E+01	Sm-145	54	Y-91	8.1
Cs-134	1.90E+01	Pa-234	N/A	Sm-146	54	Zn-65	5.40E+01
Cs-135	2.70E+01	Pa-234m	N/A	Sm-147	Unlimited	Zr-93	Unlimited
Cs-137	1.60E+01	Pb-209	N/A	Sm-148	N/A	Zr-95	2.20E+01
Dy-159	16	Pb-210	1.4	Sm-151	2.70E+02		

APPENDIX B. DETAILS OF THE TRUPACT-II IMPACT MODELING

This Appendix provides a detailed list of the model element blocks and material, a list of the stainless-steel material properties used in the analysis and also used to calculate the ASME strain-based failure limits and finally, detailed results of the finite element calculation for the free-drop analyses of the Type-B hypothetical accident condition (HAC) environments (10 CFR Part 71).

B.1. Model block numbers and materials

Table B-2. Model Block Numbers and Materials.

Block	Description	Element	Thickness (in.)	material
10	ICV elements to tie upper dome to upper flange	shell	0.25	Stainless
15	ICV upper dome attached to block 10	shell	0.25	Stainless
20	ICV side cylinder shell	shell	0.25	Stainless
25	ICV bottom dome	shell	0.25	Stainless
50	ICV Upper aluminum honeycomb	hex		Alum foam
55	ICV lower aluminum honeycomb	hex		Alum foam
70	ICV Upper flange attached to block 10	hex		Stainless
80	ICV Lover flange	hex		Stainless
90	ICV lock ring	hex		Stainless
95	Payload upper (CGOC only) other only concrete	hex		concrete
96	Payload lower (GCOC model only) not in others	hex		concrete
100	OCV 1/4 " shell to tie dome to thin (0.075) flange shell upper head	shell	0.25	Stainless
110	OCV Upper dome	shell	0.25	Stainless
120	OCA upper thin shell to tie upper flange horizontally	shell	0.075	Stainless
130	OCA upper thin shell near flange (excluding block 120)	shell	0.075	Stainless
200	OCV lower shell to tie to lower flange (top angle section)	shell	0.25	Stainless
210	OCV lower shell side and lower dome	shell	0.25	Stainless
220	OCA lower thin shell connected to lower	shell	0.075	Stainless
230	OCA lower thin shell near flange (excluding block 220)	shell	0.075	Stainless
300	OCA outer shell upper dome and shell upper side	shell	0.25	Stainless
400	OCA outer shell lower side and flat bottom	shell	0.25	Stainless
500	OCA upper head foam	hex		Foam
510	OCA lower side and bottom foam	hex		Foam
558	ICV lower honeycomb plate between honeycomb and concrete	shell	0.25	Alum 6061
559	ICV upper honeycomb plate between honeycomb and concrete	shell	0.25	Alum 6061
700	OCV upper flange	hex		Stainless
800	OCV lower flange	hex		Stainless
900	OCV lock ring	hex		Stainless

B.1.1. 304L Test Data Tables

Table B-3. INL 304L Test Data 70 °F [2].

304 L Base Material								
Temp	Fracture Strength (ksi)	Fracture Strain	Neck Strain	Reduction in Area (%)	Ultimate Strength (Ksi)	Ultimate Strain	Yield Strength (Ksi)	Total Strain
70	333	1.648	0.5	81	95.7	0.642	40.2	0.763
70	277	1.687	0.48	81	95.7	0.616	39.2	0.762
70	352	2.017	0.46	87	96	0.584	44.3	0.711
70	334	1.814	0.52	84	97.3	0.691	37.8	0.818
Average	324	1.7915	0.49	83.25	96.175	0.63325	40.375	0.7635
304L Weld Material								
70	266	1.45	0.37	77	94.5	0.445	60.7	0.603
70	295	1.585	0.39	79	88.3	0.484	35.9	0.602
Average	280.5	1.5175	0.38	78	91.4	0.4645	48.3	0.6025

Table B-4. INL 304L Test Data -20 °F [2].

304 L Base Material								
Temp	Fracture Strength (ksi)	Fracture Strain	Neck Strain	Reduction in Area (%)	Ultimate Strength (Ksi)	Ultimate Strain	Yield Strength (Ksi)	Total Strain
-20	329	1.426	0.36	76	140	0.442	51.1	0.573
-20	392	1.714	0.36	82	134.9	0.437	47.9	0.579
-20	376	1.637	0.38	81	140.7	0.468	46.5	0.585
-20	383	1.666	0.44	81	136	0.542	46.2	0.677
Average	370	1.61075	0.385	80	137.9	0.47225	47.925	0.6035
304L Weld Material								
-20	305	1.398	0.38	75	118.2	0.472	65.2	0.597
-20	346	1.526	0.47	78	114	0.604	48	0.704
Average	325.5	1.462	0.425	76.5	116.1	0.538	56.6	0.6505

B.2. 30-mph Impact Results

This section will provide more details of each HAC analysis and examine the response of the ICV which is the primary containment boundary.

B.2.1. Top Impact

The overall model deformation for the 30-mph top impact is shown in Figure B-1. Showing the compression of the polyurethane foam and outer OCA shell. Plots of the kinetic energy and the impact force on the target are shown in Figures B-2 and B-3. Note that these represent the energy and force in the half -symmetry model, not the full package.

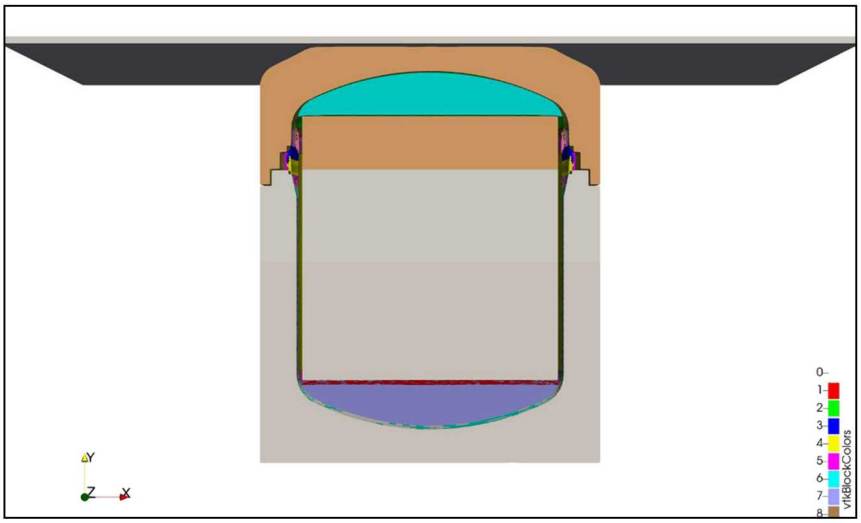

Figure B-1. Deformation for 30-mph top Impact Orientation

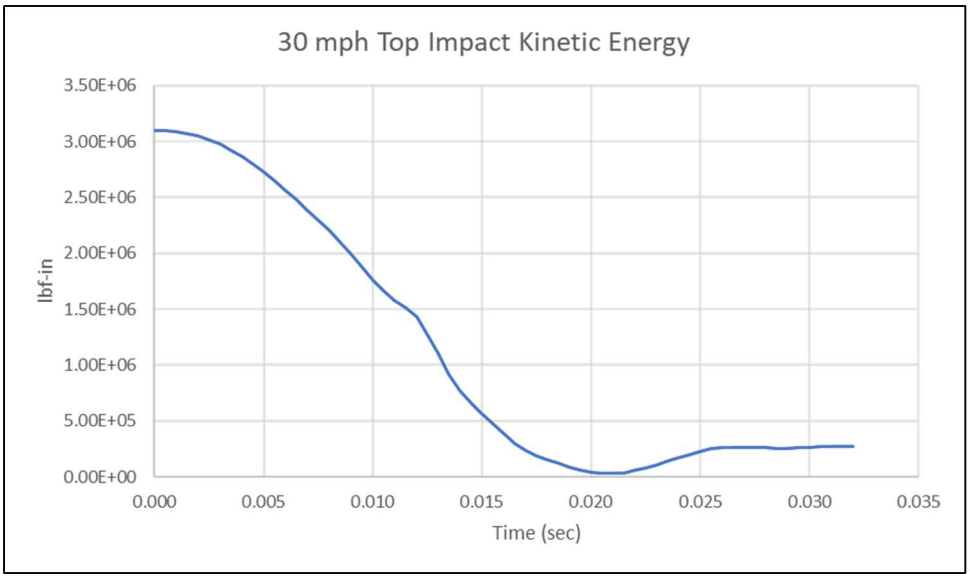

Figure B-2. Kinetic Energy versus Time 30-mph Top Impact

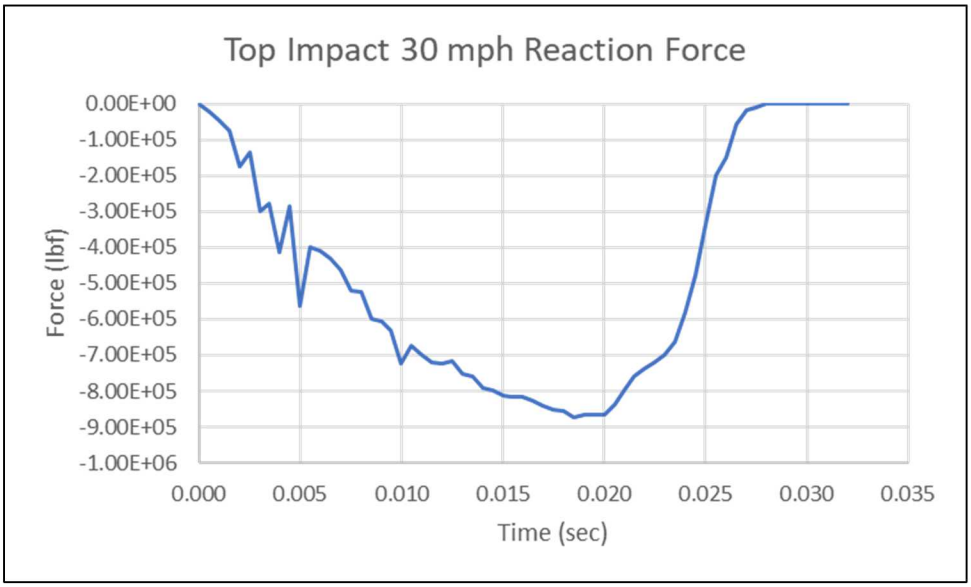

Figure B-3. Reaction Force for 30-mph Top Impact Orientation.

The impact and rebound takes approximately 0.027 sec with some residual kinetic energy remaining in the rebounding package. A peak reaction force of 8.72 x 10^5 lbf is reached at 0.0185 sec. The ICV is the containment boundary for the TRUPACT-II. Therefore, its response will be evaluated to determine the success or failure of the package. As previously discussed, the ASME strain-based acceptance criteria is used to evaluate the ICV components. Figure B-4 presents the $[TF\epsilon^p]_{max}$ values calculated for the hex flange elements and highest integration point value in the shell elements. Figure B-5 presents the EQPS values in the shell and flange. As expected for the 30-mph impact, there is only a small amount of plastic strain and the $[TF\epsilon^p]_{max}$ values are over an order of magnitude lower than the allowable limit.

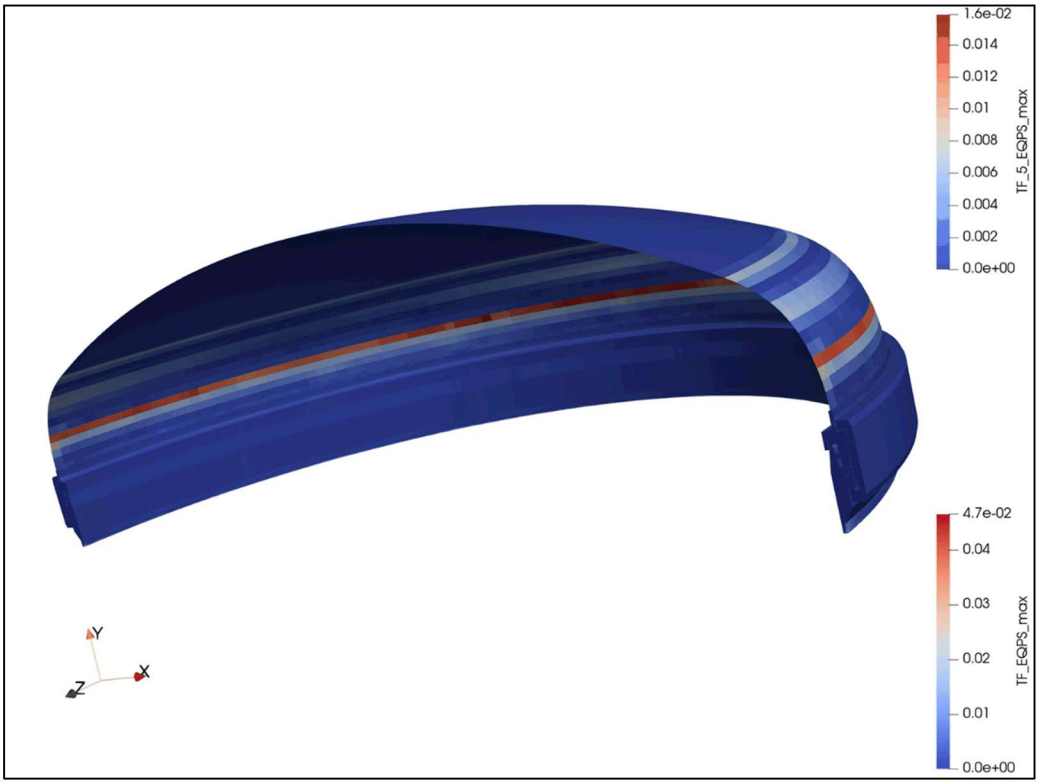

Figure B-9-4. Top Impact 30-mph TF_EQPS.

Figure B-5. Top Impact 30-mph EQPS.

B.2.2. Side Impact

The overall model deformation for the 30-mph side impact is shown in Figure B-6. Showing the compression of the polyurethane foam and outer OCA shell. A magnified view of the flange region is shown in Figure B-7.

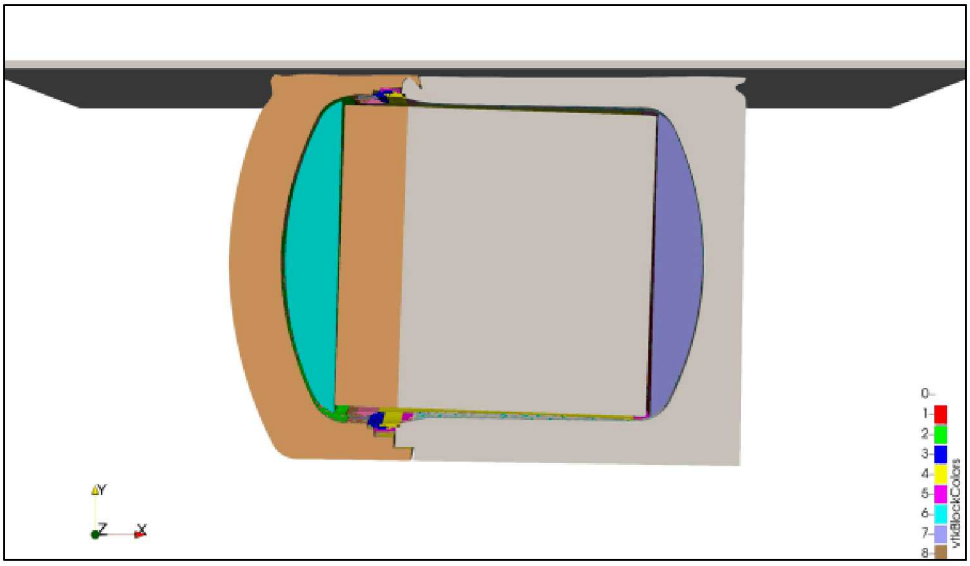

Figure B-6. Deformation for 30-mph Side Impact Orientation

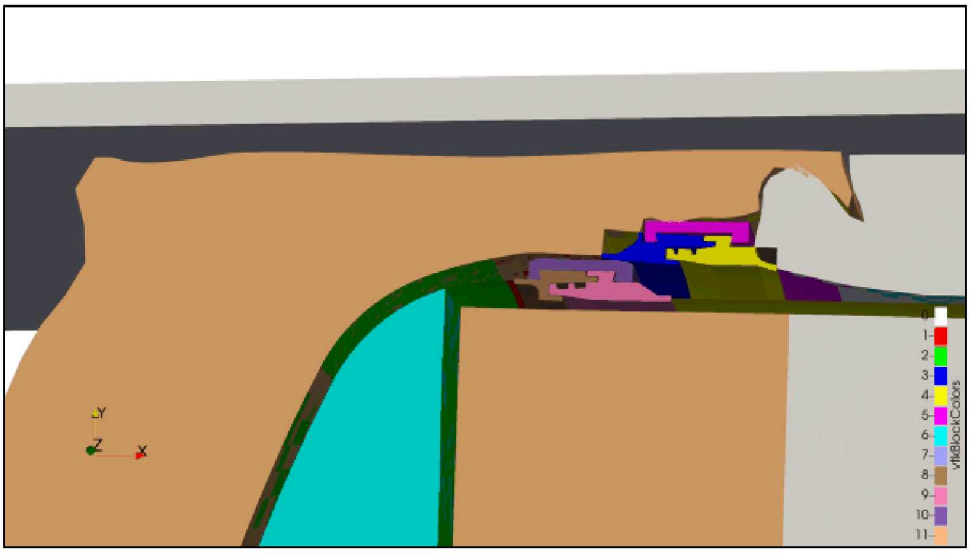

Figure B-7. Deformation for 30-mph Side Impact Orientation.

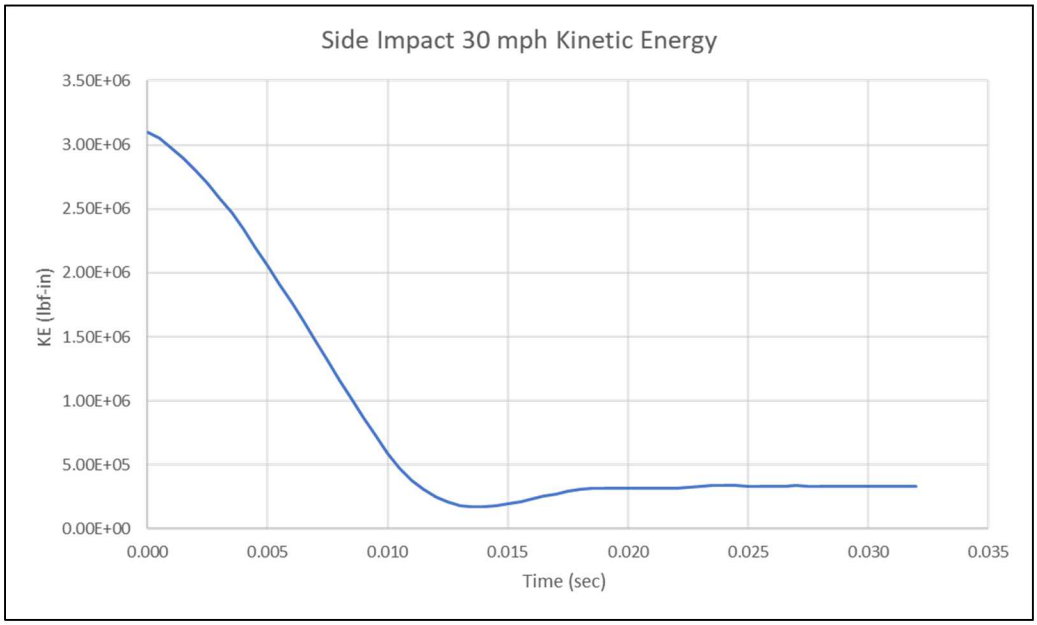

Figure B-8. Kinetic Energy Side Impact 30-mph.

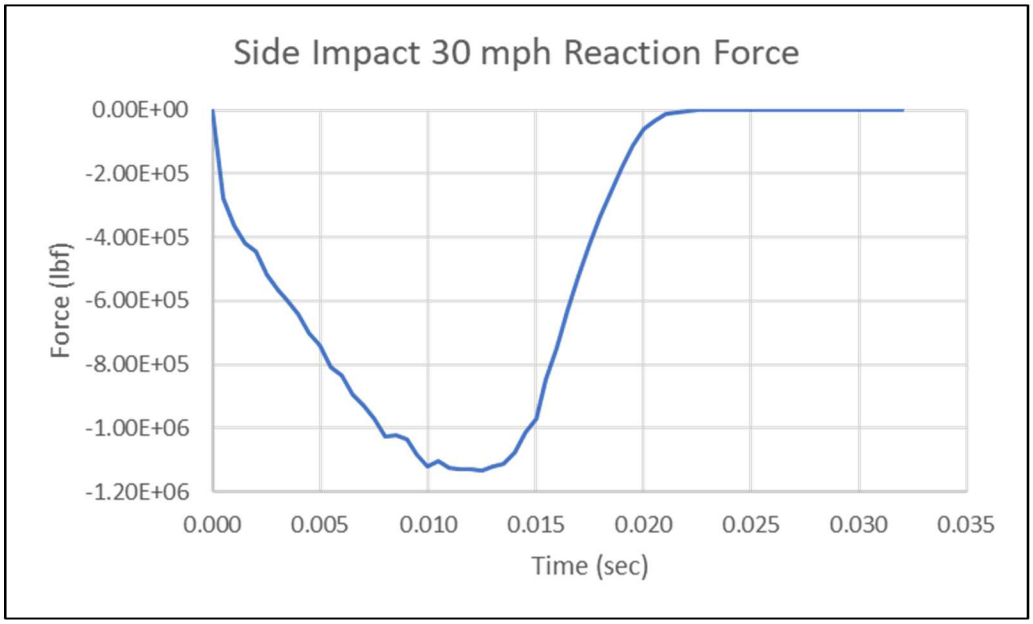

Figure B-9. Reaction Force Side Impact 30-mph.

Plots of the Kinetic energy and the impact force on the target for the half symmetry model are shown in Figures B-8 and B-9. The impact and rebound takes approximately 0.022 sec with some residual kinetic energy remaining in the rebounding package. A peak reaction force of 1.132 x 10^6 lbf is reached at 0.0125 sec.

Figure B-10 presents the $[TF\epsilon^p]_{max}$ values calculated for the hex flange elements and highest integration point value in the shell elements and Figure B-11 presents the EQPS values. As expected for the 30-mph

impact, there is only a small amount of plastic strain and the $[TF\epsilon^p]_{max}$ values are over an order of magnitude lower than the allowable limit.

Figure B-10, $[TF\epsilon^p]_{max}$. for 30-mph side impact orientation

Figure B-11. EQPS for the 30-mph side orientation

B.2.3. CGOC Impact

The overall model deformation for the 30-mph CGOC impact is shown in Figure B-12. A magnified view of the impact region is presented in Figure B-13. There is significant compression of the foam material and buckling of the outer OCA shell. This resulted in the death and removal of 326 foam elements.

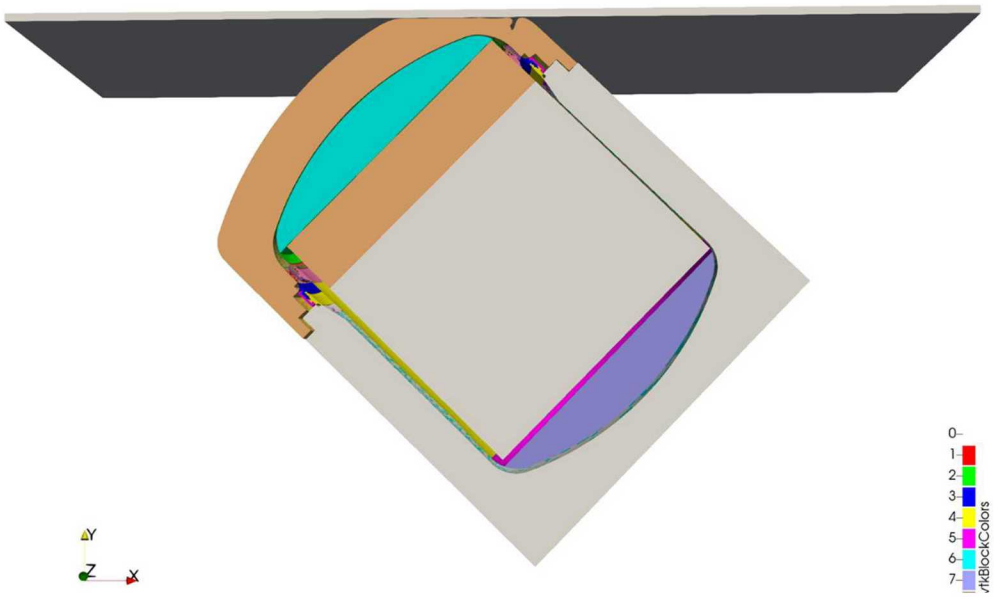

Figure B-12. Deformation for 30-mph CGOC Impact Orientation.

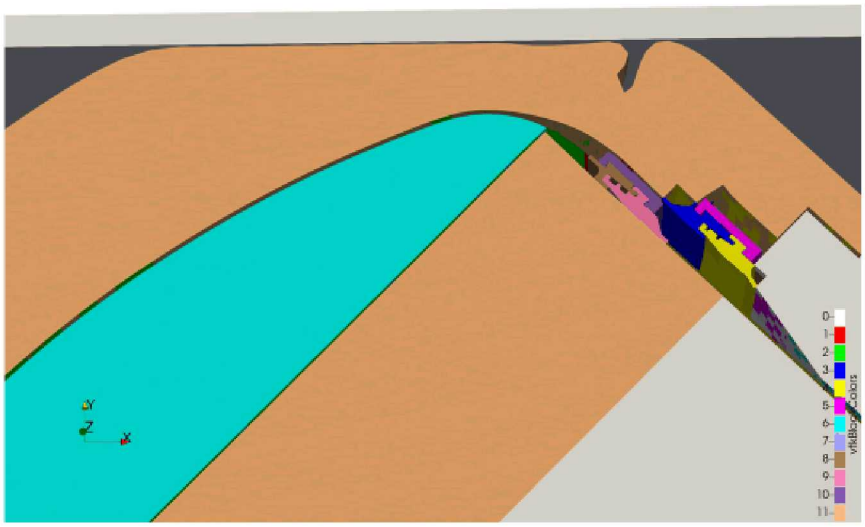

Figure B-13. Deformation for 30-mph CGOC Impact Orientation Magnified View.

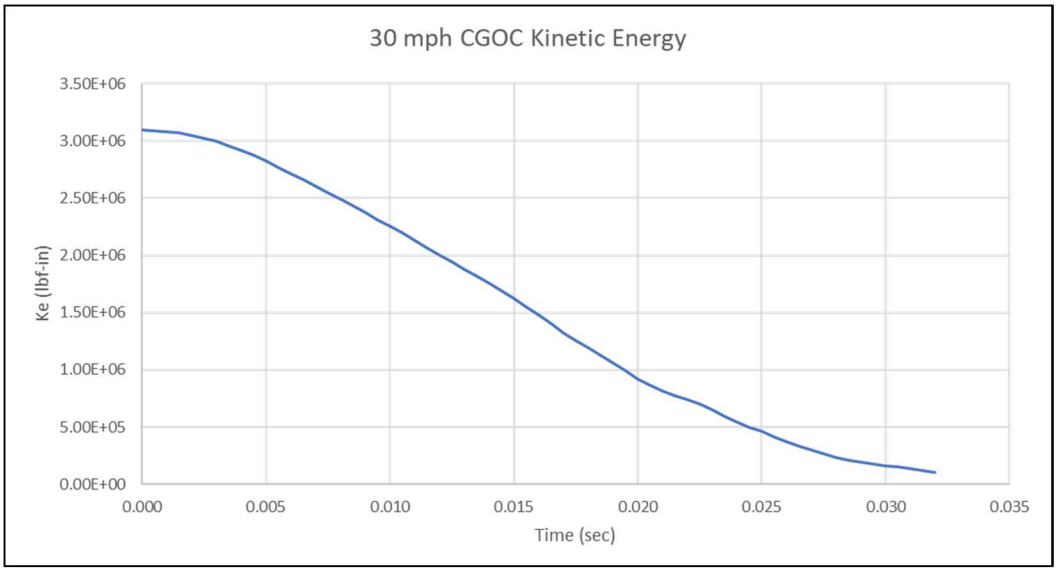

Figure B-14. Kinetic Energy CGOC Impact 30-mph.

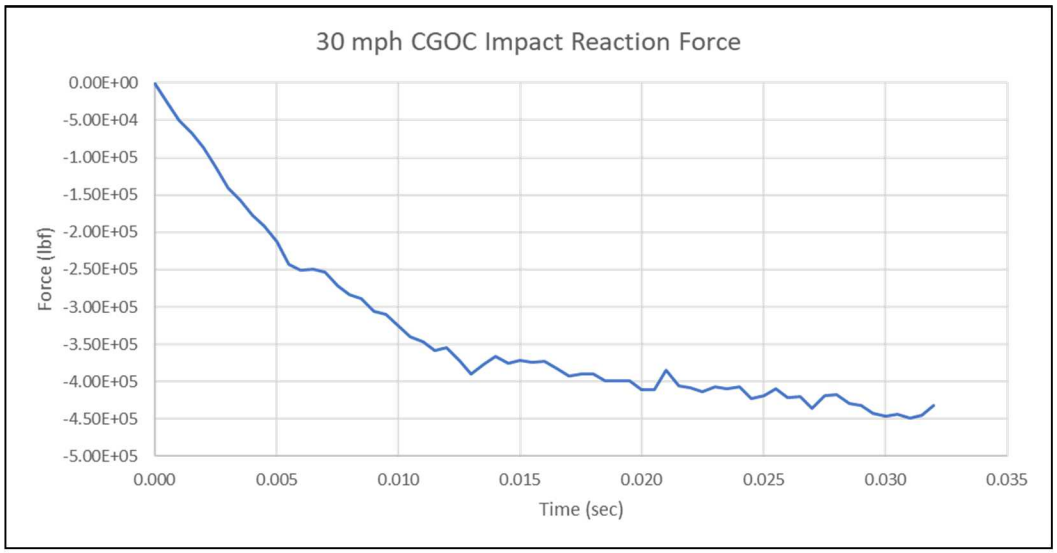

Figure B-15. Reaction Force CGOC impact 30-mph.

Plots of the kinetic energy and the impact force on the target for the half symmetry model are shown in Figures B-14 and B-15. For this velocity and orientation, the impact takes the full 0.032 sec of the analysis run time. A peak reaction force of 4.49 x 10^5 lbf is reached at 0.030 sec. Figure B-16 presents the $[TF\epsilon^p]_{max}$ values calculated for the hex flange elements and highest integration point value in the shell elements. Figures B-17 through B-19 show the $[TF\epsilon^p]_{max}$ in the flanges and lock ring. The high values are in the corner regions of the components. As expected for the 30-mph impact, there is only a small amount of plastic strain and the $[TF\epsilon^p]_{max}$ values are over an order of magnitude lower than the allowable limit.

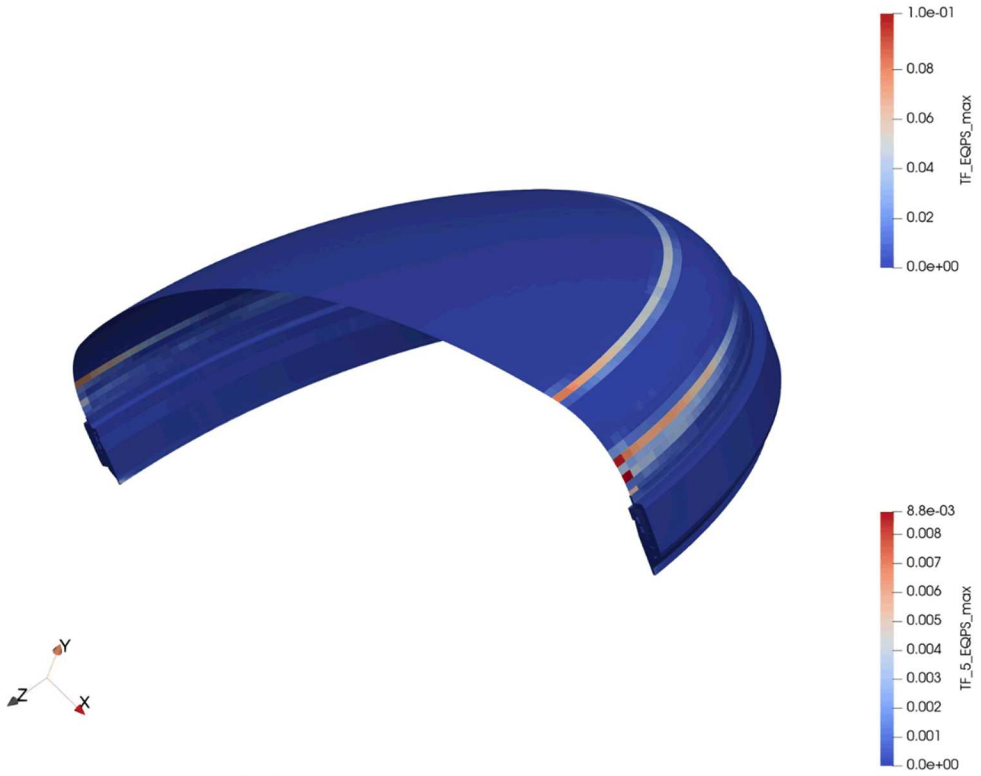

Figure B-16. CGOC Impact 30-mph $[TF\epsilon^p]_{max}$ top shell and flange.

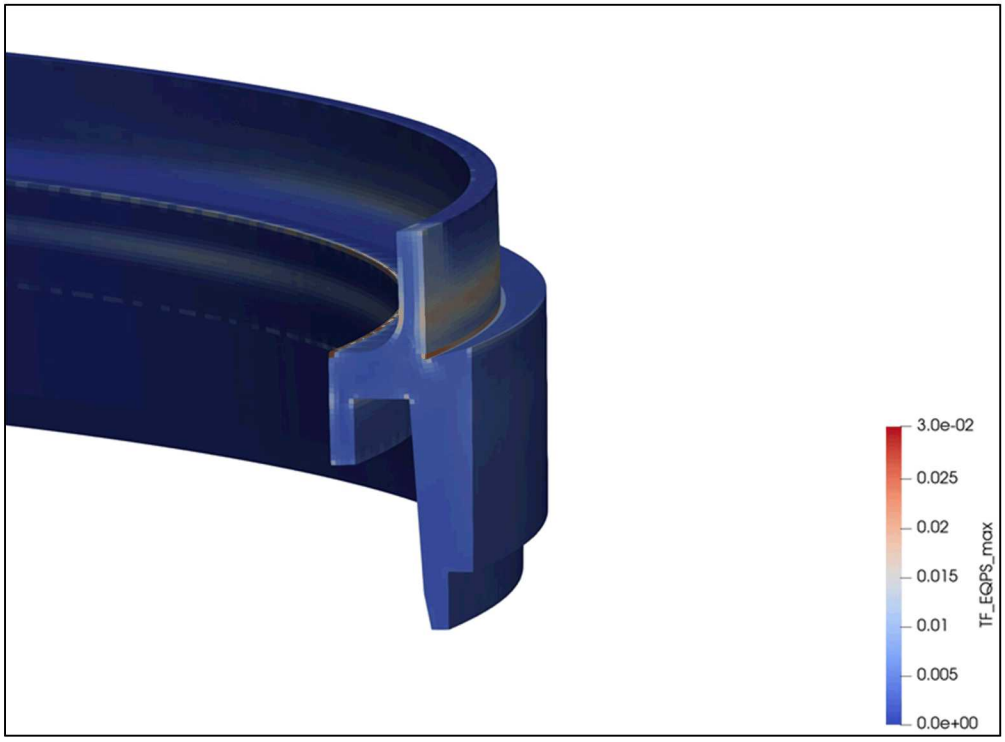

Figure B-17. CGOC Impact 30-mph $[TF\epsilon^p]_{max}$ upper flange.

Figure B-18. CGOC Impact 30-mph $[TF\epsilon^p]_{max}$ lower flange.

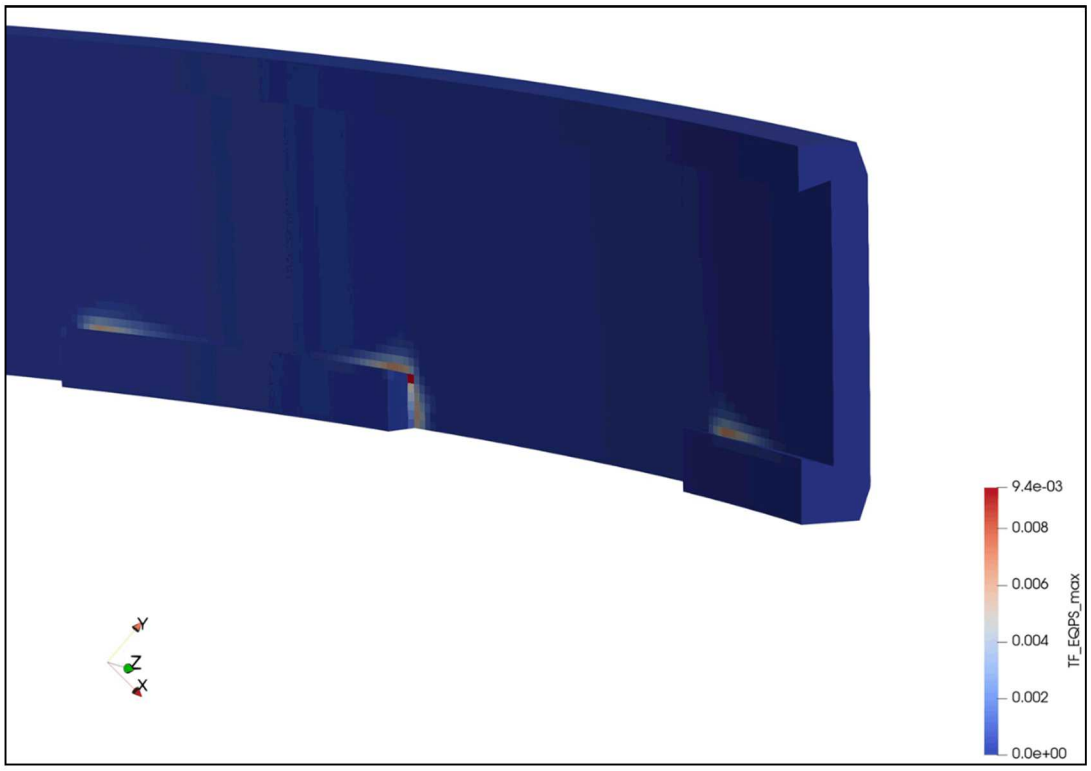

Figure B-19. CGOC Impact 30-mph.